SYNTHESIS, *IN-SILICO* MOLECULAR MODELLING AND BIOLOGICAL STUDIES OF 1,4-DIHYDROXYANTHRAQUINONE AND ITS DERIVATIVES

Thesis

Submitted in Fulfillment of the Requirements for the degree of

Doctor of Philosophy

Of

RHODES UNIVERSITY, SOUTH AFRICA

Department of Chemistry

Faculty of Science

By

Lydia Mboje Kisula

October 2021

ACKNOWLEDGEMENTS

I would like to express my sincere thanks to Prof. Rui WM Krause for accepting to be my supervisor. I am grateful for pursuing my doctorate studies under his supervision his passion and willingness to give time have given me a great opportunity to develop my career as a chemist. His support will always be remembered in my life

Special thanks are also due to the following

Rhodes University and the Organization for Women in Science for the developing world (OWSD) for provision of financial support during the entire period of my doctorate studies

Rhodes University, Chemistry department staffs Prof Rosalyn Klein, Prof Kevin Lobb, Prof Kyanye Setshaba, Dr. Vincent Smith, Dr. Xavier Siwe Noundou, technicians Mr. Adrian and Mr. Dondashe and secretaries Mrs. Benita Tarr for always been there whenever needed their help. My gratitude is also extended to my fellow workers at Tanzania Industrial research and development organization (TIRDO) through his Director-General Prof. Mtambo Mkumbukwa for their encouragement and for offering a study leave

I would always like to thank my colleagues in F22 just to mention a few names Bertha Chitambo, Melody Manyeruke, Ogunyemi Oderinlo, Mziyanda Mbaba, Ayanda Zulu, Alain Bapolis, Richard Beteck, Fostino Bokosi, Nmandi Ikemefuna, Izichukwu Charles, Douglas Kemboi, and many others for their good moral support and for being the good family since the starting of my doctorate studies up to the end. Their presence has been always warm and conducive to the creation of a productive learning environment.

I would like to thank Prof Heinrich Hoppe and Ms. Tarryn at the Biochemistry and Microbiology Department, Rhodes University for conducting the bioassay studies; the MRC AMR Hub for antimicrobial studies.

My heartfelt gratitude goes to my family and friends whose prayers and emotional support have been always warm to me. I would like to thank the organization of frontiers church and River of Life Church (Grahamstown) for their endless love and spiritual support during the whole period of my doctorate studies

I would like to thank my parents Rebecca Michael and my late father Benjamin Mboje for being good parents and for growing me and enabling me to fulfill my path towards getting proper education

Above all, I would like to thank the Almighty God the source of all creation and the one he who all the Glory belong to him

ABSTRACT

This current study of investigation reports on the synthesis of 1,4-dihydroxyanthraquinone and its derivatives on explorations of their medicinal potential. The study initially aimed to synthesize an analogue of a natural anthraquinone, *1,3,6-trihydroxy-7-((S)-1-hydroxyethyl)anthracene-9,10-dione* **5** using Friedel-Crafts acylation of phthalic anhydride and a benzene derivative. Synthetic transformation of anacardic acid **63,** obtained as a by-product of the cashew industry successfully afforded *4-ethoxyisobenzofuran-1,3-dione* **89.** However, when attempted to couple *4-ethoxyisobenzofuran-1,3-dione* **89** with *2-hydroxyacetophenone* **91** in a Friedel-Crafts acylation manner to form *2-acetyl-1,8-dihydroxyanthracene-9,10-dione* **87** the reaction did not work efficiently. A simple derivative of benzene which is; *benzene-1,4-diol* **102** was reacted instead with *3-ethoxyphthalic acid* **71** and *isobenzofuran-1,3-dione* **96** to form *1,4,5-trihydroxy anthraquinone* **72** and *1,4-dihydroxyanthraquinone* **42***,* respectively. A modified Marschalk reaction was then used to introduce the hydroxyl alkyl group to 1,4-dihydroxy anthraquinone **42**, which allowed further elaboration of the hydroxyl-substituent in moderate to good yields (22-80%).

A molecular docking study was performed using Schrödinger software to predict the binding affinity of the test compounds to the target protein trypanothione reductase (PDB ID: 6BU7). An *in-vitro* screening of 1,4-dihydroxyanthraquinone derivatives and some selected precursors for antitrypanosomal, antiplasmodial, antibacterial, and cytotoxicity activities produced encouraging results. Derivatives of anacardic acid and cardanol from CNSL were found to have moderate activity against trypanosomes with no activity against *Plasmodium falciparum*. Almost 63% of synthesized 1,4-dihydroxyanthraquinone derivatives displayed activity against trypanosomes. The *in-vitro* evaluation and the *in silico* molecular docking studies revealed that 1,4-dihydroxyanthraquinone derivatives can be potential drug-like candidates active against *T.brucei* parasites (IC_{50} = 0.70-1.20 μM). Only four 1,4-

dihydroxyanthraquinone derivatives with thiosemicarbazone, chloride, pyrrole, and diethanolamine functionality displayed activity against *Plasmodium falciparum* (IC_{50} = 3.17-14.36 μM).

In-vitro evaluated of test compounds against antibacterial screen and cytotoxicity effects significantly showed that *2-hydroxy-6-pentadecylbenzoic acid* **63a** and *2-((2-chlorophenyl)(piperazin-1-yl) methyl)-1,4-dihydroxyanthracene-9,10-dione* **78** have potency against *Staphylococcus aureus* and reduced the viability of the cells below 20% at an initial concentration of 50 μg/mL. Only 1,4-dihydroxyanthraquinone derivatives with thiosemicarbazone **76**, piperazine **78**, and diethanolamine **80** motifs were active against HeLa cells and reduced the viability of cells below 20% at a concentration of 50 μg/mL.

In conclusion, this current reported study has generated useful knowlege on the applicability of the agro-waste CNSL as an agent active against trypanosomiasis but also as a low-cost starting material to synthesize hydroxy anthraquinones. The study has further given an overview to the understanding of the medicinal value 1,4-dihydroxyanthraquinone derivatives as promising candidates towards developing drugs suitable for treating neglected tropical diseases particularly trypanosomiasis.

LIST OF ABBREVIATIONS

NMR	Nuclear Magnetic Resonance Spectroscopy
^{1}H NMR	Proton Nuclear Magnetic Resonance Spectrum
^{13}C NMR	C-13 Nuclear Magnetic Resonance Spectrum
DEPT	Distortionless Enhancement by Polarization Transfer
HSQC	Heteronuclear Single Quantum Coherence
HMBC	Heteronuclear Multiple bond Correlation
ppm	Parts per million
TLC	Thin layer Chromatography
EtOAc	Ethyl acetate
DCC	*N,N*'-Dicyclohexylcarbodiimide
DMAP	4-Dimethylaminopyridine
DMP	Dess-Martin periodinane
Et_3N	Triethyl amine
IC_{50}	Half-maximal inhibitory concentration
FDA	Food and Drug Administration
DCM	Dichloromethane
PPL	Porcine Pancreatic Lipase
MeOH	Methanol
HRMS	High Resolution Mass Spectroscopy
ESI	Electrospray Ionisation

Calcd	Calculated
m/z	*mass per charge*
μM	Micromolar

TABLE OF CONTENTS

ACKNOWLEDGEMENTS i

ABSTRACT iii

LIST OF ABBREVIATIONS v

TABLE OF CONTENTS vii

CHAPTER 1 1

INTRODUCTION 1

1.1 Introduction to the chapter 1

1.2 The rationale of the study 1

1.3 Significance of the study 3

1.4 Leishmaniasis and trypanosomiasis 4

1.5 Purpose of the study 8

1.5.1 Specific objectives 8

CHAPTER 2 10

LITERATURE REVIEW 10

2.1 Introduction to the chapter 10

2.2 Medicinal applications and biological activities of anthraquinones 10

2.3 The therapeutic importance of heterocycles 14

2.4 The synthesis of anthraquinones 18

2.4.1 Friedel–Crafts reactions 18

2.4.2 Diels–Alder reactions, [4+2]-cycloaddition reaction (DA) 19

2.4.3 Organocatalyzed [4 + 2] benzannulation 20

2.4.4 Ring-closing metathesis 20

2.4.5 Anionic condensation reactions 21

2.5 The application of Marschalk reaction 22

2.6 A modified Marschalk reaction 23

2.7 The chemistry of cashew nut shell liquid 24
2.8 Graphical representation 27
CHAPTER 3 30
EXPERIMENTAL PROCEDURES 30
3.1 Introduction to the chapter 30
3.2 General procedures 30
3.3 Extraction of cashew nut shell liquid 31
3.3.1 Isolation and purification of anacardic acid 31
3.4 Synthesis of (E)-ethyl 2-ethoxy-6-(pentadec-1-en-1-yl)benzoate from (E)-2-hydroxy-6-(pentadec-8-en-1-yl) benzoic acid 32
3.4.1 The preparation of benzoyl peroxide 34
3.5 Oxidation of (E)-ethyl 2-ethoxy-6-(pentadec-1-en-1-yl)benzoate to 3-ethoxy-2-(ethoxycarbonyl)benzoic acid **71** 36
3.5.1 Method A: Using mild oxidation by oxygen 36
3.5.2 Method B: Iron-catalyzed oxidative cleavage of olefins 36
3.6 Synthesis of phthalic anhydrides 37
3.6.1 Preparation of 4-ethoxyisobenzofuran-1,3-dione 37
3.6.2 Preparation of isobenzofuran-1,3-dione 38
3.7 Preparation of 2-hydroxyacetophenone 38
3.8 Synthesis of 2-acetyl-1-hydroxyanthracene-9,10-dione 40
3.8.1 Method C: Friedel-Crafts acylation 40
3.9 Preparation of *meta*-iodo acetophenone from acetophenone 40
3.9.1 Nitration of acetophenone to 3-nitroacetophenone 40
3.9.2 Reduction of 3-nitroacetophenone to 3-aminoacetophenone 41
3.9.3 Sandmeyer reaction of 3-aminoacetophenone to 3-iodo acetophenone 42
3.10 New synthetic methods 42

3.10.1 Method D: Modified Marschalk reaction 44
3.10.2 The reaction of alcohol with thionyl chloride 47
3.11 Preparation of anthraquinone thiosemicarbazone 53
3.12 Esterification of anacardic acid with 1,4-dihydroxy-2-(1-hydroxyethyl)anthracene-9,10-dione 55
3.13 Preparation of saturated anacardic acid 56
3.14 Preparation of cardanol by decarboxylation of anacardic acid 56
3.15 Reduction of cardanol 57
3.16 Biological studies procedures 57
3.16.1 *In vitro* antitrypanosomal assay 57
3.16.2 *In vitro* anti-Plasmodium falciparum assay 58
3.16.3 *In vitro* antibacterial assay 58
3.16.4 *Staphylococcus aureus* antibacterial assay 58
3.16.5 *E. coli* antibacterial assay 59
3.16.6 *In vitro* cytotoxicity assay 59
3.17 *In silico* molecular docking analysis procedure 60
3.17.1 Knime workflow docking 60
3.17.2 Glide grid docking 61
3.18 SwissADME pharmacokinetic properties prediction 61
3.19 Lipinski rule of five 62
CHAPTER 4 63
RESULTS AND DISCUSSION 63
4.1 Introduction to the chapter 63
4.2 Retrosynthetic analysis 63
4.3 Preliminary experiments on the synthetic strategies towards the analogue 64
4.4 Extraction and isolation of anacardic acid 65

4.5 Synthetic conversion of anacardic acid to (S)-1,6-dihydroxy-7-(1-hydroxyethyl)anthracene-9,10-dione **6** 66
4.6 Oxidation of (E)-ethyl 2-ethoxy-6-(pentadec-1-en-1-yl)benzoate **70** 76
4.7 Preparation of phthalic anhydrides 80
4.8 Preparation of the 2-hydroxyacetophenone 82
4.9 Friedel-Crafts acylation 84
4.10 Synthesis of 2-acetyl-3-hydroxyanthracene-9, 10-dione **87** 85
4.11 Synthetic transformation of acetophenone to 3-iodoacetophenone **101** 86
4.12 New synthetic approaches and the modified Marschalk reaction 88
4.13 The modified Marschalk reaction 93
4.14 Functional group modifications 98
4.15 Synthesis of 1,4-dihydroxyanthraquinone thiosemicarbazone **76** 98
4.16 Synthesis of anthraquinone amines 103
4.17 Synthesis of 1-(9,10-dihydro-1,4-dihydroxy-9,10-dioxoanthracen-3-yl)ethyl 2-hydroxy-6-pentadecylbenzoate 116
4.18 Hydrogenation of anacardic acid **63** 119
4.19 Decarboxylation of anacardic acid 119
CHAPTER 5 122
BIOASSAY STUDIES AND *IN SILICO* MOLECULAR DOCKING ANALYSIS 122
5.1 Introduction to the chapter 122
5.2 Biological evaluation of the target compounds 122
5.3 Biological results and discussion 122
5.31 Trypanosoma brucei assay 123
5.32 pLDH (Malaria) assay – single concentration screen 127
5.33 Antibacterial assays 129
5.34 Cytotoxicity assays 129

5.4 *In silico* molecular docking analysis 130
5.5 *In silico* molecular docking results and discussion 136
5.6 Swiss ADME results for ligands that were active against trypanosomiasis 140
5.7 Lipinski Rule of Five results 141
CHAPTER 6 143
CONCLUSIONS 143
RECOMMENDATIONS FOR FUTURE WORK 144
REFERENCES 145
APPENDIX 169
AA 1: Mass spectrometry of carboxylic **71** 169
AA2: Mass spectrometry of imidazole anthraquinone **83** 170
AA3: Mass spectrometry of thiazole anthraquinone **85** 171
AA4: Protein ligand interaction-LK09 172
AA5: Protein ligand interaction-LK18 173
AA6: Protein ligand interaction-LK20 174
AA7: Protein ligand interaction-LK21 175
AA8: Protein ligand interaction- pentamidine 176
AA9: Protein ligand interaction- eflornithine 177
AA10: Protein ligand interaction- camptothecin 178
AA11: Trypanosoma brucei brucei % cell viability for compounds at the varied concentration 179
AA12: Graph of % viability (T. brucei cells) against log [C] for sample LK01-LK21 180
AA13: P. falciparum parasite % cell viability at the varied concentration (μM) 181

CHAPTER 1

INTRODUCTION

1.1 Introduction to the chapter

This chapter gives a general overview of anthraquinones, their structure and uses in the field of medicinal chemistry, and routes to their synthesis. The significance of the study is also described especially as it relates to the treatment of several neglected tropical diseases.

1.2 The rationale of the study

An anthraquinone pharmacophore is a physiologically active ingredient occurring in many plants, microorganisms, insects, and marine animals [1]. The therapeutic potential of anthraquinone derivatives such as antibacterial [2], anticancer [3] [4], antifilarial [5], and antileishmanial [6] has attracted researchers from diverse fields and hence are considered as targets in organic synthesis [7]. In addition to their useful medicinal value, their bright-colored nature of most anthraquinone derivatives has confirmed them as safe colorants in cosmetics, drugs, and foods [7] [8].

Many anthraquinone derivatives, particularly anthracycline antibiotics have long been used as anti-infective agents, and also in the treatment of different types of human cancer [9] [10]. There are many anticancer drugs, ranging from nitrogen mustards (e.g. chlorambucil) to antimetabolites (e.g. 5-fluorouracil) that are approved worldwide [11], but several anthracycline drugs such as daunomycin **1**, doxorubicin **2**, epirubicin **3,** and idarubicin **4** (**Figure 1.1**) remain as first-line choices in terms of efficacy and potency [12].

The general structure of the anthracycline drugs includes the anthraquinone backbone, linked to an amino sugar molecule that helps to impart specific functions [13]. The planar, electron-deficient anthracene quinone ring typically works by inserting itself into the electron-rich

purine-pyrimidine bases causing a distorted DNA helix and interfering with the normal functioning of DNA polymerases, RNA polymerases, topoisomerases, and other related enzymes required for DNA replication and RNA synthesis [14]. The amino sugar is mostly inactive, but dramatically improves the water solubility of the anthracyclines [13].

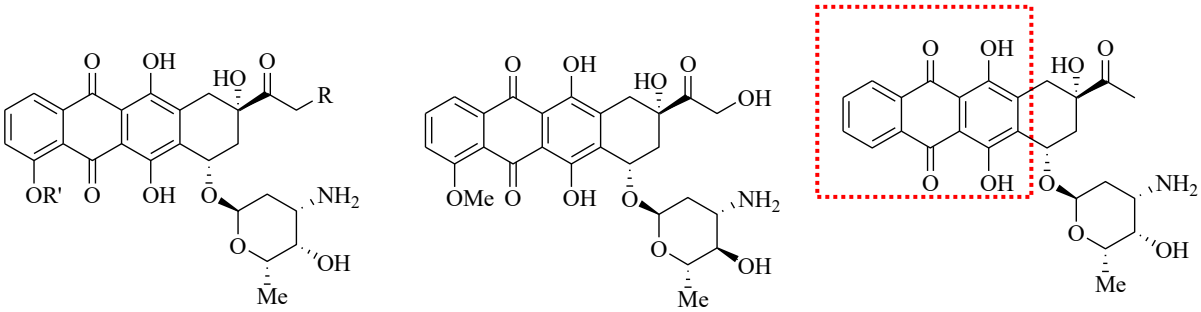

Figure 1. 1: The anthracycline anticancer drugs daunorubicin (1), adriamycin (2), epirubicin (3), and idarubicin (4)

Clinically, anthracycline drugs are used to treat a variety of cancers ranging from leukemia, lymphomas, breast, uterine and ovarian cancer to lung cancer [15]. Like any other chemotherapeutic agents, anthracycline drugs induce some side effects and their use is limited due to cardiotoxicity that develops after prolonged treatment with lower doses or after acute treatment with high doses [15]. This feature has necessitated the search for other anticancer drugs inevitable.

Almost all anthracycline drugs share a unique feature namely 1,4-dihydroxyanthraquinone moiety. This common feature has in recent times raised the attention of many chemists to serve as a motif for structural modifications towards the enhancement of other cytotoxic anticancer agents. Routes to the synthesis of 1,4-dihydroxyanthraquinone **(Figure 1.1)** have evolved at the hands of medicinal chemists, and these systems have been extensively studied

both as a building block for the synthesis of other possible antitumor agents and in the development of other therapies [16] [17].

1.3 Significance of the study

Recently, a hitherto new unreported chiral hydroxyanthraquinone **5** (**figure 1.2**) was isolated from marine fungus *Negrospora spp.* Due to its paucity; the biological activities of compound **5** were not tested [18]. Several other derivatives of anthraquinones with hydroxyalkyl functionality similar to structures **5** and **6** are known to have good antimicrobial activity and as well as antitumor activity [19] [20]. From this overview, it was considered necessary to design a study to synthesize compound **6**, which is the analogue of a chiral natural anthraquinone **5** and to test for its biological activities.

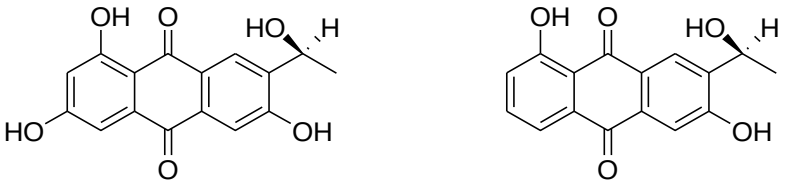

Figure 1.2: Chemical structure of 1,3,6-trihydroxy-7-((*S*)-1-hydroxyethyl)anthracene-9,10-dione 5 and its analogue 6

Based on this background, the current reported study aimed at finding a general route to the synthesis of **5** and its analogue **6** from the agro-waste cashew nutshells, and then to further elaborated the moiety for evaluation as anti-infective leads. The components of the cashew nut shell liquid from *Anacardium occidentale* are a source of valuable phenolic compounds that have been in recent days used in organic synthetic works. The utilization of cashew nut shells is sought to be of importance in adding value to the cashew crop particularly in the countries where it is planted like Tanzania. As based on this, a study was designed to synthesize an analogue of a chiral natural anthraquinone **6** from anacardic acid **63** using the

Friedel-Crafts acylation method (**Scheme 1.1**). This current study made use of 1,4-dihydroxyanthraquinone in the synthesis of several other anthraquinone derivatives with varied functionalities such as amines and heterocyclics. The compound synthesized were tested for their potency for antitrypanosomal, antiplasmodial and antibacterial activities.

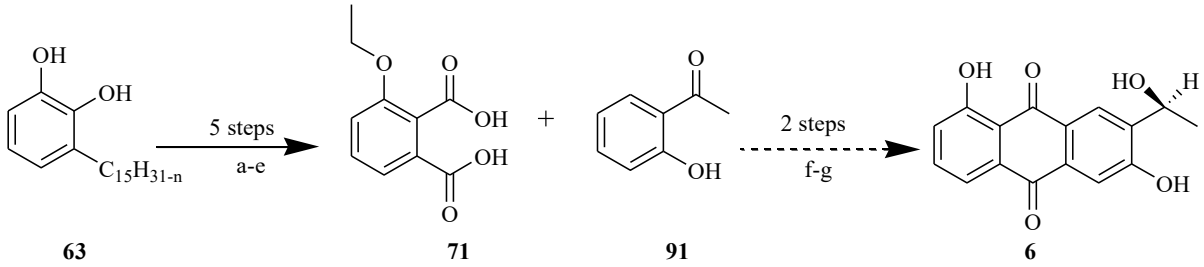

63 **71** **91** **6**

Scheme 1.1: Proposed route to 1,6-dihydroxy-7-((*S*)-1-hydroxyethyl)anthracene-9,10-dione 6 (a) DES, K_2CO_3, ACN, 24 h, 90 ℃ (b) Pd/C, methanol, 24 h (c) NBS, BPO, CCl_4, 3 h, 90 ℃ (d) DBU, 5 h, toluene, 110 ℃ (e) $FeCl_3.6H_2O$, aq. 70% TBHP, 36 h, NaOH, H_2O, 80 ℃ (f) NaCl/$AlCl_3$, 180-220 ℃, 1½ h (g) PPL, Buffer

1.4 Leishmaniasis and trypanosomiasis

Leishmaniasis and trypanosomiasis are a group of protozoan diseases of the genus *Leishmania* and *Trypanosoma* [21] [22]. The two genera belong to the family Trypanosomatidae of the order Kinetoplastida [22]. Trypanosomatid parasites affect both humans and animals such as cattle, sheep, and goats leading to poor productivity particularly in the areas of rural Africa [23] [24] [25].

The parasites responsible for human diseases are *Leishmania*, *Trypanosoma brucei* and *Trypanosoma cruzi* which are respectively the causative of leishmaniasis, African sleeping sickness and Chagas disease [26]. The parasites, *Leishmania* and *Trypanosoma* have unique mechanisms for circumventing the immune systems of their vertebrate hosts [25]. *Leishmania spp* are obligate intracellular parasites that invade and proliferate in monoclonal phagocytic cells, the blood cell responsible for vertebrate immune defence [27] [28]. All

Trypanosomes with exception of *Trypanosoma cruzi* on the other hand are extracellular parasites living in the bloodstream and cerebrospinal fluid [25] [29]

The WHO regards human African trypanosomiasis (HAT or sleeping sickness), Chagas disease (South American trypanosomiasis), and leishmaniasis as "Neglected Tropical Diseases" (NTDs) [30] [31]. It has been reported that none of the approved drugs for the treatment of trypanosomatid disease are satisfactory. The reason for this situation has been largely due to lack of funding, especially when the target group of the disease is the rural and poor in society, who cannot afford to fund the development of new treatments through payment for future drugs [31] [32].

Furthermore, all the currently available therapeutic drugs for these three conditions are largely ineffective and highly toxic: they include benznidazole and nifurtimox to treat Chagas diseases, paromomycin, miltefosine, amphotericin B, glucantine for treating leishmaniasis and eflornithine, pentamidine, and melarsoprol for treating HAT (**Figure 1.3**) [32].

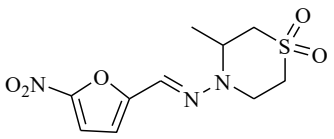

Nifurtimox **7**

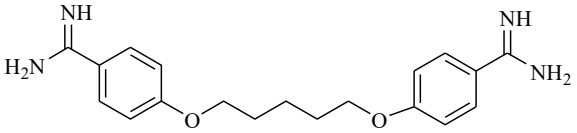

Pentamidine **8**

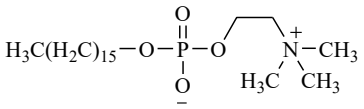

Miltefosine **9**

Figure 1.3: Some examples of approved drugs for the treatment of trypanosomatid diseases [31]

The need for new and alternative drugs is therefore quite clear. In addition to toxicity, some of the available drugs suffer pharmacodynamic and pharmacokinetic disadvantages such as poor solubility requiring complex routes of administration. To add insult to injury, the

emergence of drug resistance and high costs further limit their use in areas where these parasites are endemic [31] [32].

Trypanothione reductase (TR) is a genetically validated drug target enzyme of the unique trypanothione-based thiol metabolism of Trypanosomatidae (**Figure 1.4**) [33]. Trypanothione reductase is a key enzyme of the parasite antioxidant defence and does not occur in mammalian hosts [34].

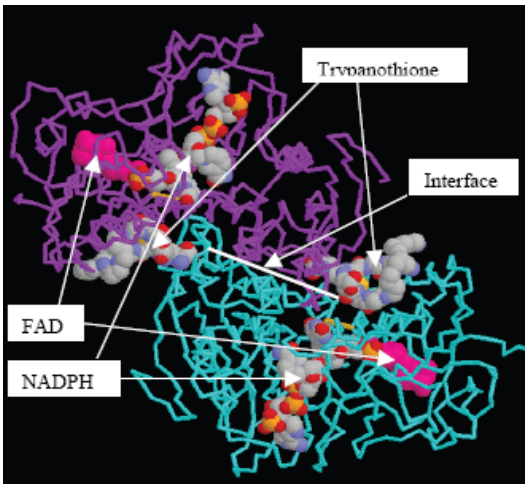

Figure 1.4: Structure of trypanothione reductase enzyme with FAD, NADPH and trypanothione bound [35]

TR is an essential enzyme in the catalysis of the NADPH –dependent reduction of trypanothione disulphide ($T[S]_2$) to dithiol trypanothione [bis(glutathio-nyl) spermidine, ($T[SH]_2$) (**Figure 1.5**) [36].

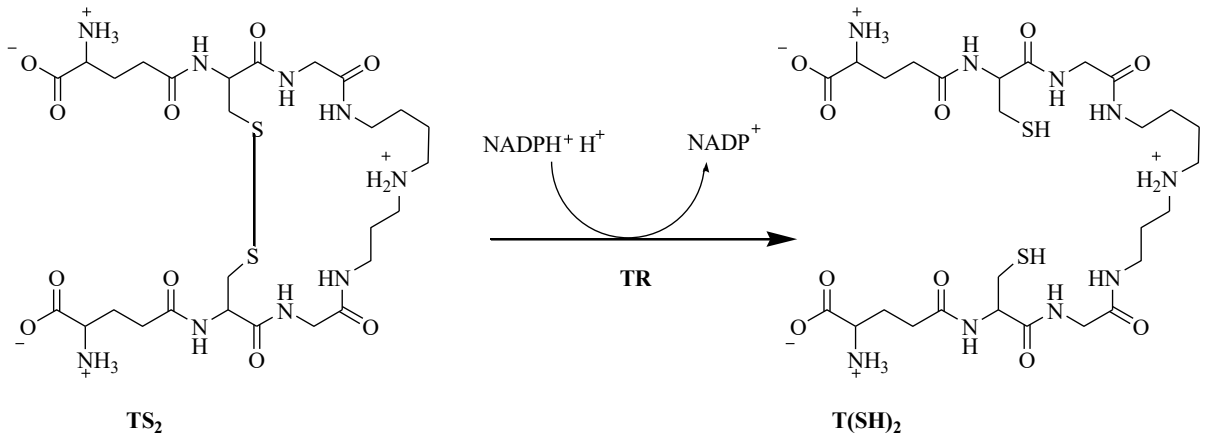

Figure 1.5: Reduction of trypanothione disulfide (TS_2) to the dithiol trypanothione ($T(SH)_2$) catalyzed by the enzyme TR

Genetic approaches have validated TR to be essential for the proliferation of *Leishmania* and *Trypanosoma* [36]. The inhibition of TR is one of the strategies towards developing drugs against leishmaniasis and trypanosomiasis [33] [36]. Trycyclic derivatives such as chlomipramine, chlorpromazine, and prochlorperazine were reported to be the potent trypanothione reductase inhibitor are considered as the leads for developing effective drugs against trypanosomiasis and Leishmaniasis [37] [38]. Anthraquinone core structure is tricyclic with a keto group either at 9 and 10, 1 and 4 and 1 and 2 (Figure 2.11); however none of these systems have been widely studied as both potential inhibitors of trypanothione reductase and trypanosomatid parasites.

The work of a medicinal chemist is to discover new libraries that can be used to combat infectious diseases [39]. Nature has always been providing fascinating insights and inspirations that can lead to the discovery of potential chemotherapeutic agents for the treatment of various diseases on our planet [40] [41]. Cashew nut shell liquid (CNSL), the by-product of the cashew industry has been proven to be one of the most versatile food wastes for use as low-cost starting materials in organic synthesis works [42].

To date, there are several chemical libraries of CNSL-derived hybrids that have been investigated for their potential anti-trypanosomal activity [42]. This successful result has given hope for the use of CNSL and its components in combating trypanosomiasis. This is particularly true in lower-income countries where often the cultivation of cashew coincides with endemic areas for trypanosomiasis [42] [43]. In this work derivatives of anacardic acid from CNSL and 1,4-dihydroxy anthraquinones were synthesized and screened against trypanosomiasis causing parasite. Furthermore, the *in-silico* molecular docking studies were conducted on the selected compound to determine their mode of interaction with TR and their drug-likeness.

1.5 Purpose of the study

The main objective of the study was to synthesize 1,4-dihydroxy-anthraquinone derivatives as potential anti-infective agents.

1.5.1 Specific objectives

The specific objectives were

i. to synthesize 4-ethoxyisobenzofuran-1,3-dione from anacardic acid

ii. to synthesize *(S)*-1,6-dihydroxy-7-(1-hydroxyethyl)anthracene-9,10-dione from 3-ethoxyphthalic acid

iii. to synthesize 1,4,5-trihydroxyanthraquinone from 4-ethoxyisobenzofuran-1,3-dione

iv. to synthesize hydroxyalkyl-1,4-dihydroxyanthraquinone derivatives from 1,4-dihydroxyanthraquinone

v. to carry out bioassay studies on each of the pure synthesized compounds

vi. to perform a docking study to elucidate the mode of interaction of anacardic acid derived structures and that of 1,4-dihydroxyanthraquinone with trypanothione

reductase enzyme; PDB Id: 6BU7

vii. to kinetically resolve the hydroxyalkylanthraquinones to enantiomerically pure alcohols

CHAPTER 2

LITERATURE REVIEW

2.1 Introduction to the chapter

This chapter describes the medicinal applications and biological properties of anthraquinones; several key methodologies developed to synthesize anthraquinones are outlined here. The chemistry of the components of cashew nut shell liquid and the therapeutic importance of heterocycles is also discussed in a detailed way.

2.2 Medicinal applications and biological activities of anthraquinones

Anthraquinones are secondary metabolites occurring in some plants, fungi, lichens, and insects [44] [45]. Besides being used as colorants, anthraquinone derivatives have been used for centuries for medical applications such as laxatives, antimicrobial and anti-inflammatory agents [46] [47].

Despite these useful medical applications only two biosynthetic pathways have been proposed; the polyketide pathway and the chorismate/δ-succinylbenzoic acid pathway [48]. The polyketide pathway leads to the "emodin" type of anthraquinones **10** (**Figure 2.1**) and have both rings substituted. The chorismate/δ-succinylbenzoic acid pathway leads to the alizarin type of anthraquinones **11** and has one of the rings un-substituted [48].

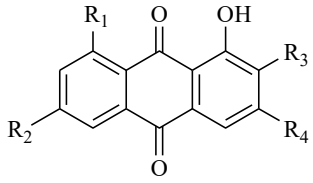

10 Emodin R_1 =OH, R_2 =CH_3, R_3 =H, R_4= OH

11 Alizarin R_1=R_2= R_4 =H R_3 =OH

Figure 2. 1: Structure of the emodin 10 and alizarin anthraquinones 11

The emodin type of anthraquinone **10** and its derivative have received considerable attention due to their broad-spectrum biological activities as such as antibacterial, anticancer, anti-

inflammatory, anti-diabetic, and anti-oxidative activities [49] [50]. However, research studies have indicated that the biological activities of the emodin-type anthraquinones are closely related to their chemical structure [51]. The presence of the hydroxyl, methyl, amino, and carbonyl groups displayed by the emodin type play a practical significance in their diverse biological activities [52].

The emodin-type molecules, as well as some of their derivatives, have been recently reported to display significant activity against malaria parasites [53]. The relatively high affinity of emodin with FIKK kinase has been the key factor for the enhanced antimalarial activity, making these anthraquinones (**Figure 2.1**) potential lead compounds for the development of antimalarial drugs targeting FIKK kinase [54].

Many natural anthraquinones from plants of the genus *Senna* occur as anthraquinone glycosides (anthraquinones linked to sugar molecules) (**Figure 2.2**) and; are the causative agents for the laxative activity [53] [55]. Laxatives are defined as the type of drugs that help a person empty their bowel. The laxative property of anthraquinones is explained by their ability to cause alteration in colonic absorption and secretion, resulting in fluid accumulation and consequently diarrhea [55]. This property allows the leaves from several *Senna* plants (*Cassia acutifolia* and *Cassia angustifolia*) to be used in commercial herbal teas for use as laxatives and also for slimming effects [56].

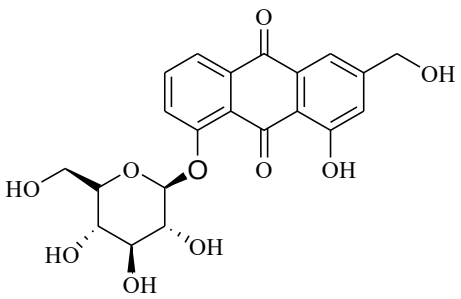

Aloe-emodine-8-O-*β*-D-glucopyranoside **12**

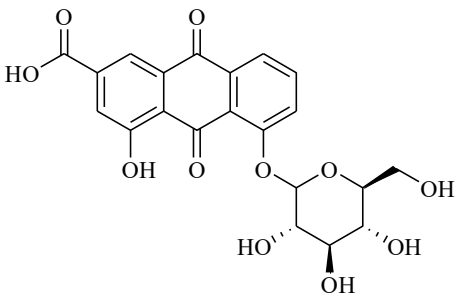

Rhein-8-O-*β*-D-glucopyranoside **13**

Figure 2. 2: Examples of anthraquinone derivatives in form of glycosides [56]

The anthraquinone moiety is an important constituent of the traditional Chinese medicine and has long been used in cancer treatment [57]. Several amino-substituted anthraquinones (**Figure 2.3**) have shown to display significant anti-proliferative activity against human/mammalian cancer cells with less toxicity to normal cells [58]. For example amino alkyl-functionalized anthraquinones such as mitoxantrone **14** and ametantrone **15** were developed in an attempt to increase therapeutic effectiveness and reduce toxicity by the anticancer drugs anthracyclines and anthraquinone during chemotherapy [59].

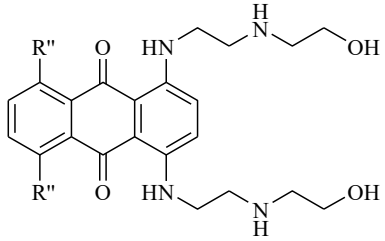

14 R" = OH Mitoxabtrone

15 R" = H Ametantrone

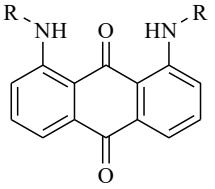

16 R = $CH_2CH_2CH_3$

Figure 2. 3: Chemical structure of the amino-substituted anthraquinones [59]

Because of this Sweidan and his co-workers in 2018 synthesized novel *N*1-anthraquinon-2-yl amidrazones of structures **17** and **18** (**Figure 2.4**) incorporating *N*-piperazines moieties [60]. The *in vitro* activity of **17** and **18** against MCF-7 breast cancer, K562 chronic myelogenous leukemia, and dermal fibroblasts cell lines gave good results which suggest the two structures to be promising potential anticancer drugs [60].

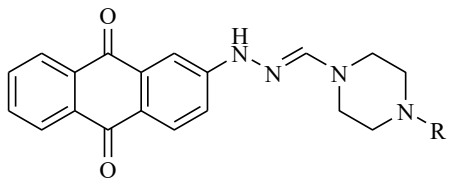

Novel amidrazones with their IC_{50} (µM)

Structure	MCF-7	K562	Fibroblast
17 R = H	20	2.1	2.2
18 R = CH_2CH_2OH	4.5	1.1	15

Figure 2. 4: The chemical structure of the novel N1-anthraquinon-2-yl amidrazone [60]

The mechanism of cytotoxicity of anthraquinones compounds and their derivatives is reported to be due to their ability to non-covalently binding to DNA duplex and therefore

interfering with the activity of DNA topoisomerase II [61]. Since topoisomerases regulate cellular processes such as replication and transcription by altering the topology of DNA; inhibition of the activity of topoisomerases has shown to be an effective strategy in cancer chemotherapy [62]. Ever since their discovery in 1971 DNA topoisomerases have been established as molecular targets for developing new anticancer agents with low toxicity [63]. Several other compounds such as camptothecins, indolocarbazoles, and indenoisoquinolines have been reported to be the human topoisomerases I (top I) inhibitors [64]. Gattinoni *et. al* 2007 discovered four types of topopyrones A-D **(19-22)** as inhibitors of topoisomerase I (**Figure 2.5)** which were isolated from the cultures of a fungus, *Phoma* sp, and from *Penicillium* sp [64].

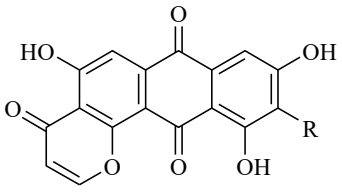

19 Topopyrone A R= Cl

20 Topopyrone C R= H

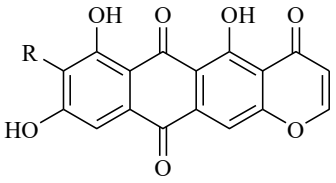

21 Topopyrone B R= Cl

22 Topopyrone D R = H

Figure 2. 5: Some natural topopyrones (19-22) [64]

The wide range biological properties of anthraquinone such as laxative, anti-inflammatory, antioxidant, antifungal, antimicrobial, antitumor, larvicidal, and many others, render them to be considered as a privileged scaffold in drug discovery [65] [66] .

Despite all of the efforts that have been made in understanding the chemistry and the biology of the anthraquinones in recent years, research studies on their structural-functional relationship, mode of action, and therapeutic potential are limited [67] [68] [69].

This is the reason making the synthesis of anthraquinone and its derivatives inevitable in the process of drug development. Nevertheless, the history of medicinal chemistry has indicated

the importance heterocyclic compounds for pharmaceuticals development. The section that follows discusses the application of heterocyclic compounds in drug development.

2.3 The therapeutic importance of heterocycles

Heterocyclic compounds are a class of organic compounds whose molecules contain one or more rings of atoms with at least one atom (the heteroatom) being an element other than carbon, most frequently oxygen, nitrogen, or sulphur [70]. Heterocycles find many applications in our daily lives as herbicides, photo stabilizers, dyes, sensitizers, flavoring agents, and agrochemicals [70] [71].

Human diseases like inflammation, tuberculosis, cancer, and diabetes have been treated with drugs containing heterocyclic scaffolds [72]. Many heterocyclic scaffolds particularly nitrogen heterocycles are reported to be a valuable source of therapeutic agents in the field medicinal chemistry [72]. Approximately 75% of drugs approved by the FDA and currently available in the market are nitrogen-containing heterocyclic moieties [72]. Compounds such as aryl imidazolium salts and aryl triazolium, aryl piperazines and piperadine, and aryl thiosemicarbazides are of considerable interest due to their useful biological and pharmacological activities especially antitumor activity [73] [74] [75]

Fused heterocyclic systems such as benzimidazole are reported to be good scaffolds present in many drugs that are in clinical application [76]. Benzimidazole systems and their derivatives possess a wide range of biological properties such as antibacterial, antifungal anthelmintic, and anti-inflammatory activity [76].

Compounds containing imidazolium and triazolium salts have received considerable attention among chemists because of their broad range of biological and pharmacological activity especially antitumor activity [77].

Recently, several novel -3-substituted fluorene–imidazolium salt **23** and **24** (**Figure 2.6**) derivatives were synthesized and were found to be active against human tumor cell lines [73].

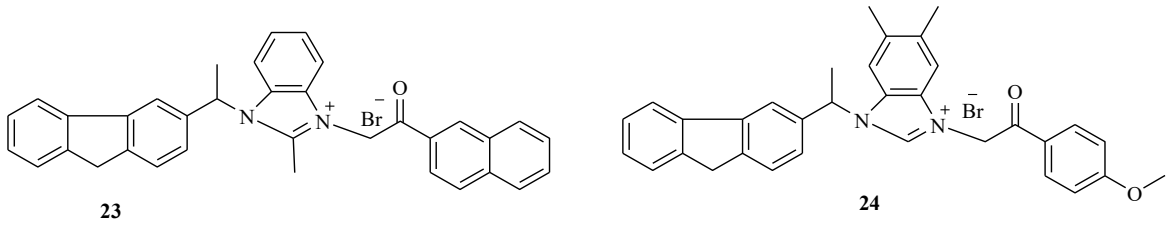

Figure 2. 6: Representative structures of fluorene derivatives and imidazolium salts [73]**.**

Several other studies have highlighted the applicability of the piperazine ring (**Figure 2.7**) as a good motif for the construction of pharmaceutically important drugs for the treatment of diseases like cancer, Alzheimer's disease, and fungal diseases [78] [79] [80].

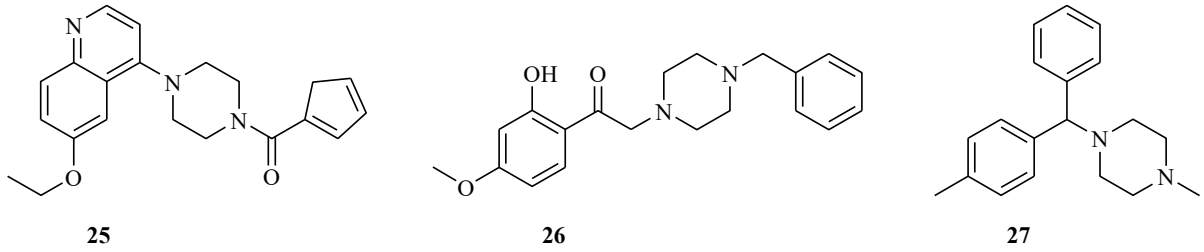

Figure 2.7: Representative bioactive piperazine containing compounds [74] [78]

Several morpholine (tetrahydro-1,4-oxazine) containing compounds are known to exhibit a wide range of biological activities such as analgesic, anti-inflammatory, antioxidant, anti-obesity, and anticancer activity [81]. In addition to this, the ring structure of morpholine has been reported to be an important pharmacophore present in many pharmaceutically active ingredients [82]. Drugs reported to be available on the market such as gefitinib **28**, phendimetrazine **29,** and puparlisib **30** contain a morpholine ring (**Figure 2.8**) [82].

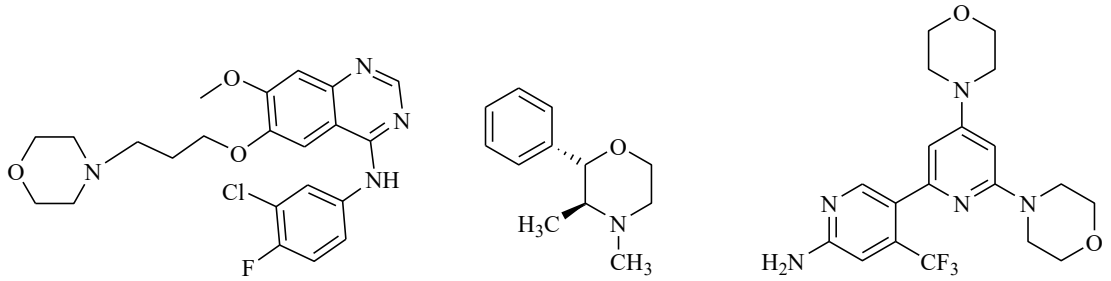

28 **29** **30**

Figure 2. 8: Representative bioactive morpholine containing drugs [82]

On the other hand, heterocyclic frameworks containing thiazole analogues have emerged to be a new topic in modern drug discovery [71]. Modern research has reported on the diverse biological activities of thiazole derivatives such as antibacterial, antifungal, analgesic, antidiabetic, antimicrobial, anticancer, antihypertensive, and anti-inflammatory. This has aroused the interest of many researchers to design studies to synthesize molecules that contain more than one thiazole moiety [71] [83].

2-Arylbenzothiazoles motif has gained the attention of chemists in being used as a synthetic building block for the construction of molecules with anticancer, antitumor, anti-hepatitis C virus, antioxidant, and antiglutamic acid [84]. Recently a series of antitumor aromatic benzothiazole molecules **31-33** (**Figure 2.9**) were designed and synthesized [84] [85].

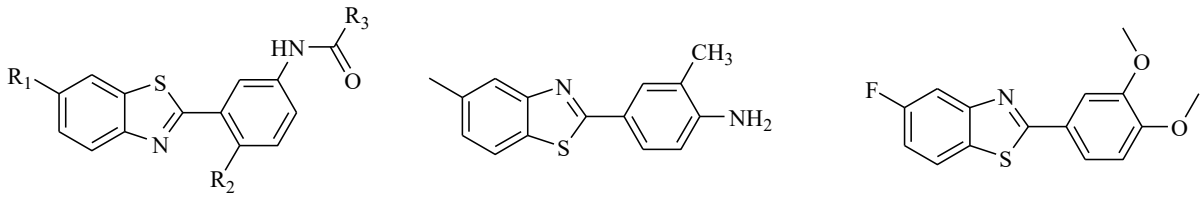

31 **32** **33**

Figure 2. 9: Representative bioactive 2-arylbenzothiazole compounds [84]

Several nitrogen-containing compounds known as thiosemicarbazone (TSC) (**Figure 2.10**) constitute a group of pharmaceutically important scaffolds with varied bioactivities particularly as antiparasitic, antibacterial, and antitumoral agents [86] [87].

Thiosemicarbazone is the Schiff base derivatives of thiosemicarbazide, obtained by condensation of the thiosemicarbazide with aldehydes or ketones [88]. The biological activities of thiosemicarbazone depend on the parent aldehyde or ketone [89]. This property has aroused the interest of medicinal chemists to design different studies on their synthesis. To date, several thiosemicarbazone derivatives have been successfully synthesized such as **34**, **35** and **36** and evaluated for their anticancer [90], antibacterial [91], and antimicrobial activities [92].

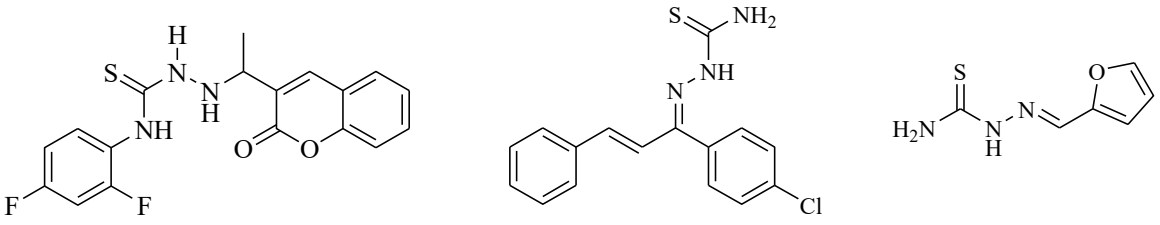

34 **35** **36**

Figure 2.10: Some biologically active thiosemicarbazones derivatives [88] [90] [93]

Therefore, considering the interesting biological activities of imidazole, triazole, piperazine, and thiosemicarbazide motifs in the drug discovery process, it was desirable to incorporate these compounds into the anthraquinone moiety for improved bioactivity. Moreover, Marschalk reaction has evolved to be a plausible mechanism for functional group modification of the anthraquinone structure which can lead to the discovery novel compounds of that can be used as anti-infective agents. Nevertheless, there is no sufficient information in the database on these compounds being successfully synthesized and tested.

2.4 The synthesis of anthraquinones

Theoretically, there are three isomeric forms of anthraquinones (anthracenequinones) (**Figure 2.11**) namely, 1,2-anthraquinone **37**, 1,4-anthraquinone **38,** and 9,10-anthraquinones **39** that could exist [94]. In terms of diversity and application in industrial sectors, the 9,10-anthraquinones followed by the 1,4-anthraquinones are reported to be the major groups [95]. The diversity, chemistry, and biological activities of the anthra-9,10-quinones render them to be an important class, covered by several extensive reviews [96]. The section below discusses several methods used to prepare anthra-9,10-quinones.

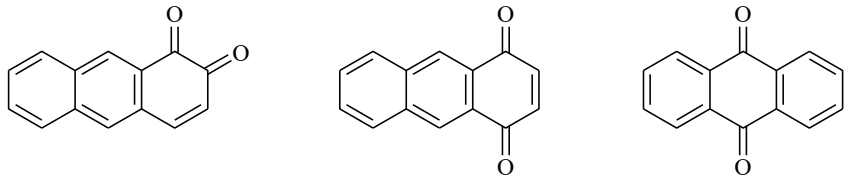

37 **38** **39**

Figure 2.11: The three isomeric forms of anthraquinones

2.4.1 Friedel–Crafts reactions

The Friedel–Crafts reaction plays a major role in the synthesis of anthra-9,10-quinones, particularly in their industrial production [96]. The Friedel-Crafts reaction has been used in the preparation of various anthraquinones and it is a one-pot reaction of phthalic acid/ anhydride and some benzene derivatives (**Scheme 2.1**) catalyzed, by a eutectic mixture of aluminium trichloride and sodium chloride at elevated temperature [97]. Although several other catalysts, such as $AlCl_3/H_2SO_4$, montmorillonite clay, and $AlCl_3$/NaCl melt, montmorillonite K10 clay, and thin-layer chromatography (TLC) grade silica gel have been employed in these transformations there is still the need for simpler methods [98]. This is due to the disadvantages such as low yields of products and harsh reaction conditions posed by this method [97] [98]. For the unsymmetrical compounds, the use of this method is limited

due to a Hayashi rearrangement and hence leading to mixtures of regioisomers that are difficult to separate [99] [100].

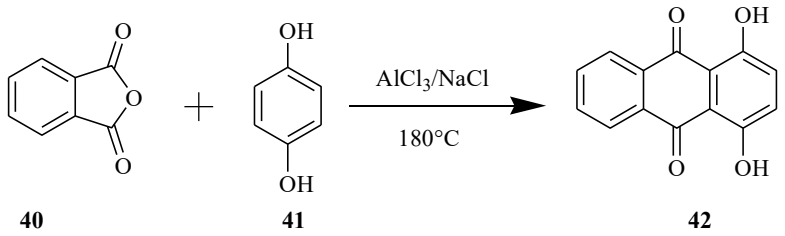

40 **41** **42**

Scheme 2. 1: Friedel-Crafts acylation between phthalic anhydride and benzene-1,4-diol [97]

2.4.2 Diels–Alder reactions, [4+2]-cycloaddition reaction (DA)

The Diels–Alder reaction or [4+2] cycloaddition reaction serves as a powerful tool for the introduction of complexity in chemical structures, and hence it is an important method for the synthesis of many natural products [101][102]. Important carbocyclic scaffolds such as hydroanthraquinones which are building blocks of a large number of drugs and natural products are one of the typical products of DA cycloadditions with activated napthoquinone [101][103]

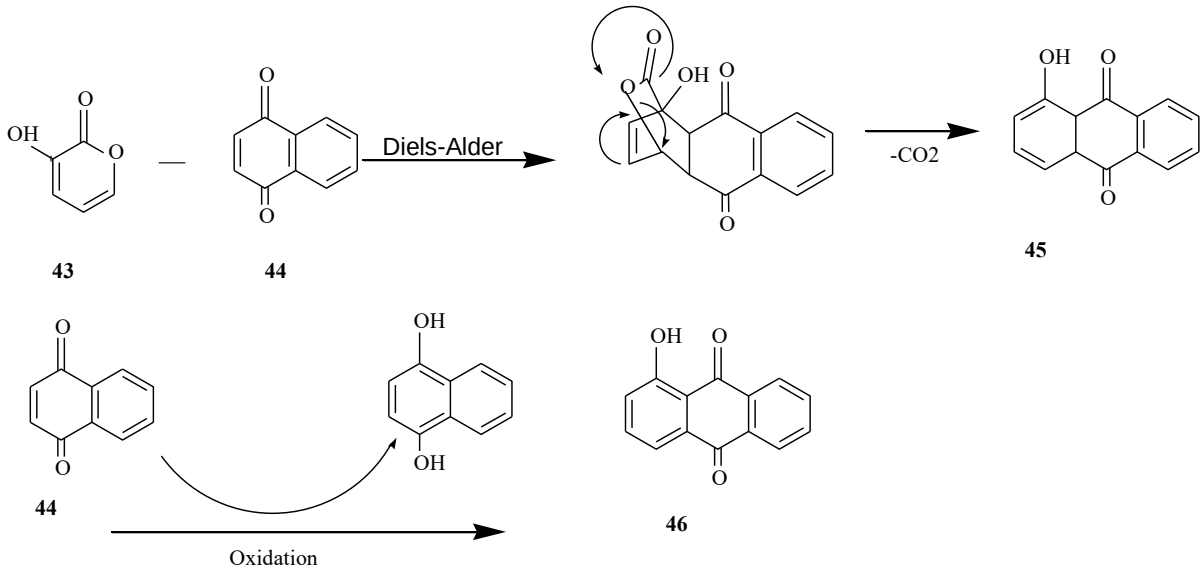

Scheme 2. 2: Mechanism of reaction of a Diels-Alder reaction [104]

One interesting example of Diels-Alder is the reaction of 3-hydroxy-2-pyrone **43** 1,4-naphthoquinone **44** to form 1-hydroxyanthraquinone **45** (**Scheme 2.2**)**.** The mechanism of the

reaction first involves a base-catalyzed Diels–Alder reaction of **43** and **44**, followed by decarboxylation form dihydroanthraquinone **45**, then oxidation of **45** by **44** afford 1-hydroxyanthraquinone **46** [104]. From an experimental point of view, reports have shown that the Diel-Alder reaction procedeeds smoothly with easy operational procedures [104] [105]. The Diels-alder reaction is the core approach in the total synthesis of many potent anthraquinones such as kwanzoquinone C and related natural products [105] [106].

2.4.3 Organocatalyzed [4 + 2] benzannulation

A recently reported, novel and efficient method for the synthesis of anthraquinone and tetracenedione derivatives uses L-proline catalyzed [4+2] cycloaddition of in situ generated azadiene from α,β-unsaturated aldehydes and 1,4-naphthoquinones or 1,4-anthracenedione the presence of organocatalysts (**Scheme 2.3**) [102].

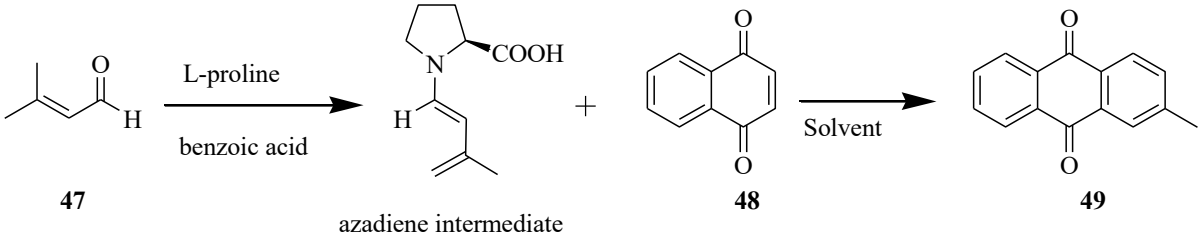

Scheme 2. 3: Synthesis of 2-methylanthracene-9,10-dione 49 by the 4＋2 cycloaddition reaction [102]

2.4.4 Ring-closing metathesis

The ring-closing metathesis (RCM) has been reported to be a general and straightforward synthetic design towards naturally occurring anthraquinones [1]. An example, shown below involves the diallylation of 1,4-naphthoquinones (**Scheme 2.4**), followed by RCM using Grubbs' first-generation catalyst and subsequent aromatization to afford the desired anthraquinones in a very efficient and elegant way with regio-control of substituent on the one ring [1].

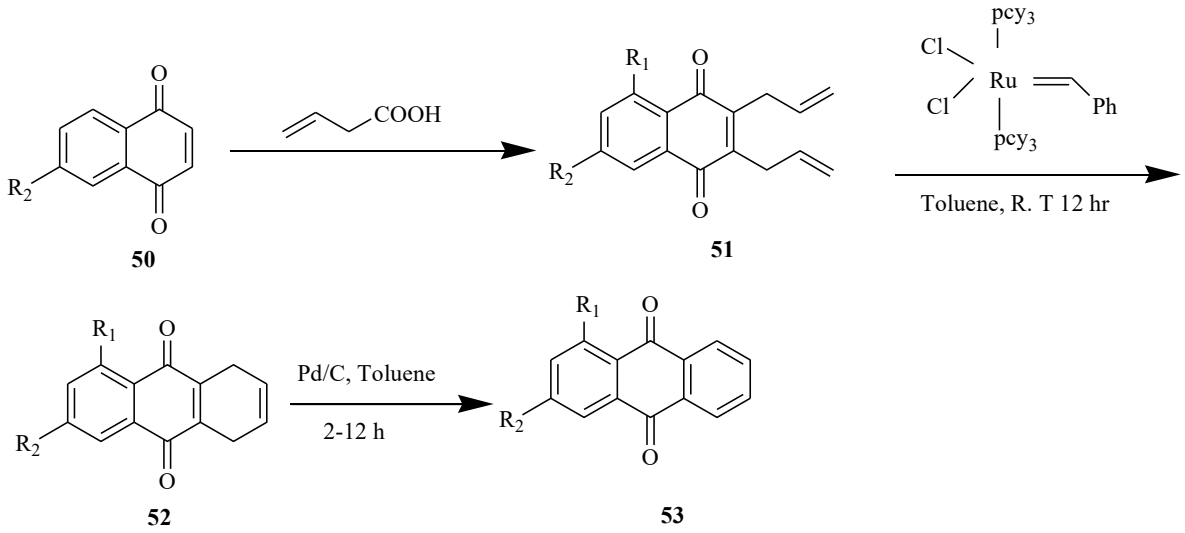

Scheme 2. 4: Synthesis of anthraquinone by ring closing metathesis [1]

2.4.5 Anionic condensation reactions

The Hauser annulation is a general, powerful, and regiospecific method that has been successfully applied to the total synthesis of quinonoid natural products [100]. Operationally the Hauser Kraus annulation involves the one-pot reaction of isobenzofuranones with *p*-benzoquinones as a Michael acceptor (**Scheme 2.5**) in the presence of LiO*t*Bu [100].

The reaction is viewed as a domino reaction sequence consisting of initial lateral deprotonation, Michael addition, followed by Dieckmann/Claisen cyclization and elimination of the phenyl sulfinate ion [100]. The annulation has been reported to work better when 3-cyanoisobenzofuran-1(3H)-ones 1 are used in place of sulfonylisobenzofuran-1(3H)-ones [100].

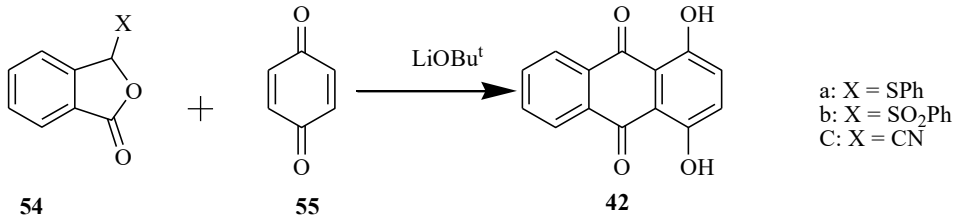

Scheme 2. 5: An example Hauser Kraus annulation reaction [100]

The use anionic of condensation reaction was reported by Roy and co-workers in 2016 in the synthesis of anthraquinone **58** (**Scheme 2.6**) which is the main intermediate towards the synthesis of proisocrinin **60**.

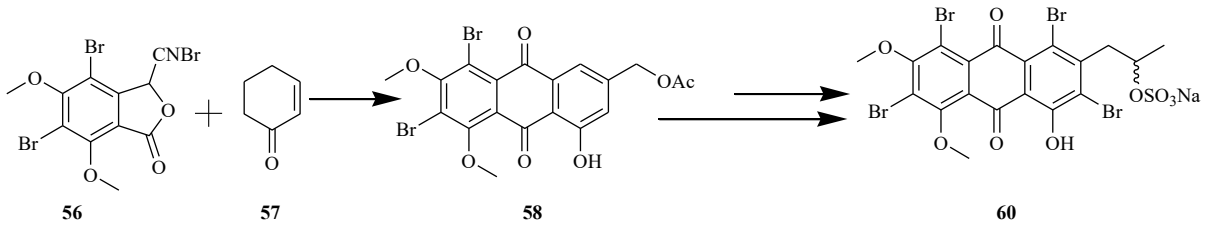

56 57 58 60

Scheme 2. 6: The application of Hauser Kraus annulation [107]

2.5 The application of Marschalk reaction

Marschalk reaction is an old reaction reported in 1936 by Marschalk as a powerful means of adding carbon atoms and functionalized side-chains to certain highly deactivated anthraquinones [108]. The reaction reports on the introduction of an alkyl group into the 2-position of 1-amino- or l-hydroxyanthraquinones, and into the 1-position in the case of 2-hydroxyanthraquinones. The reaction proceeds by the action of an aldehyde on amino- or hydroxy-anthraquinone under basic conditions [109]. However, the reaction was later employed in the synthesis of anthracycline anticancer drugs [108]. Krohn and Priyono in 1984 reported the synthesis of anthracyclinones, feudomycinones and rhodomycinones by an intramolecular Marschalk reaction [110]. The traditional form of Marschalk reaction **(Scheme 2.7)** is time-consuming, as it involves many steps to accomplish to arrive at the desired product. Recent studies have reported simplified Marschalk reactions under cold conditions could produce better results [12].

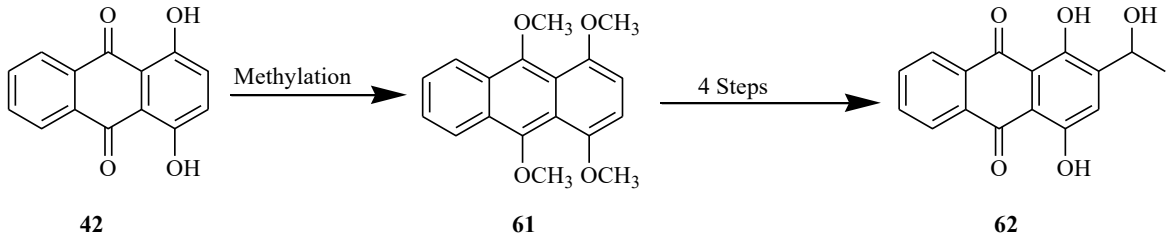

42 61 62

Scheme 2.7: Traditional Marschalk strategy for the elaboration of 1,4-dihydroxyanthraquinone [12]

2.6 A modified Marschalk reaction

The modified Marschalk reaction is a method that has emerged recently as a direct means to derivative and functionalize highly deactivated anthraquinones [12]. The Marschalk reaction is a C–C bond-forming reaction which can generate the 2-alkylated anthraquinones via sodium dithionite reduction of 1-hydroxyanthraquinones to its leuco-form under basic conditions followed by condensation with aldehydes [111].

The mechanism of this reaction as proposed by Zhao *et.al* [12] involves the conversion of anthraquinone into its leuco form **I** in the presence of NaOH and $Na_2S_2O_4$ (**Scheme 2.8**). This step is followed by the condensation of **I** with the aldehyde to afford adduct **II**, which further isomerizes to afford the hydroxyalkyated anthrahydroquinone anion **III**. Upon oxidation, at low temperature, the desired hydroxyalkyated product **IV** is generated.

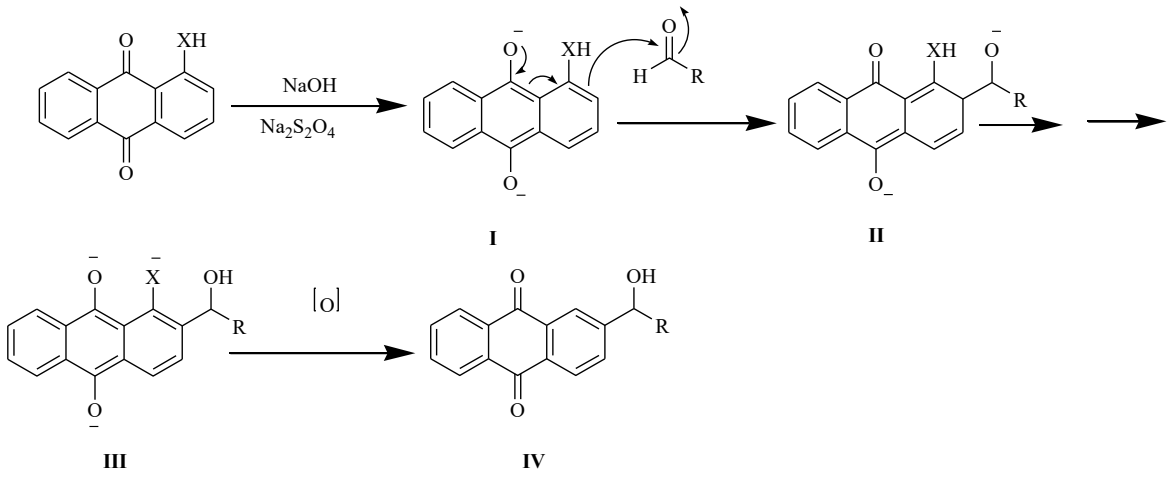

Scheme 2. 8: The modified Marschalk reaction mechanism

Unlike the traditional strategy which requires protection and deprotection for the introduction of the 2-hydroxyalkyl group to the 1-hydroxyanthraquinones, the modified Marschalk method offers a simple method, to introduce the hydroxyl alkyl group to the 1-hydroxy anthraquinone.

As based on the usefulness of Marschalk reaction in the medicinal application of anthraquinones, it was important to use 1,4-dihydroxyanthraquinones to synthesize anthraquinones with varied functional groups. The hydroxyalkyanthraquinone was linked to a variety of nitrogen-containing compounds and were tested for biological activities.

2.7 The chemistry of cashew nut shell liquid

The cashew nut shell liquid is a by-product of the cashew agribusiness that has in recent days been used green in chemistry as a renewable material [112]. The CNSL is a natural source for unique unsaturated long-chain phenols that are considered as an abundant low-cost starting material in organic synthesis [113].

CNSL can be natural or technical depending on the methods of extraction such as solvent extraction or dry heat extraction [113]. Natural CNSL (**Figure 2.12**) contains a mixture anacardic acid (60–65%), cardol (15–20%), cardanol (10%) and traces of methyl cardol whilst technical CNSL obtained by roasting shells contains mainly cardanol (60–65%), cardol (15–20%), polymeric material (10%) and with traces of methyl cardol [114].

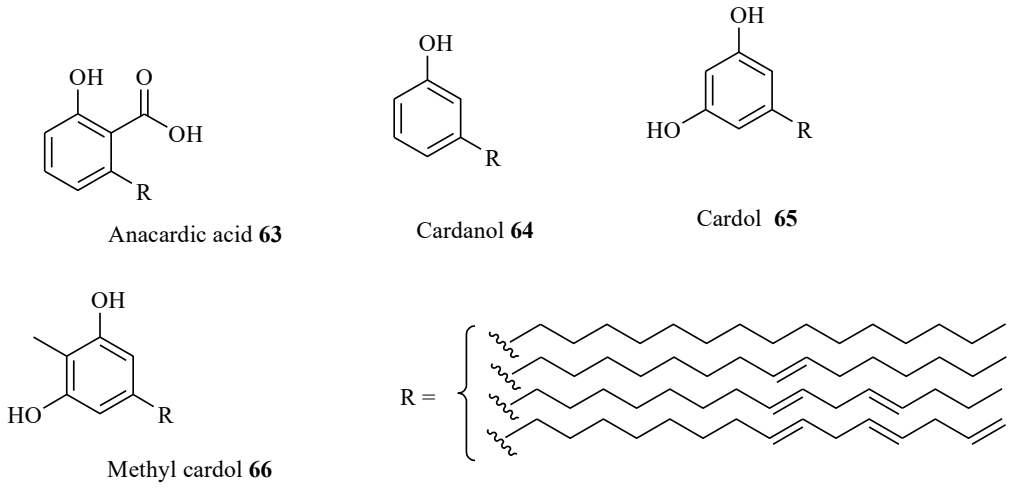

Figure 2. 12: The components of cashew nut shell liquid

The presence of an aromatic nucleus and several functional groups on the components of CNSL render them to be of use in a variety of fine chemicals industries [115] [116].

One of the most critical applications of CNSL is the production of resins and polymeric derivatives which are used as exchange resins, anticorrosive paints, waterproof materials, flame retardants, coating of surfaces, friction materials, and rubber modifiers [117] .

Past research has indicated various biological properties of CNSL itself such as antibacterial, anti-inflammatory, and antioxidant activity, enzymatic inhibition, and anti-proliferative activity [116].

On the other hand, anacardic acid (AA) the major phenolic constituent of cashew nut shell liquid has received great attention, not only due to diverse biological activities but due to its usefulness in the synthesis of various advanced intermediates [118] [119] [120]. Anacardic acid has been renowned as a Brazilian natural substance with several therapeutic uses such as antimicrobial, antioxidant, anticancer, anti-inflammatory, antibacterial, antitrypanosomal, antiviral, and many others [118] [121] [122]. Recent studies have reported the application of CNSL in the nanodispersion technology in formulations of nanoemulsions that have antitumor efficacy for breast cancer [123].

The applicability of the cashew nut shell liquid is the ultimate source of the current research among chemists. The wide biological activities of the CNSL prove it to be the best candidate for use in our daily life in food, dyes, and the field of medicine [117].

Based on this background, it was considered necessary to explore ways of adding value to the components of cashew nut shell liquid (CNSL), which to the most part forms the major type of waste in cashew nut processing industries. The abundance of anacardic acid, its chemical structure, and functionalities are key features for its use in our current research

As explained earlier the chiral natural anthraquinone **5** (**Figure 1.2**) was isolated from the marine fungus *Negrospora spp* [18]. However, it was reported that the biological activities of compound **5** were not tested because it was obtained in minute quantities.

Since natural products can form the basis for the discovery of drugs of pharmaceutical importance. It was necessary to use compound **5** to synthesize its analogous compound **6** with the same equivalent features. Accordingly, a synthetic strategy that would utilize anacardic acid **63** (**Figure 2.13**)**,** a constituent of CNSL, to prepare a phthalic anhydride derivative was designed in such a manner that could be coupled with a benzene derivative to generate an anthraquinone moiety.

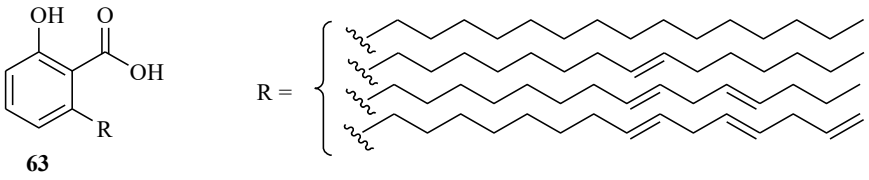

63

Figure 2.13: Anacardic acid 63 as a mixture of the saturated, monoene, diene, and triene side chain

Thus, this thesis aimed at synthesizing anthraquinone **6** (**Figure 1.2**)**,** an analogue of the natural anthraquinone **5**, using Friedel-Crafts acylation of a benzene derivative and a substituted phthalic anhydride derived from anacardic acid **63** (**Figure 2.13**).

The preliminary results on the synthesis of an analogue of a chiral anthraquinone **6** were not promising due to the lack of symmetry of 3-ethoxyphthalic acid **71** leading to the Hayashi rearrangement. This prompted the use of other methods that would avoid the Hayashi rearrangements. A thorough literature search indicated the use of 1,4-dihydroxyanthraquinone as a synthon for the synthesis of a variety of anticancer drugs. Thus, it was necessary to use the 1, 4-dihydroxyanthraquinone and to derivative into compounds with varied functionalities and to test them for antibacterial, antitrypanosomal, and for antiplasmodial activity.

2.8 Graphical representation

Anacardic acid **63** isolated from cashew agro-waste was synthetically transformed to 1,4,5-trihydroxyanthraquinone (**Scheme 2.9**). Modified Marschalk reaction was used to the hydroxyalkyl group to the 1,4-dihydroxyanthraquinone **42** (**Scheme 2.10**). The resulting hydroxyaryl anthraquinone was chlorinated with thionyl chloride, and further reacted with various amines (**Scheme 2.11**). On the other hand, the hydroxy aryl anthraquinone **73** was oxidized to a carbonyl and then reacted with thiosemicarbazide (**Scheme 2.10**).

Studies on the ester formation were done first with the aliphatic hydroxyanthraquinone **62** which was reacted with saturated anacardic acid (**Scheme 2.12**). This step is the starting point towards the racemic resolution of the prepared alcohols.

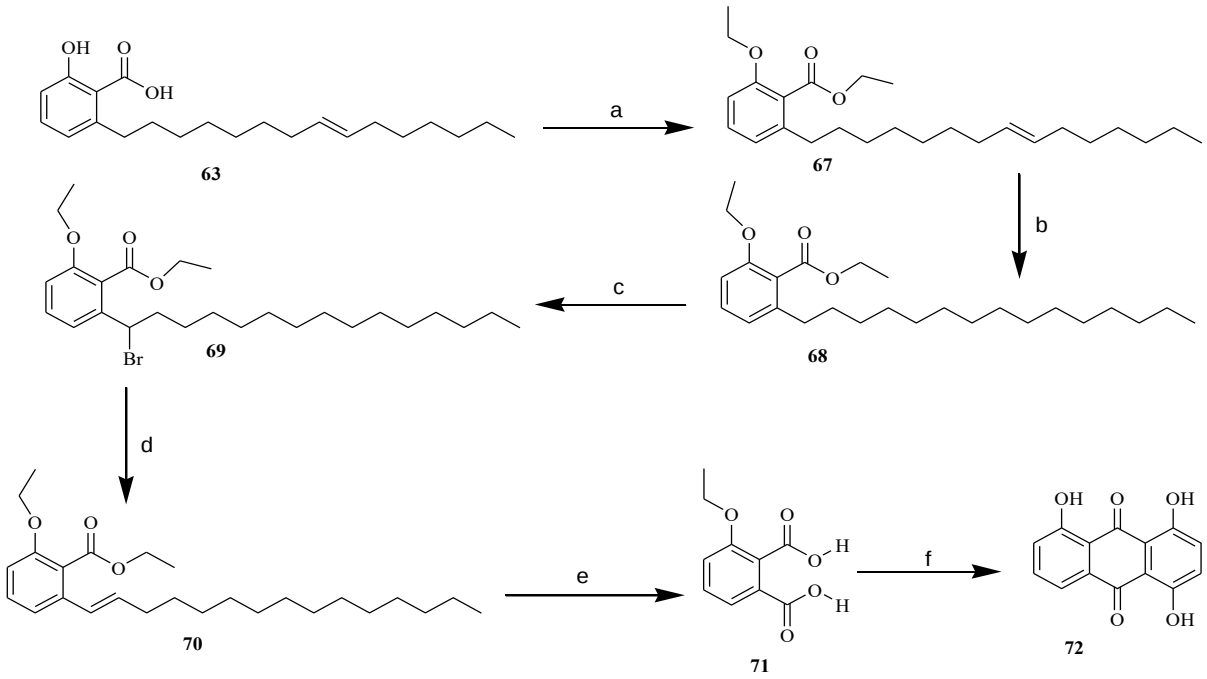

Scheme 2. 9: Schematic synthetic transformation of anacardic acid to 1,4,5-trihydroxy anthraquinone 72 (a) DES, K_2CO_3, ACN, 24 h, 90 ℃ (b) Pd/C, methanol, 24 h (c) NBS, BPO, CCl_4, 3 h, 90 ℃ (d) DBU, 5 h, toluene, 110 ℃ (e) $FeCl_3.6H_2O$, aq. 70% TBHP, 36 h, NaOH, H_2O, 80 ℃ (f) NaCl/$AlCl_3$, benzene 1,4-diol, 180-220 ℃, 1½ h

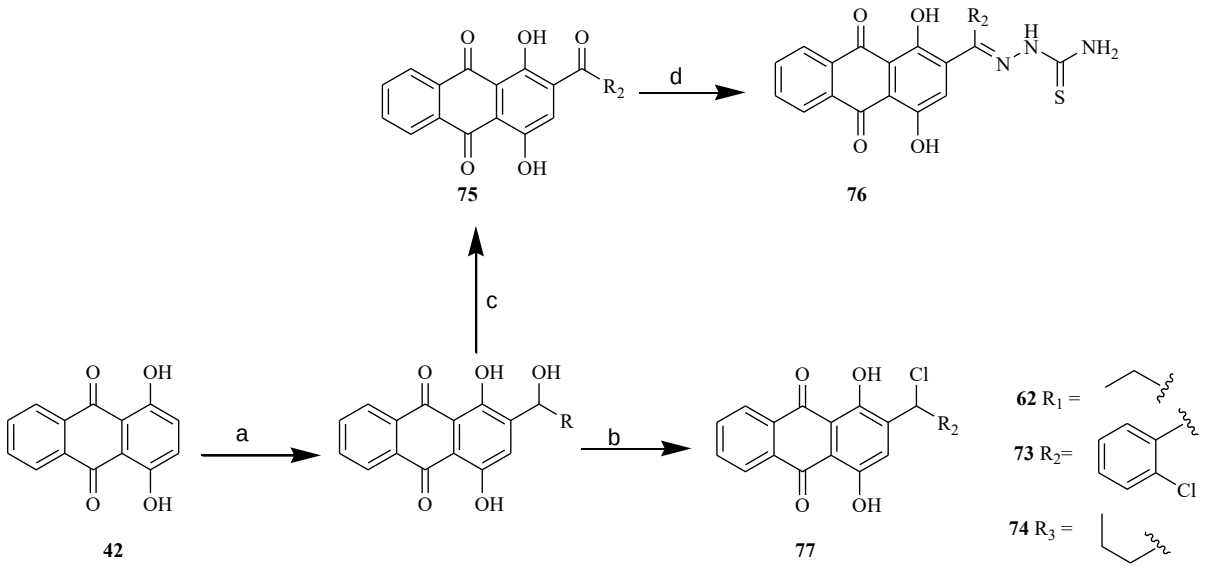

Scheme 2. 10: Alkylation of 1,4-dihydroxyanthraquinone 42 (a) NaOH, $Na_2S_2O_4$, 0 ℃, N_2, (acetaldehyde or propionaldehyde or 2-chlorobenzaldehyde) (b) $SOCl_2$, 50 ℃ (c) Dess Martin reagent/DCM (d) thiosemicarbazide, methanol, 90 ℃

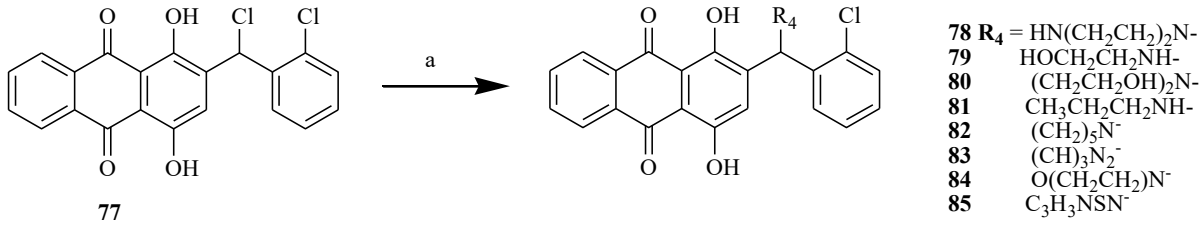

Scheme 2. 11: Synthesis of anthraquinone amine derivatives (78-85) (a) amines/DCM

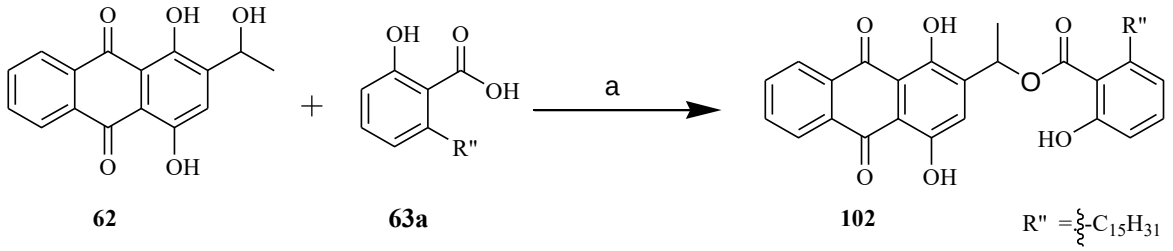

Scheme 2. 12: Esterification of 1, 4-dihydroxy-2-(1-hydroxyethyl)anthracene-9,10-dione 62 with anacardic acid (a) DCC/DMAP, dichloromethane, rt

CHAPTER 3

EXPERIMENTAL PROCEDURES

3.1 Introduction to the chapter

This chapter describes the detailed procedures that were used in the synthesis, purification, and characterization of the compounds.

3.2 General procedures

Raw cashew nuts were obtained from small-scale farmers in Dar es Salaam (Tanzania). All other chemicals and reagents were purchased from Sigma-Aldrich Company limited. Reactions were carried out in clean oven-dried glassware. All air or moisture-sensitive reactions were carried under a nitrogen or argon atmosphere. All solvents used unless otherwise specified were distilled and dried over molecular sieves. Acetaldehyde was distilled before use. Methanol was purified by adding a significant amount of CaH_2 letting it stand for 24 hours, distilling and drying over molecular sieves. Reactions were monitored by thin-layer chromatography (TLC) of type silica-gel 60 F254 using UV light as a visualizing agent. Products were purified using Silica gel 60Å, 70-230 mesh, 63-200 μm. Melting points were measured by using a hot-stage melting point apparatus and are reported as uncorrected.

^{1}H-NMR and ^{13}C-NMR spectra were recorded on Bruker Nuclear Magnetic Resonance spectrometers (300 MHz, 400 MHz and 600 MHz, ^{1}H-NMR chemical shifts (δ_H) and ^{13}C-NMR chemical shifts (δ_C) are recorded in parts per million (ppm) downfield from trimethylsilane (TMS) and coupling constants (J) are quoted in Hertz (Hz). Abbreviations for NMR data are s (singlet), br (broad), d (doublet), t (triplet), q (quartet), quin (quintet) and sxt (sextet) and m ((multiplet)

^{1}H-NMR and ^{13}C-NMR spectra were assigned with the aid of HSQC, HMBC, and DEPT 135 NMR techniques. Infrared (IR) spectra were recorded on a Perkin Elmer spectrum 100 FT-IR

spectrometer and mass spectra were recorded on a Bruker qToF Compact LC MS. Raw mass spectrometry data were processed using MZmine software (version 2.38).

Antimicrobial assays were performed by two organizations the AMR Hub at Rhodes University (RU) and the H3D in Cape Town. Trypanosoma assay and malaria assay were performed by the Rhodes University Centre for Chemical and Bio-medicinal Research.

3.3 Extraction of cashew nut shell liquid

Dry cashew nut shells (1000.00 g) contained in a closed bottle were soaked in methanol for 5 days and after filtration and evaporation of solvents yielded 270.00 g of cashew nut shell liquid (CNSL)

3.3.1 Isolation and purification of anacardic acid

CNSL (100.00 g) was dissolved in 5% aqueous methanol (600.00 mL) and calcium hydroxide (50.00 g) was added in portions under stirring. Afterward, the temperature was raised to 50 ℃ and stirring was maintained for 3 h. The reaction mixture was filtered under Buchner funnel and washed with (200.00 mL) methanol to yield 110.00 g of calcium anacardate

To a powdered calcium anacardate, 40.00 g dissolved in 160.00 mL distilled water, was added 21. 80 mL of 11M HCl and the resulting mixture stirred for 1 h. The reaction mixture was extracted with ethyl acetate, the organic layer was washed with water and dried over anhydrous Na_2SO_4. The crude product was then chromatographed over silica gel using 10% methanol in dichloromethane yielding 23.18 g of anacardic acid **63** as a dark brown liquid which was used directly as the starting material to synthesize the 1,4,5-trihydroxyanthraquinone (**Scheme 2.9**)

3.4 Synthesis of (*E*)-ethyl 2-ethoxy-6-(pentadec-1-en-1-yl)benzoate from (*E*)-2-hydroxy-6-(pentadec-8-en-1-yl) benzoic acid

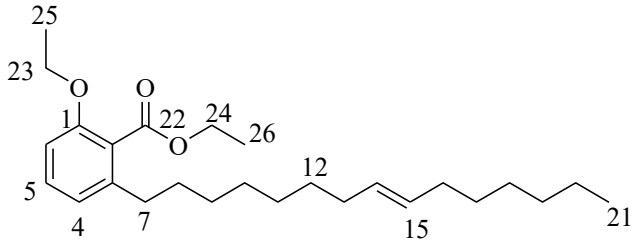

67

A solution of anacardic acid **63** (19.48 g, 0.06 mol) in acetonitrile (150 mL) was added (39.22 g, 0.28 mol) K_2CO_3 and diethyl sulphate (35.00 g, 0.23 mol). The content was heated to reflux at 90 ℃ for 24 hrs. The reaction mixture was cooled to room temperature, filtered and the filtrate concentrated, re-dissolved in ethyl acetate, and washed with water (2 × 200 mL). The organic layer obtained was dried over $MgSO_4$, filtered and the solvent evaporated in vacuo. The resultant crude product was subjected to column chromatography using silica gel (10% ethyl acetate in petroleum ether) yielding ester **67** (14.90 g, 66%) as a reddish-yellow liquid, FTIR υmax(ATR)/cm-1 2900-2844 (O-H) carboxylic, 1730 (C=O); ^{1}H NMR (300 MHz, $CDCl_3$): δ_H 0.89 (3H, m, CH_3), 1.30 (10H, m, CH_2), 1.37 (6H, td, J = 7.0, 3.2 Hz, $2CH_3$), 1.52 (2H, m, CH_2), 1.99 (2H, m, CH_2), 2.63 (2H, m, CH_2), 2.84 (2H, m, CH_2), 4.04 (2H, q, J = 6.90 Hz, OCH_2), 4.39 (2H, q, J = 7.10 Hz, OCH_2), 5.34 (2H, m, =CH_2), 6.73 (d, J = 8.3 Hz, 1H), 6.79 (d, J = 7.7 Hz, 1H) and 7.21 (1H, t, J = 8.00 Hz, H5). ^{13}C-NMR (75 MHz, $CDCl_3$): δ_C 13.3, 13.7, 24.5, 26.2, 27.9, 28.2, 28.3, 28.4, 28.5, 28.7, 30.2, 30.6, 30.7, 32.4, 59.9, 63.2, 108.4, 120.3, 123.1, 126.6, 128.3, 128.9, 135.8, 154.6 (C1) and 167.5 (C22).

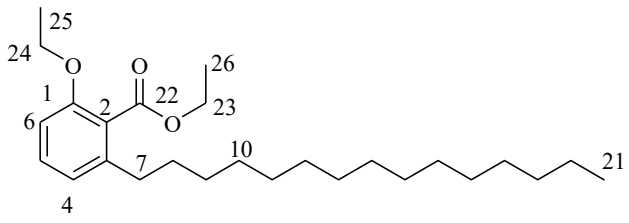

68

To a two neck 100 mL round-bottomed flask a solution of ester **67** (1.27 g, 3.42 mmol) in 40 mL degassed methanol was added 0.13 g of 10% palladium on carbon (w/w). The two necks were well fitted with a rubber septum and hydrogen gas filled in two balloons was allowed to enter the solution with stirring for 24 h. After the completion of the reaction the mixture was filtered over a Celite bed, the solvent evaporated to yield the saturated compound **68** as a light-yellow liquid (1.22 g, 96 %), ^{1}H NMR (300 MHz, $CDCl_3$): δ_H 0.88 (3H, t, *J* = 6.7 Hz, H21), 1.26 (30H, m, (H9-H20), H25 and H26), 1.57 (2H, m, H8), 2.55 (2H, t, H7), 4.03 (2H, q, *J* = 7.0 Hz, H24), 4.39 (2H, q, *J* = 7.1 Hz, H23), 6.73 (1H, d, *J* = 8.3 Hz, H6), 6.79 (1H, d, *J* = 7.7 Hz, H4) and 7.22 (1H, t, *J* = 8.0 Hz, H5). δ_C ^{13}C NMR (75 MHz, $CDCl_3$): δ_C 14.15 (21), 14.38 (25), 14.68 (C26), 22.70 (C20), 29.39 - 29.71 (C9-C18), 31.27 (C19), 31.95 (C8), 33.47 (C7), 60.82 (C23), 63.61 (C24), 109.83 (C6), 121.42 (C4), 124.21 (C2), 130.16 (C5), 141.00 (C3), 155.68 (C1) and 168.32 (C22).

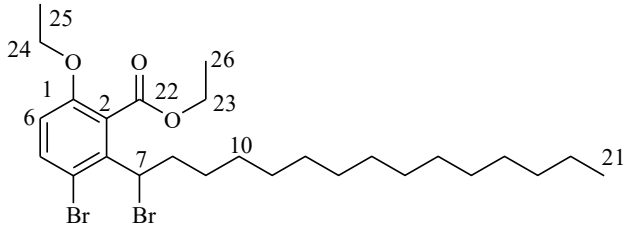

69a

A solution of saturated compound (0.22 g, 0.59 mmol) **68** in 4 mL absolute dichloromethane was added with MnO_2 (0.10 g, 1.50 mmol) at room temperature. This was followed by the drop-wise addition of liquid bromine (0.10 g, 0.59 mmol) in 2 mL dichloromethane. Stirring was maintained for 30 minutes up until completion of the reaction as indicated from the TLC. The reaction was quenched with water, filtered, and washed with dichloromethane, dried over $NaSO_4$, and after solvent evaporation, the dibromide **69a** was obtained as a white solid (0.25 g, 92%). This was not the expected product and hence it was not used in any reaction as it

was difficult to characterize it through the presence of two doublets in the aromatic region the ^{1}H NMR spectrum indicated the presence of extra bromine in the aromatic region

3.4.1 The preparation of benzoyl peroxide

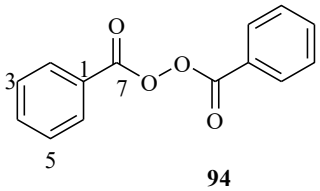

94

In a 25 mL round-bottomed flask containing 2 mL of benzoyl chloride **93** was added 1.50 mL of diethyl ether and cooled to 0 ℃. To this was added 586.00 µL of H_2O_2. The temperature of the reaction was maintained between 0-10 ℃, this was followed with the addition of sodium hydroxide 0.87 g in 2 mL water. The reaction mixture was left to stir for one hour. The precipitates formed were filtered and benzoyl peroxide **94** as white pure solids (1.32 g, 51%) m.p 103 °C; FTIR υmax(ATR)/cm-1 1752 (C=O); ^{1}H NMR (600 MHz, $CDCl_3$): δ_H 7.55 (2H, t, J = 7.6 Hz, H3 and H5), 7.69 (1H, t, J = 7.2 Hz, H4) and 8.11 (2H, d, J = 7.9 Hz, H2 and H6). ^{13}C NMR (150 MHz, $CDCl_3$): δ_C 125.6 (C1), 128.8 (C3 and C5), 129.8 (C2 and C6), 134.3 (C4), 163.1 (C7).

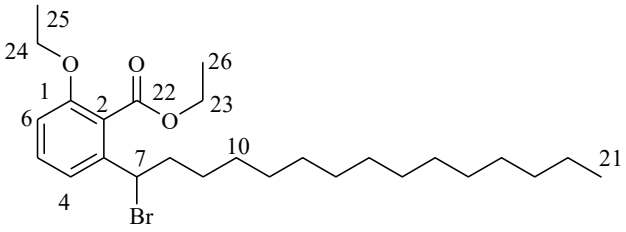

69

To a solution of **68** (2.32 g, 5.90 mmol) in dry CCl_4 was added NBS (1.27 g, 7.16 mmol) and benzoyl peroxide 0.23 g (10% w/w). The resulting mixture was heated to reflux conditions at 90 ℃ while stirring for 3 h. The reaction mixture was filtered, and the filtrate was added with water, extracted with ethyl acetate, washed with saturated $NaHCO_3$, brine, and dried over

sodium sulphate. The solvent was evaporated to yield bromine **69** as a yellowish liquid (2.57 g, 91%); FTIR υmax(ATR)/cm-1 2916-2847 (C-H), 671 (C-Br); ^{1}H NMR (300 MHz, $CDCl_3$): δ_H 0.8 (3H, t, *J* = 6.7 Hz, H21), 1.28 (30H, m H9-H18, H25 and H26), 2.08 (2H, m, H8), 3.97 (2H, q, *J* = 7.0 Hz, H24), 4.34 (2H, q, *J* = 7.1 Hz, H23), 4.89 (1H, t, *J* = 7.4 Hz, H7), 6.74 (1H, d, *J* = 8.3 Hz, H6), 7.12 (1H, d, *J* = 8.0 Hz, H4) and 7.25 (1H, t, *J* = 8.1 Hz, H5). ^{13}C NMR (75 MHz, $CDCl_3$): 14.1 (21), 14.3 (25), 14.6 (C26), 22.2 (C20), 28.0- 29.7 (C9-C18), 31.7 (C19), 39.9 (C8), 50.6 (C7), 61.5 (C23), 64.6 (C24), 111.4 (C6), 119.4 (C4), 123.1 (C2), 130.8 (C5), 140.4 (C3), 155.3 (C1) and 167.3 (C22).

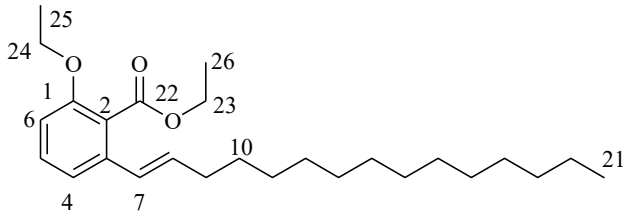

70

To a solution of bromide **69** (1.25 g, 2.50 mmol) in toluene was added (1.18 g, 7.75 mmol) DBU. The reaction mixture was refluxed at 110 ℃ for 6 h under an argon atmosphere. The reaction mixture was allowed to cool to room temperature and quenched with 10% hydrochloric acid (50 mL) and then extracted with ethyl acetate. The combined organic extracts were washed with 10% hydrochloric acid (50 mL), brine (2 mL), and dried over sodium sulphate. The organic phase was concentrated to give a yellow solid, purified on column chromatography with 5% ethyl acetate: hexane mixture to obtain alkene **70** as a light yellow liquid (0.91 g, 87%), FTIR υmax (ATR)/cm-1 2916-2847 (C-H), 1773 (C=C); ^{1}H NMR (400 MHz, $CDCl_3$): δ_H 0.95 (3H, t, *J* = 6.7 Hz, H21), 1.33 (30H, m, H11-H20, H25 and H26), 1.50 (2H, m, H10), 2.24 (2H, q, *J* = 7.1 Hz, H9), 4.08 (2H, q, *J* = 6.9 Hz, H24), 4.46 (2H, q, *J* = 7.1 Hz, H23), 6.27 (1H, m, H8), 6.44 (1H, d, *J* = 15.7 Hz, H7), 6.78 (1H, d, *J* = 8.2 Hz, H6), 7.14 (1H, d, *J* = 7.9 Hz, H4), 7.27 (1H, t, *J* = 8.0 Hz, H5). ^{13}C NMR (100 MHz, $CDCl_3$): δ_C 14.1(C21), 14.3 (C25), 14.6 (C26), 22.2 (C20), 29.1- 29.2 (C10-C18), 31.9 (C19),

33.2 (C9), 60.9 (C23), 64.3 (C24), 110.0 (C6), 117.5 (C4), 122.9 (C2), 126.1 (C7), 129.9 (C5), 134.3 (C8), 136.4 (C3), 157.7 (C1) and 168.1 (C22)

3.5 Oxidation of (*E*)-ethyl 2-ethoxy-6-(pentadec-1-en-1-yl)benzoate to 3-ethoxy-2-(ethoxycarbonyl)benzoic acid 71

3.5.1 Method A: Using mild oxidation by oxygen

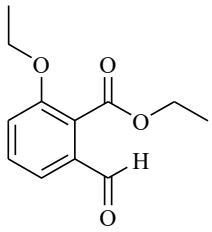

71a

In a two-neck round-bottomed flask a solution of alkene **70** (1.13 g, 3.00 mmol) and benzoic acid (0.18 g, 1.50 mmol) and was added sodium nitrite (0.31 g, 4.49 mmol) under an oxygen gas atmosphere. The reaction mixture was stirred at 80 ℃ for 48 h. TLC was used in monitoring the reactions. After evaporation of solvents and chromatographic purification over silica gel from 10 % to 25% ethyl acetate/hexane, mixtures to afford aldehyde **71a** as a light yellow solid; this product confirmed the formation of aldehyde **71a**, as revealed from the ^{1}H NMR spectra the product had impurities posing difficulties for proper characterization and this could be the drawback for this method.

3.5.2 Method B: Iron-catalyzed oxidative cleavage of olefins

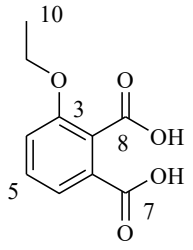

71

To a mixture of Olefin **70** (1.76 g, 4.37 mmol) and $FeCl_3.6\ H_2O$ (59.07 mg, 5 mol %) was added 70% aqueous TBHP 3.61 mL and water 4.37 mL, After stirring for one hour, NaOH (0.699 g, 17.4 mmol) was added, thereafter the temperature of the reaction was raised at 80 ℃ and stirring was maintained for 36 h. The reaction mixture was allowed to cool to room temperature and extracted with ethyl acetate and the aqueous layer was treated with dilute HCl 10% and crushed ice. This mixture was then extracted with ethyl acetate and the combined organic phase was washed with saturated brine solution, dried with anhydrous Na_2SO_4, and concentrated under reduced pressure resulting in a white solid which was filtered washed with hexane to afford the pure carboxylic acid **71** as a white solid 0.59 g, 64%, m.p 183-186 ^{o}C; FTIR υmax(ATR)/cm^{-1} 3246 (O-H) carboxylic, 1734 (C=O); *m/z* HRESIMS calcd for $C_{10}H_{10}O_5$ $[M + H]^+$: 211.0601 found 211.0591. ^{1}HNMR (400 MHz, CD_3OD): δ_H 1.40 (3H, t, J = 6.9 Hz, H10), 4.14 (2H, q, J = 6.9 Hz, H9), 7.30 (1H, d, J = 8.3 Hz, H4), 7.47 (1H, t, J = 8.1 Hz, H5) and δ 7.60 (1H, d, J = 7.8 Hz, H6). ^{13}C NMR (100 MHz, CD_3OD): δ_C 14.9 (C10), 64.7 (C9), 117.1 (C4), 121.8 (C6), 127.2 (C1), 129.3 (C2), 130.1 (C5), 155.2 (C3), 167.0 (C7) and 168.2 (C8).

3.6 Synthesis of phthalic anhydrides

3.6.1 Preparation of 4-ethoxyisobenzofuran-1,3-dione

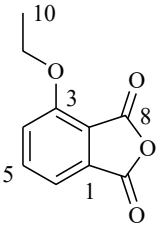

89

Carboxylic **71** (0.78 g, 3.70 mmol) in 2 mL thionyl chloride was refluxed under N_2 atmosphere at 90 ℃ for 12 h. The reaction mixture was cooled to room temperature. Excess thionyl chloride was evaporated. The crude obtained was washed twice with 10 mL of carbon

tetrachloride and consecutively evaporated. The resulting crude product was purified under column chromatography using 4: 5.5: 0.5 ethyl acetate: petroleum ether: acetic acid. To yield (0.27 g, 37.83%) of 4-ethoxyisobenzofuran-1,3-dione **89** as needle-shaped pale yellow crystals. ^{1}H NMR (600 MHz, $CDCl_3$): δ_H 1.57 (3H, t, J = 7.0 Hz, H10), 4.33 (2H, q, J = 7.0 Hz, H9), 7.33 (1H, d, J = 8.4 Hz, H4), 7.57 (1H, d, J = 7.4 Hz, H6) and 7.82 (1H, dd, J = 8.4, 7.4 Hz, H5). ^{13}C NMR (150 MHz, $CDCl_3$): δ_C 14.8 (C10), 65.5 (C9), 117.0 (C1), 117.1 (C4), 119.4 (C6), 133.1 (C2), 138.0 (C5), 157.4 (C3), 160.1 (C7) and 162.6 (C8).

3.6.2 Preparation of isobenzofuran-1,3-dione

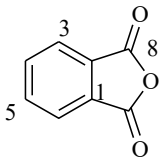

96

A solution of phthalic acid **95** (5.00 g, 33.70 mmol) and acetic anhydride (30 mL) was heated for 2 h at 140 ℃. The reaction mixture was cooled to room temperature and the excess acetic anhydride was removed under reduced pressure. The residue was washed with petroleum ether and after drying phthalic anhydride **96** was obtained as a white solid, 3.74 g, 84%; m.p 127-130 ℃**.** ^{1}H NMR (400 MHz, DMSO): δ_H 8.01 (2H, m, H3 and H6) and 8.10 (2H, m, H4 and H5). ^{13}C NMR (100 MHz, DMSO): δ_C 125.8 (C3 and C6), 131.7 (C1 and C2), 136.7 (C4 and C5), 163.7 (C7 and C8)

3.7 Preparation of 2-hydroxyacetophenone

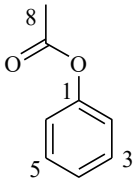

97

Phenol **92** (10.00 g, 0.10 mol) was treated with acetic anhydride under a catalytic amount of sulphuric acid for 30 minutes. TLC was used in monitoring the reaction and after the completion of the reaction, the mixture was poured into water (50 mL) with stirring, extracted with ethyl acetate (200 mL) and the layers were separated. The organic layer was dried over anhydrous sodium sulphate and the solvent was removed under reduced pressure to yield phenyl acetate **97** (9.20 g, 64%) which was obtained as a colorless liquid. ^{1}H NMR (600 MHz, $CDCl_3$): δ_H 2.31 (3H, s, H8), 7.17 (2H, d, *J* = 7.6 Hz, H3 and H5), 7.28 (1H, dd, *J* = 8.4, 7.4 Hz, H4) and 7.44 (2H, m, H2 and H6). ^{13}C NMR (150 MHz, $CDCl_3$): δ_C 21.1 (C8), 121.7 (C2 and C6), 125.9 (C4), 129.5 (C3 and C5), 151.04 (C1) and 168.67 (C7)

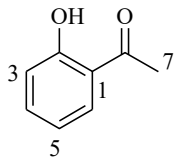

91

Powdered anhydrous $AlCl_3$ (5.90 g, 0.04 mol) was added little by little to acetic acid phenyl ester **97** (3.01 g, 0.02 mol) in a round-bottomed flask in an ice-water bath. The resultant mixture was heated to 120 ℃ for 6 h in an oil bath. Then the reaction mixture was added a lot of crushed ice for hydrolysis. The newly formed organic layer in the reaction mixture was extracted by ethylacetate, dried to yield 0.84 g of 2-hydroxyacetophenone **91** as a colorless liquid in 27%. ^{1}H NMR (400 MHz, $CDCl_3$): δ_H 2.49 (3H, s, H7), 6.77 (1H, t, *J* = 7.6 Hz, H5), 6.85 (1H, d, *J* = 8.4 Hz, H3), 7.34 (1H, t, *J* = 8.5 Hz, H4) and 7.60 (1H, d, *J* = 8.0 Hz, H2). ^{13}C NMR (100 MHz, $CDCl_3$): δ_C 26.6 (C7), 118.3 (C3), 118.9 (C4), 119.7 (C1), 130.6 (C6), 136.4 (C4), 162.3 (C2) and 204.6 (C6)

3.8 Synthesis of 2-acetyl-1-hydroxyanthracene-9,10-dione

3.8.1 Method C: Friedel-Crafts acylation

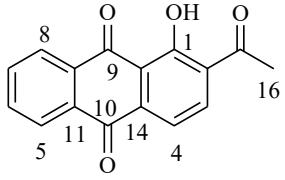

87

To an oven-dried two neck 50 mL round-bottomed flask containing a mixture of aluminium chloride (1.74 g, 13.00 mmol) and sodium chloride (0.38 g, 6.46 mmol). A condenser was well fitted, and the other neck was fitted with a balloon containing nitrogen gas. The contents were heated at 180 ℃, in an oil bath till molten. To this melt, an intimate mixture of phthalic anhydride **96** (0.25 g, 1.68 mmol), 2-hydroxy acetophenone **91** (0.22 g, 1.61 mmol), and aluminium chloride (0.58 g, 4.30 mmol) was added. The temperature was raised to 220ºC with stirring for 1½ h. The reaction mixture was first cooled to room temperature then poured into a mixture of ice/conc.HC1 10% and stirred for 2 h. This reaction did not work as it formed black tar.

3.9 Preparation of *meta*-iodo acetophenone from acetophenone

3.9.1 Nitration of acetophenone to 3-nitroacetophenone

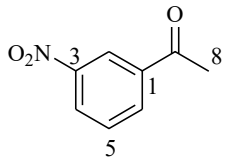

99

To a 6.30 ml of 99% fuming nitric acid that is cooled to -45 ℃ was added (1.00 g, 8.30 mmol) of acetophenone **98** dropwise while maintaining the temperature at -45 to -30 ℃. Stirring was then continued for 2½ h at -30 ℃. The reaction mixture was then poured into a water-ice mixture and kept at 0-10 °C for 2 h filtered in vacuo to obtain m-nitro

acetophenone **99** as cream powdered (0.71 g, 51%), m.p. 78 °C. ^{1}H NMR (300 MHz, $CDCl_3$): δ_H 2.62 (3H, s, H7), 7.62 (1H, t, J = 8.0 Hz, H5), 8.24 (1H, m, H6), 8.37 (1H, m, H4) and 8.76 (1H, t, J = 1.8 Hz, H2). ^{13}C NMR (75 MHz, $CDCl_3$): δ_C 26.7 (C8), 123.2 (C2), 127.3 (C4), 129.8 (C5), 133.7 (C6), 138.2 (C1), 148.4 (C3), 195. 6 (C7)

3.9.2 Reduction of 3-nitroacetophenone to 3-aminoacetophenone

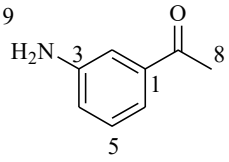

100

To (1.59 g, 9.62 mmol) suspension of m-nitro acetophenone **99** in a mixture of glacial acetic acid (10 mL), ethanol (10 mL), and water (5 mL) was added reduced iron powder (2.79 g, 5.00 mmol). The resulting suspension was exposed to ultrasonic irradiation for 5 h at 30 °C with TLC analysis monitoring for the completion of the reaction. The reaction mixture was dissolved in ethyl acetate, the filtrate was partitioned with 2 M KOH, and the basic layer was further extracted with ethyl acetate. The combined organic extracts were washed with brine and water, dried over $MgSO_4$, and concentrated under reduced pressure to give a crude product that was subjected to flash silica gel column chromatography (10 - 25 % ethyl acetate in hexanes) to afford 3-amino acetophenone **100** as a light brown solid. Yield = 53 %, m.p 87-92 ºC; ^{1}H NMR (300 MHz, $CDCl_3$): δ_H 2.48 (3H, s, H8), 3.77 (2H, br, H9), 6.80 (1H, dd, J = 8.0, 2.4 Hz, H4) 7.17 (1H, m, H5), 7.19 (1H, m, H2) and 7.26 (1H, m, H6). ^{13}C NMR (75 MHz, CDCl3): δ_C 26.72 (C8), 114.01 (C2), 118.81 (C6), 119.67 (C4), 129.44 (C5), 138.20 (C1), 146.64 (C3) and 198.44 (C7)

3.9.3 Sandmeyer reaction of 3-aminoacetophenone to 3-iodo acetophenone

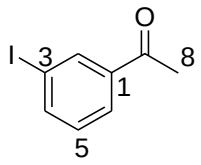

101

To (0.3 g, 2.25 mmol) solution of m-amino acetophenone **100** in concentrated hydrochloric acid (1.00 mL) was added ice-cold water (1.00 mL). The reaction mixture was then cooled to 0 ℃ by use of an ice-water bath. The reaction mixture was then diazotized by the dropwise addition with stirring of a solution of sodium nitrite (0.17 g, 2.50 mmol) in water (0.70 mL), keeping the temperature between 0-5 ℃. After stirring for 15 min, the reaction mixture was added to a solution of potassium iodide (0.83 g, 4.90 mmol) in water (4.00 mL). After stirring for 30 min, the reaction mixture was extracted with ethyl acetate. The organic phase was then concentrated in vacuo to obtain a crude product that was purified through column 10% ethyl acetate in petroleum ether) to yield 3-iodoacetophenone **101** as a brownish liquid. Yield = 54%. ^{1}HNMR (300 MHz, $CDCl_3$): δ_H 2.48 (3H, s, H8), 7.11(1H, td, J = 7.8, 4.7 Hz, H5), 7.79 (2H, m, H4 and H6) and 8.18 (1H, s, H2). ^{13}C NMR (75 MHz, $CDCl_3$): δ_C 26.6 (C8), 94.5 (C3), 127.1 (C6), 130.8 (C5), 136.0 (C2), 138.9 (C1), 141.7 (C4) and 196.6 (C7).

3.10 New synthetic methods

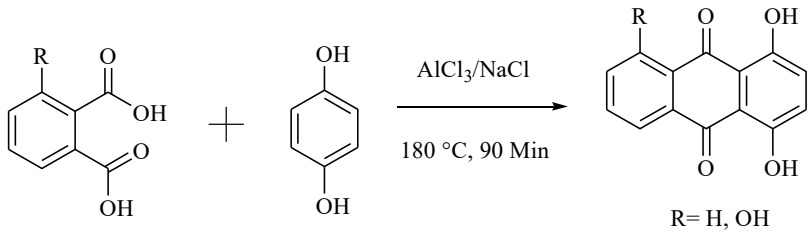

Scheme 3.1: Friedel-Crafts reaction of phthalic acid and 1,4-benzene diol

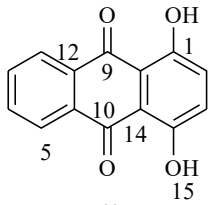

42

To an oven-dried two necks 50 mL round-bottomed flask containing a mixture of aluminium chloride (3.18 g, 23.84 mmol) and sodium chloride (0.68 g, 11.63 mmol). A condenser was well fitted, and the other neck was fitted with a balloon containing nitrogen gas. The contents were heated 180 ℃ in an oil bath till molten. To this melt, an intimate mixture of phthalic acid (0.42 g, 2.88 mmol), 1, 4-benzenediol (0.32 g, 2.96 mmol), and aluminium chloride (1.06 g, 7.94 mmol) was added. The temperature was raised to 220 ℃ with stirring for 1½ h. The reaction mixture was first cooled to room temperature then poured into a mixture of ice/conc. HC1 10% and stirred for 2 h. The solids were filtered, rinsed with water, and air-dried overnight. The filtrate was extracted with ethylacetate to afford 0.50 g of quinizarin **42** as a red-orange solid in 82% m.p 195-197 ℃, FTIR υmax(ATR)/cm-1 2906 (C-H), 1624 (C=O); ^{1}H NMR (400 MHz, DMSO): δ_H 6.62 (2H, s, H3 and H4), 7.22 (2H, m, H5 and H8), 7.45 (2H, m, H6 and H7) and 11.88 (2H, s, H15 and H16). ^{13}C NMR (100 MHz, DMSO): δ_C 113.1 (C13 and C14), 127.1 (C5 and C8), 129.8 (C2 and C3), 133.3 (C11 and C12), 135.5 (C6 and C7), 157.1 (C1 and C4) and 187.1 (C9 and C10).

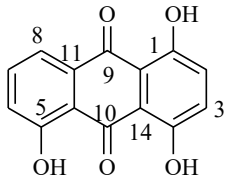

72

For the 1,4,5-trihydroxy anthraquinone method C was used the crude product obtained was first filtered over a short silica gel column and washed with 20% chloroform: petroleum ether to yield 1,4,5-trihydroxyanthraquinone **72** as a red-orange solids yield 45%, m.p 58-60 ℃,

FTIR υmax(ATR)/cm-1 2912-2848 (C-H), 1676 (C=O); HRSM m/z [M + H]$^{+}$calcd for $C_{14}H_8O_5$: 257.0444 found 257.2696. ^{1}H NMR (400 MHz, $CDCl_3$): δ_H 7.19 (1H, s, H6), 7.24 (2H, d, H2 and H3), 7.64 (1H, t, H7) and 7.81 (1H, d, H8). ^{13}C NMR (100 MHz, $CDCl_3$): δ_C 111.4 (C13), 111.6 (C14), 115.0 (C12), 118.5 (C8), 123.5 (C6), 128.5 (C2), 128.9 (C3), 132.4 (C11), 135.9 (C6), 156.7 (C1), 157.2 (C4), 161.6 (C5), 185.2 (C9) and 190.0 (C10).

Modified Marschalk reaction for 1,4-dihydroxyanthraquinones and 1,4,5-trihydroxyanthraquinone with acetaldehyde, propionaldehyde, and 2-chlorobenzaldehyde. The reaction of quinizarin with 2-chlorobenzaldehyde as compared to open chain aldehydes is advantageous because of its high yield and easiest method of purification. This was the reason for choosing 2-chlorobenzaladehydes in our reactions. Moreover, this reaction when is done with 1,4,5-trihydroxanthraquinone did not give the expected results as revealed from the NMR spectra.

3.10.1 Method D: Modified Marschalk reaction

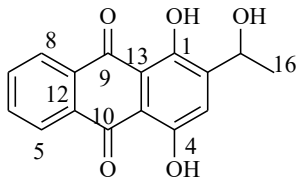

62

To a (2.00 g, 8.32 mmol) solution of anthraquinone **42** in absolute methanol (20 mL) cooled 0 ℃ to was added aqueous NaOH (1 M, 50 mL) and a solution of $Na_2S_2O_4$ (2.80 g, 2.00 mmol) in water (16.60 mL) under nitrogen. After 10 minutes of stirring, the acetaldehyde (1.83 g, 41.60 mmol) was added. The reaction mixture was stirred for 2 h at 0 ℃. The solution was poured into cold water that contained 3% H_2O_2 (12.44 mmol, 10 mL), and stirred for 10 minutes. The mixture was acidified by the addition of HCl (1 M solution, 2 mL). The resultant reaction mixture was washed four times with ethylacetate, the organic

layer dried over sodium sulphate. The solvent was evaporated in vacuo to yield a solid, which was purified through a long column over silica gel eluting with dichloromethane to yield a product which upon recrystallization from dichloromethane anthraquinone **62** was obtained as an orange solid. Yield = 16%, m.p. 87-90°C; FTIR υmax(ATR)/cm^{-1} 3246 (O-H) carboxylic, 2908 (CH_3), 1609 (Ar-C=C-); ^{1}H NMR (400 MHz, DMSO): δ_H 1.38 (3H, d, J = 6.4 Hz, H16), 5.05 (1H, q, J = 6.4 Hz, H14), 7.45 (1H, s, H3), 7.97 (2H, m, H6 and H7) and 8.23 (2H, m, H5 and H8). ^{13}C NMR (100 MHz, DMSO): δ_C 24.1 (C16), 63.2 (C15), 111.6 (C13), 112.5 (C14), 124.7 (C3), 127.0 (C5), 127.1 (C8), 133.3 (C11 and C12), 135.3 (C6), 135.5 (C7), 149.7 (C2), 154.6 (C1), 157.4 (C4), 186.4 (C9) and 187.3 (C10).

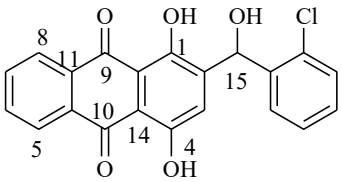

73

To a 0 °C cold solution of anthraquinone **42** (2.00 g, 8.3 mmol) in absolute methanol (20 mL) was added aqueous NaOH (1 M, 50 mL) and a solution of $Na_2S_2O_4$ (2.89 g, 16.50 mmol) in water (16.50 mL) under nitrogen. After 10 minutes of stirring, 2-chlorobenzaldehyde (4.60 g, 33.00 mmol) was added. The reaction mixture was stirred for 4 h at 0 °C. The solution was poured into cold water (50 mL) that contained 30% H_2O_2 (10 mL), and the mixture was stirred for 10 min. The mixture was acidified by the addition of HCl (1 M solution, 10 mL), forming a solid mass which was separated and was dissolved in ethyl acetate and evaporated, re-dissolved in hexane, and stirred for 2 h to form precipitates. The formed precipitates were filtered by filter paper and washed several times with hexane to remove traces of the starting material and some of the unreacted aldehydes, dried purified through column chromatography with 10% ethyl acetate/ petroleum ether to yield anthraquinone **73** as an orange solid. Yield = 75 %, m.p 195-190 ºC ; FTIR υmax (ATR)/cm^{-1} 3450 (O-H) alcohol,

1232 (C-O-). ^{1}H NMR (400 MHz, DMSO): δ_H 6.33 (1H, s, H15), 7.33 (3H, m, Ar-H), 7.42 (1H, s, H3), 7.47(m, 1H), 7.88 (2H, m, H6 and H7) and 8.16 (2H, m, H5 and H8). ^{13}C NMR (100 MHz, DMSO): δ_C 65.8 (C15), 112.3 (C13), 112.7 (C14), 126.3 (C3), 126.9 (C5), 127.0 (C8), 127.7 (Ar-C), 129.3 (Ar-C), 129.7 (Ar-C), 129.9 (Ar-C), 133.0 (Ar-C), 133.2 (C11), 133.3 (C12), 135.3 (C6), 135.5 (C7), 140.2 (Ar-C), 145.2 (C2), 154.9 (C1), 156.8 (C4), 186.5 (C9) and 187.4 (C10).

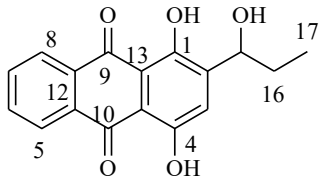

74

To a (0.4 g, 1.6 mmol) cold solution of anthraquinone **42** in absolute methanol (10 mL) maintained at 0 °C was added aqueous NaOH (1 M, 10 mL) and a solution of $Na_2S_2O_4$ (0.58 g, mmol) in water (3 mL) under nitrogen. After 10 minutes of stirring, the propionaldehyde (0.76 g, 13.6 mmol) was added. The reaction mixture was stirred for 2 h while maintaining a temperature of 0 °C. The solution was poured into cold water that contained 3% H_2O_2 (2.49 mmol, 5.6 mL), and stirred for 10 minutes. The mixture was acidified by the addition of HCl (1 M solution, 1 mL). The resultant reaction mixture was washed four times with ethyl acetate, the organic layer dried over sodium sulphate. The solvent was evaporated in vacuo to yield a solid. This solid was purified through a long column over silica using 100% Dichloromethane to yield product **74** as an orange solid. Yield = 14 %, m.p. 120-125 °C; FTIR υmax (ATR)/cm^{-1} 3183 (O-H) alcohol, 2916 (CH_3), 1593 (Ar-C=C-); ^{1}H NMR (400 MHz, $CDCl_3$): δ_H 1.03 (3H, t, J = 6.4 Hz, H17), 1.77 (1H, m, H16), 1.90 (1H, m, H16), 5.01 (1H, m, H15), 7.41 (1H, s, H3), 7.81 (2H, m, H6 and H7) and 8.32 (2H, m, H5 and H8). ^{13}C NMR (100 MHz, $CDCl_3$): δ_C 10.0 (C17), 29.5 (C16), 70.7 (C15), 111.7 (C13), 112.4 (C14),

126.0 (C3), 126.9 (C5), 127.0 (C8), 133.4 (C11), 133.5 (C12), 134.4 (C6), 134.5 (C7), 145.9 (C2), 155.5 (C1), 157.9 (C4), 186.4 (C9) and 187.3 (C10).

3.10.2 The reaction of alcohol with thionyl chloride

To further our reaction 2-((2-chlorophenyl)(hydroxy)methyl)-1,4-dihydroxyanthracene-9,10-dione obtained from the reaction 1,4-dihydroxyanthraquinone and 2-chlorobenzaldehyde was used in structure modification as stipulated in the procedure below:

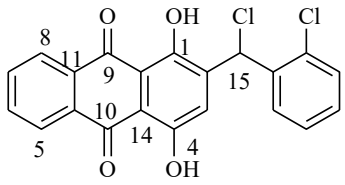

77

Thionyl chloride 2 mL was added dropwise to the parent alcohol **73** (0.50 g, 1.30 mmol) cooled in an ice bath after stirring for 10 minutes. The temperature of the reaction was raised to 50 ℃ and stirring was maintained for 2 h. Excess thionyl chloride was dried in vacuo; the solid obtained was dissolved in dichloromethane and distilled off. The resulting solid was further re-dissolved in a mixture of dichloromethane/ hexane to form precipitates which were filtered washed several times with hexane and dried to obtain anthraquinone a crude product. Further purification with a mixture of 10% ethylacetate in petroleum ether afforded compound **77** as an orange solid Yield = 51.7%, m.p 200-204 ℃; FTIR υmax (ATR)/cm^{-1} 1738 (C=O); *m/z* HRESIMS calcd for $C_{21}H_{12}Cl_2O_4$ $[M + H]^+$: 399.0185.found 399.1771. ^1H NMR (400 MHz, $CDCl_3$) δ 6.94 (1H, s, H15), 7.31 (2H, m, Ar-H), 7.41 (2H, m, Ar-H), 7.62 (1H, m, Ar-H), 7.83 (2H, m, H6 and H7), and 8.35 (2H, m, H5 and H8). ^{13}C NMR (100 MHz, $CDCl_3$) δ 53.6 (C15), 112.8 (C13 and C14), 127.1 (Ar-C), 127.2 (Ar-C), 127.3(Ar-C), 128.0 (Ar-C), 129.5 (Ar-C), 129.9 (C5), 130.0 (C8), 133.2, 133.3 (C11), 133.4 (C12), 134.6 (C6), 134.7 (C7), 136.3 (C2), 140.5 (Ar-C), 155.1 (C1), 157.1 (C4), 186.7 (C9) and 187.2 (C10).

Method E: Reaction of the alkyl chloride with amines

Method E as highlighted below was used in the synthesis of various amines by reaction with the chloride

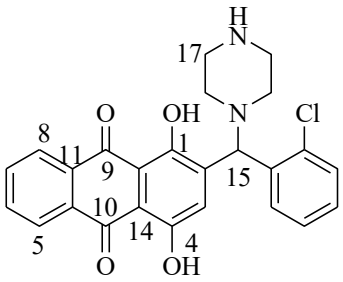

78

A solution of anthraquinone **77** (0.10 g, 0.25 mmol) in dry dichloromethane (10 mL), was added with various amines (0.17 g, 1.97 mmol, 6 equiv) and the resulting mixture was stirred at room temperature to completion of the reaction as showed from TLC. The reaction mixture was poured into water and extracted with ethylacetate. The organic layer was washed with water, dried, and concentrated. The solid obtained was purified by column chromatography using a mixture of 4% MeOH/ DCM as a solvent system to yield anthraquinone **78** as a deep purple solid.Yield = 71%, m.p 100-120 °C; FTIR υmax (ATR)/cm^{-1} 3057 (O-H) alcohol, 1620 (Ar-C=C); *m/z* HRESIMS calcd for $C_{25}H_{21}ClN_2O_4$ $[M + H]^+$: 449.1263 found 449.3618. ^{1}H NMR (400 MHz, $CDCl_3$): δ_H 2.48 (2H, m, H16), 2.55 (2H, m, H16), 2.91 (4H, m, H17), 5.55 (1H, s, H15), 7.19 (2H, m, Ar-H), 7.36 (1H, dd, *J* = 7.8, 1.3 Hz, Ar-H), 7.51 (1H, dd, *J* = 7.7, 1.7 Hz, Ar-H), 7.60 (1H, s, H3), 7.80 (2H, m, H6 and H7) and 8.31(2H, m, H5 and H8). ^{13}C NMR (100 MHz, $CDCl_3$): δ_C 45.2 (C17), 51.4 (C16), 61.5 (C15), 111.0 (C13), 111.5 (C14), 125.8 (C5), 125.9 (C8), 126.1 (Ar-C), 127.1 (Ar-C), 127.6 (Ar-C), 128.8 (C3), 129.1 (Ar-C), 132.4 (C11), 132.5 (C13), 133.4 (Ar-C), 134.0 (C6 and C7), 136.1 (Ar-C), 142.1 (C2), 155.9 (C1), 156.5 (C4), 185.6 (C9) and 186.0 (C10)

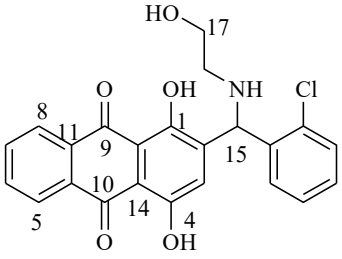

79

Purified by column chromatography using a mixture of 4% MeOH/DCM as a solvent system to yield anthraquinone **79** as a deep purple solid. Yield = 22%, m.p 147-150 ℃; FTIR υmax(ATR)/cm^{-1} 3285 (O-H) alcohol, 1609 (Ar-C=C-); *m/z* HRESIMS calcd for $C_{23}H_{18}ClNO_5$ $[M + H]^+$: 424.0946 found 424.1253. ^{1}H NMR (400 MHz, $CDCl_3$): δ_H 2.75 (2H, m, H16), 3.58 (2H, m, H17), 5.67 (1H, s, H15), 7.15-7.22 (3H, m, Ar-H and H3), 7.33 (1H, d, d, *J* = 7.6 Hz, Ar-H), 7.45, (1H, d, *J* = 7.4 Hz, Ar-H), 7.74 (1H, m, H6 and H7) and 8.25 (2H, m, H5 and H8). ^{13}C NMR (100 MHz, $CDCl_3$): δ_C 48.7 (C17), 55.5 (C15), 60.3 (C16), 112.0 (C13), 112.7 (C14), 127.0, 127.1 (C5), 127.2 (C8), 127.6 (Ar-C), 128.9 (Ar-C), 129.1 (Ar-C), 130.0 (Ar-C), 133.4 (C6), 133.5 (C7), 134.2 (Ar-C), 133.4 (C6), 134.5 (C7), 137.6 (Ar-C), 142.9 (C2), 156.3 (C1), 157.5 (C4), 186.5 (C9) and 186.2 (C10).

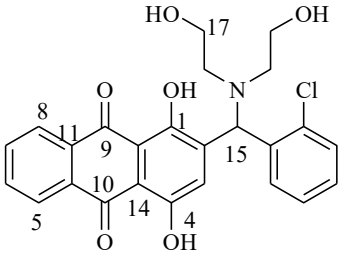

80

Purified by column chromatography using 4% MeOH in dichloromethane to give anthraquinone **80** as an orange solid. Yield = 72%, m.p 130-140 ℃; FTIR υmax(ATR)/cm^{-1} 3332 (O-H) alcohol, 1585 (Ar-C=C-); *m/z* HRESIMS calcd for $C_{25}H_{22}ClNO_6$ $[M + H]^+$: 468.1208 found 468.1544. ^{1}H NMR (400 MHz, $CDCl_3$): δ_H 2.99 (4H, m, H16), 3.42 (2H, m, H17), 3.51 (2H, m, H17), 5.95 (1H, s, 1H), 6.99 (1H, s, H3), 7.22 (2H, m, Ar-H), 7.33 (1H, d,

J = 7.4 Hz, Ar-H), 7.43 (1H, d, *J* = 7.1 Hz, Ar-H), 7.74 (2H, m, H6 and H7) and 8.24 (2H, m, H5 and H8). ^{13}C NMR (100 MHz, $CDCl_3$): δ_C 54.4 (C16), 59.7 (C17), 60.8 (C15), 112.2 (C13), 112.7 (C14), 127.0 (C5), 127.2 (C8), 128.6 (Ar-C), 129.1 (Ar-C), 129.5 (Ar-C), 130.5 (C3), 133.4 (C11), 133.5 (C12), 134.4 (Ar-C), 134.5 (C11), 134.7 (C12), 137.1 (Ar-C), 142.4 (C2), 156.4 (C1), 157.2 (C4), 186.6 (C9) and 187.4 (C10).

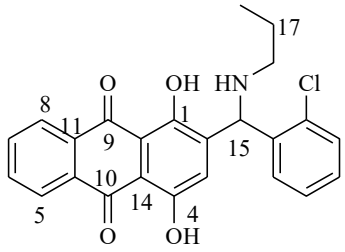

81

Purified by column chromatography using a mixture of 10% ethylacetate/ petroleum ether as a solvent system to yield compound **81** as an orange solid. Yield = 90%, m.p 98-120 °C; FTIR υmax (ATR)/cm^{-1}3069 (O-H) alcohol, 1581 (Ar-C=C-); *m/z* HRESIMS calcd for $C_{24}H_{20}ClNO_4$ $[M + H]^+$: 422.1154 found 422.3618. ^{1}H NMR (400 MHz, $CDCl_3$): δ_H 0.86 (3H, t, *J* = 7.4 Hz, 7.4 Hz, H18), 1.5 (2H, dq, *J* = 14.9, 7.6, 7.0 Hz, H17), 2.57 (2H, t, *J* = 7.1 Hz, 7.1 Hz, H16), 5.59 (1H, s, H15), 7.15 (2H, m, Ar-H), 7.30 (1H, m, Ar-H), 7.33 (1H, m, Ar-H), 7.36 (1H, s, H3), 7.69 (2H, m, H6 and H7) and 8.18 (2H, m, H5 and H8). ^{13}C NMR (100 MHz, $CDCl_3$): δ_C 11.8 (C18), 23.4 (C17), 50.6 (C16), 57.3 (C15), 111.8 (C13), 112.4 (C14), 126.8 (Ar-C), 127.0 (C5 and C8), 127.7 (Ar-C), 128.7 (Ar-C), 129.0 (Ar-C), 129.8 (C3), 133.4 (C11 and C12) 134.0 (Ar-C), 134.3 (C6), 134.4 (C7), 138.5 (Ar-C), 144.1 (C2), 156.7 (C1), 158.1 (C4), 186.4 (C9) and 187.0 (C10).

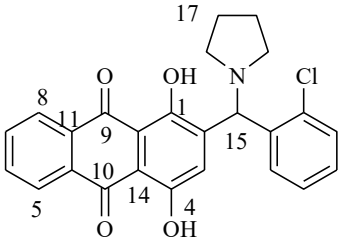

82

Purified with 10% ethylacetate/petroleum ether mixtures to give anthraquinone **82** as a dark orange solid. Yield = 44%, m.p 148-150 ℃. FTIR υmax (ATR)/cm^{-1} 3065 (O-H) alcohol, 1577 (-Ar-C=C-); *m/z* HRESIMS calcd for $C_{25}H_{20}ClNO_4$ $[M + H]^+$: 434.1154 found 434.3386. ^{1}H NMR (400 MHz, CD_6O): δ_H 1.65 (4H, m, H17), 2.38 (2H, m, H16), 2.48 (2H, m, H16), 5.37 (1H, s, H15), 7.12 (1H, td, *J* = 7.6, 1.7 Hz, Ar-H), 7.22 (1H, td, *J* = 7.6, 1.2 Hz, Ar-H), 7.28 (1H, dd, *J* = 7.9, 1.2 Hz, Ar-H), 7.50 (1H, s, H3), 7.55 (1H, dd, *J* = 7.8, 1.6 Hz, Ar-H), 7.84 (2H, m, H6 and H7) and 8.34 (2H, m, H5 and H8). ^{13}C NMR (100 MHz) $CDCl_3$: δ_C 23.3(C17), 52.2 (C16), 61.4 (C15), 111.9 (C13), 112.6 (C14), 126.7 (C5), 126.8 (C8), 127.2 (C3), 127.8 (Ar-C), 128.7 (Ar-C), 129.6 (Ar-C), 130.4 (Ar-C), 133.4 (C11), 133.5 (C12), 133.8 (C6), 134.8 (C7), 134.9 (Ar-C), 138.7(Ar-C), 144.0 (C2), 156.2 (C1), 157.5 (C4), 186.8 (C9) and 187.5 (C10).

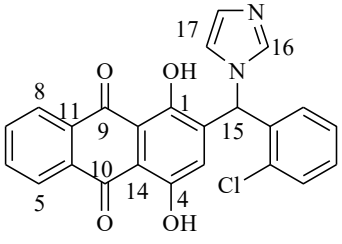

83

Purified with 1% methanol/chloroform to yield compound **83** as an orange solid. Yield = 46 %, m.p 180-200 °C; FTIR υmax (ATR)/cm^{-1}(1617 (-C=N), 1573 (Ar-C=C-); *m/z* HRESIMS calcd for $C_{24}H_{15}ClN_2O_4$ $[M + H]^+$: 431.0793 found 431.0796. ^{1}H NMR (400 MHz, $CDCl_3$): δ_H 6.76 (1H s, H15), 6.91 (2H, d, *J* = 7.8 Hz, H17), 7.19 (1H, s, H16), 7.28 (2H, m, Ar-H), 7.35 (1H, t, *J* = 7.6 Hz, Ar-H), 7.47 (1H, d, *J* = 7.8 Hz, Ar-H), 7.54 (1H, s, H3), 7.86 (2H, m,

H6 and H7), 8.37 (2H, m, H5 and H8), 12.79 (1H, s, -OH) and 13.29 (1H, s, -OH). ^{13}C NMR (100 MHz, $CDCl_3$): δ_C 56.3 (C15), 113.1 (C13), 113.2 (C14), 119.3 (Ar-C), 127.1 (Ar-C), 127.2 (C5), 127.3 (C8), 128.4 (C17), 129.2 (C16), 130.4 (Ar-C), 130.5 (Ar-C), 133.3 (C11), 133.4 (C12), 133.8 (Ar-C), 134.7 (Ar-C), 134.8 (C6), 134.9 (C7), 138.5 (C2), 155.0 (C1), 157.0 (C4), 186.8 (C9) and 187.3 (C10).

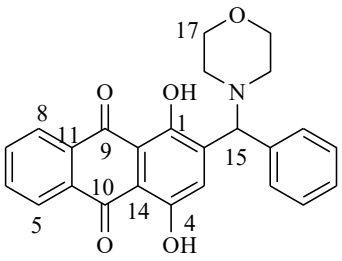

84

Purified with 10% Ethylacetate/petroleum ether mixtures to give compound **84** as an orange solid. Yield = 80%, m.p. 180-182 ℃, FTIR υmax (ATR)/cm^{-1}3057 (O-H) alcohol, 1577 (Ar-C=C-); *m/z* HRESIMS calcd for $C_{24}H_{20}ClNO_5$ $[M + H]^+$: 450.1103 found 450.3422. ^{1}H NMR (400 MHz, $CDCl_3$): δ_H 2.50 (2H, m, H16), 2.60 (2H, m, H16), 3.72 (4H, m, H17), 5.51 (1H, s, H15), 7.20 (2H, m, Ar-H), 7.37 (1H, dd, *J* = 7.8, 1.5 Hz, Ar-H), 7.53 (1H, dd, *J* = 7.7, 1.8 Hz, Ar-H), 7.62 (1H, s, H3), 7.81 (2H, m, H6 and H7) and 8.34 (2H, m, H5 and H8). ^{13}C NMR (100 MHz, $CDCl_3$): δ_C 50.8 (C16), 61.3 (C15), 66.2 (C17), 111.0 (C13), 111.5 (C14), 125.9 (Ar-C), 126.0 (C5), 126.1 (C8), 127.1 (Ar-C), 127.7 (C3), 128.9 (Ar-C), 129.1(Ar-C), 132.3 (C11), 132.4 (C12), 133.43 (C6 and C7), 134.1 (Ar-C), 135.7 (Ar-C), 141.8 (C2), 155.9 (C1), 156.4 (C4), 185.6 (C9) and 186.1 (C10)

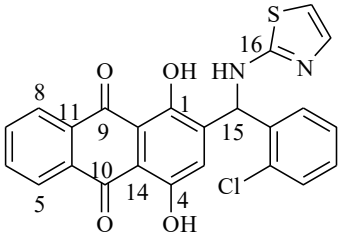

85

Purified with 1% methanol/chloroform to yield anthraquinone **85** as a black solid 27 % m.p 137 ℃; FTIR υmax (ATR)/cm^{-1} 33 52 (-NH-), 1629 (C=N); *m/z* HRESIMS calcd for $C_{24}H_{15}ClN_2O_4S$ [M + H]: 463.0514 found 463.0508. ^{1}H NMR (400 MHz, $CDCl_3$): δ_H 6.44 (1H, s, H15), 6.96 (1H, d, *J* = 3.6 H, Ar-H), 7.19 (3H, m, Ar-H), 7.75 (2H, m, H6 and H7) and 8.24 (H5 and H8). ^{13}C NMR (100 MHz, $CDCl_3$): δ_C 55.1 (C15), 109.5 (Ar-C), 111.5 (C13), 111.9 (C14), 126.0, 126.1, 126.2 (C5), 126.3 (C8), 127.5 (Ar-C), 128.7 (Ar-C), 129.2 (Ar-C), 132.3 (C11), 132.4 (C12), 133.2 (Ar-C), 133.5 (C6), 133.6 (C7), 135.2 (Ar-C), 137.5(Ar-C), 139.5 (C2), 155.0 (C1), 156.3 (C4), 168.1 (C16) 185.6 (C9) and 186.1 (C10).

3.11 Preparation of anthraquinone thiosemicarbazone

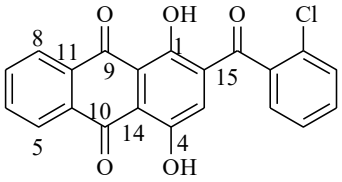

75

A solution of alcohol anthraquinone **73** (0.22 g, 0.58 mmol) in CH_2Cl_2 (20 mL) was treated at 25 ℃ with Dess–Martin periodinane (0.36 g, 0.84 mmol) and stirred for 20 min. Afterward, saturated aq. $NaHCO_3$) was added and extracted with ethyl acetate. The organic layer was washed with brine and dried over sodium sulphate. The solvent was evaporated in vacuo; the crude product recrystallized from methanol/ petroleum ether to afford compound **75** as an orange solid. Yield = 99%, m.p. 140-153 ℃; FTIR υmax(ATR)/cm^{-1} 1738 (C=O); ^{1}H NMR (400 MHz) $CDCl_3$: δ_H 7.35 (2H, m, Ar-H), 7.41 (1H,m, Ar-H), 7.51 (1H, s, H3), 7.79 (2H, m, H6 and H7) and 8.28 (2H, m, H5 and H8).^{13}C NMR (100 MHz) $CDCl_3$: δ_C 113.7 (C13), 115.3 (C14), 127.0 (C3), 127.2 (C5), 127.3 (C8), 129.6 (Ar-C), 130.4 (Ar-C), 130.6 (Ar-C), 132.3 (Ar-C), 132.7 (C-2), 133.2 (C11), 133.4 (C12), 134.8 (C6), 134.9 (C7), 138.0 (Ar-C), 138.1 (Ar-C), 156.1 (C1), 156.5 (C4), 187.0 (C9), 187.1 (C10) and 192.2 (C15)

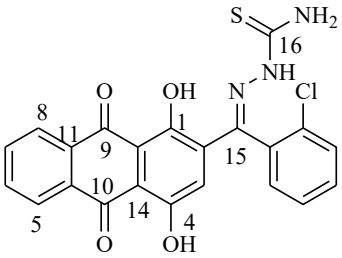

76

To the thiosemicarbazide (0.14 g, 1.86 mmol) in absolute methanol (20 mL), carbonyl **75** (0.10 g, 0.26 mmol) was added afterward and three drops of sulphuric acid were added. The reaction mixture was refluxed at 90 ℃ for 24 h till the completion of the reaction as monitored by TLC. The reaction mixture was allowed to cool to room temperature. The solvent was evaporated, and the crude product was purified by column chromatography from 2:1, petroleum ether/ethylacetate mixture to chloroform as solvent system to yield a solid which was recrystallized from CH_2Cl_2/petroleum ether giving thiosemicarbazone **76** as a red-orange. Yield = 45%, solid m.p 137-139 ℃; FTIR υmax (ATR)/cm^{-1} 3222 (-NH_2), 1624 (C=N), 1164 (C=S); *m/z* HRESIMS calcd for $C_{22}H_{14}ClN_3O_4S$ M + H]: 452.0466 found 452.0366. ^{1}H NMR (400 MHz, $CDCl_3$): δ_H 7.34 (1H, dd, J = 7.3, 1.9 Hz, Ar-H), 7.39 (1H, s, H3), 7.50 (3H, m, 3H), 7.84 (2H, m, H6 and H7), 8.34 (2H, m, H5 and H8), 12.78 (1H, s, -OH), 13.68 (1H, s, -OH). ^{13}C NMR (100 MHz, $CDCl_3$) δ_C 112.5 (C13), 112.7 (C14), 126.1 (C5), 126.2 (C8), 127.1 (Ar-C), 128.2 (Ar-C), 128.9 (Ar-C), 129.1 (Ar-C), 129.9 (C3), 131.0 (Ar-C), 131.8 (Ar-C), 132.2 (C11), 132.3 (C13), 133.7 (C6), 133.8 (C7), 134.5 (C2), 142.5 (C15), 155.4 (C1), 156.1 (C4), 178.6 (C16), 185.7 (C9) and 186.3 (C10)

3.12 Esterification of anacardic acid with 1,4-dihydroxy-2-(1-hydroxyethyl)anthracene-9,10-dione

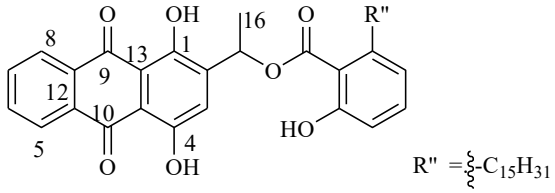

102

To a stirred solution of 2-hydroxymethyl-1,4-dihydroxy-9,10-anthraquinine **62** (0.20 g, 0.70 mmol) in dichloromethane was added DCC (0.16 g, 0.77 mmol) and DMAP (0.04 g, 34.3 mmol) at 0-5 ℃, followed by the addition of Anacardic acid **63a** (0.27 g, 0.77 mmol). The solution was stirred for 4 h at 0-5 ℃. Afterward, hexane 10 mL was added and stirred for 10 minutes, the precipitates formed were filtered and the filtrate evaporated. The crude product was purified through chromatography using 10% ethyl acetate /petroleum ether to afford ester **102** as an orange solid (0.041, 9.5%), m.p. 99-101 °C; FTIR υmax(ATR)/cm-1 2912-2845 (C-H), 1658 (C=O); ^{1}H NMR (400 MHz, $CDCl_3$): δ_H 0.84 (3H, t, J = 6.8 Hz, H-Alky), 1.21 (26H, m, H-alkyl), 1.72 (3H, d, J = 6.6 Hz, H16), 2.88-3.03 (2H, m, H-alkyl), 6.52 (1H, q, J = 6.6 Hz, H16), 6.71 (1H, d, J = 7.4 Hz, Ar-H), 6.80 (1H, d, J = 8.2 Hz, Ar-H), 7.28 (1H, t, J = 7.9 Hz, Ar-H), 7.33 (1H, s, H3), 7.81 (2H, m, H6 and H7) and 8.31 (2H, m, H5 and H8). ^{13}C NMR (100 MHz, $CDCl_3$): δ_C 13.1- 35.8 (C-Alkyl), 67.2 (C15), 110.6 (Ar-C), 111.5 (C13), 111.9 (C14), 114.8 (Ar-C), 121.5 (Ar-C), 124.0 (C3), 126.0 (C5), 126.1 (C8), 132.3 (C11), 132.4 (C12), 133.5 (Ar-C), 133.6 (C6), 133.7 (C7), 141.2 (Ar-C), 145.1 (C-2), 153.8 (C1), 156.5 (C4), 161.9 (Ar-C-O-), 169.5 (C-17), 185.6 (C-9) and 186.3 (C-10).

3.13 Preparation of saturated anacardic acid

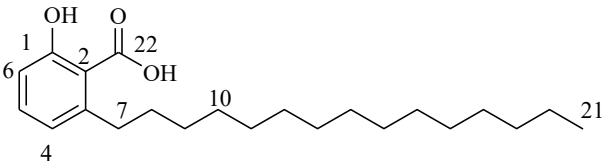

63a

To a two neck 200 mL round-bottomed flask containing (10.00 g, 0.03 mol) of anacardic **63** dissolved in 150 mL absolute methanol, was added (1.00 g, 10% w/w) of powdered Pd/C. The two necks were closed by a septum and an inlet allowed hydrogen gas in the balloon to enter. The reaction was stirred for 24 h at room temperature, and it was filtered and concentrated to obtain a solid which upon recrystallized from petroleum ether afforded pure 2-hydroxy-6-pentadecylbenzoic acid **63a** as a white solid. Yield = 19.9 %, m.p. 78-80 °C, υmax(ATR)/cm-1 3440 (O-H) carboxylic, 2911-2843 (C-H); ^{1}H NMR (400 MHz $CDCl_3$): δ_H 0.87 (3H, t, J = 6.8 Hz, H21), 1.25 (24H, m, H9-H20), 1.59 (2H, quin, H8) 2.97 (2H, m, H7), 6.77 (1H d, J = 7.4 Hz, H6), 6.86 (1H, d, J = 8.2 Hz, H4) and 7.35 (1H, t, J = 7.9 Hz, H5). ^{13}C NMR (100 MHz $CDCl_3$): δ_C 13.1 (C21), 21.7 (C8), 28.4-31.1 (C9-C20), 35.5 (C7), 109.5 (C6), 114.8 (C4), 121.7 (C2), 134.3 (C5), 146.7 (C3), 162.5 (C1) and 174.4 (C22).

3.14 Preparation of cardanol by decarboxylation of anacardic acid

Natural CNSL (50.00 g) and calcium hydroxide (1.00 g, 2%, 0.01 mol) were dissolved in 200 mL toluene and heated at 250 °C for 2 h. The mixture was allowed to cool to ambient temperature and extracted with petroleum ether, filtered, and concentrated to give as a dark brown oil (5.00 g, 11.4%). FTIR υmax (ATR)/cm-1 3264 (O-H), 2918 (C-H); ^{1}H NMR (400 MHz, $CDCl_3$): δ_H 1.07 – 0.85 (m, 1H), 1.40 (s, 36H), 1.83 – 1.49 (m, 2H), 1.83 – 1.49 (m, 2H), 2.13 (s, 1H), 2.70 – 2.41 (m, 1H), 2.91 (d, J = 13.7 Hz, 1H), 6.83 (d, J = 7.6 Hz, 1H) and 7.20 (t, J = 7.7 Hz, 1H)

3.15 Reduction of cardanol

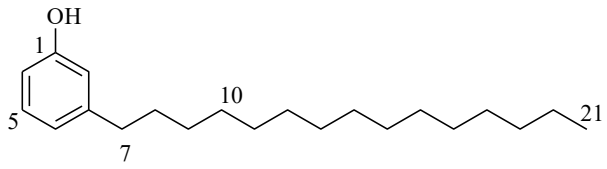

64a

To a two neck 50 mL round-bottomed flask containing (5.00 g, 0.016 mol) of cardanol **64** dissolved in 20 mL absolute methanol, was added (0.50 g, 10% w/w) of powdered Pd/C. The two necks were closed by a septum and an inlet allowed hydrogen gas in a balloon to enter. The reaction was stirred for 24 hours at room temperature, and it was filtered and concentrated to yield the 3-pentadecylphenol **64a** as a white solid. Yield = 92%. m.p. 47-49 °C, υmax(ATR)/cm-1 3280 (O-H), 2909-2842 (C-H); ^{1}H NMR (400 MHz, $CDCl_3$): δ_H 0.90 (3H, t, J = 6.7 Hz, H21), 1.29 (24H, m, H9-H20), 1.59 (2H, quin, H8), 2.56 (2H, t, H7), 6.65 (1H, d, H2 and H6), 7.75 (1H, d, J = 8.8 Hz, H4) and 7.14 (1H, t, J = 7.7 Hz, H5)

^{13}C NMR (100 MHz, $CDCl_3$): δ_C 14.2 (C21), 22.7 (C20), 29.3-29.74 (C9-C19), 31.9 (C8), 35.87 (C7), 112.5 (C6), 115.3 (C2), 120.9 (C4), 129.4 (C5), 144.9 (C3) and 155.5 (C1)

3.16 Biological studies procedures

3.16.1 *In vitro* antitrypanosomal assay

To assess for anti-trypanocidal activity, test compounds were added to *in vitro* cultures of *T.b. brucei* in 96-well plates at a fixed concentration of 20 µM, after an incubation period of 48 hours, numbers of parasites surviving drug exposure were determined by adding a resazurin based reagent. The reagent contains resazurin which was reduced to resorufin by living cells. Resorufin is a fluorophore (Exc_{560}/Em_{590}) and was quantified in a multiwell fluorescence plate reader. Results were expressed as % parasite viability – the resorufin fluorescence in compound-treated wells relative to untreated controls.

3.16.2 *In vitro* anti-*Plasmodium falciparum* assay

Malaria parasites (*Plasmodium falciparum* strain 3D7) were maintained in RPMI 1640 medium containing 2 mM L-glutamine and 25 mM Hepes (Lonza). The medium was further supplemented with 5% Albumax II, 20 mM glucose, 0.65 mM hypoxanthine, 60 µg/mL gentamycin, and 2-4% hematocrit human red blood cells. The parasites were cultured at 37ºC under an atmosphere of 5% CO_2, 5% O_2, and 90% N_2 in a sealed T75 culture flask.

Single concentration screening was conducted using compounds at 20 µM added to parasite cultures in 96-well, clear plates and incubated for 48 hours in a 37ºC CO_2 incubator. After 48 hours, 20 µL of culture was removed from each well and combined with 125 µL of a mixture of Malstat and NBT/PES solutions in a fresh 96-well plate. These solutions measure the activity of the parasite lactate dehydrogenase (pLDH) enzyme in the cultures. A purple product was formed when pLDH was present, and the product was quantified in a Spectramax M3 microplate reader (Abs_{620}). The Abs_{620} reading in each well was quantified which is an indication of the pLDH activity and hence the number of parasites present. For each compound concentration, % parasite viability – the pLDH activity in compound-treated wells relative to untreated controls – was calculated.

3.16.3 *In vitro* antibacterial assay

3.16.4 *Staphylococcus aureus* antibacterial assay

To assess the effect of the compounds on the growth of *S. aureus* cells, they were incubated at a fixed concentration of 50 µg/mL in 96-well plates containing *S. aureus* for 6 hours. The numbers of cells remaining viable after exposure to the compound were determined by using the resazurin-based reagent and reading resorufin fluorescence in a multiwell plate reader.

Results were expressed as % viability – the resorufin fluorescence measured in compound-treated wells relative to untreated controls.

3.16.5 *E. coli* antibacterial assay

To assess the effect of the compounds on the growth of *E. coli* cells, they were incubated at a fixed concentration of 50 µg/ml in 96-well plates containing *E. coli* for 6 hours. The numbers of cells remaining viable after exposure to the compound were determined by using the resazurin-based reagent and reading resorufin fluorescence in a multiwell plate reader. Results were expressed as % viability – the resorufin fluorescence measured in compound-treated wells relative to untreated controls. Compounds were usually tested in duplicate.

3.16.6 *In vitro* cytotoxicity assay

To assess the cytotoxicity effects of the compounds, they were incubated at a fixed concentration of 50 µg/ml in 96-well plates containing HeLa cells for 24 hours. The numbers of cells surviving drug exposure were determined by using the resazurin-based reagent and reading resorufin fluorescence in a multiwell plate reader.

Results were expressed as % viability – the resorufin fluorescence measured in compound-treated wells relative to untreated controls. Compounds were usually tested in duplicate. For the cytotoxicity assay, results are expressed as % cell viability, based on fluorescence reading in treated wells vs. untreated control well.

3.17 *In silico* molecular docking analysis procedure

Docking analysis was performed on Schrödinger suite software which was used both in the Knime workflow and in the glide grid docking.

3.17.1 Knime workflow docking

The 21 ligands were sketched in chemdoodle and were saved as Sdf files, and they were visualized in the discovery studio where they were saved as PDB files. The 3D structure of target protein trypanothione reductase; PDB Id, 6BU7 was downloaded from the PDB sum [124]. After downloading the structure in PDB format it was visualized in the Discovery Studio Visualizer [125] and saved as a PDB file.

A Knime workflow is a powerful tool designed to perform multitask scientific jobs such as docking and many other physico chemical properties of ligands as based on the Schrödinger software. Once the workflow was created the target protein (6BU7) was added to node 1 the ligands in PDB format are loaded in the PDB reader (node 6) (**figure 3.1**)

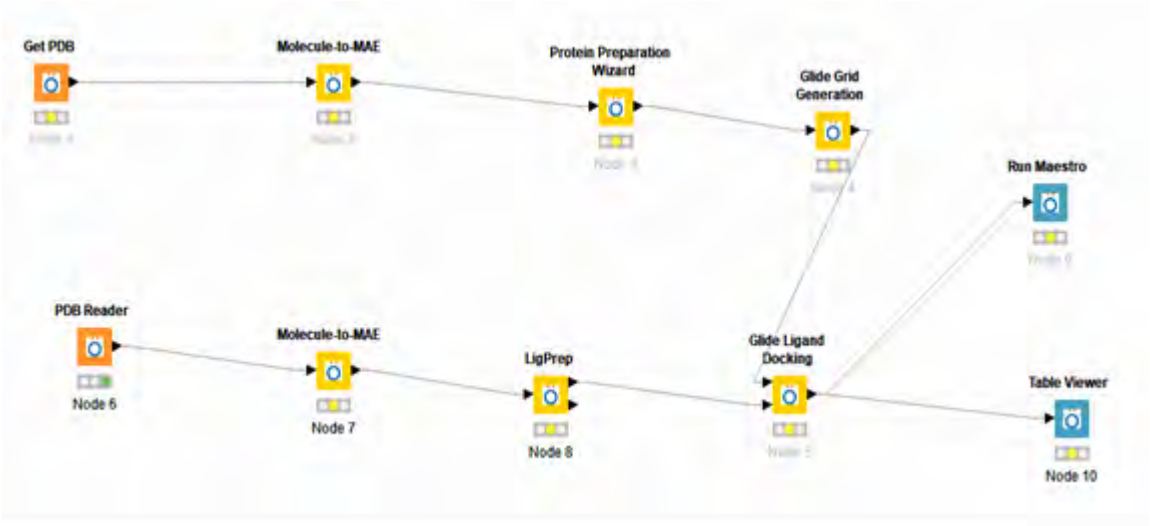

Figure 3. 1: The knime workflow summarizing the docking procedure

The software prepared the target protein and the ligands into different conformers automatically and it was executed in the table viewer (node 10).

3.17.2 Glide grid docking

The docking procedure was performed in the Maestro 12.6 which comes with the Schrödinger suite software. Each ligand in Sdf format or PDB format was prepared to suitable conformers and was docked into the active sites of the prepared protein prepared. The PDB of the target protein was downloaded by going into the file menu, selecting get PDB and the protein 6BU7 was typed and downloaded. The target protein was to be prepared using the protein preparation wizard, in which case Chain A was removed, the solvents were removed and other chemicals such as metallic ions were removed. The remaining part of the protein which was chain B was used in the docking procedure. The protein was prepared in the protein preparation wizard in which case it was first pre-processed, refined where the H-bonding was optimized, water was removed, and the protein was minimized. The grid box was generated by going into the task menu, receptor grid generation was selected and an atom from the ligand was picked to generate the grid box for docking

Then one ligand after another was imported and each was prepared to get several suitable conformers. By going into the task menu, ligand docking was selected, and each conformer was docked with the target protein.

3.18 SwissADME pharmacokinetic properties prediction

The 15 compounds that were active against trypanosomiasis were passed on the SwissADME filter to determine the pharmacokinetic, ADME (absorption, distribution, metabolism, and excretion. The active ligands were subjected to several parameters such as molecular mass, several hydrogen donors, acceptors; log P, GI (gastrointestinal absorption, etc. These parameters help determine if the ligand has lead likeness and drug-likeness. The ligands

were drawn and submitted in smiles format on the SwissADME filter, the ligands that have passed the SwissADME filter were subjected to the SCFBioserver to predict their drug-likeness as based on Lipinski Rule of Five.

3.19 Lipinski rule of five

The SCFBioserver was used to identify test compounds that have drug-likeness based on the RO5. During this procedure twelve test compounds from the first filter were prepared by drawing their chemical structure in the Marvin sketch where explicit hydrogen was added, afterwards, the structure was converted to 3D, saved in pdb format on desktop, and uploaded on the Lipinski drug filter.

CHAPTER 4

RESULTS AND DISCUSSION

4.1 Introduction to the chapter

This chapter discusses the observations and the challenges encountered in each experimental work. The full spectrum of each result obtained during the experimental work, including the characterization of several synthesized compounds and their intermediates, is discussed.

4.2 Retrosynthetic analysis

This study aimed first at designing a synthetic strategy towards an analogue of a chiral natural anthraquinone **6**. As described several synthetic approaches have been successfully employed in the synthesis of many anthraquinone derivatives [1] [97] [100]. However, the Friedel-Crafts acylation reaction between phthalic anhydride and benzene derivative was being envisaged to be exploited more in this transformation. The retro-synthetic analysis of the analogue of the natural chiral anthraquinone **6** (**Scheme 4.1**) yields first 2-acetyl-3-hydroxyanthracene-9,10-dione **88** and the latter yields two building blocks, namely 3-alkoxy phthalic anhydride **89** and benzene derivatives **91**. The phthalic anhydride **89** was sought to be suitable to react with 2-hydroxyacetophenone **91** in the Friedel-Crafts acylation manner and it could be derived from alkene **67.** The source of the alkene is anacardic acid **63** which is derived from the agro-waste cashew nut shells.

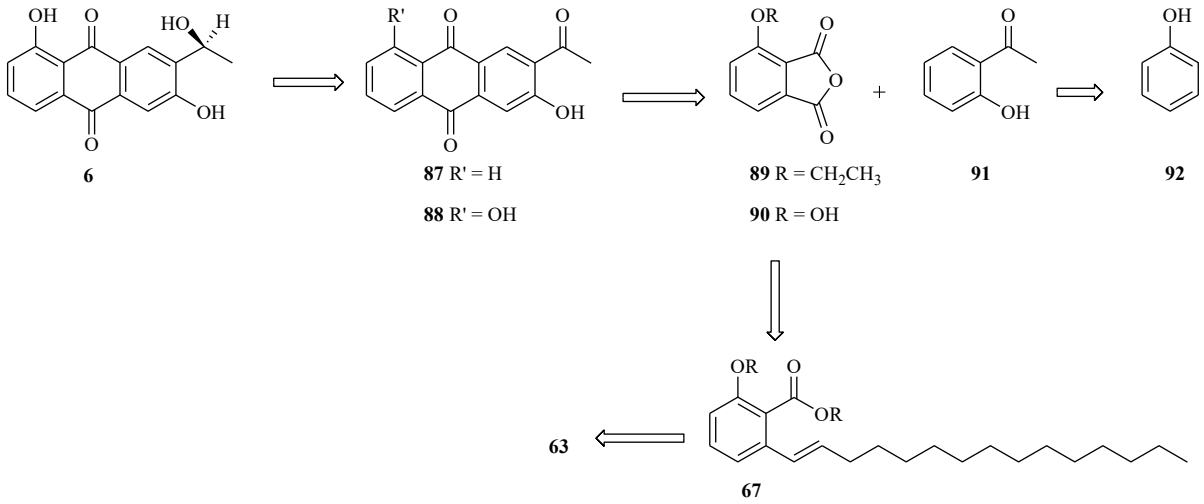

Scheme 4.1: The retrosynthetic analysis of the analogue of a chiral natural Anthraquinone 6

As reported earlier the versatility of the phenolic constituents of cashew nut shell liquid (CNSL) render them to be used as starting materials in organic synthesis [115] [116]. The chemical structure of anacardic **63** (**Figure 2.13**), the carboxylic acid functionality, the pentadecyl side chain are ortho to each other making possible for structural modifications to yield phthalic anhydride **89** (**Scheme 2.9** and **Scheme 4.1**)**.** As noted earlier anthraquinones, particularly of emodin type, are known to be of therapeutic potential due to their diverse biological properties such as antibacterial, anticancer, antiviral, antifungal, and antiprotozoal activities [50] [51]. The hydroxyl group of anacardic acid makes it possible to arrive at an emodin type of anthraquinone

4.3 Preliminary experiments on the synthetic strategies towards the analogue

A list of synthetic steps has been employed in the conversion of anacardic acid **63** to the analogue of chiral natural anthraquinone **6** (**Figure 1.2**). These synthetic strategies emanated from the extraction and the isolation of anacardic acid from the cashew nut shells. However, the finding obtained from this research provides an overview for the exploitation of anacardic acid to synthesize the 1,4,5-dihydroxyanthraquinone

4.4 Extraction and isolation of anacardic acid

Attempt to extract the cashew nut shells was first done using petroleum ether as a solvent. The use of this solvent could not give expected better results due to relatively low yields of the cashew nut shell liquid obtained in approximately 5% yield. Further extraction of the cashew nut shells using methanol as solvent could give better yields of CNSL in 27%. (**Figure 4.1**). The anacardic acid from the cashew nut shell liquid could be isolated in an acid-base reaction manner employing the method reported by Paramashivappa *et.al* [126]. In this method, 2 eq weight of CNSL in 5% aqueous methanol were reacted with 1 eq weight of calcium hydroxide forming calcium anacardate as a stable salt (**Scheme 4.2**).

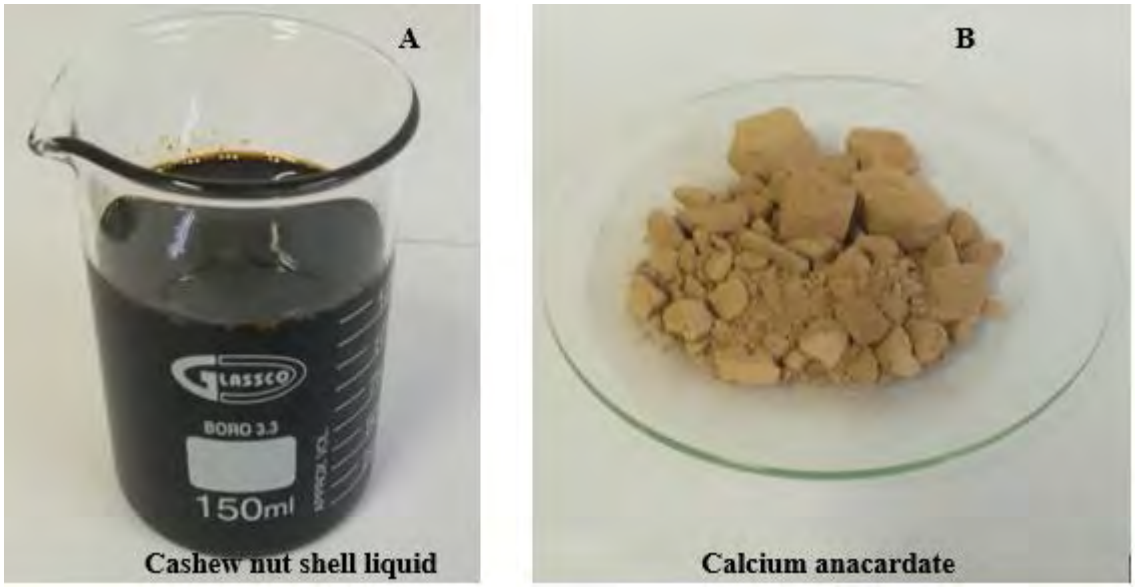

Figure 4. 1: Methanol extracted CNSL (A) and dried calcium anacardate (B)

The fine cake of the calcium anacardate was subsequently dried and hydrolysed at room temperature with 11M hydrochloric acid. The resultant mixture was stirred for one hour and extracted with ethyl acetate. The organic layer obtained after extraction with ethyl acetate was dried to give crude anacardic acid. After purification by column chromatography with 10% methanol/DCM anacardic acid **63** in 56% yields was obtained as a brownish liquid.

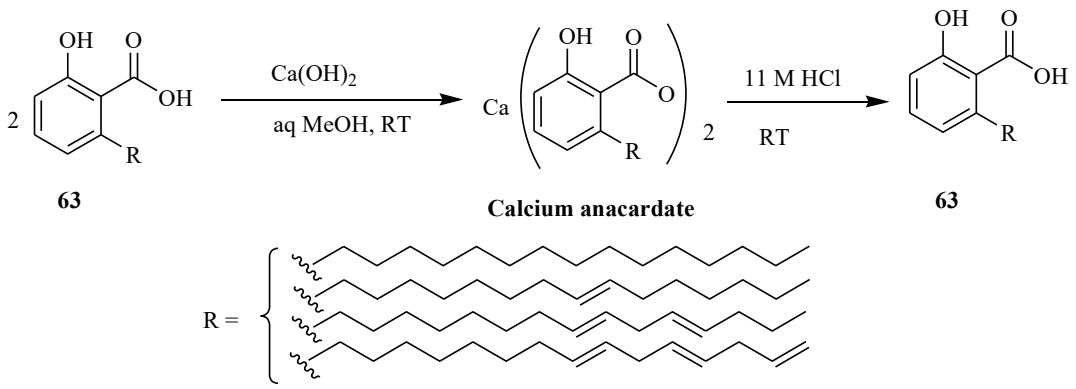

Scheme 4. 2: Isolation of anacardic acid from cashew nut shell liquid

4.5 Synthetic conversion of anacardic acid to (*S*)-1,6-dihydroxy-7-(1-hydroxyethyl)anthracene-9,10-dione 6

To synthesize the analogue of a chiral natural anthraquinone **6**, it was important to first prepare 4-ethoxyisobenzofuran-1,3-dione **89** (**Scheme 4.1**) an important precursor in the synthesis of anthraquinones. The 3-hydroxyphthalic anhydride **90** on the other hand is regarded as a synthon in preparation of anticancer drugs such as adriamycin and daunomycin (**Figure 1.1**). Many methods used in the preparation of this intermediate 3-hydroxyphthalic anhydride **90** (**Scheme 4.1**) suffer from the disadvantages of many reaction steps, low yields and the use of expensive chemicals [5] [6]. Thus, in this study, we are presenting an alternative source of 3-hydroxyphthalic anhydride from the readily available cashew nut shells. Moreover, the chemicals used in this transformation are readily available and cheap. During the preparation of this intermediate, the hydroxyl and carboxylic group of the anacardic **63** (**Scheme 4.3**) were to be first protected. The protecting agents of choice were diethyl carbonate and diethyl sulphate. The reaction of anacardic acid with diethyl carbonate in dimethylformamide under conditions of refluxing using potassium carbonate did not work better. This was evident by observing no change of starting material after developing a TLC plate of the reaction medium. However, by using a different protocol as reported by Reddy *et. al* [127] it was possible to protect acid **63** (**Figure 2.13**). In this method, the anacardic acid **63**

was ethylated in dry acetonitrile using diethyl-sulfate under reflux conditions (**Scheme 4.3**). After evaporation of solvent and column chromatography, the ester **67** was obtained in high yields 66%.

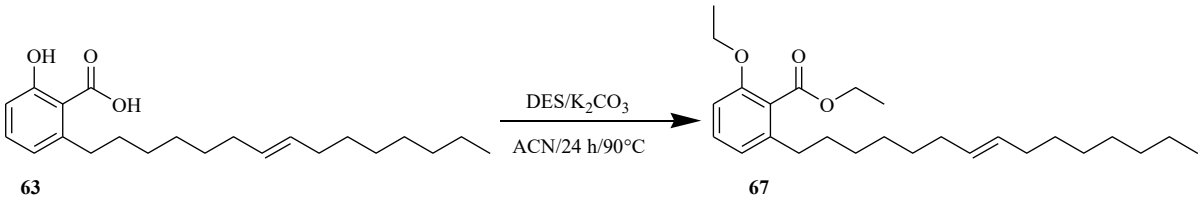

63 **67**

Scheme 4. 3: Alkylation of anacardic acid 63 to ester 67

The ^{1}H NMR spectrum of ester **67** exhibited two quartets at δ_H 3.95 and 4.32 ppm each integrating two protons. These two peaks signified the formation of the ether group and each corresponded to the two hydrogens of the ethoxy group of the phenolic and the carboxylic functionality. The aromatic protons were found to be resonating at δ_H between 6.62 to 7.16 ppm. This region exhibited a triplet at δ_H 7.12 ppm and two doublets at δ_H 6.72 and 6.64 ppm, each one integrated one proton. A multiplet at δ_H 5.28 ppm was assigned for the two protons carrying the alkene functionality

The ^{13}C NMR spectrum of compound **67** displayed signals at δ_C 59.8 and 63.3 ppm. The two signals were assigned to the methylene groups of the ethoxy group carrying the phenoxy functionality and the carboxylic acid functionality.

Three signals at δ_C 13.1, 13.3, and 13.7 ppm were being assigned for the terminal methyl group of the pentadecyl side chain and of two ethoxy groups. A peak at δ_C 167.3 ppm was being assigned for the carbonyl carbon of the carboxylic acid functionality.

The double bonds of the alkenyl side chain ester **67** were reduced using hydrogen gas under palladium 10% (w/w) as a catalyst. After 24 hours the reaction mixture was filtered over a Celite bed, the solvent evaporated giving the saturated compound **68** in 96% yields.

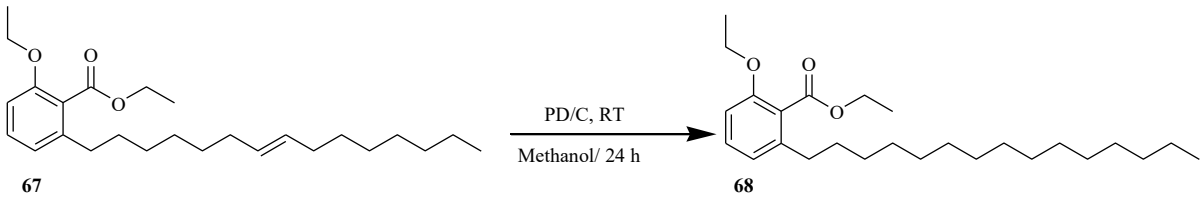

67 68

Scheme 4.4: Palladium-catalyzed hydrogenation of ester 67

The ^{1}H NMR spectrum of compound **68** (**Figure 4.2**) displayed two quartets at δ_H 3.92 and 4.30 ppm each integrating two protons. These two peaks corresponded each to the two hydrogens of the methylene groups of the ethoxy group functionality of phenoxy and carboxylic group.

This spectrum showed a remarkable disappearance of the multiplet at the δ_H between 4.87 and 5.69 ppm. This confirmed the consumption of the alkene functionality of the starting material **68**. A triplet at δ_H 2.55 ppm integrating two protons was being assigned for the two hydrogens of the benzylic protons. A quintet at δ_H 1.55 ppm integrating to two protons was being assigned for the two methylene hydrogens next to the benzylic group. A multiplet at δ_H 1.27 and 1.36 ppm which integrated to thirty protons was being assigned for the remaining hydrogens of the methylene groups of the pentadecyl side chain and the two methyl groups of the two ethoxy group

A triplet at δ_H 0.88 ppm integrating to three protons was being assigned for three hydrogens of the terminal methyl group of the pentadecyl side chain group. The downfield aromatic region showed a remarkable two doublets at δ_H 6.72 ppm and 6.79 ppm ortho to each integrating one proton. These two doublets were consecutively being assigned for the hydrogen ortho to phenoxy group and the pentadecyl side chain.

A triplet integrating one proton appeared at δ_H 7.21 ppm was being assigned to the aromatic proton para to the carboxylic group.

The ^{13}C NMR spectrum of the saturated compound **68** (**Figure 4.2**) showed two peaks next to each other at δ_C 60.9 and 64.2 ppm. These peaks were respectively being assigned for the two methylene carbons of the two ethoxy groups of the carboxylic and phenoxy functionality. Three peaks at δ_C 14.1, 14.3, and 14.7 ppm were being accounted for the three-terminal methyl groups of pentadecyl side chain of the two ethoxy groups.

This compound displayed its signal for the carbonyl and phenoxy group at δ_C 168.3 and 155.7 ppm respectively

Another signal at δ_C 130.0 ppm was being assigned for C-5 which is para to the carboxylic acid group functionality. A signal at δ_C 109.4 ppm was being assigned to C-6 which is ortho to the phenolic group.

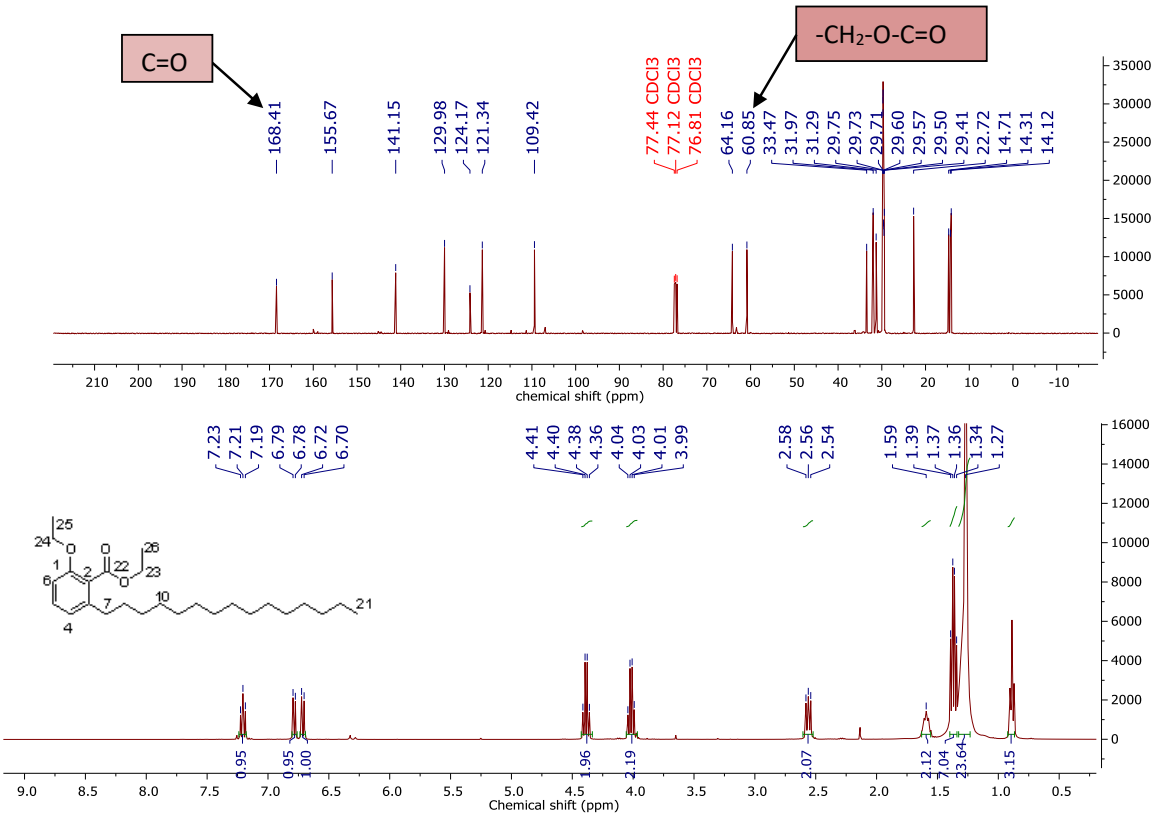

Figure 4.2: 400MHz ^{1}H and ^{13}C NMR spectrum of ethyl 2-ethoxy-6-pentadecylbenzoate 68 in $CDCl_3$)

A peak at δ_C 121.3 ppm was being assigned to C-4 while a signal at δ_C 141.2 ppm accounted for the carbon carrying the pentadecyl side-chain group. A signal at δ_C 124.2 ppm was assigned to C-2.

Different bromination methods to brominate compound **68** at benzylic position were attempted. The first trial involved the use of the method proposed by Xu *et. al* [128], In this protocol, alkane **68** in dichloromethane was brominated with molecular Br_2 under MnO_2 (non-activated) catalyst (**Scheme 4.5**). After half an hour the product formed was isolated and well-characterized through NMR spectroscopic methods. However, the NMR results, revealed that the target product **69** was not formed but product **69a** due to loss of regioselectivity.

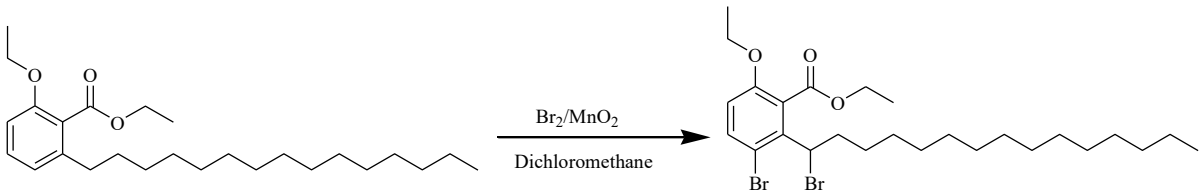

Scheme 4.5: Bromination of 68 to ethyl 3-bromo-2-(1-bromopentadecyl)-6-ethoxybenzoate

The target product was not formed and our desire was to brominate at the benzylic position, the search for a suitable bromination method was therefore necessary. The use of N-Bromosuccinamide and radical initiators such as benzoyl peroxide or 2,2′-azobisisobutyronitrile (AIBN) has been used for benzylic bromination in many syntheses [129] [130].

The most prominent solvents that are used in this reaction are benzene and CCl_4. The use of these solvents is mostly not recommended due to their toxicity. Green solvents such as ethyl acetate, water, acetonitrile, and chlorobenzene for substituting hazardous CCl_4 are being encouraged these days [130]. However, when attempted to brominate the saturated compound **68** with NBS and using a catalytic amount BPO in chlorobenzene at 80 ℃ for 12 hours as indicated by the TLC of the reaction medium no change of the starting material was observed. The trial to brominate saturated compound **68**, as reported by Lograd*o et.al* [131] in CCl_4 could result to the formation target product **69** (**Scheme 4.6**). In this method, 1.2 equivalents of N-Bromosuccinamide and 10% (w/w) of a suitable free radical initiator were used. The radical initiators of choice that were used were AIBN and benzoyl peroxide. The AIBN was to be first air dried to get the pure crystals before it was used. Using AIBN initiator in this reaction target bromide **69** was obtained in 91% yields with easy purification procedures. The radical initiator benzoyl peroxide (BPO) (**Scheme 4.7**) was to be synthesized from benzoyl chloride by adopting the method reported by Flowers and Leffler [132].

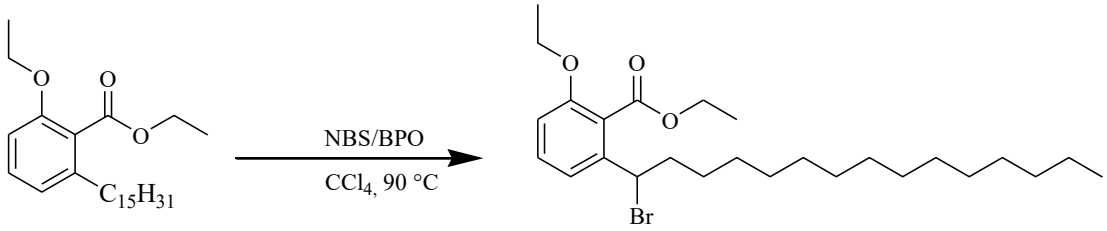

68 **69**

Scheme 4.6: Benzylic bromination of the saturated alkane 68

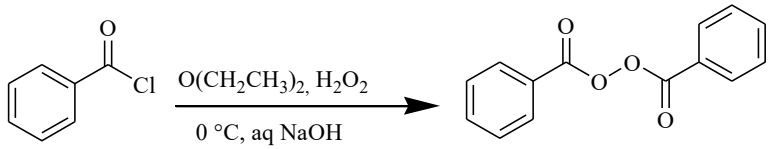

93 **94**

Scheme 4.7: Preparation of benzoyl peroxide 94 from benzoyl chloride [132]

The ^{1}H NMR spectrum of the target bromide **69** exhibited a remarkable appearance of a triplet at δ_H 4.91 ppm which integrated one proton. This signal accounted for the benzylic proton and signified a proof of the formation of the target product **69**.

This spectrum showed two quartets as well at the chemical shift of 3.99 and 4.38 ppm each integrating two protons. These two signals corresponded each to the two hydrogens of methylene groups of the ethoxy group functionality of phenoxy and carboxylic group.

A multiplet at δ_H 2.13 ppm integrating to two protons was being assigned for the two hydrogens next to the benzylic group.

A multiplet at δ_H between 1.17 to 1.33 ppm which integrated thirty protons was being assigned for the remaining hydrogens of the methylene groups of the pentadecyl side chain and the two methyl groups of the ethoxy group.

A triplet at δ_H 0.84 ppm integrating three protons was being assigned for the three hydrogens of the terminal methyl group of the pentadecyl side-chain group.

The region showed three signals which were observed two doublets at δ_H 6.78 and 7.12 ppm. These peaks each integrated one proton and were accounted for the hydrogen ortho to both the phenoxy and the aliphatic group.

A triplet integrating to one proton appeared at δ_H 7.28 ppm was being assigned to the aromatic proton para to the carboxylic group.

The ^{13}C NMR spectrum of bromide **69** showed two peaks next to each other at δ_C 61.4 and 64.4 ppm. These peaks were respectively being assigned for the two methylene groups of carboxylic functionality and phenoxy functionality. Three peaks at δ_C 14.1, 14.3 and 14.7 ppm were being assigned for the three terminal methyl groups of pentadecyl side chain and of the terminal ethoxy group (phenoxy and carboxylic group respectively).

The carbonyl group ester functionality of this compound displayed its signal at δ_C 167.4 ppm. Another signal at δ_C 155.4 ppm was acquainted for the aromatic carbon carrying the phenoxy group. The HSQC and HMBC spectra were in conjunction used to assign each carbon present in the compound. A signal at δ_C 130.8 ppm was being assigned for the carbon para to the carboxylic acid group functionality. A peak at δ_C 111.5 ppm was being assigned C-6. A signal at δ_C 120.0 ppm was assigned to C-4 (carbon meta to the carboxylic acid functionality). A peak at δ_C 140.4 ppm was being assigned for the carbon carrying the pentadecyl side-chain group. A peak at δ_C 123.1 ppm was being assigned for the carbon carrying carboxylic functionality.

Dehydrobrominated of compound **93** was first attempted using potassium *tert*-butoxide, however as indicated from the TLC the reaction could not work. Wolkoff P in 1981 conducted a study highlighting on the effectiveness of this base when applied to primary alky bromides [133]. This scholar further indicated the superiority of 1,8-Diazabicyclo [5.4.0] undec-7-ene (DBU) in the dehydrohalogenation of secondary and tertiary bromides [133]. In

this present work bromide **69** was reacted with DBU in dry toluene under conditions of refluxing (**Scheme 4.8**). After six hours the reaction was quenched with 10% HCl and extracted with ethyl acetate. After evaporation of solvent and purification through column chromatography desired alkene **70** in 87 % yields was obtained.

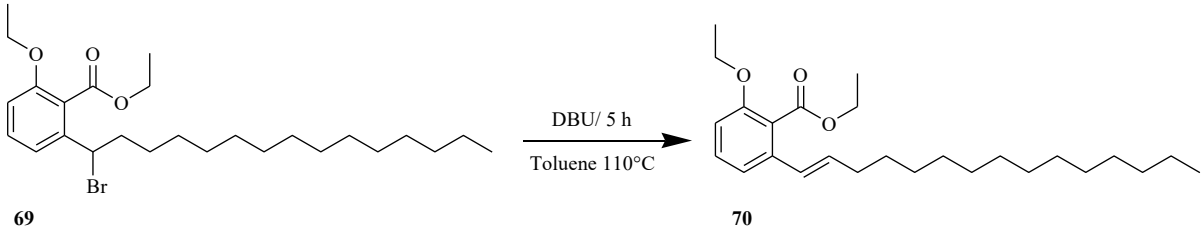

69 **70**

Scheme 4. 8: Dehydrobromination of ethyl 2-(1-bromopentadecyl)-6-ethoxybenzoate to Alkene 70

The ^{1}H NMR spectrum of alkene **70** (**Figure 4.3**) was acquainted with the presence of a doublet at δ_H 6.44 and a multiplet at δ_H 6.27 ppm each integrating one proton. These two hydrogens respectively accounted for two hydrogens of the alkene functionality next to each other. The coupling constant (*J*) of alkene **70** was found to be 15.7 Hz which is characteristic to *trans* configurations [134]. Two quartets at δ_H 4.09 and 4.46 ppm each integrating two protons were each assigned to the two hydrogens of methylene protons for the phenoxy and carboxylic group. A quartet at δ_H 2.24 ppm integrating two protons accounted for the methylene hydrogen next to the alkene group. A triplet at δ_H 0.95 ppm integrating to three protons was assigned for the three hydrogens of the terminal pentadecyl group. A multiplet at δ_H 1.33 ppm integrating twenty-eight protons was assigned to the twelve methylene hydrogens of the pentadecyl side chain and for the two methyl groups of the ethoxy group.

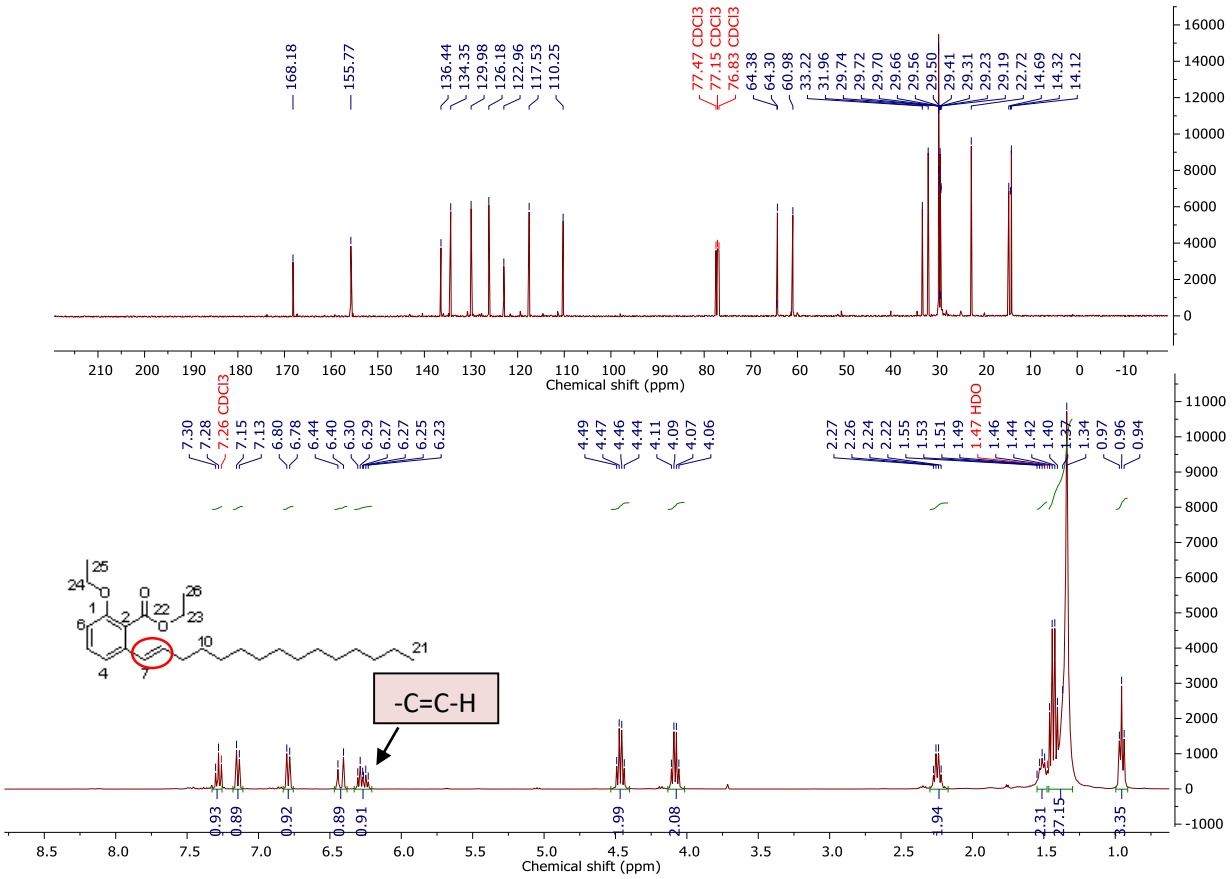

Figure 4.3: 400MHz ^{1}H NMR and ^{13}C NMR spectrum of (*E*)-ethyl 2-ethoxy-6-(pentadec-1-en-1-yl)benzoate 70 in $CDCl_3$

The aromatic region of this spectrum exhibited two doublets at δ_H 6.78 and 7.14 ppm integrating one proton. These were respectively assigned to the hydrogen *ortho* to the phenoxy group and *ortho* to the pentadecyl side chain. A triplet integrating one proton appeared at δ_H 7.27 ppm was being assigned to the aromatic proton para to the carboxylic group.

The ^{13}C NMR spectrum of this alkene **70** displayed signals at δ_C 61.0 and 64.3 ppm (**Figure 4.3**). These signals accounted for the two methylene carbons of the ethoxy group of the carboxylic acid functionality and the phenoxy. The terminal methyl groups of the pentadecyl side chain and the two ethoxy groups resonated at δ_C 14.1, 14.3, and 14.6 ppm, respectively. The aromatic region of this spectrum displayed an increased number of two extra peaks as

compared to the respective starting material **69**. A signal displayed at δ_C 110.2 ppm was being assigned (C-6) the carbon ortho to the phenoxy group. Another signal at δ_C 130.0 ppm was assigned (C-5) carbon para to the carboxylic acid functionality. A signal at δ_C 117.5 ppm was assigned to (C-4) the carbon ortho to the pentadecyl side chain. A signal at δ_C 126.15 ppm was assigned to the benzylic carbon of the alkene functionality. A signal at δ_C 134.4 ppm was assigned to (C-8) the alkene carbon next to the benzylic position.

A signal at δ_C 136.4 ppm was assigned to the carbon carrying the pentadecyl side chain. A signal at δ_C 122.9 ppm was assigned for the carbon carrying the carboxylic acid functionality. Two signals at δ_C 155.8 and 168.2 ppm accounted for C-1 and the carbonyl group, respectively. These results were pretty enough to confirm the successful formation of the compound and perfectly matched with the results reported by Lograd*o et.al* [131]

4.6 Oxidation of (*E*)-ethyl 2-ethoxy-6-(pentadec-1-en-1-yl)benzoate 70

The oxidative cleavage of alkenes is a synthetically useful transformation in the synthesis of bioactive natural products, pharmaceuticals, agrochemicals [135]. Mechanistically, there are only two main options available to perform this transformation; ozonolysis and dihydroxylation using RuO_4 and OsO_4. Each one of these methods is toxic in the sense that they require the use of toxic high-valent oxometals while the former generates ozonide intermediate which is explosive [129]. These reasons necessitated the search for environmentally friendly methods to cleave alkene **70**

In this aspect, a couple of methods were chosen and attempted to oxidize the alkene **70** to its respective oxidative product. The oxidizing agents of the first choice were potassium permanganate and sodium periodate. However, when each of these was used as observed from the TLC results, there was no indication of the formation of the desired product. These challenging result paved the way for more literature search of oxidizing agents to be used. It

was later found that when alkene **70** was oxidized under mild conditions of an oxygen atmosphere, utilizing sodium nitrite and benzoic acid adopting a protocol reported by Yin *et.al* [129]. By acquiring this procedure the respective aldehyde **71a** was formed (**Scheme 4.9**). This protocoal as well did not give better results as expected, due to its shortcoming of long reaction times and yielded product **71a** which was not easily purified under normal chromatography columns.

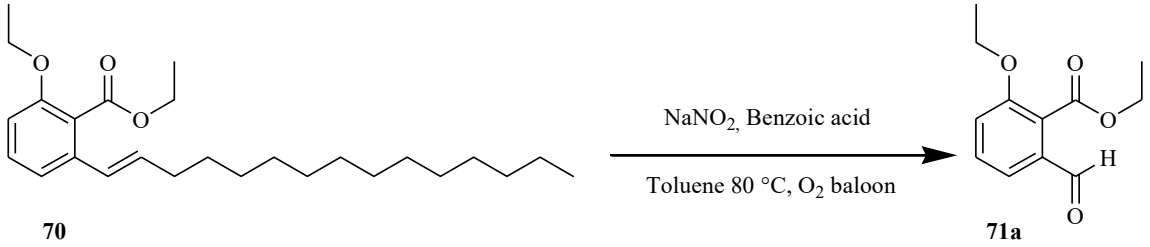

70 **71a**

Scheme 4.9: Mild oxidation of (*E*)-ethyl 2-ethoxy-6-(pentadec-1-en-1-yl)benzoate with sodium nitrite

The ^{1}H NMR spectrum of aldehyde **71a** showed a singlet at the chemical shift of 9.90 ppm which accounted for the aldehydic proton. The ^{13}C NMR spectrum of this product displayed a signal at 190.4 ppm which corresponded to the carbonyl carbon of the aldehyde functional group.

The use of iron as a cheap catalyst to cleave C=C bonds has recently evolved the interests of chemists to be used in green chemistry works [136][137]. From this point of view, we cleaved alkene **70** successfully using inexpensive *tert*-butyl Hydroperoxide under iron catalysis, adopting a method reported by Shaikh and Hong [138]. In this procedure (*E*)-ethyl 2-ethoxy-6-(pentadec-1-en-1-yl) benzoate **70** to carboxylic acid was treated with aqueous *tert*-butyl hydroperoxide (TBHP) after 2.5 days the ethoxy phthalic acid **71** was obtained in 64% yields as a white solid (**Scheme 4.10**). In this current study, it is worthy to note that the ethoxy phthalic acid **71** was obtained in good yields with the easiest purification procedure.

This confirms that the cashew nut shell liquid is a good candidate for synthesizing 3-hydroxyphthalic anhydride which is an intermediate for the synthesis of anthracycline anticancer drugs.

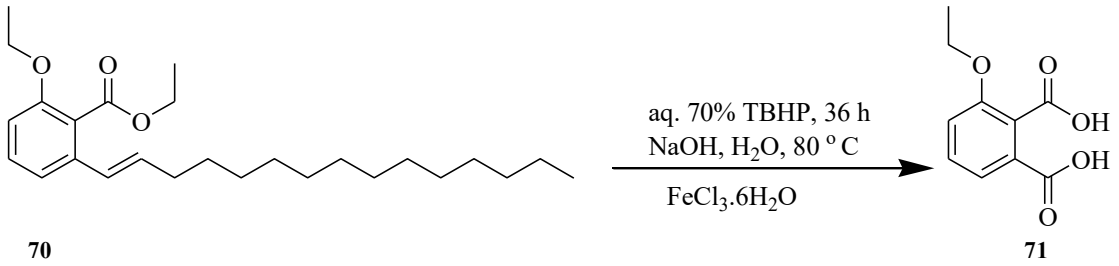

70 **71**

Scheme 4.10: $FeCl_3 \cdot 6H_2O$-catalyzed oxidation of (*E*)-ethyl 2-ethoxy-6-(pentadec-1-en-1-yl)benzoate to carboxylic acid

The ^1H NMR spectrum (**Figure 4.4**) of the carboxylic acid **71** showed a remarkable disappearance of the aliphatic side chain. A single quartet at δ_H 3.84 ppm integrating two hydrogens indicated the presence of protons of the $-CH_2-$ of the ethoxy group of the phenolic group. The presence of a single quartet implies that the other ethoxy group of the carboxylic group was hydrolyzed. A triplet at δ_H 1.04 ppm integrating three protons was assigned to the three methyl hydrogens of the ethoxy group. The aromatic region displayed a doublet at δ_H 7.24 ppm which integrated to one proton and a multiplet at δ_H 7.44 ppm which integrated to two protons.

The ^{13}C NMR spectrum of carboxylic **71 (Figure 4.4**) was marked by the appearance of 10 peaks which indicated the presence of 10 carbon atoms. This spectrum displayed two signals at δ_C 168.3 and 166.6 ppm which confirmed the presence of two carboxylic groups. The ^{13}C DEPT 135 experiment (**Figure 4.5**) displayed a maximum of five peaks, which corresponded to the number of carbon atoms carrying hydrogen atoms. In this spectrum, the CH_3 and C-H displayed positive signals while the CH_2 displayed a negative signal.

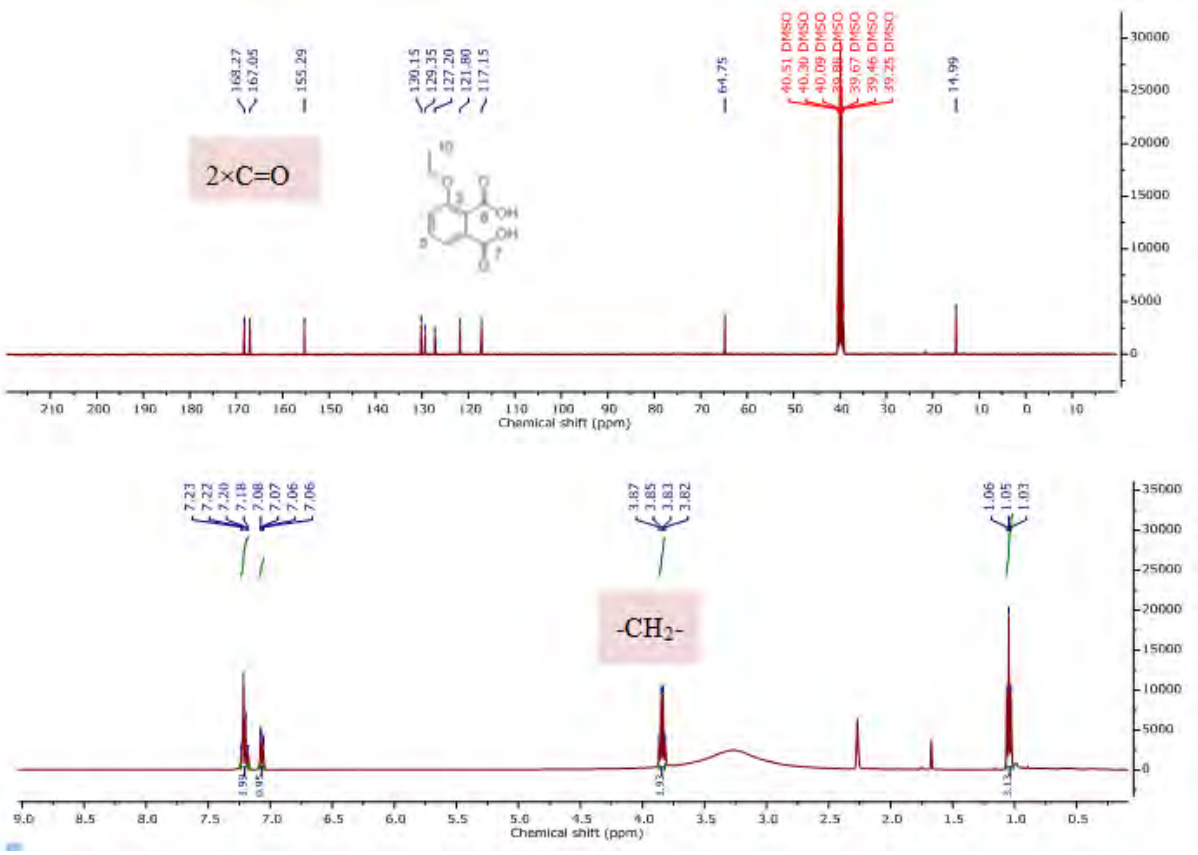

Figure 4.4: 400MHz ^{1}H and ^{13}C NMR spectrum of 3-ethoxyphthalic acid 71 in DMSO

This carboxylic can also be obtained commercially but it is very expensive and hence synthesizing it from cashew nut shells offers another source of 3-hydroxyphthalic acids.

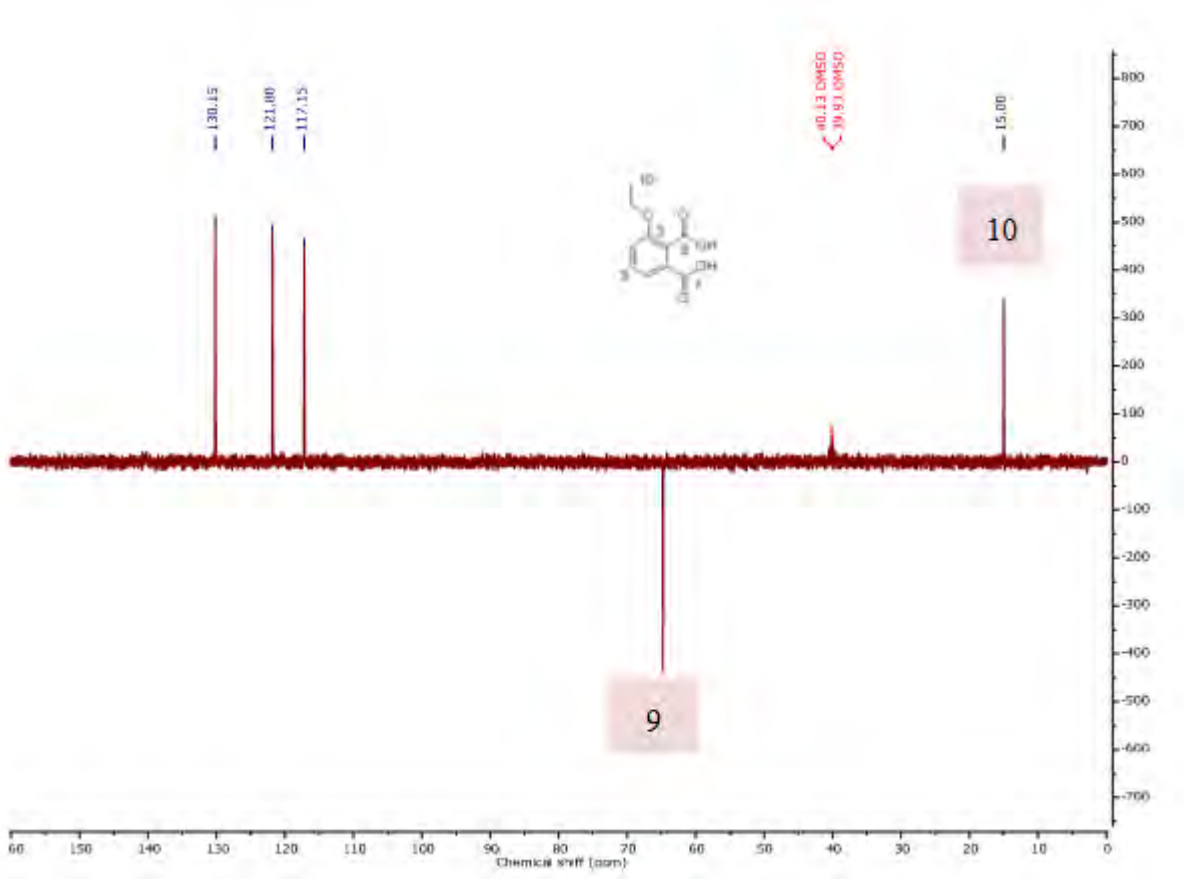

Figure 4.5: 400MHz ^{13}C DEPT-135 spectrum of carboxylic 71 in DMSO

4.7 Preparation of phthalic anhydrides

The 4-ethoxyisobenzofuran-1, 3-dione was prepared from 3-ethoxyphthalic acid **71** (**Scheme 4.11**). In this case under nitrogen condition, 3-ethoxyphthalic acid was treated with thionyl chloride and heated to reflux at 90 ℃ for 12 hours.

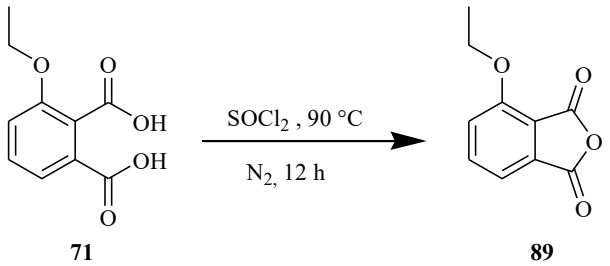

71 **89**

Scheme 4.11: Synthesis of 4-ethoxyisobenzofuran-1, 3-dione from 3-ethoxyphthalic acid

After evaporation of the solvent and chromatographic purification compound, the anhydride **89** was formed in a 37% yield. The ^{1}H NMR spectrum of 4-ethoxyisobenzofuran-1,3-dione **89**, showed a triplet at δ_H 7.84 ppm which integrated one proton. This proton was being assigned to the hydrogen *meta* to the phenoxy group. A doublet at δ_H 7.57 ppm integrating one proton was assigned to the hydrogen para to the Ethoxy group. Another doublet at δ_H 7.34 ppm which integrated one proton was assigned for the hydrogen ortho to the ethoxy group.

A quartet at δ_H 4.33 ppm two protons accounted for the two hydrogens of the methylene groups. A triplet at δ_H 3.20 ppm integrating three protons was assigned to the three hydrogens of the terminal methyl group.

The ^{13}C NMR of the anhydride **89** displayed the signals for the carbonyl group resonating at δ_C 162.6 and 160.1 ppm. These peaks were a significant confirmation of the formations of the 4-ethoxyisobenzofuran-1, 3-dione.

A signal displayed at δ_C 157.4 ppm was accounted for the carbon carrying the phenoxy group. The methylene carbon of this compound was found to be resonating at δ_C 65.5 ppm. Another signal at δ_C 14.4 ppm was accounted for the terminal methyl group. It was of curiosity find to other alternative sources of phthalic anhydride so that it could be coupled first with 2-hydroxy acetophenone **91.** The commercially available phthalic acid was converted to phthalic anhydride by refluxing in acetic anhydride at 140 ℃ (**Scheme 4.12**) by adopting the method reported by Zhang *et. al* [139]. After evaporation of the solvent, the product formed **97** was used for the next reaction.

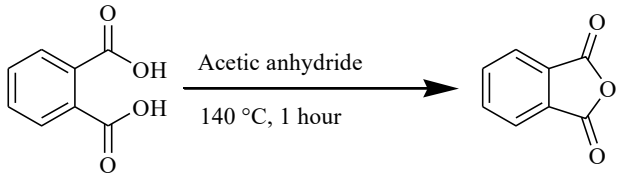

Scheme 4.12: Synthesis of isobenzofuran-1, 3-Dione 96 from phthalic acid

4.8 Preparation of the 2-hydroxyacetophenone

The 2-hydroxyacetophenone (**Scheme 4.13**) was prepared by the O-acetylation of phenol **92** with acetic anhydride using a catalytic amount of sulphuric acid Tu *et.al* [140]. The phenyl ester **97** was then reacted under anhydrous conditions using aluminium trichloride in a Fries rearrangement manner to afford the 2-hydroxyacetophenone **91**. Fries rearrangement can be defined as a type of organic reaction which transforms phenyl esters to acyl phenols in the presence of a Friedel-Crafts catalyst [141] [142].

The ^{1}H NMR spectrum of phenylacetate **97** displayed a significant number of four peaks. A signal at δ_H 2.32 ppm integrating three protons this peak was accounted for the three hydrogens of the acetyl group. The aromatic region had a doublet at δ_H 7.17 ppm integrating to two protons. These protons were being assigned for the two hydrogens ortho to the phenyl ester. A triplet at δ_H 7.30 ppm integrating one proton was being assigned to hydrogen para to the phenyl ester.

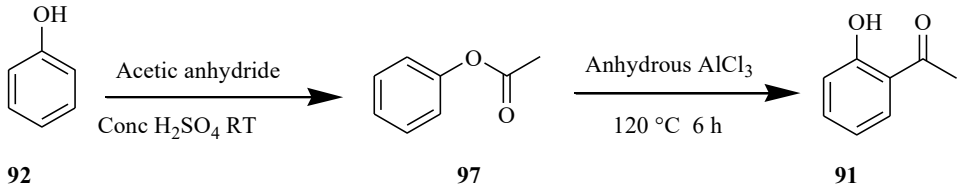

Scheme 4.13: Synthesis of 2-hydroxy acetophenone 91 from phenol 92

A triplet at δ_H 7.45 ppm integrating to two protons was being assigned for the two hydrogens Meta to the phenyl ester group. The ^{13}C NMR spectrum of the phenylacetate **97** displayed a total of six peaks which confirmed the successful formation of the compound

The ^{1}H NMR of the 2-hydroxy acetophenone **91** (**Figure 4.6**) showed two triplets at δ_H 6.77 and 7.36 and another two doublets at δ_H 6.86 and 7.61 ppm which each was integrating into one proton. These four protons corresponded to the four aromatic hydrogens of the 2-hydroxy acetophenone. A signal at 2.49 ppm integrating to three protons accounted for the three hydrogens of the acetyl group. The ^{13}C NMR spectrum of 2-hydroxy acetophenone **91** had its signals resonating at δ_C 26.6 ppm which was assigned to the aliphatic carbon of the acetyl group. A signal at δ_C 204.6 ppm accounted for the carbonyl group. Another signal at δ_C 162.4 ppm was assigned for the carbon carrying the phenol group. The remaining five aromatic carbons were found to be resonating at δ_C 118.3, 118.9, 119.7, 130.8, and 136.8 ppm. The appearance of these eight peaks confirmed the successful formation of the 2-hydroxy acetophenone

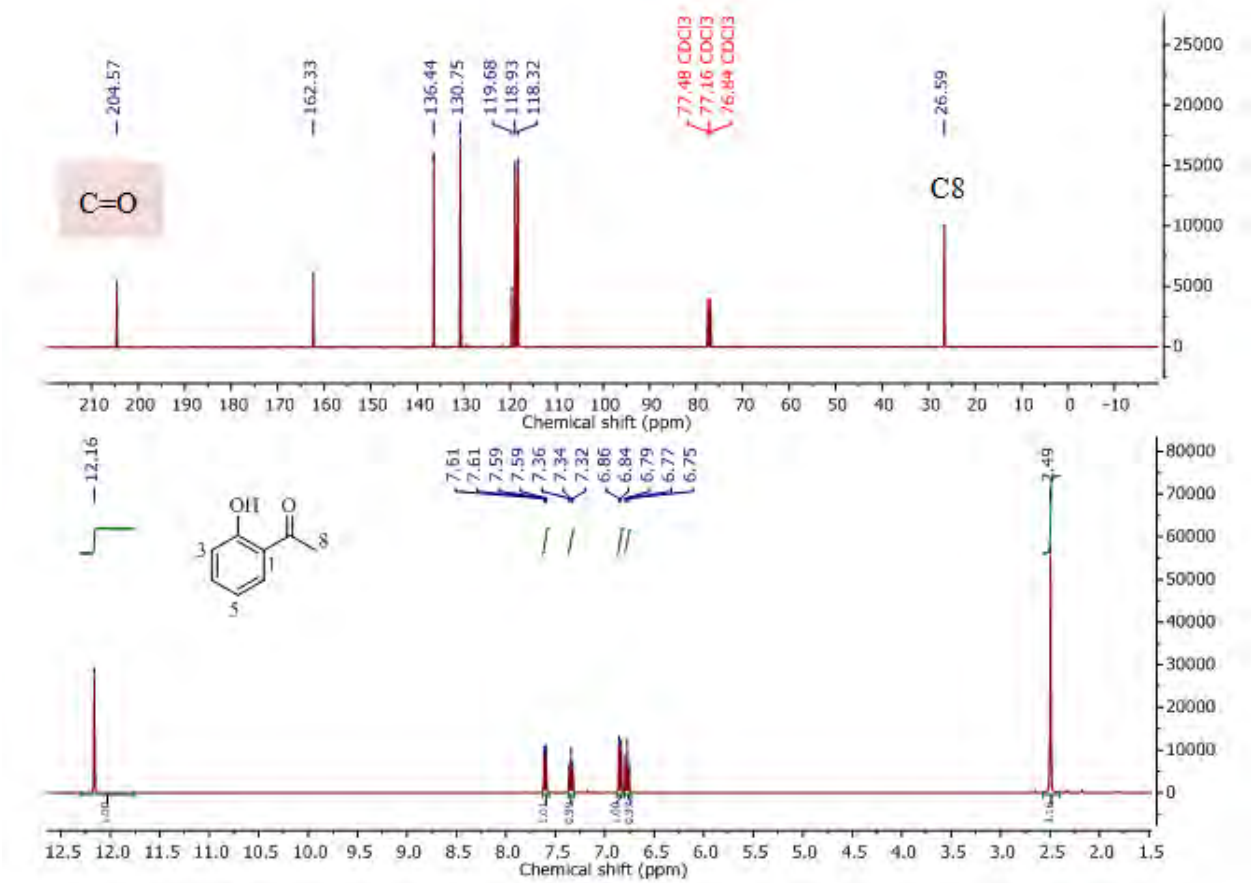

Figure 4.6: 400MHz ^{1}H and ^{13}C NMR spectrum of 2-hydroxyacetophenone in $CDCl_3$

4.9 Friedel-Crafts acylation

In the present study, the Friedel-Crafts acylation was envisaged to couple the 4-ethoxyisobenzofuran-1,3-dione **89** and 2-hydroxy acetophenone **91** by using a mixture of $AlCl_3$/NaCl as a catalyst. The main task was to synthesize the analogue of a chiral natural anthraquinone **6**. In this context, the 4-ethoxyisobenzofuran-1,3-dione **89** was prepared from anacardic acid **63** which is a by-product of the cashew industry (**Scheme 4.12**). Moreover, isobenzofuran-1, 3-dione **96** as shown from above was prepared (**Scheme 4.13**) it was first coupled with the 2-hydroxyacephenone **91** to create the anthraquinone nucleus.

4.10 Synthesis of 2-acetyl-3-hydroxyanthracene-9, 10-dione 87

As discussed earlier the approach towards the synthesis of 2-acetyl-3-hydroxyanthracene-9, 10-dione **87** was Friedel-Crafts acylation between isobenzofuran-1,3-dione **96** and 2-hydroxyacetophenone **91** (**Scheme 4.14**). This could result to 2-acetyl-3-hydroxyanthracene-9,10-Dione **87** by adopting the methodology reported by Hicks *et.al* [143]. Enzymatic reduction of anthraquinone carbonyl **87** would afford the target anthraquinone **6**.

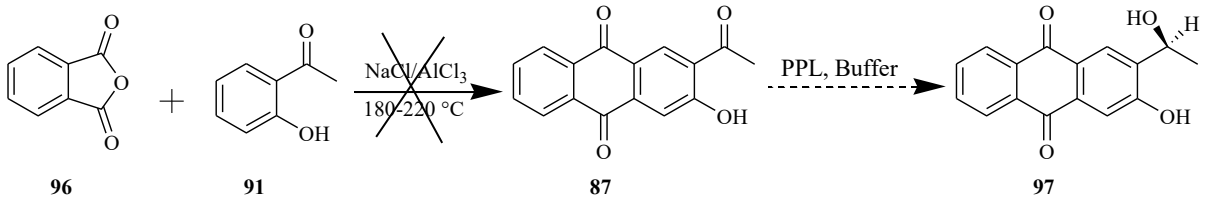

96 **91** **87** **97**

Scheme 4.14: Friedel-Crafts reaction of phthalic anhydride and 2-hydroxyacetophenone

However, when attempted the reaction (**Scheme 4.14**) did not work as the product formed was black as tar which was not verified by NMR spectroscopic method. The reason for this failure was due to the lack of symmetry properties of one of the reactants. Another reason that attributed to this discouraging result, is that the two groups of the 2-hydroxyacetophenone **91** *ortho* to each other para directors and meta directors unfavourable for the cyclization process.

Apart from synthesizing 2-hydroxyacetophenone, other benzene derivatives such as 3-nitroacetophenone, 3-aminoacetophenone, and 3-iodoacetophenone were consecutively synthesized from acetophenone. Moreover, due to the discouraging results from above, none of them were coupled with the phthalic anhydride. The section below discussed the synthetic transformation of acetophenone to 3-iodoacetophenone.

4.11 Synthetic transformation of acetophenone to 3-iodoacetophenone 101

The 3-nitroacetophenone was prepared by adding acetophenone dropwise to cold fuming nitric 99% at -45 °C (**Scheme 4.15**) while maintaining this temperature for 2½ hours. After workup procedures, the 3-nitroacetophenone was obtained as a creamy powder 51%

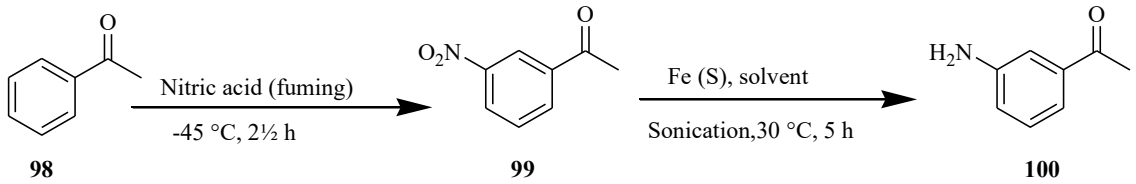

98 **99** **100**

Scheme 4. 15: Synthesis of 3-amino acetophenone 100 from acetophenone 98

The ^{1}H NMR of the 3-nitroacetophenone **99** showed a maximum number of 5 peaks. The hydrogen between the acetyl and the nitro group appeared as a singlet and was found to be resonating at δ_H 8.70 ppm. Two consecutive doublets and a triplet were each found to be resonating at δ_H 8.37, 8.24, and 7.62 ppm. Each of these three protons was found to be integrating to one proton. These four protons were being assigned to the four aromatic protons.

The aliphatic region was being characterized by a singlet at δ_H 2.62 ppm integrating three protons. These three protons were being assigned to the three protons of the acetyl group.

The ^{13}C NMR spectrum 3-nitroacetophenone **99** showed the remarkably number 8 peak in which case a peak at δ_C 195.4 ppm was being assigned to the carbonyl functionality of the acetyl group

Reducing the 3-nitroacetophenone using hydrogen gas under palladium catalysts gave 3-amino acetophenone in approximately low yields 10%. The yield was only sufficient for NMR characterizations. However, when attempting to reduce using Iron powder under ultrasonic irradiation adopting the method reported by Gamble *et.al* [144], target 3-amino

acetophenone was obtained in 53%. The ^{1}H NMR spectrum of the 3-amino acetophenone **100** showed a doublet at the δ_H of 7.23 ppm integrating one proton. Another doublet at δ_H 6.77 ppm integrating one proton and a multiplet at the δ_H 7.17 to 7.14 ppm integrating two protons were assigned for the aromatic protons. A broad peak at δ_H 3.77 ppm integrating to two protons was accounting for the two hydrogens of the amine group. A singlet at δ_H 2.48 ppm integrating three protons was assigned to the protons of the acetyl group.

The 3-iodoacetophenone **101** was synthesized from 3-aminoacetophene **100** (**Scheme 4.16)** by using the method reported by Jiang *et.al* [145]. This unique transformation of an aromatic amino group to halide is called the Sandmeyer reaction. The Sandmeyer reaction is a versatile tool in transforming an amino group attached to an aromatic ring to an aryl halide via diazonium salt intermediates [146]. In this method m-aminoacetophenone in concentrated hydrochloric acid was diazotized by using sodium nitrite under cold conditions, and then reacted with potassium iodide to yield the 3-iodoacetophenone 54%.

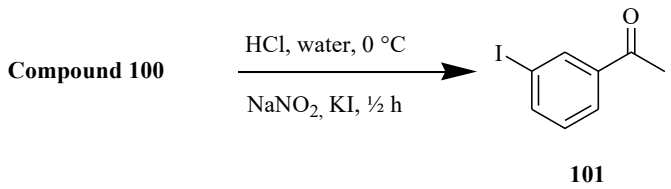

101

Scheme 4.16: Synthesis of 3-iodoacetophenone 100 from 3-amino acetophenone 101

The ^{1}H NMR spectrum of the 3-iodoacetophenone **101 (Figure 4.7)** showed a singlet at δ_H 8.19 ppm which was integrating one proton. This proton was assigned for the aromatic hydrogen atom situated between the two substituent groups (the acetyl substituent group and the iodo substituent group)

A multiplet at the δ_H 7.78 ppm which was integrated two protons was accounting for the two aromatic hydrogens ortho to the acetyl group and the iodo group. A triplet of doublet

appeared at the δ_H of 7.11 ppm which integrated one proton was assigned to the hydrogen meta to the acetyl substituent group. The ^{13}C NMR spectrum of the 3-iodoacetophenone **101** was characterized with the appearance of 8 signals. A signal at δ_C 94.5 ppm was assigned for the carbon carrying the iodo-substituent group. A signal at 196.6 ppm was accounted for the carbonyl carbon of the acetyl substituent group.

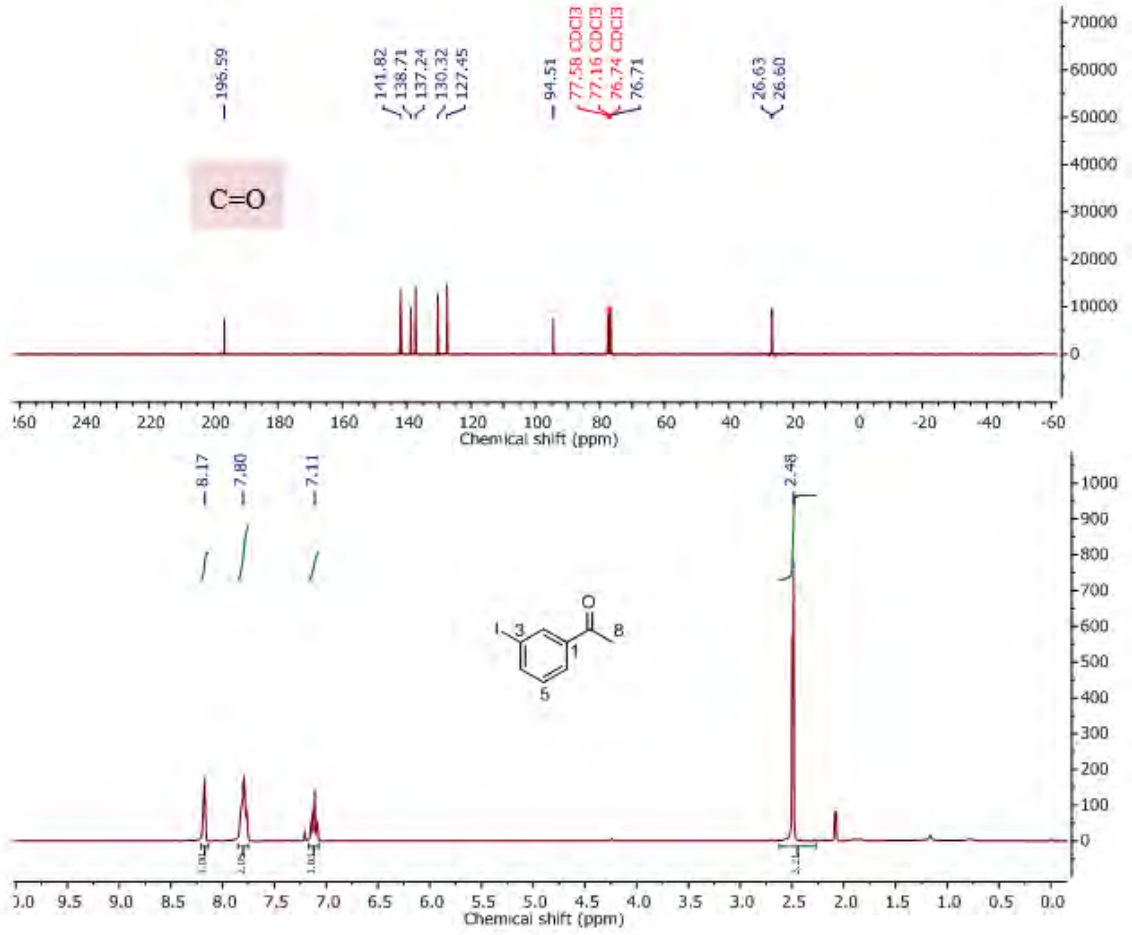

Figure 4. 7: 400MHz ^{1}H NMR spectrum of1-(3-iodophenyl)ethanone 101 in $CDCl_3$

4.12 New synthetic approaches and the modified Marschalk reaction

The use of the 1,4-dihydroxyanthraquinone as a synthon as described earlier has recently gained attention to be used for the synthesis of anticancer drugs [12] [16].

In this present study, we successfully synthesized the 1,4-dihydroxyanthraquinone from phthalic anhydrides **89** and **96** (**Scheme 4.12 and Scheme 4.13**) and 1, 4-benzenediol **102**.

Marschalk reaction was later employed in the introduction of the hydroxyalkyl group to the 1, 4-dihydroxyanthraquinone **42**. The Friedel-Crafts acylation was used in the coupling of the two anhydrides with the 1,4-benzenediol to form 1,4-dihydroxyanthraquinones **42** and **72**. However it was observed that phthalic acid without converting to its respective anhydride reacted with 1,4-benzenediol **102** preferably to give the anthraquinone (quinizarin) (**Scheme 4.17**)

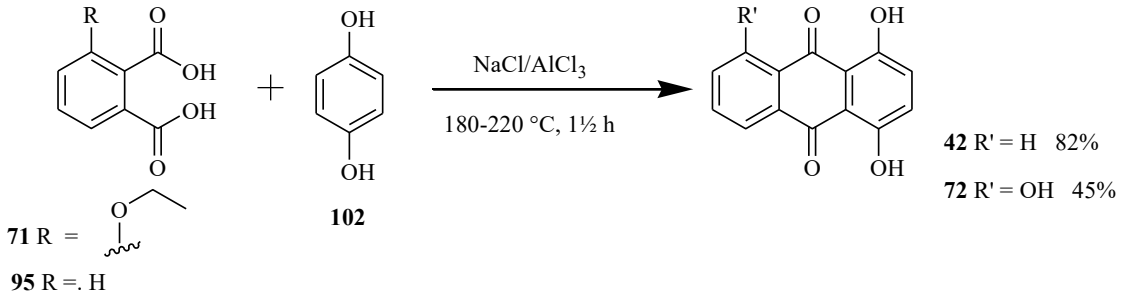

Scheme 4.17: Synthesis of the 1, 4-dihydroxyanthraquinone from phthalic acid

The same methodology reported by Hicks *et al* [143] as described above was used to prepare the 1,4-dihydroxyanthraquinone **42** and 1,4,5-trihydroxyanthraquinone **71**. From the experimental point of view, it was observed that 1, 4-dihydroxyanthraquinone **42** is favorably formed as compared to 1,4,5-trihydroxyanthraquinone **72** in terms of yield and easiest purification procedures.

Characterization of quinizarin **42** by ^{1}H NMR spectrum (**Figure 4.8**) displayed a singlet at δ_H 6.22 ppm which was integrating to two protons, these protons were being assigned to the two hydrogens ortho to the hydroxyl group. The two multiplets at δ_H 7.16 and 7.44 ppm which were each integrating to two protons were being assigned for the four hydrogens of the un-substituted ring of anthraquinones. The ^{13}C NMR spectrum of quinizarin **42** showed a maximum number of seven peaks (**Figure 4.8**). This reduced number of carbon peaks was

due to the symmetry properties of compound **72**. A signal at δ_C of 187.1 was accounted for the carbonyl group.

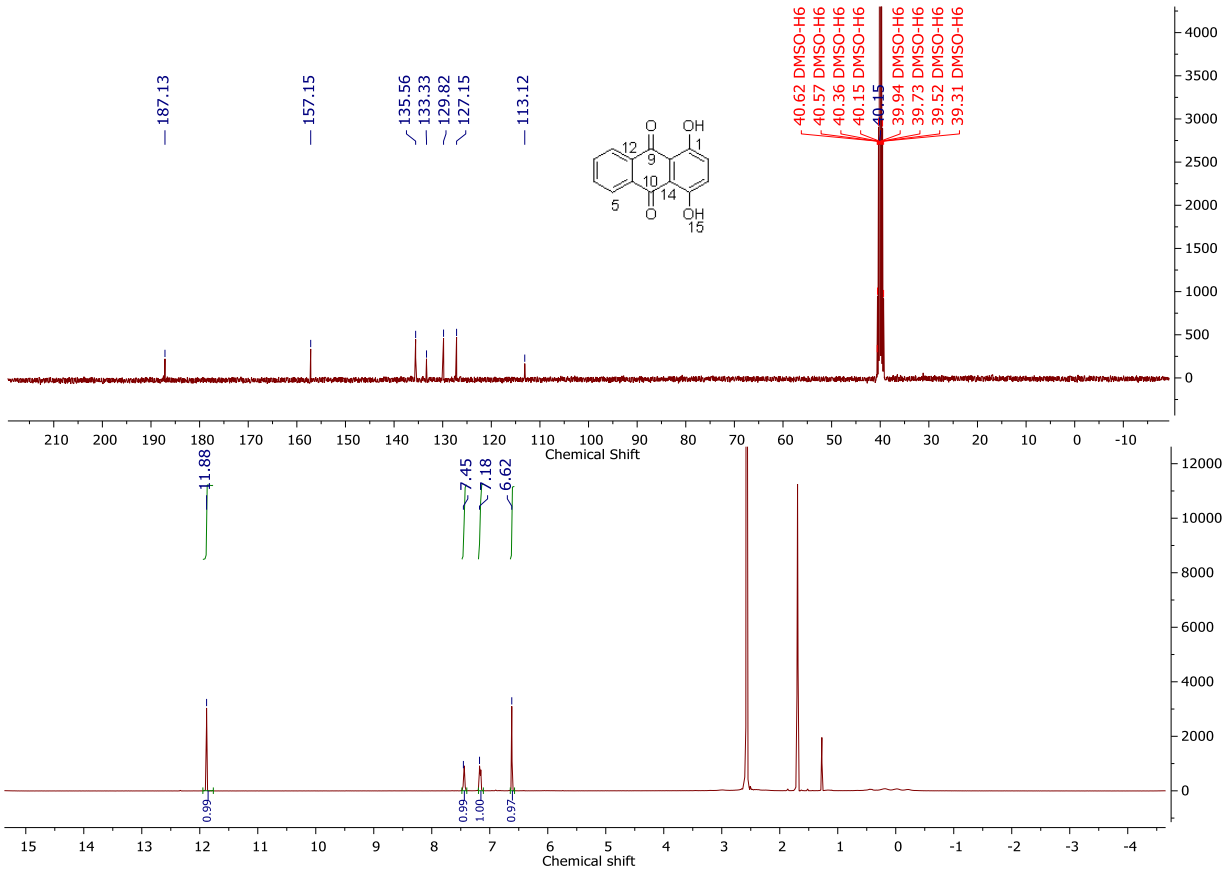

Figure 4.8: 400 MHz ^{1}H and ^{13}C NMR spectrum of quinizarin 42 in DMSO

The low yield results and impurity properties of compound **72** were being attributed to the lack of region-selectivity of the Friedel-Crafts acylation method. Both ^{1}H NMR, ^{13}C NMR and ^{13}C DEPT 135 experiments were used in confirming the structure of this anthraquinone. The ^{1}H NMR spectrum (**Figure 4.10**) was marked by the appearance of a doublet at δ_H 7.84 ppm which was integrating one proton was assigned to H-6. A triplet at 7.66 ppm which was integrating one proton accounted for H-7. The hydrogens, H-2 and H-3 were found to be resonating at 7.27 ppm and these protons were integrated into two protons.

These two peaks had a closer similarity to the ones reported by Ubbani *et a*l [6]. A singlet at 7.27 ppm corresponded to H-8. Signals at δ_H 12.14, 12.23, and 12.95 ppm were assigned for the three hydroxyl groups of anthraquinone

The ^{13}C DEPT 135 (**Figure 4.11**) experiment displayed five positive signals. This provided a proof of the number of C-H atoms that are situated in the aromatic region. Furthermore, the ^{1}H NMR results of **72** showed the disappearance of the ethoxy substituent as it hydrolyzed during the reaction [98].

The TLC (**Figure 4.9**) of 1,4,5-trihydroxy **72** anthraquinone exhibited two spots lying over one another posing difficulty of purification. The reason for the lack of regiochemical control in the intermolecular Friedel-Crafts reaction was due to Hayashi rearrangement [9].

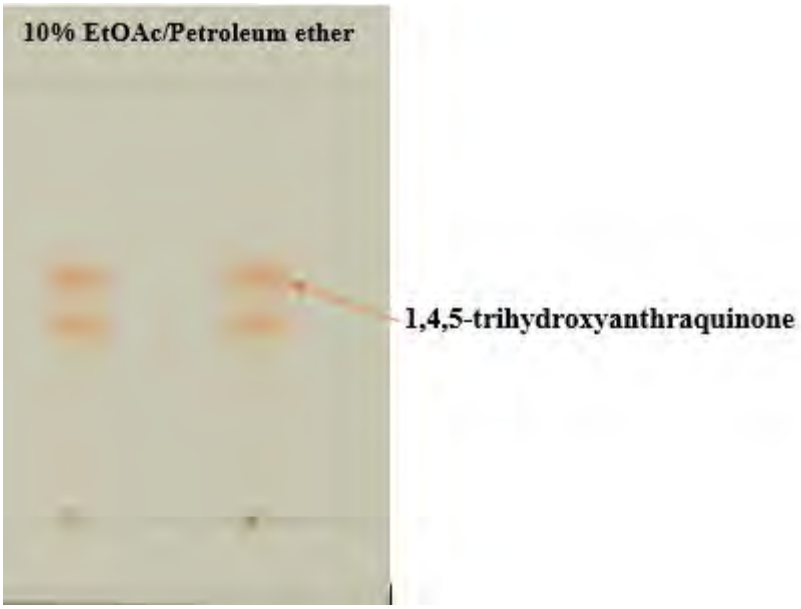

Figure 4. 9: TLC for the 1, 4, 5-trihydroxy anthraquinone

The ^{13}C NMR spectrum (**Figure 4.10**) of 1,4,5-trihydroxyanthraquinone **72** exhibited two peaks at δ_C 190.0 and 185.2 ppm corresponding to the two carbonyl groups of the anthraquinone. A signal at δ_C 161.7 ppm accounted for the carbon five. Another two consecutive signals at δ_C 157.3 and 156.8 ppm was being assigned for carbon one and four.

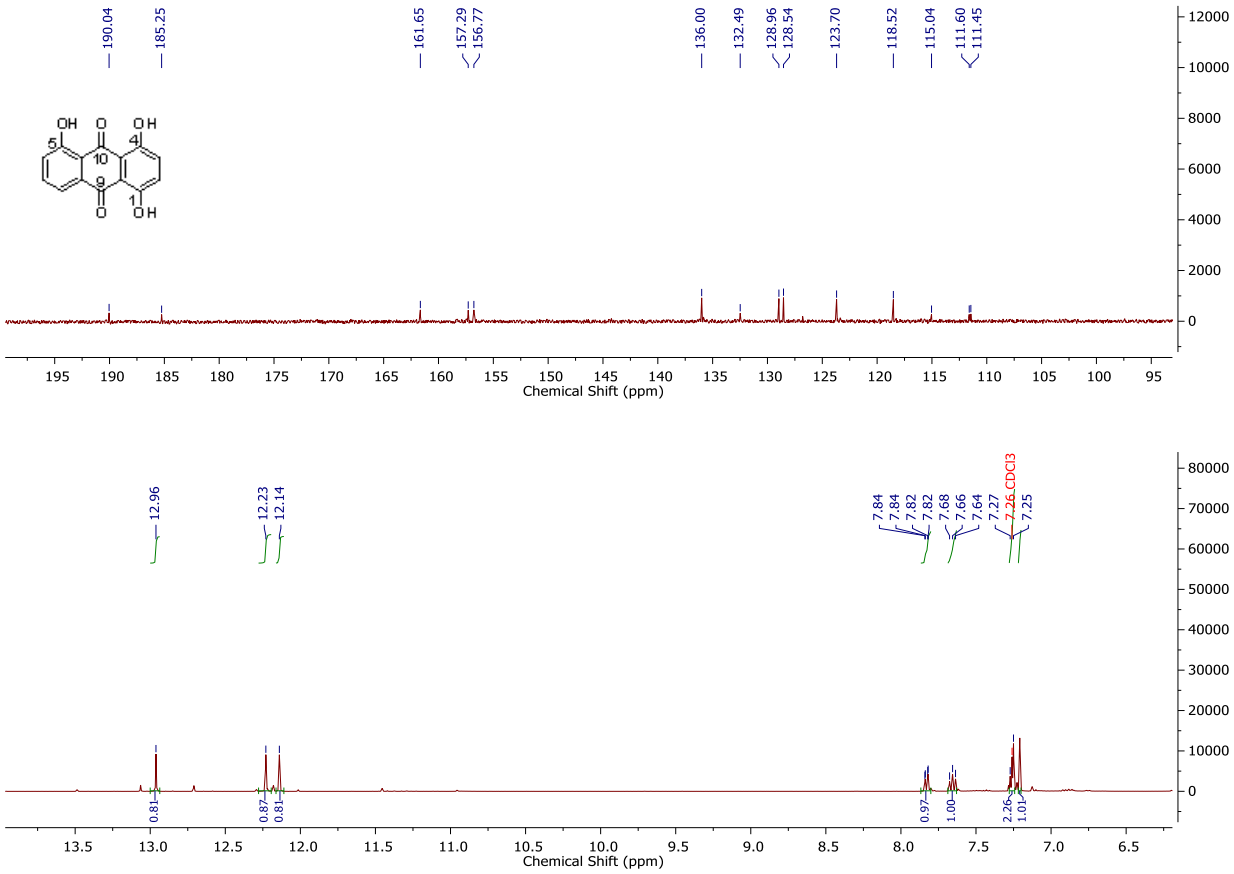

Figure 4.10: 400MHz ^{1}H and ^{13}C NMR spectrum of 1, 4, 5-trihydroxyanthracene-9,10-dione 72 in $CDCl_3$

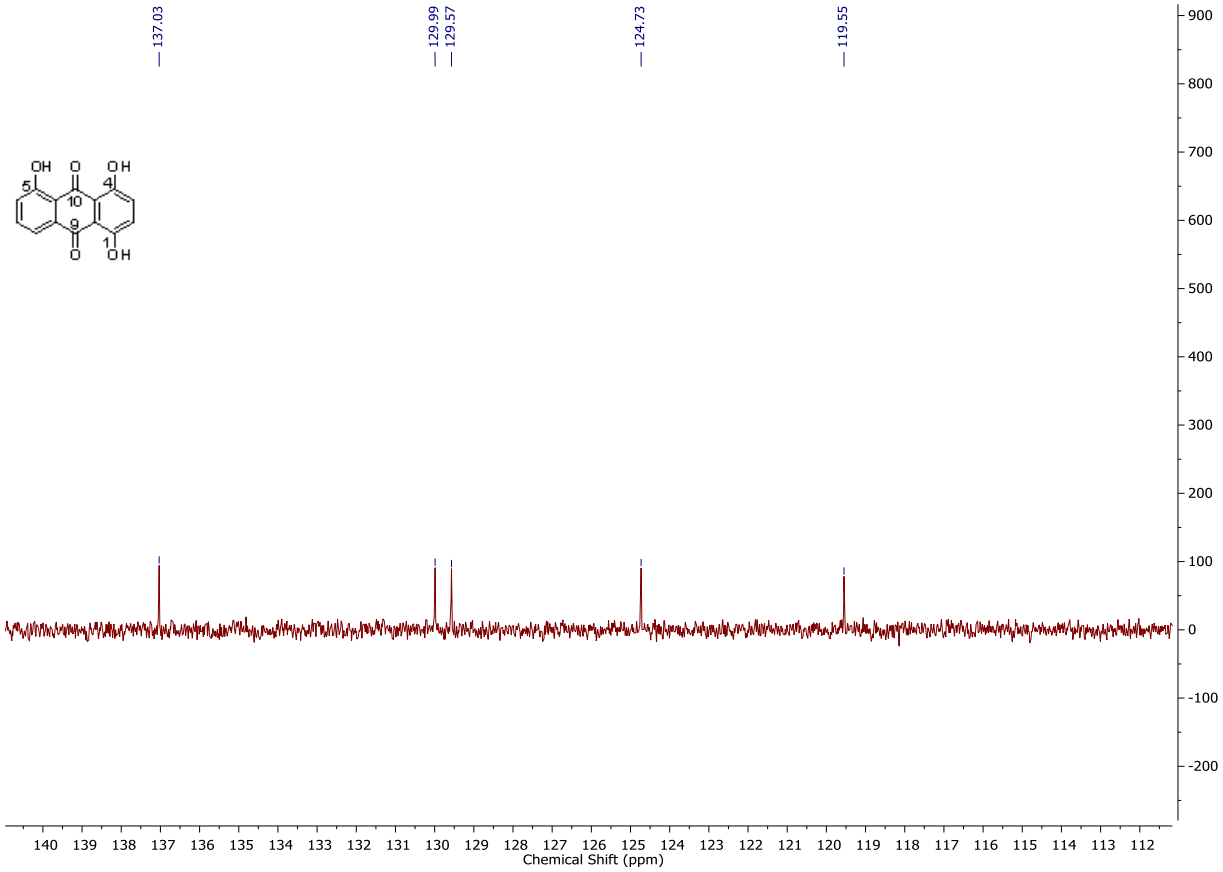

Figure 4.11: 400MHz ^{13}C DEPT-135 of 1,4,5-trihydroxyanthracene-9,10-dione 72 in $CDCl_3$

4.13 The modified Marschalk reaction

The two compounds; 1,4-dihydroxyanthraquinone **42** and the 1,4,5-trihydroxyanthraquinone **72** were differently reacted with aldehydes such as acetaldehyde, propionaldehyde, and 2-chlorobenzaldehyde under Marschalk reaction. However, the reaction of these three aldehydes with the 1,4,5-trihydroxyanthraquinone **72** under the same conditions, formed unwanted products which were isolated in very low yields. This discouraging prompted considerations alternative methods for the preparation of the 1,4,5-trihydroxyanthraquinone that would avoid Hayashi rearrangements. We further considred that the hydroxyalkylation of 1,4,5-trihydroxy anthraquinone **72** requires first the protection of the hydroxy group at position 5.

Quinizarin **42** was reacted successfully with the chosen aldehydes under basic conditions using dithionite reduction adopting the method reported by Zhao *et.al* [98] to form alcohol anthraquinones **62**, **73,** and **74** (**Scheme 4.18**) in moderate yields. In this reaction, 1,4-dihydroxyanthraquinone **42** in absolute methanol under inert atmosphere at 0 °C was first reacted with 1 M sodium hydroxide (6 eq), an orange solution immediately turned purple, and afterward, a freshly prepared solution of the dithionite was added and stirred for 10 minutes, followed by the addition of aldehyde. The reaction mixture was stirred for a maximum of four hours while maintaining the same conditions except for entries 2 and 3 (**Table 4.1**).

Longer reaction times were omitted for entry 1; this is because after two hours undesired products started forming. It was necessary to use a maximum of 5.2 equivalent amount of the acetaldehyde. The reaction is followed by the addition of an aqueous solution of H_2O_2, for the re-oxidation of the dihydroxyanthraquinones [147]. It was noted that during the re-oxidation process higher amount of hydrogen peroxide could affect the formation of anthraquinone **62**.

During the formation of dihydroxyanthraquinones **62**, the amount of H_2O_2 of 3%, unlike 30% H_2O_2 which was for the re-oxidation of **73.** From experimental observation, it was was found the reaction of quinazarin **42** and aromatic aldehyde formed hydroxyalkylanthraquinone **73** with better yields and easiest purification procedures.

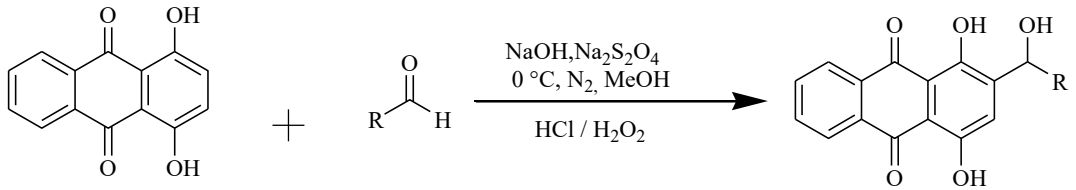

42 **62, 73** or **74**

Scheme 4.18: The modified Marschalk reaction with aldehydes

As indicated from the TLC plate of the reaction alkylated anthraquinones were more polar than the starting material **42**. The hydrogen bonding on each of the alcohol accounts for this polarity.

Table 4. 1: The reaction of aldehydes with the 1,4-dihydroxyanthraquinone.

Entry	Aldehyde	R Alkyl	Time (h)	Product	Yield %
1	Acetaldehyde	methyl	2	**62**	20
2	2-chlorobenzaldehyde	2-ClC_6H_4	4	**73**	75
3	Propionaldehyde	Ethyl	3	**74**	20

The results from the ^{1}H NMR spectrum of dihydroxyanthraquinone **62** showed a doublet at δ_H 1.38 ppm integrating three protons which were accounting for the three hydrogens of the methyl group; a quartet at δ_H 5.04 ppm which was integrating one proton was assigned for the benzylic hydrogen of the anthraquinone. The aromatic region displayed singlet at δ_H 7.45 ppm integrating one proton, which accounted for the proton ortho to the hydroxyethyl substituent. Multiplets at δ_H 7.96 and 8.24 ppm each integrating two protons were assigned for the protons of the unsubstituted aromatic ring of the anthraquinone.

The ^{13}C NMR spectrum of the dihydroxyanthraquinone **62** showed a peak at δ_C 24.1 ppm which was being assigned for the terminal methyl carbon in the aliphatic group. Another signal at δ_C 63.3 ppm was assigned for the benzylic carbon of the anthraquinone. The carbons of the two carbonyl groups of the dihydroxyanthraquinone **62** were found to be resonating at δ_C 186.5 and 187.2 ppm. These NMR results successfully confirmed the formation of compound **62** and were comparable with the results reported by Zhao *et. al* [12]

The ^{1}H NMR spectrum of compound **73** (**Figure 4.12**) displayed a signal at δ_H 6.32 ppm which was assigned for hydrogen the benzylic group. Signals from δ_H 7.34 to 8.19 ppm integrating nine protons accounted for the aromatic hydrogen.

^{13}C NMR spectrum of alcohol **73** was marked by the appearance of two new signals at δ_C 186.6 and 187.4 ppm which were accounting for the carbonyl groups of anthraquinone. The slightly different chemical environment, associated with these groups was the resultant effect of its chemical shifts.

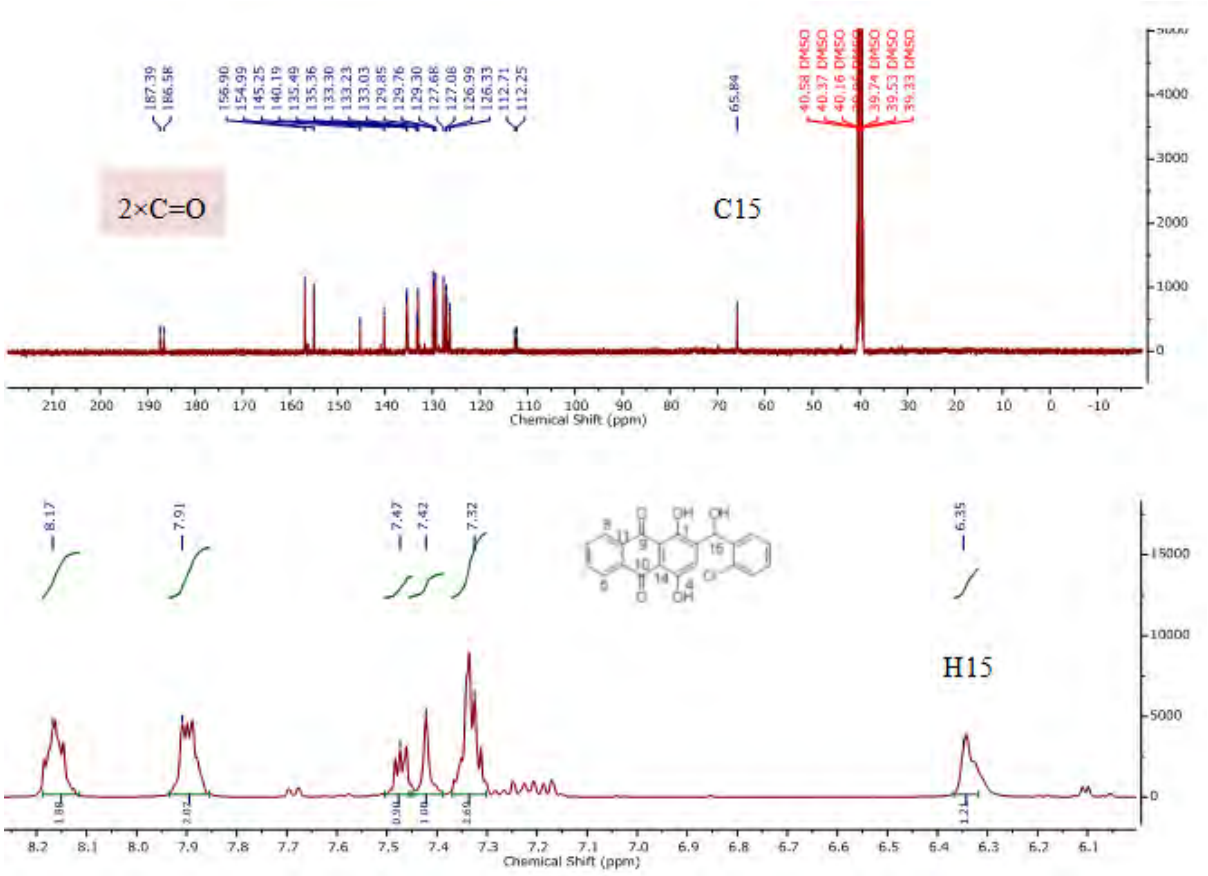

Figure 4.12: 400MHz ^{1}H, ^{13}CNMR spectrum of 2-((2-chlorophenyl)(hydroxy)methyl)-1,4-dihydroxyanthracene-9,10-dione 73 in DMSO

The ^{1}H NMR spectrum of anthraquinone **74** (**Figure 4.13**) showed a triplet at δ_H 0.97 ppm integrating three protons accounting for the three protons of the terminal methyl groups. The appearance of multiplets at δ_H 1.75 and 1.85 ppm each integrating one proton was assigned

for the two hydrogens next to the terminal methyl groups. A multiplet at δ_H 4.90 ppm integrating to one proton was accounted for the benzylic proton.

The aromatic region was characterized with a singlet at δ_H 7.35 ppm integrating one proton which was assigned to the aromatic proton ortho to the hydroxy-Propyl group of the anthraquinone. Multiplets at δ_H 7.44 and 8.26 ppm each integrating two protons were assigned to the four protons of the un-substituted ring.

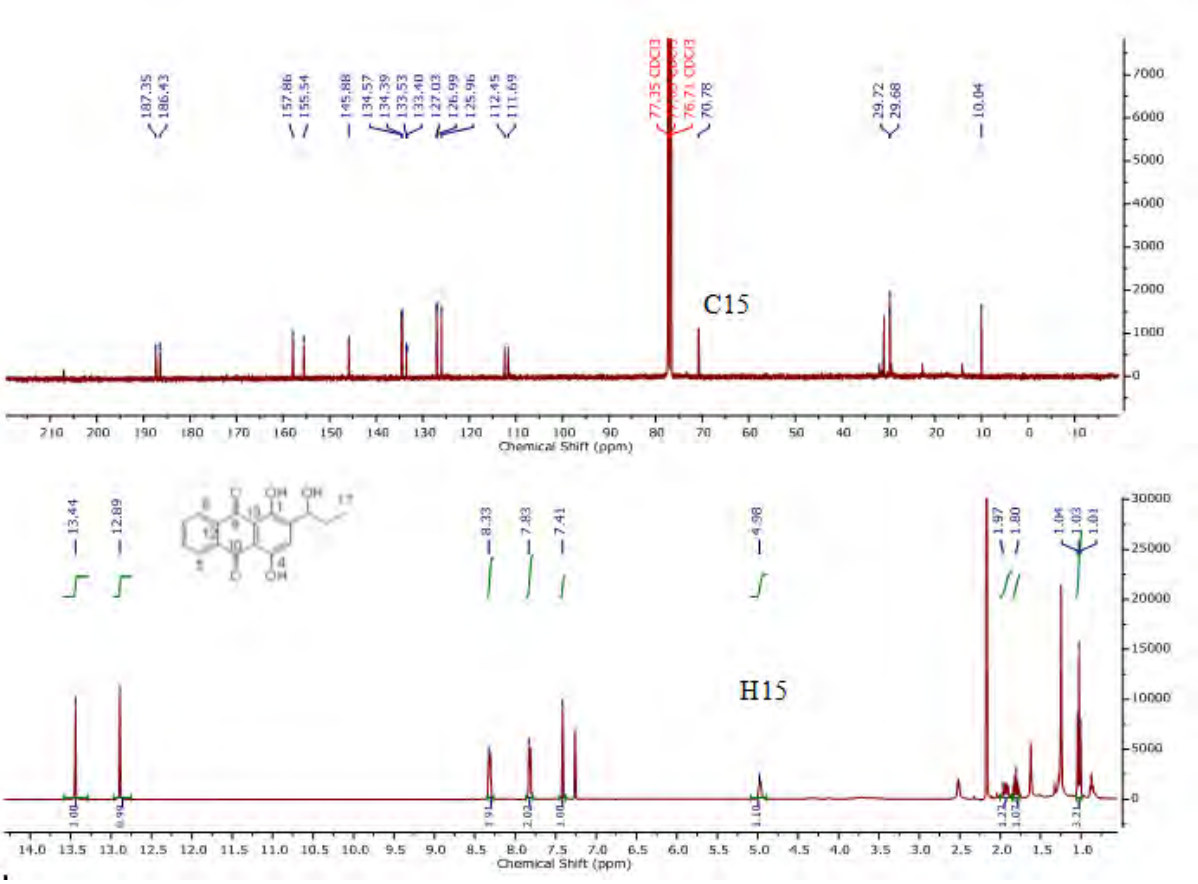

Figure 4.13: 400MHz ^{1}H, ^{13}CNMR spectrum of 1,4-dihydroxy-2-(1-hydroxypropyl)anthracene-9,10-dione 74 in DMSO

The ^{13}C NMR of this compound **74** showed a signal at δ_C 10.0 ppm, which accounted for the methyl group. Another signal at δ_C 29.8 ppm was being assigned for the carbon of the methylene group of the aliphatic side chain. The benzylic carbon of this anthraquinone was found to be resonating at δ_C 70.8 ppm. A signal at δ_C 126.0 ppm accounted for the aromatic

carbon ortho to the aliphatic side chain. The four carbons carrying hydrogens in the unsubstituted aromatic ring were found to be resonating at δ_C 127.0, 127.0, 134.4, and 134.6 ppm. The two carbonyl groups of this anthraquinone resonated at δ_C 187.4 and 186.4 ppm

4.14 Functional group modifications

As illustrated earlier in chapter 1, the Marschalk reaction provides a plausible mechanism for the functional group modifications of the anthraquinone moiety [17]. In the current study, we report some of the few possibilities on how the alcohol was converted into various groups ranging from carbonyl to halide functionality. From our experimental observations, it was observed that 2-((2-chlorophenyl)(hydroxy)methyl)-1,4-dihydroxyanthracene-9,10-dione **73** is stable to chlorination with thionyl chloride as compared to 1,4-dihydroxy-2-(1-hydroxypropyl)anthracene-9,10-dione **74** and 1,4-dihydroxy-2-(1-hydroxyethyl)anthracene-9,10-dione **62**. Furthermore, the esterification reaction of hydroxyalkyl 1,4-dihydroxyanthraquinone with aromatic carboxylic is favored as compared to aliphatic carboxylic acid. In our first trial it 1,4-dihydroxy-2-(1-hydroxyethyl)anthracene-9,10-dione **62** was esterified with excess anacardic acid (**Scheme 4.21**)

4.15 Synthesis of 1,4-dihydroxyanthraquinone thiosemicarbazone 76

Alcohol **73** was being oxidized to the carbonyl compound **75** in absolute dichloromethane in approximately good yield (**Scheme 4.19**) by using 1.5 eq of Dess Martin periodinane according to the procedure reported by Tietze *et. al* [8]. After proper workup procedure, solvent evaporation of the carbonyl **75** was obtained as an orange solid in 99 % yield.

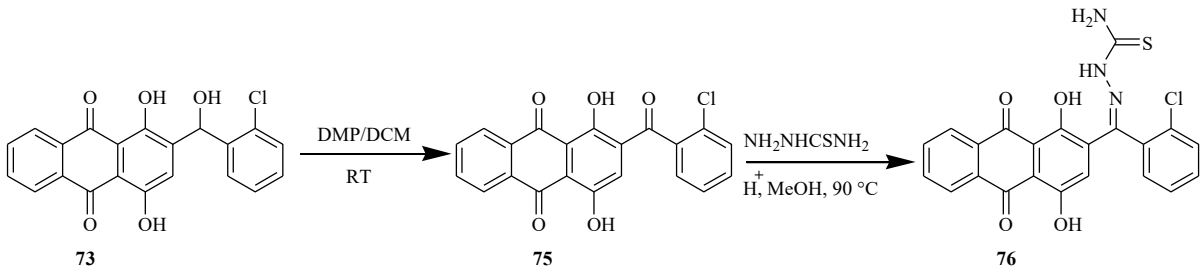

73 **75** **76**

Scheme 4.19: Synthesis of (*E*)-2-((2-chlorophenyl)(1,4-dihydroxy-9,10-dioxo-9,10-dihydroanthracen-2-yl)methylene)hydrazinecarbothioamide from anthraquinone 73

^{1}H NMR spectrum of 2-(2-chlorobenzoyl)-1,4-dihydroxyanthracene-9,10-dione **75** displayed two signals at 8.27 and 7.79 ppm, each integrating two protons. The four protons accounted for the four hydrogens of the unsubstituted anthraquinone ring. The absence of a signal at 6.32 ppm in this spectrum was the indicator that the benzylic hydrogen was consumed.

The ^{13}C NMR spectrum (**Figure 4.14**) of carbonyl **75** was characterized by the appearance of the new peak at the δ_C 192.0 ppm which was accounting for the presence of the carbonyl group (C15). The absence of a signal at δ_C 65.5 ppm was an indication that the consumption of benzylic carbon

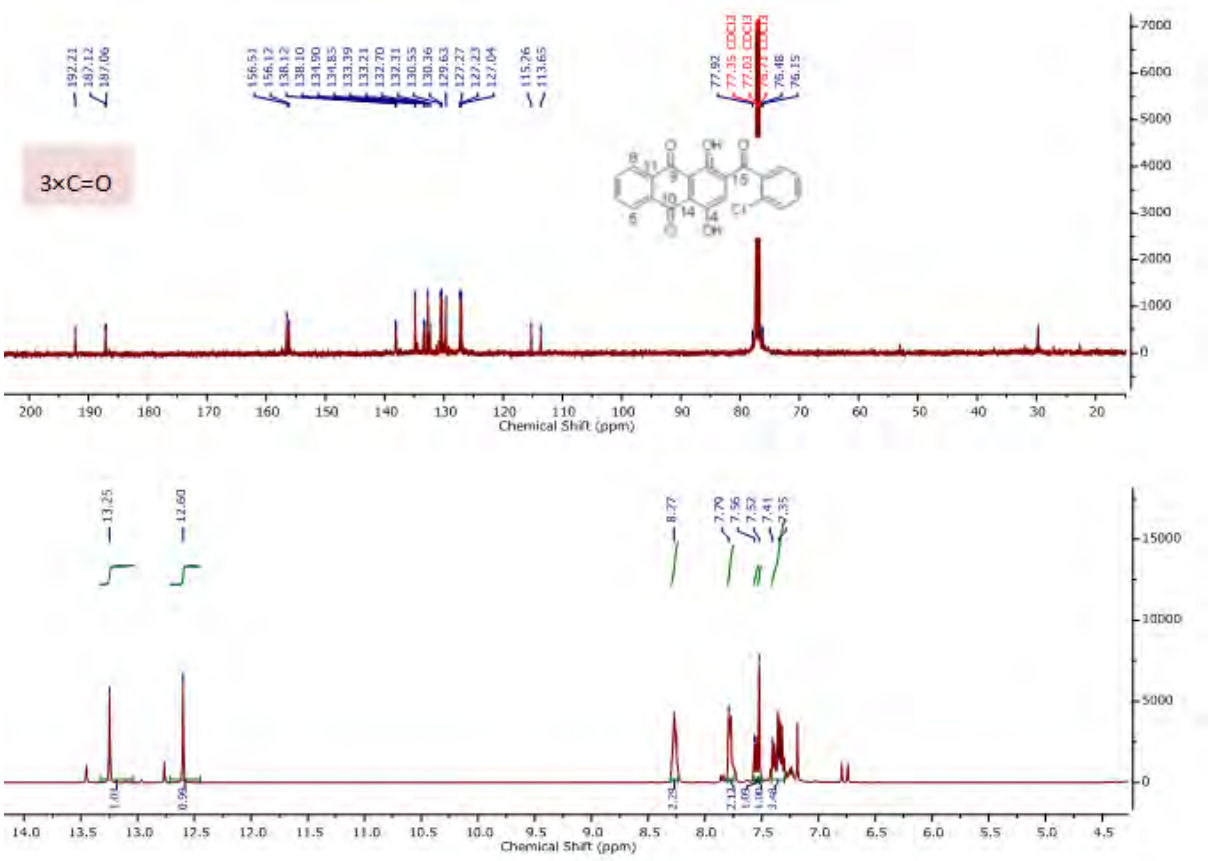

Figure 4.14: 400MHz ^{1}H and $^{13}CNMR$ spectrum of 2-(2-chlorobenzoyl)-1,4-dihydroxyanthracene-9,10-dione 75 in $CDCl_3$

The preparation of thiosemicarbazone **76** using involved the use of catalytic amounts of acid. The acids used in this catalysis were acetic acid, trifluoroacetic acid, and hydrochloric acid. These catalysts did not work better as expected, as it was observed from the TLC of the reaction medium. This tremendous discouraging result necessitated the search for a stronger catalyst.

Using a protocol suggested by Saeed *et al*., [88] with some slight modifications, carbonyl compound **75** reacted with 6 equivalent of thiosemicarbazide in methanol under sulphuric acid catalyst stirred overnight at 90 °C (**Scheme 4.19**). It was observed that during the experiment, higher amounts of sulphuric acid could result in the formation of undesired

products. The addition of three drops of this acid was found to be an appropriate amount for the formation of the thiosemicarbazone **76.**

After 24 hours of reflux, the reaction was cooled down and the solvent was evaporated. The resultant crude product was purified through column chromatography to give the desired product 45% yields as a red solid.

The ^{1}H NMR spectrum of thiosemicarbazone **76** (**Figure 4.15**) was characterized with a new broad peak at the δ_H 8.84 ppm. This broad peak was integrating to two protons and was assigned for the hydrogens of the terminal thiosemicarbazone functionality. The ^{13}C NMR spectrum of thiosemicarbazone **76** displayed a new signal at δ_C 178.6 ppm this signal accounted for the thioamide carbon C=S (C16). The appearance of a peak at this region δ_C 178.6 or 177.6 ppm signifies the presence of a thioamide as it being reported by several scholars [148][149]

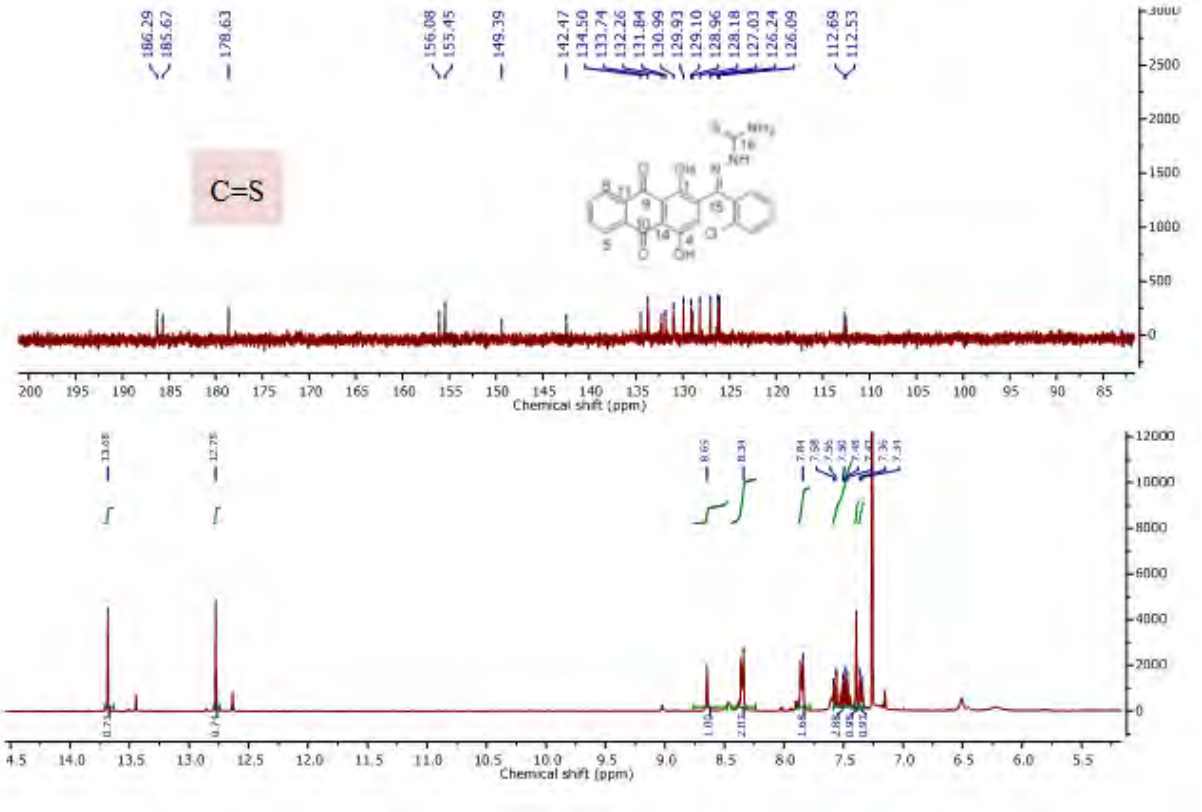

Figure 4.15: 400MHz ^{1}H and ^{13}CNMR spectrum of (*Z*)-1-((2-chlorophenyl)(9,10-dihydro-1,4-dihydroxy-9,10-dioxoanthracen-3-yl)methylene)thiosemicarbazide 76 in $CDCl_3$

Alcohol **73** was first attempted to be chlorinated according to the method reported Venkanna *et.al* [150]. In this method, a mixture of trichloroisocyanuric acid/ dimethylformamide was used as a chlorinating agent. This chlorination methodology did not work better as it formed a very low yield of product. The information obtained from the TLC of the reaction was a significant clue that the product was forming. This necessitated the search for a good chlorinating agent with particular; thionyl chloride was chosen.

However, the reaction of alcohol **73** with thionyl chloride in dichloromethane formed a low yield product. When the solvent was eliminated and therefore excess amount thionyl chloride was used the desired product **77** formed in good yield 51%. This crude product was used in the next reaction (**Scheme 4.20**).

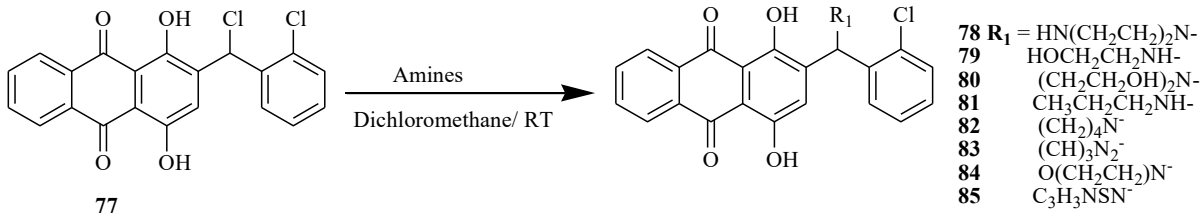

Scheme 4.20: The reaction of anthraquinone chloride 77 with various amines

4.16 Synthesis of anthraquinone amines

The series of amino-substituted anthraquinone derivatives (**Table 4.2**) were synthesized by treating chloride **77** in dichloromethane with a suitable alkyl amine using the method reported by Zhao *et. al* [17] with some slight modifications. Anthraquinones are inherently chemically stable aromatic compounds, the two carbonyl group have a deactivating influence therefore, it was important to use excessive amount of amine to get approximately good yields [151]. The reaction did not require the use of bases such as potassium carbonate and triethylamine. After suitable workup procedure and purification, amines were obtained in moderately good yields

Table 4. 2: Reaction of reaction of dihydroxyanthraquinone 77 with various amines

Compound	R-Group	Yield (%)	Compound	R-Group	Yield (%)
78	$H_2N(CH_2CH_2)_2N$-	71	**82**	$(CH_2CH_2)_2N$-	44
79	$HOCH_2CH_2NH$-	22	**83**	CNC_2H_3N-	46
80	$(CH_2CH_2OH)_2N$-	61	**84**	$O(CH_2CH_2)_2N$-	80
81	$CH_3CH_2CH_2NH$-	90	**85**	NC_3H_3SN-	27

The ^{1}H NMR of piperazine anthraquinone moiety **78** (**Figure 4.15**) was characterized with multiplets at δ_H 2.39 and 2.48 ppm: each of these integrated two protons. Another multiplet appeared at δ_H 2.86 ppm and integrated four protons. These multiplets corresponded to the methylene protons of the piperazine group. The benzylic proton of this anthraquinone (H15)

was found to be resonating at δ_H 5.43 ppm and integrated one proton. The HSQC experiment (**Figure 4.17**) which is the correlation between proton and carbon was used in the assignments of these protons. The aromatic protons were observed to resonate at δ_H 7.13 to 8.24 ppm were marked with protons integrating to nine protons as equals to the total number of aromatic hydrogens.

The ^{13}C NMR spectrum of piperazine anthraquinone moiety **78** (**Figure 4.16**) showed a remarkable appearance of signals at δ_C 45.2 and 51.4 ppm corresponding to the two methylene groups of the piperazine ring.

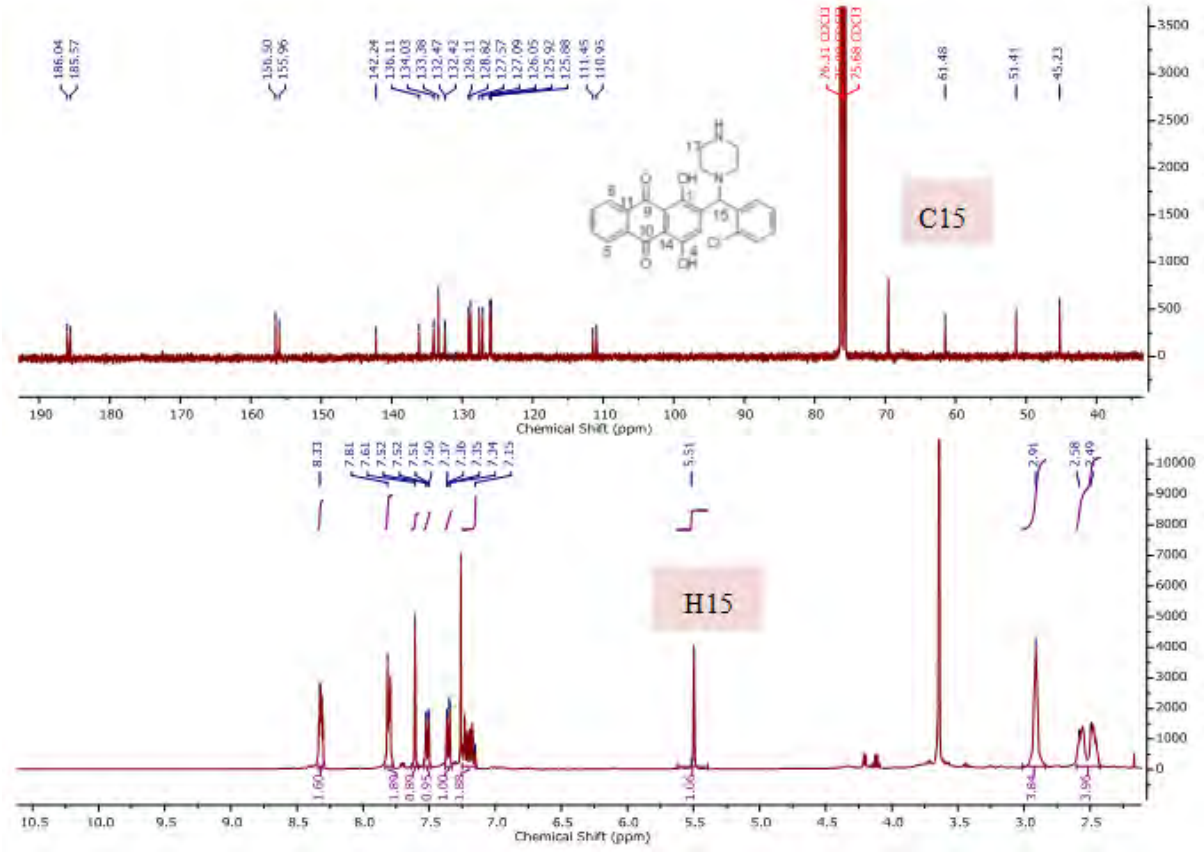

Figure 4.16: 400MHz ^1H and ^{13}CNMR spectrum of 2-((2-chlorophenyl)(piperazin-1-yl)methyl)-1,4-dihydroxyanthracene-9,10-dione 78 in $CDCl_3$

A signal at δ_C 61.5 ppm was assigned for the benzylic carbon (C15) of one of the anthraquinone ring. The carbonyl carbons of this anthraquinone were found to be resonating at δ_C 185.6 and 186.1 ppm (**Figure 4.16**).

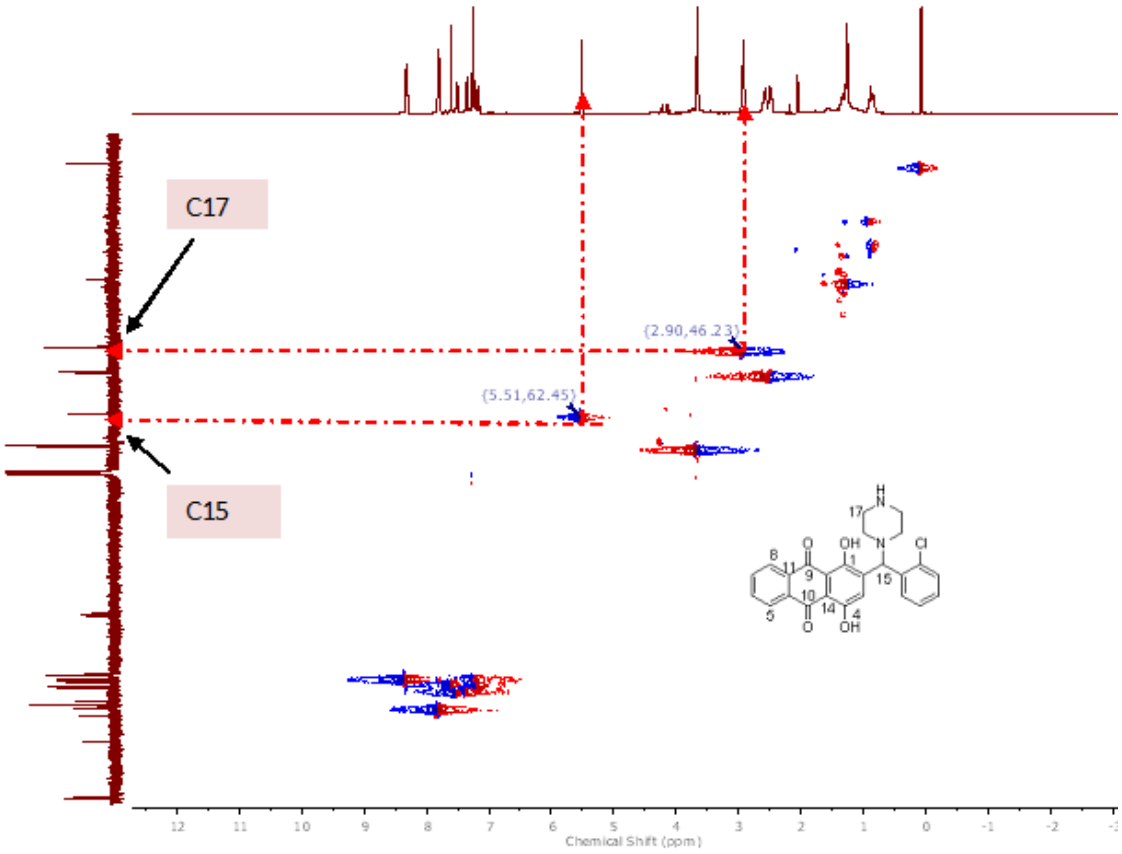

Figure 4. 17: 400MHz HSQC spectrum of 2-((2-chlorophenyl)(piperazin-1-yl)methyl)-1,4-dihydroxyanthracene-9,10-dione 78

The ^{1}H NMR spectrum of the ethanolamine anthraquinone **79** displayed two multiplets at δ_H 2.84 and 3.72 ppm each integrating two protons (**Figure 4.18**). These protons were assigned for four hydrogens of the ethylene group substituent group. A singlet at δ_H 5.66 ppm integrating one proton accounted for the benzylic proton (H15). The aromatic protons were found to be resonating at δ_H 7.15 - 8.28 ppm and were found to integrate a total of nine protons.

The ^{13}C NMR of the ethanolamine anthraquinone **79** displayed signals at δ_C 49.7 and 61.1 ppm (**Figure 4.18**); these signals were assigned to the $-CH_2-$ groups of the ethanolamine

substituent. A signal at δ_C 56.3 ppm was being assigned to the benzylic carbon (C15) of one of the anthraquinone ring carrying the alkyl group (**Figure 4.19**). The carbonyl group of this anthraquinone resonated at δ_C 186.5 to 186.2 ppm.

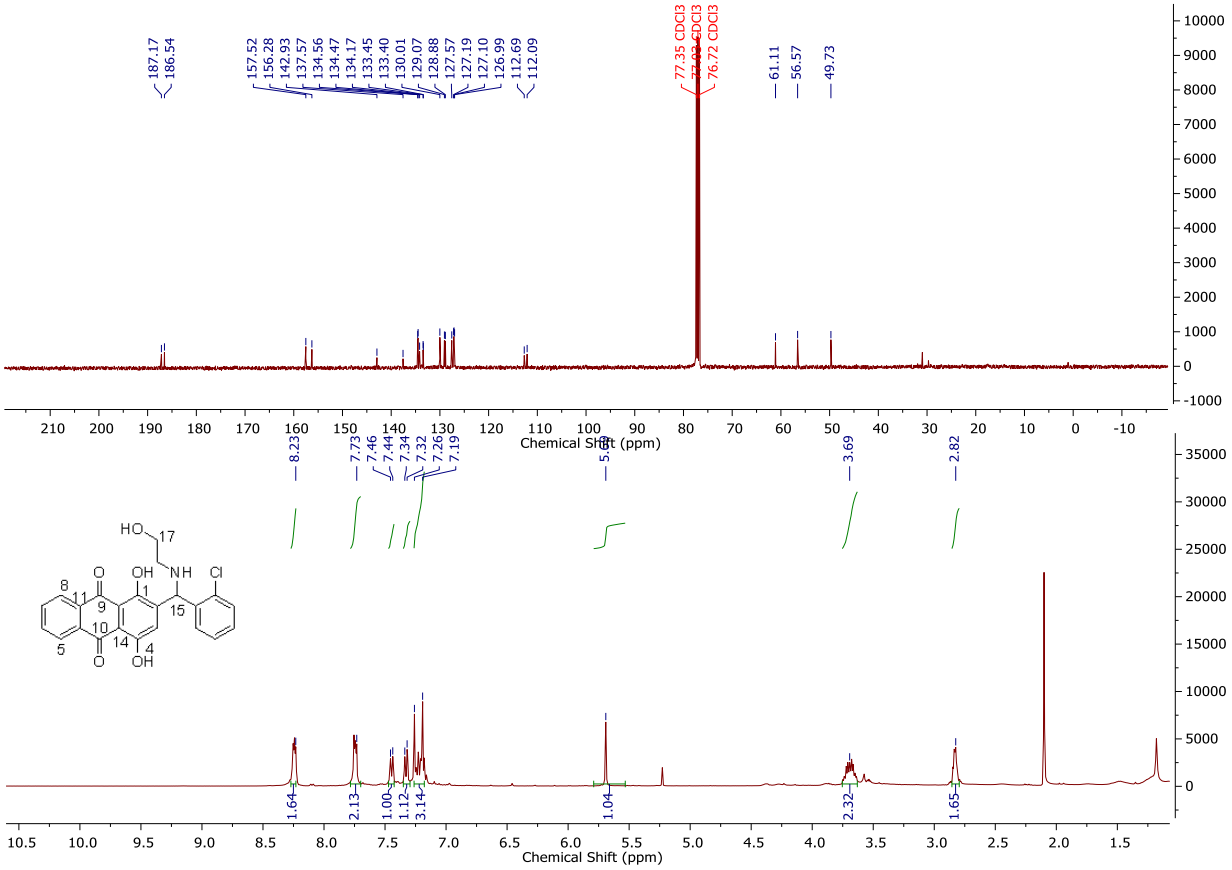

Figure 4.18: 400MHz ^{1}H and ^{13}C NMR spectrum 2-((2-hydroxyethylamino)(2-chlorophenyl)methyl)-1,4-dihydroxyanthracene-9,10-dione 79 in $CDCl_3$

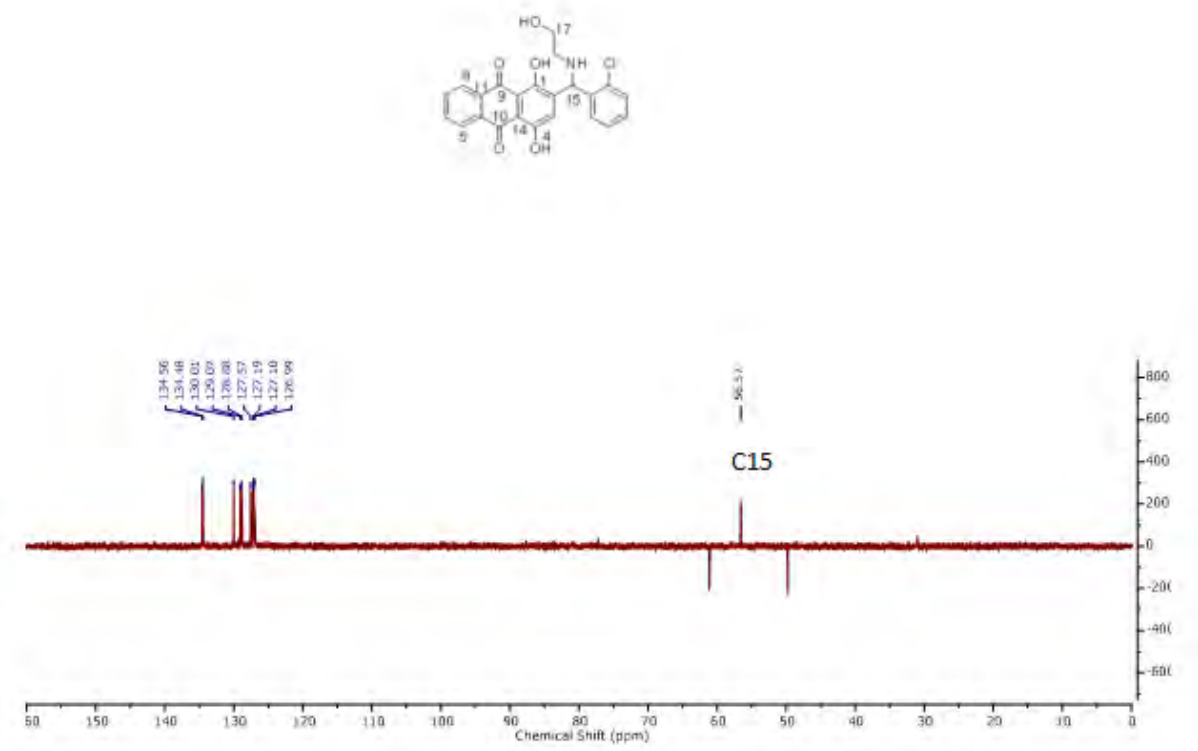

Figure 4.19: 400MHz ^{13}C DEPT 135 spectrum of 2-((2-hydroxyethylamino)(2-chlorophenyl)methyl)-1,4-dihydroxyanthracene-9,10-dione 79 in $CDCl_3$.

The ^{1}H NMR spectrum of diethanolamine anthraquinone **80** (**Figure 4.20**), displayed a multiplet at δ_H 2.82 ppm integrating four protons. These four protons were being assigned for the four methylene hydrogens next to the amine group. Another two multiplets at δ_H 3.42 and 3.52 ppm each integrating two protons, each corresponded to the two methylene hydrogens next to the hydroxyl group. The benzylic hydrogen of one of the aromatic rings was found to be resonating at the δ_H 5.79 ppm and integrated one proton. The aromatic hydrogens were found to resonate in the region between δ_H 6.83 - 8.09 ppm. These protons integrated a total of nine hydrogens.

The ^{13}C NMR spectrum of diethanolamine anthraquinone **80** (**Figure 4.20**) showed three peaks in the low field region. A signal at δ_C 54.4 ppm was being assigned for the two-methylene carbon (C16) next to the amine group. Another signal at δ_C 60.9 ppm was being

assigned for two methylene carbons (C17) next to the hydroxyl group. Signals at δ_C 156.3 and 157.3 ppm were being assigned for the two aromatic carbons carrying the hydroxyl group. The two carbonyl carbons of the anthraquinone ring were found to be resonating at δ_C 186.6 and 187.4 ppm. They are both in the same chemical environment. The benzylic carbon (C15) of one of the aromatic rings was found to be resonating at δ_C 59.8 ppm (**Figure 4.20** and **Figure 4.21)**

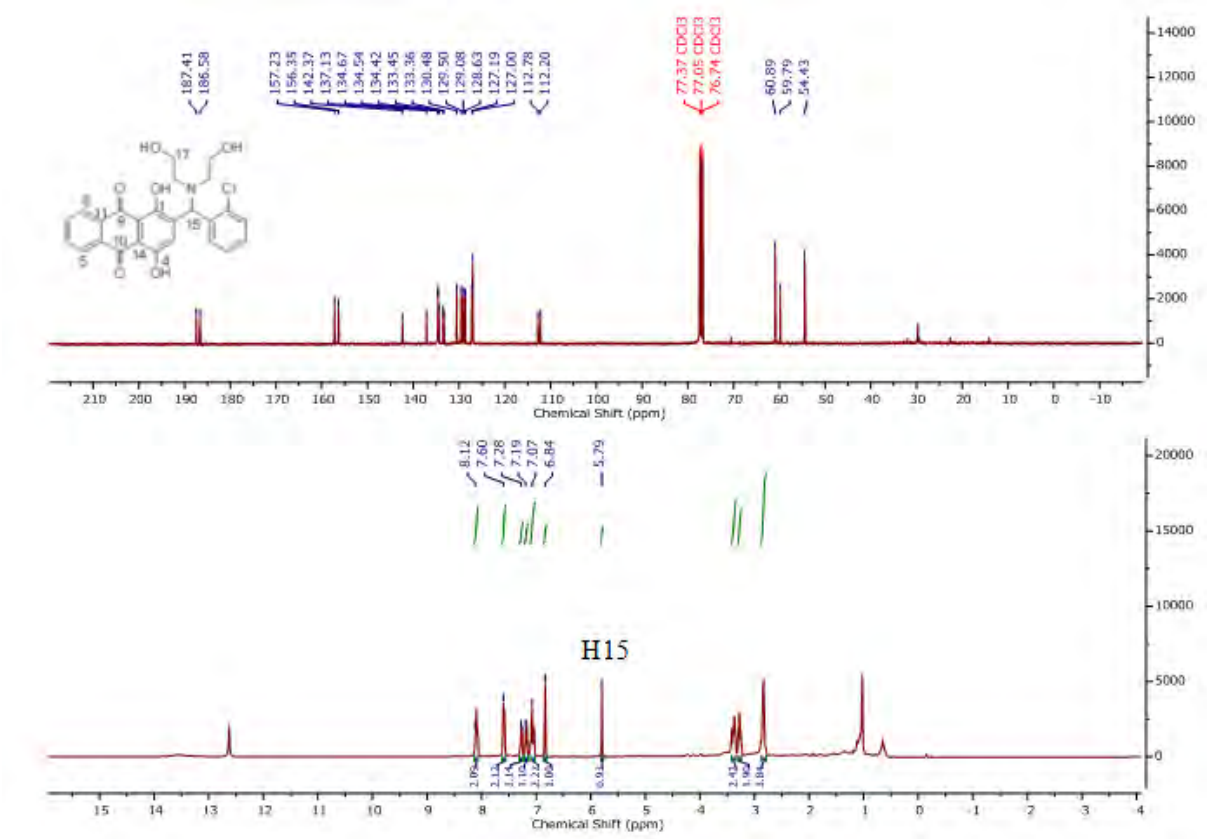

Figure 4.20: 400MHz ^{1}H and ^{13}C NMR 2-((*bis*(2-hydroxyethyl)amino)(2-chlorophenyl)methyl)-1,4-dihydroxyanthracene-9,10-dione 80 in $CDCl_3$

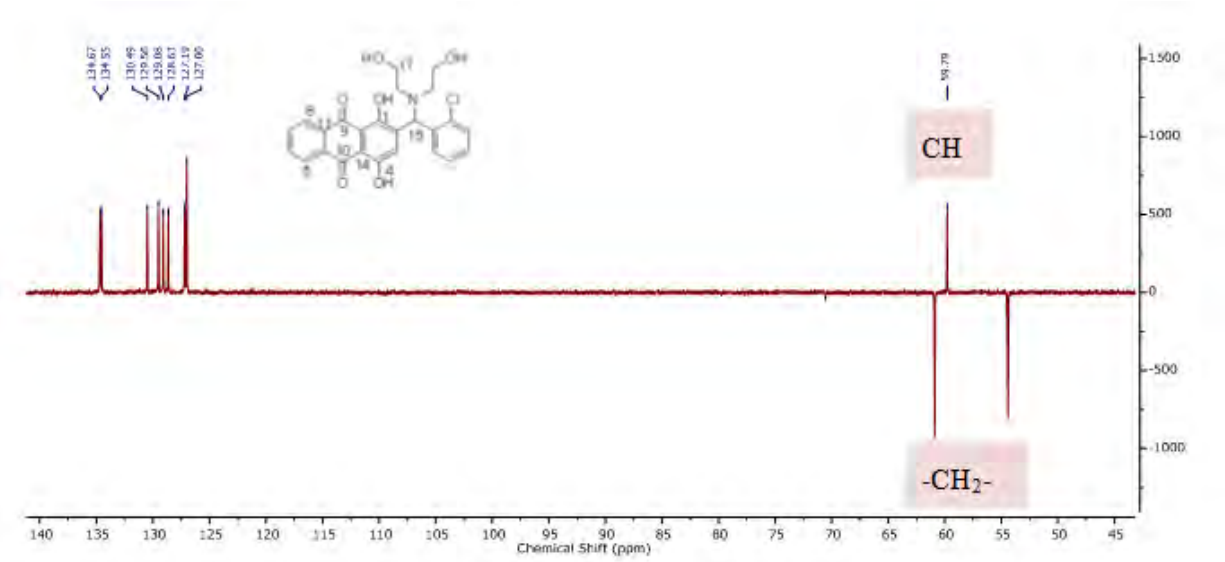

Figure 4.21: 400MHz ^{13}C DEPT 135 spectrum of 2-((bis(2-hydroxyethyl)amino)(2-chlorophenyl)methyl)-1,4-dihydroxyanthracene-9,10-dione 80 in $CDCl_3$

The ^{1}H NMR of amino anthraquinone **81** showed a triplet at δ_H 0.86 ppm integrating three protons was assigned to the terminal methyl group (**Figure 4.22)**. A sextet at δ_H 1.49 ppm integrating two protons was being assigned to the protons of the methylene group (-CH_2-) next to the methyl group. Another triplet integrating two protons which was found to be resonating at δ_H 2.59 ppm was assigned for the methylene protons next to the amine group. The aromatic protons were found to be resonating at δ_H 7.14-8.24 ppm and these protons integrated to a total of nine protons

The ^{13}C DEPT-135 experiments for compound **81** showed a peak at δ_C 11.9 ppm which was being assigned for the carbon of the terminal methyl group (**Figure 4.23)**. Another signal at δ_C 23.4 ppm was assigned for the methylene carbon next to the terminal methyl group. The methylene carbon next to the amine group was found to be resonating at δ_C 50.9 ppm. The carbon of the (-CH-) of the benzylic group was found to be resonating at δ_C 57.5 ppm. The aromatic region showed a maximum of nine peaks.

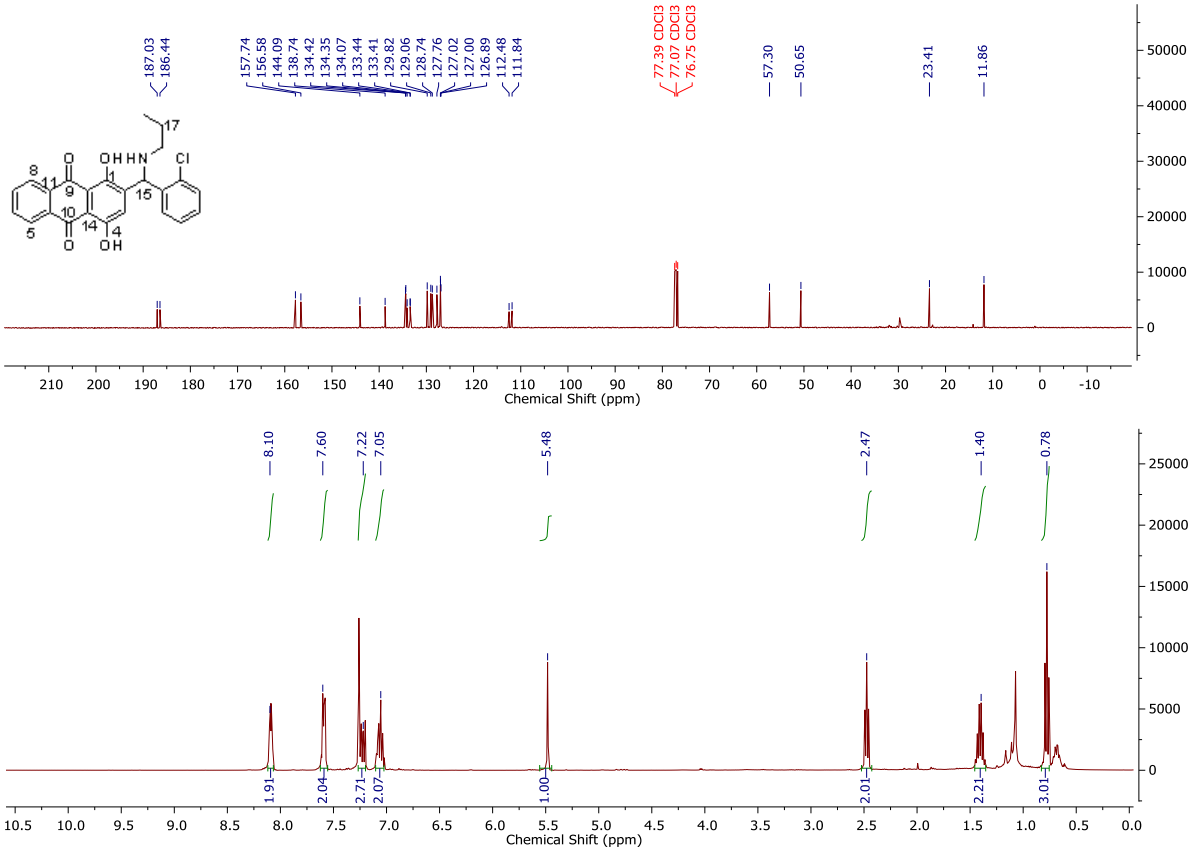

Figure 4.22: 400MHz ^{1}H NMR, ^{13}C NMR spectrum of 2-((2-chlorophenyl)(propylamino)methyl)-1,4-dihydroxyanthracene-9,10-dione 81 in $CDCl_3$

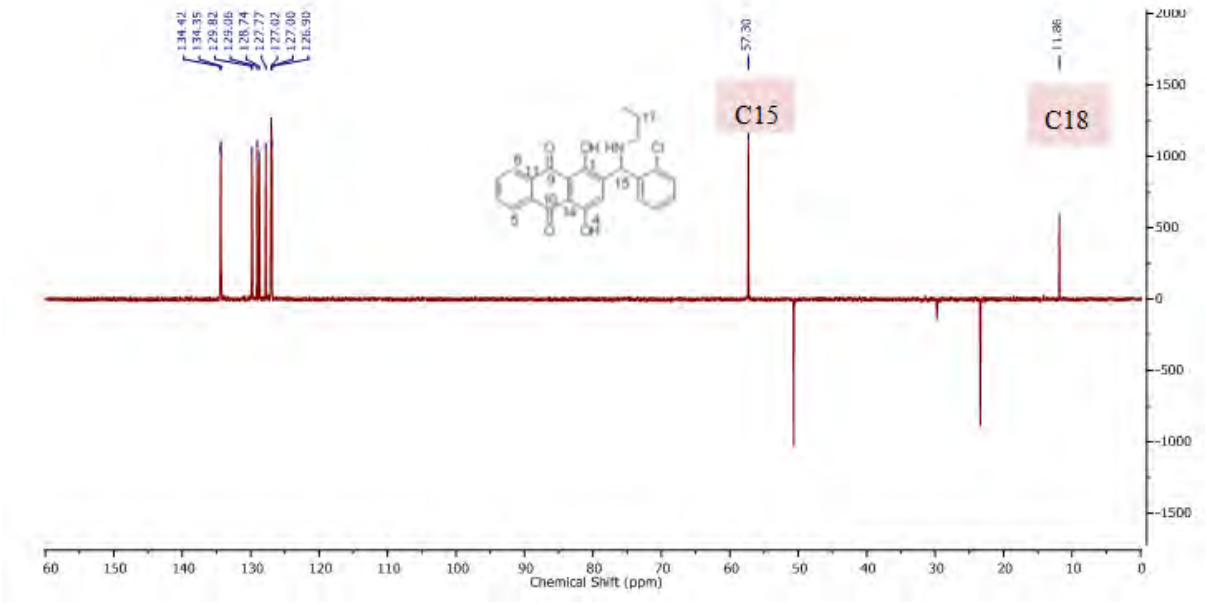

Figure 4.23: 400MHz DEPT-135 spectrum of 2-((2-chlorophenyl)(propylamino)methyl)-1,4-dihydroxyanthracene-9,10-dione 81 in $CDCl_3$

The same procedure as above was used in the synthesis of anthraquinones bearing pyrrolidine **82**, imidazole **83,** morpholine **84,** and amino thiazole **85**. The hydrogen and the carbon NMR respectively were used in the characterization of these compounds. However, the anthraquinone imidazole **83** was insoluble in many of the deuterated solvents. Mass spectrometry (Appendix AA2) was as well be used in the characterization of this compound.

The ^{1}H NMR spectrum of the anthraquinone pyrrolidine **82** (**Figure 4.24**) was characterized by two consecutive multiplets at δ_H1.65 and 2.48 ppm. Each one of these integrated four protons and corresponded to the eight methylene hydrogens of the pyrrolidine substituent group. A singlet atδ_H 5.37 ppm integrating one proton was appointed for the benzylic hydrogen.

The aromatic region had its protons characterized by two consecutive triplets at δ_H 7.14 and 7.22 ppm, two doublets at δ_H 7.29 and 7.55 ppm, each integrated one proton. These corresponded to the four hydrogens of the 2-chlorophenyl substituent group.

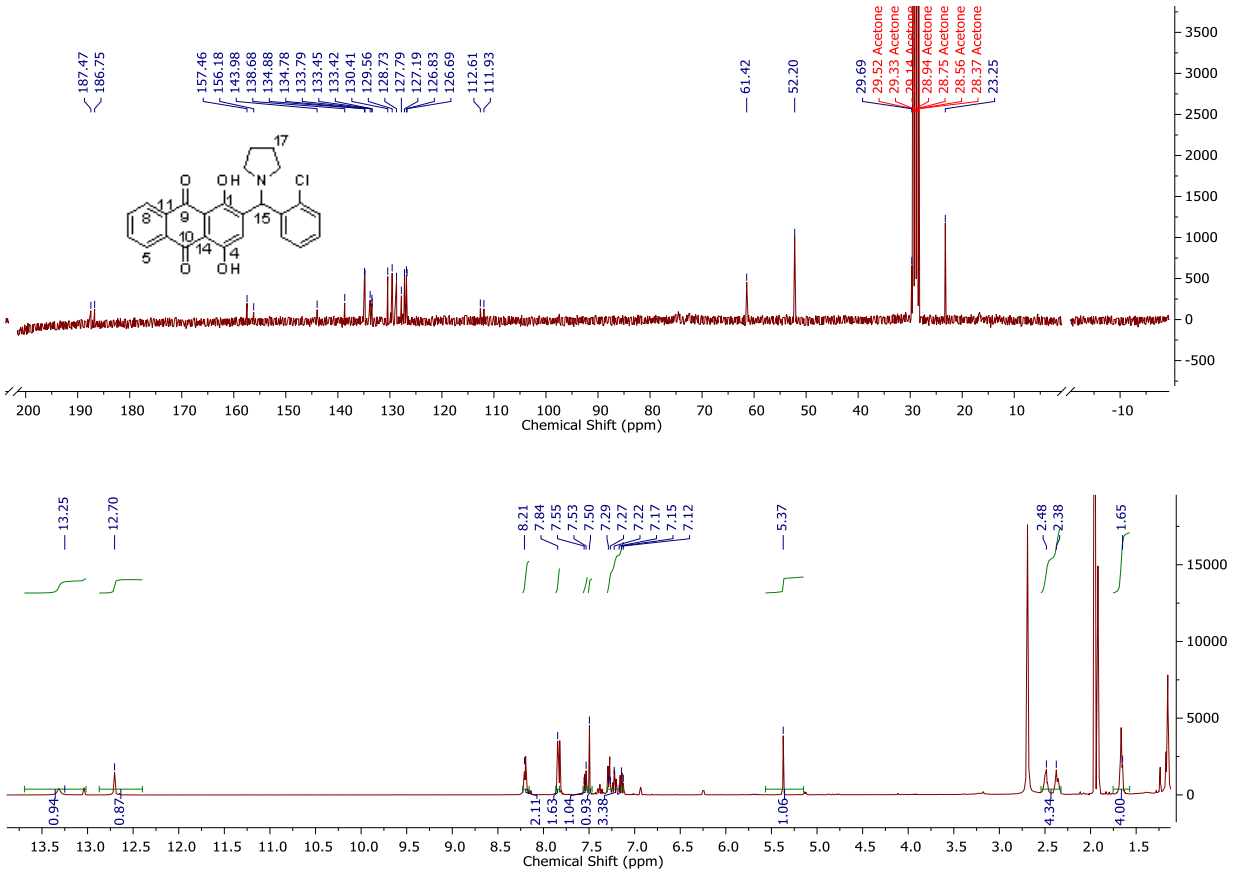

Figure 4. 24: 400MHz ^{1}H and ^{13}C NMR spectrum of 2-((2-chlorophenyl)(pyrrolidin-1-yl)methyl)-1,4-dihydroxyanthracene-9,10-dione 82 in acetone

A singlet at δ_H 7.49 ppm integrating one proton was assigned to the hydrogen next to the aliphatic substituent group. Two multiplets at δ_H 7.84 and 8.20 ppm each integrating two protons was assigned to the four hydrogens of the un-substituted anthraquinone ring.

The ^{13}C NMR spectrum of this compound exhibited three signals at the aliphatic region. A signal at δ_C 61.4 ppm accounted for the benzylic carbon (**Figure 4.24**). The consecutive signals at δ_C 23.3 and 52.2 ppm were assigned to the methylene carbons. The two-carbonyl groups of the anthraquinone were resonating at δ_C 186.8 and 187.5 ppm. The ^{13}C DEPT-135 of compound **82** (**Figure 4.25**) displayed two signals negative at δ_C 23.2 and 52.1 ppm, this

revealed the presence of two methylene groups (C16 and C17). A positive signal at δ_C 61.4 accounted for the C15 group.

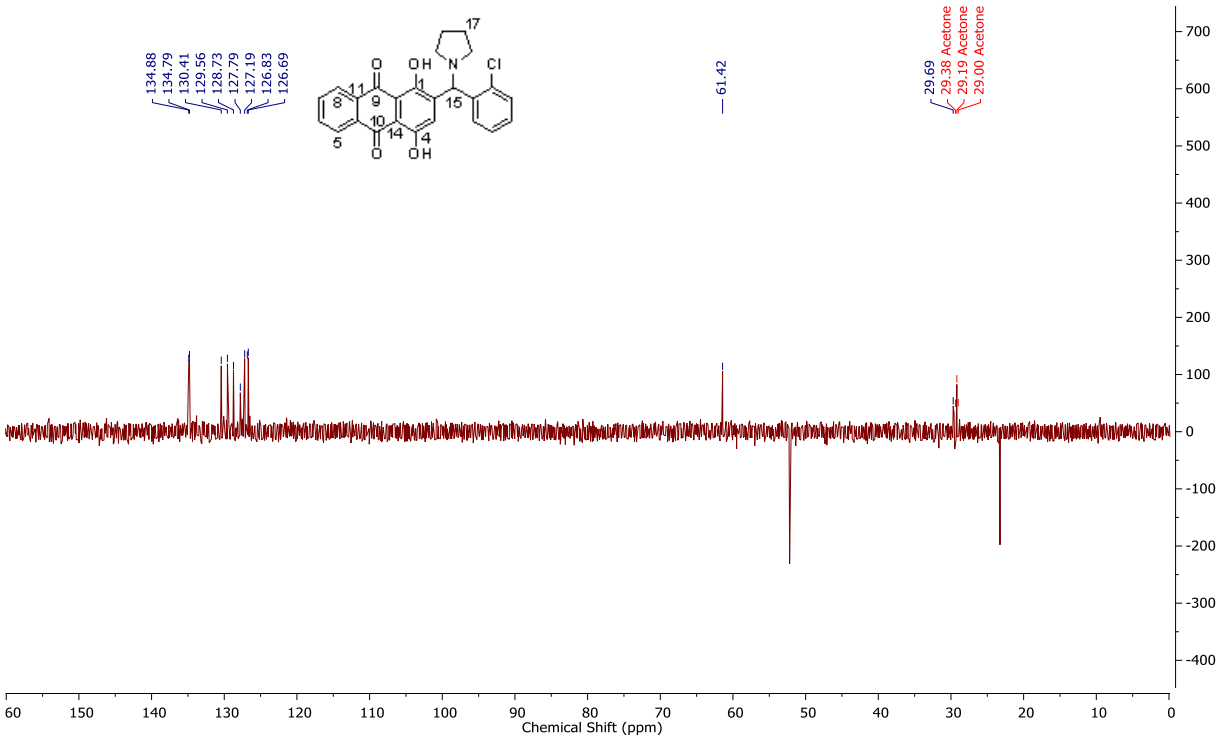

Figure 4.25: 400MHz DEPT-135 spectrum of 2-((2-chlorophenyl)(pyrrolidin-1-yl)methyl)-1,4-dihydroxyanthracene-9,10-dione 82 in acetone

Characterization of the imidazole anthraquinone **83** was observed to be challenging due to the overlap of atoms. Moreover, the compound was found to be insoluble in many making it difficult to observe some other peaks. The ^{1}H NMR spectrum of anthraquinone imidazole **83 (Figure 4.25)** displayed two signals at δ_H 7.86 and 8.36 ppm each integrating two protons. These two signals accounted for the four hydrogens of the unsubstituted ring anthraquinone ring. A singlet at δ_H 6.69 ppm integrating one proton accounted for the benzylic hydrogen. A doublet at δ_H 6.79 ppm (signal b) integrating two protons was assigned to the two-imidazole hydrogen next to each other (H17) (**Figure 4.26**). A singlet at δ_H 7.18 ppm (signal a) which was integrating one proton was assigned to one hydrogen of the imidazole substituent group

(H16). Wang *et.al* has previously reported the ^{1}H NMR spectrum of an imidazole ring to be characterized with a doublet for the two hydrogens (H17) at the chemical shift of 6.65 and 6.75 ppm; they further assigned a singlet at δ_H 7.75 ppm to be the signal for (H16) [152]

The ^{13}C NMR spectrum (**Figure 4.26)** of the anthraquinone imidazole **83** displayed 23 signals, whereby the signal for the benzylic carbon resonated at δ_C 56.1 ppm. The mass spectrometry of this compound displayed the parent peak of 431.07 *m/z* which is equivalent to the calculated.

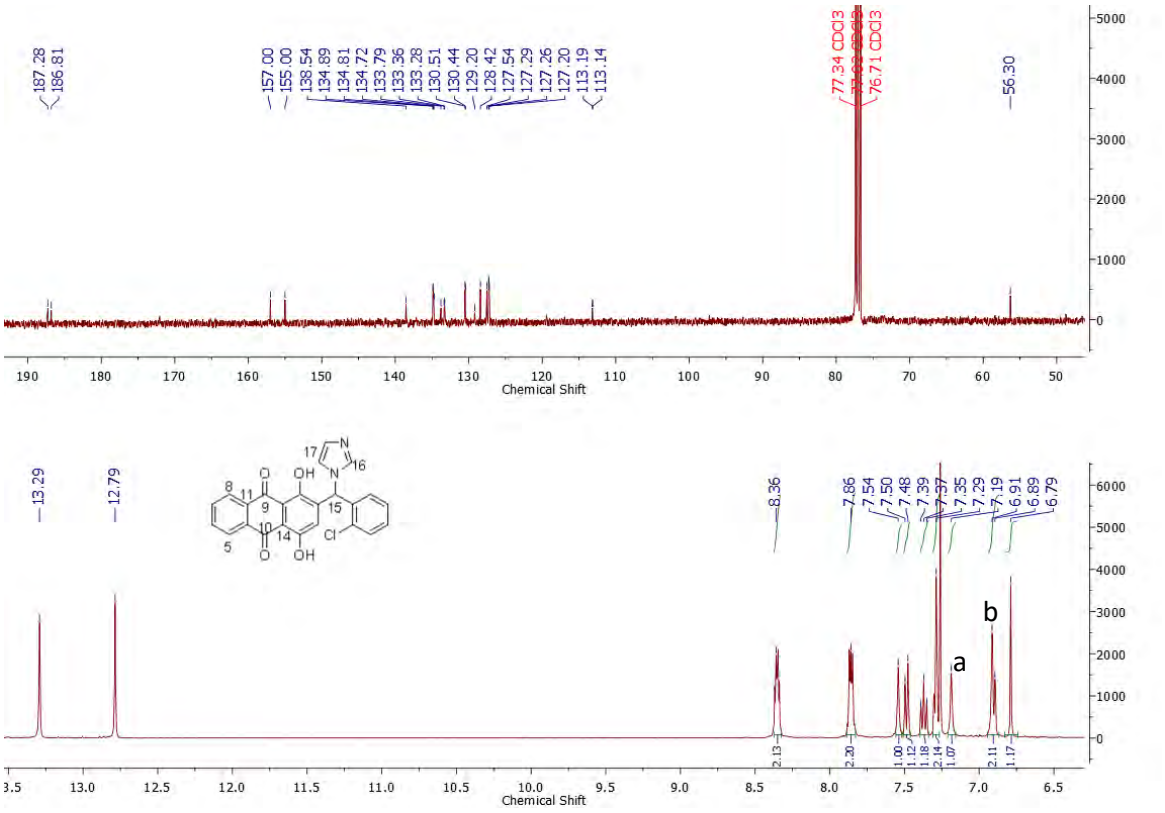

Figure 4. 26: 400MHz ^{1}H and ^{13}C NMR spectrum of 2-((2-chlorophenyl)(1H-imidazol-1-yl)methyl)-1,4-dihydroxyanthracene-9,10-dione 83 in $CDCl_3$

The ^{1}H NMR spectrum of morpholine anthraquinone **84** (**Figure 4.27**) displayed two multiplets at δ_H 2.43 and 2.49 ppm each integrating two protons. These were assigned to the two methylene groups next to the nitrogen atom. The four protons of the two methylene

groups next to the oxygen atom were found to be resonating to δ_H 3.6 ppm. These protons integrated four hydrogens. A singlet at δ_H 5.47 ppm integrating to one proton was assigned to the benzylic hydrogen of one of the aromatic rings. The ^{13}C NMR spectrum displayed signals at δ_C 61.3 and 66.2 ppm (**Figure 4.27**); these peaks were assigned to two methylene groups. A signal at δ_C 50.8 ppm accounted for the benzylic carbon of one of the aromatic rings. Two signals at δ_C 185.6 and 186.0 ppm were being assigned for the carbonyl carbons of the anthraquinone.

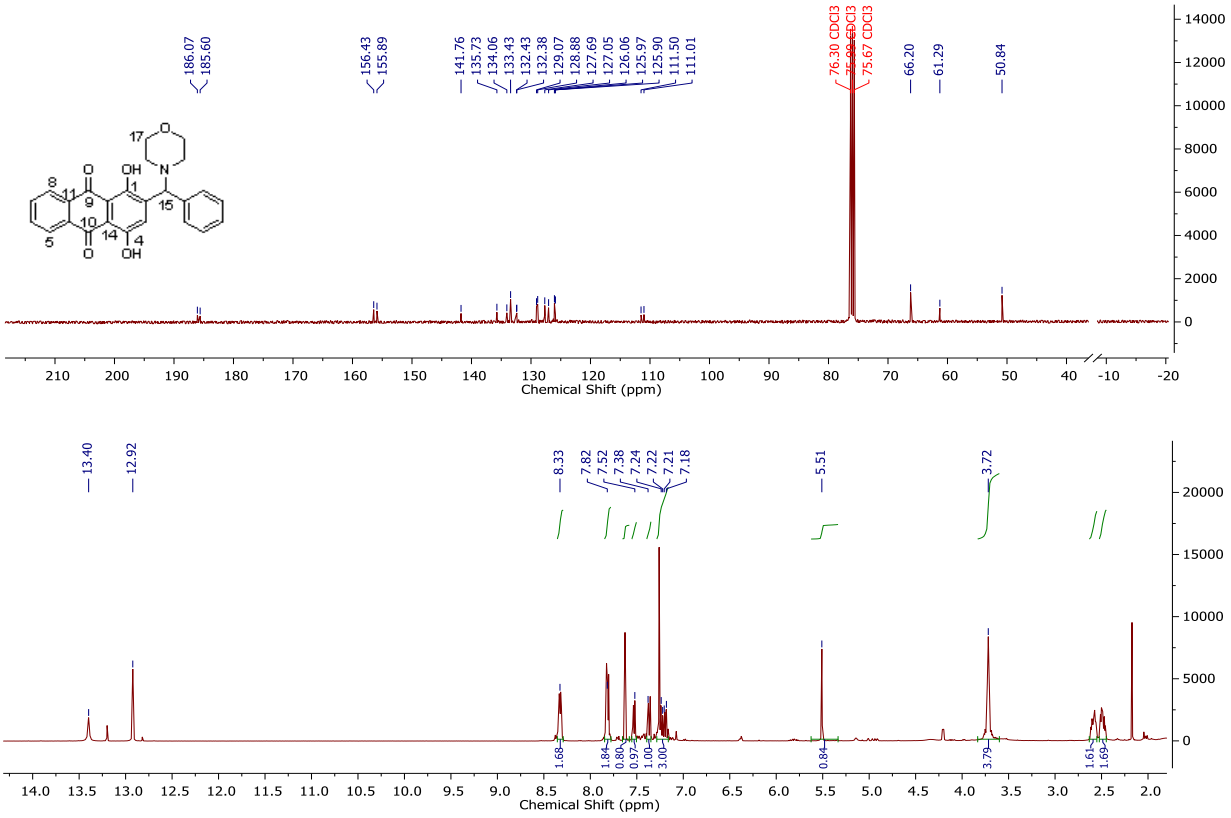

Figure 4.27: 400MHz ^1H and ^{13}C NMR spectrum of 2-((2-chlorophenyl)(morpholino)methyl)-1,4-dihydroxyanthracene-9,10-dione 84 in $CDCl_3$

The ^1H NMR spectrum of anthraquinone amino thiazole **85** (**Figure 4.28**), was being marked with the appearance of a multiplet at δ_H 6.42 ppm. This multiplet integrated one proton and it was corresponding to the benzylic hydrogen (H15). The degree of electronegativity of the compound caused the increase in the deshielding effect of this hydrogen. The aromatic region

has its protons resonating at δ_H 6.95-8.23 ppm. These multiplets integrated a total of eleven protons. These number of hydrogens perfectly corresponded to the number of C-H peaks that appeared in the ^{13}C DEPT-135 experiments which displayed eleven signals. The mass spectrometry data of this compound **85** (**Appendix AA3**) perfectly matched the theoretical molecular mass.

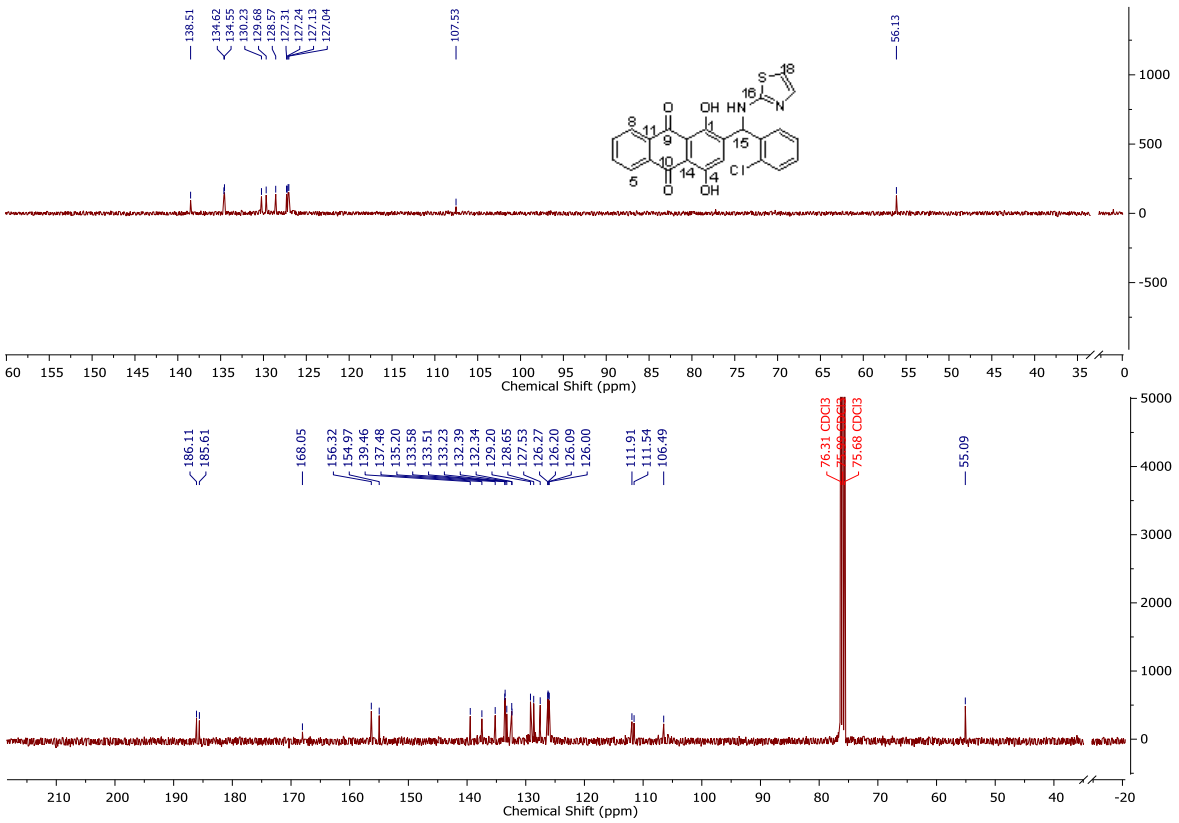

Figure 4.28: 400MHz DEPT-135 and ^{13}C NMR spectrum of 2-((2-chlorophenyl)(thiazol-2-ylamino)methyl)-1,4-dihydroxyanthracene-9,10-dione 85 in $CDCl_3$

4.17 Synthesis of 1-(9,10-dihydro-1,4-dihydroxy-9,10-dioxoanthracen-3-yl)ethyl 2-hydroxy-6-pentadecylbenzoate

The ester of 1, 4-dihydroxy-2-(1-hydroxyethyl)anthracene-9,10-dione **102** and anacardic acid was synthesized according to the method reported by Jin and his co-workers [153]. In this method saturated anacardic acid was to be prepared first by reducing anacardic acid **63** using hydrogen gas (**Scheme 4.22**). The named Steglich esterification requires an *in-situ* activation

of carboxylic acid **63a** (**Scheme 4.21**), by dicyclohexylcarbodiimide under the catalysis of 4-dimethylaminopyridine [154].

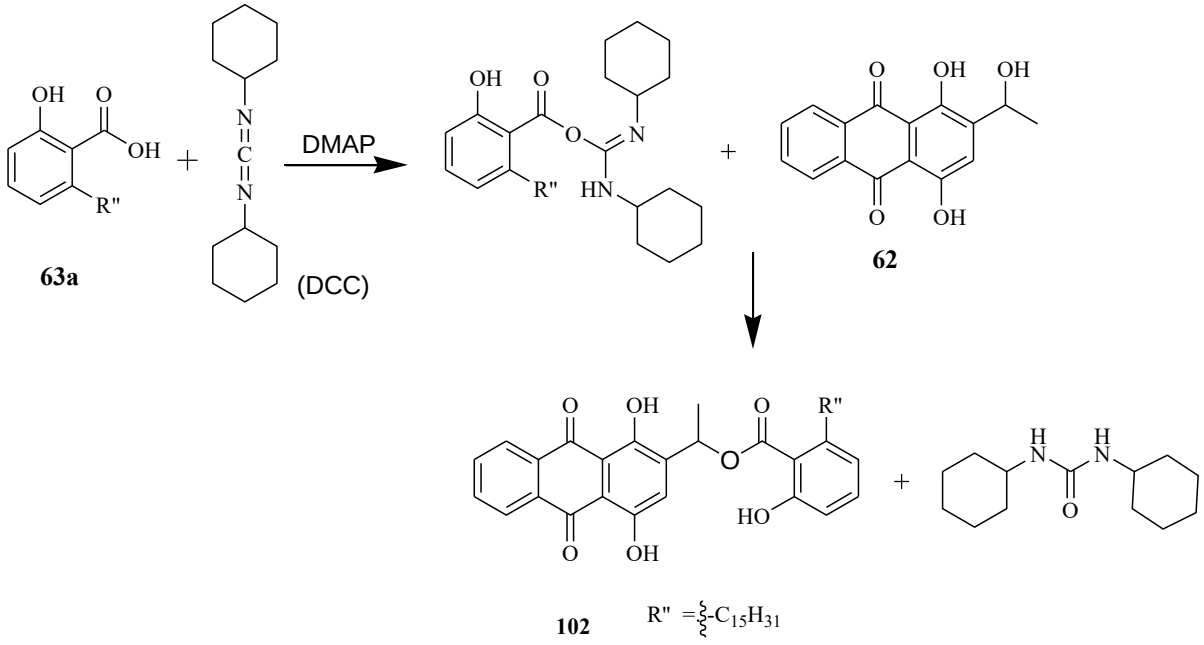

Scheme 4.21: Synthesis of the ester of anacardic acid and 1,4-dihydroxy-2-(1-hydroxyethyl)anthracene-9,10-dione

In the procedure, a cold solution of 1,4-dihydroxy-2-(1-hydroxyethyl)anthracene-9,10-dione was reacted first with DCC and DMAP and then with powdered anacardic acid. After two hours the reaction was quenched with hexane, filtered, and dried to obtain the crude product. This was be purified through column chromatography and after evaporation, the 1,4-dihydroxy anthraquinone ester **102** was obtained as an orange solid 9.5 %. The excess amount of saturated anacardic acid **63a** was needed during the reaction process (2-2.5eq).

The ^{1}H NMR spectrum was characterized with a triplet at δ_H 0.87 ppm integrating to three protons was assigned for terminal -CH_3- groups of the anacardic acid pentadecyl chain (**Figure 4.29**). Another multiplet at δ_H 1.25 ppm integrating to twenty-four was assigned to the 12-CH_2- of the anacardic acid pentadecyl side chain. A doublet at δ_H 1.63 ppm integrating

to three protons was assigned to the -CH_3- groups of the hydroxyethyl group of anthraquinone (H16).

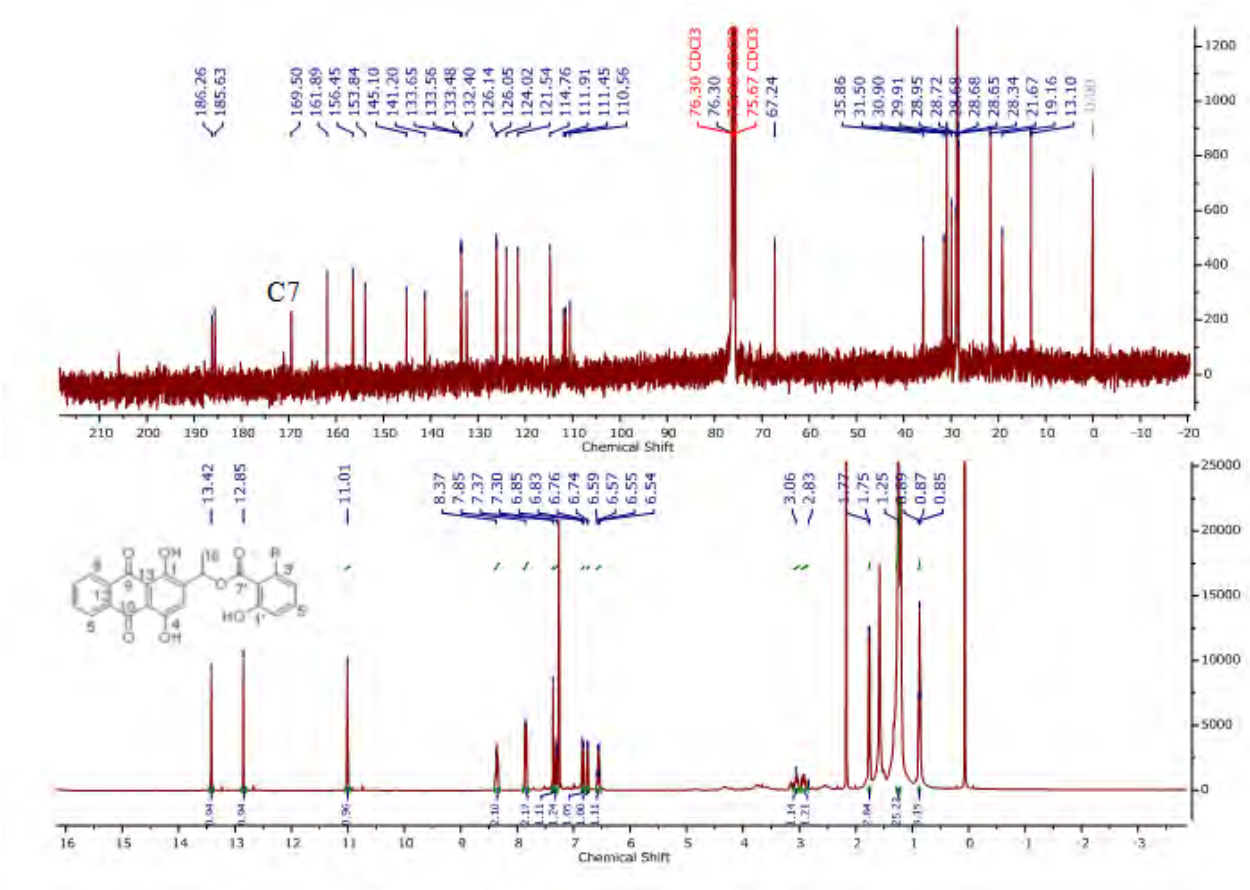

Figure 4. 29: 400MHz ^{1}H and ^{13}C NMR of 1,4-dihydroxyanthraquinone ester 110 in $CDCl_3$

A quartet at δ_H 6.30 ppm integrating to one proton was assigned to the benzylic proton of the anthraquinone ring (H15). Two doublets at δ_H 6.69, 6.83 and a triplet at δ_H 7.17 ppm each integrating to one proton was assigned to the aromatic protons of the anacardic acid ring.

A singlet at δ_H 7.36 ppm integrating to one proton was assigned to the aromatic proton ortho to the hydroxyl ethyl group of the anthraquinone (H3). Multiplets at δ_H 8.20 and 7.94 ppm each integrating to two protons were assigned to the four protons of the un-substituted ring.

The ^{13}C NMR spectrum of anthraquinone ester **102** (**Figure 4.29)** displayed a significant signal at δ_C at 169.5 ppm accounting for the presence of the carbonyl ester group and was

assigned to C7'. A signal at δ_C 121.5 ppm was assigned to C6' while another one at δ_C 114.7 ppm was being assigned to C4'

4.18 Hydrogenation of anacardic acid 63

This was done under hydrogen gas in methanol using a catalytic amount of Pd/C 10% with stirring for 24 hours at room temperature (**Scheme 4.22**). The reaction mixture was afterward filtered to remove the palladium, the solvent was evaporated and the saturated anacardic acid **63a** recrystallized from petroleum ether and was obtained as a white solid 19.9%.

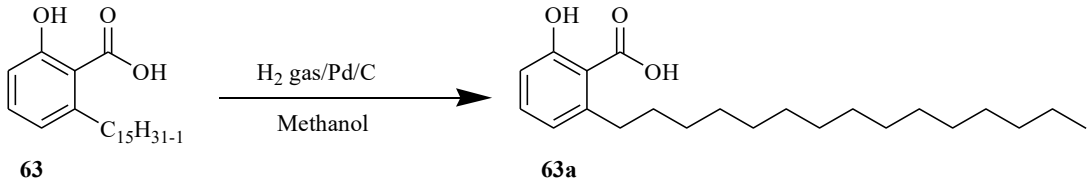

63 **63a**

Scheme 4. 22: Hydrogenation of anacardic acid 63

4.19 Decarboxylation of anacardic acid

The decarboxylation of natural cashew nut-shell liquid was done by dissolving a mixture of CNSL and 2% $Ca(OH)_2$ in toluene and heating to 250 °C as suggested by Tyman [155] with some slight modifications. After two hours the mixture was allowed to cool to room temperature and extracted with petroleum ether filtered and concentrated to yield cardanol as a dark brown oil. The double bonds of cardanol were reduced by hydrogen gas in methanol using a catalytic amount of Pd/C 10% to obtain saturated cardanol **64a** as a white solid in 92%.

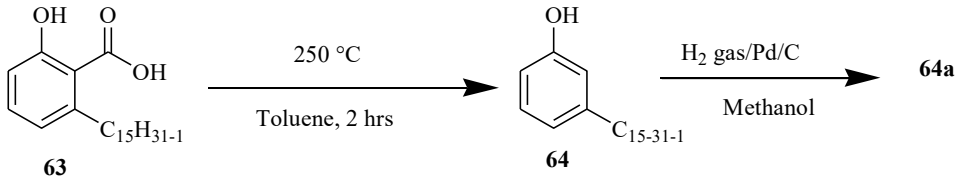

63 **64**

Scheme 4.23: Decarboxylation of anacardic acid 63 to cardanol

The ^{1}H NMR spectrum of cardanol **64a** (**Figure 4.30**) displayed a triplet at δ_H 7.05 ppm integrating one proton which was assigned to the hydrogen meta to the hydroxyl group. A doublet at δ_H 6.67 ppm integrating one proton accounted for the hydrogen ortho to the pentadecyl side chain. A multiplet at δ_H 6.58 ppm integrating two protons was assigned to the two hydrogens ortho to the hydroxyl group. The aliphatic group of this spectrum was acquainted with a triplet at δ_H 2.46 ppm integrating one proton and was assigned to the benzylic hydrogen. A multiplet at δ_H 1.50 ppm integrating two hydrogens was being assigned to the methylene hydrogens next to the benzylic group. A triplet at δ_H 0.81 ppm integrating to three protons accounted for the terminal methyl group of the pentadecyl side chain.

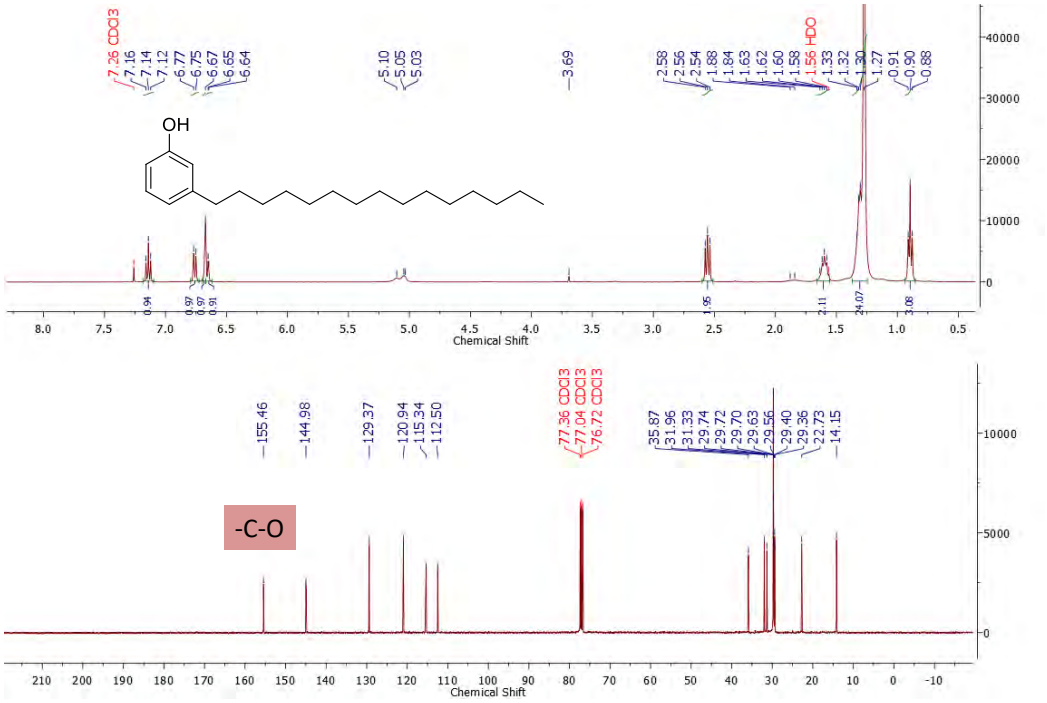

Figure 4. 30: 400MHz ^{1}H NMR, ^{13}C NMR of cardanol 64a in $CDCl_3$ cardanol

The ^{13}C NMR spectrum of compound **64a** (**Figure 4.30**) had its aromatic region displaying six signals. A signal at δ_C 155.5 ppm accounted for the carbon carrying the hydroxyl group. The aliphatic region of this spectrum had its signals resonating at δ_C 14.2 - 35.9 ppm.

CHAPTER 5

BIOASSAY STUDIES AND *IN SILICO* MOLECULAR DOCKING ANALYSIS

5.1 Introduction to the chapter

This chapter describes the *in vitro* biological evaluation of the target compounds against *Trypanosoma brucei (T.b.),* Malaria parasites (*Plasmodium falciparum* 3D7), bacteria parasites, and HeLa cell line. The molecular docking analysis of the 21 ligands docked against the active sites of the protein trypanothione reductase (6BU7) is given in this chapter

5.2 Biological evaluation of the target compounds

The subspecies *Trypanosoma brucei brucei* (*T.b.b*.) which is responsible (animal African trypanosomiasis) is not infective to humans [156], was used for drug screening. Malarial assays were done on chloroquine-sensitive strain 3D7 (*P. falciparum*) [157]. The full sequence genome of the (*Plasmodium falciparum* 3D7) is known hence making it possible for providing new exciting possibilities for discovering novel potent anti-malarial drugs with target-specific pathways [157]. The antibacterial activity was carried out against *Staphylococcus aureus* (ATCC 25923) and *Escherichia coli* (ATCC 25922). The cytotoxicity of the synthesized compounds was done on HeLa cell lines which is the name given for cervical cancer tumors [158]. HeLa cells are extensively used as cell lines to study the cytotoxicity of a chemical compound [159]. The biological screening assays were conducted in collaboration with following laboratories: 1) Biochemistry and Microbiology Department, Rhodes University – Associate Professor Heinrich Hoppe 2) Drug Discovery and Development Centre (H3D), University of Cape Town

5.3 Biological results and discussion

The synthesized compounds LK01- LK21 (**Figure 5.1** and **Figure 5.2**) in this study were biologically evaluated *in vitro* for their inhibitory activities against Trypanosoma parasites

Trypanosoma brucei (T.b.), malaria parasites *P. falciparum* (3D7) strains, bacterial and cytotoxicity assay. A detailed description for the first two assays is provided with pentamidine and chloroquine being used as control drugs, respectively.

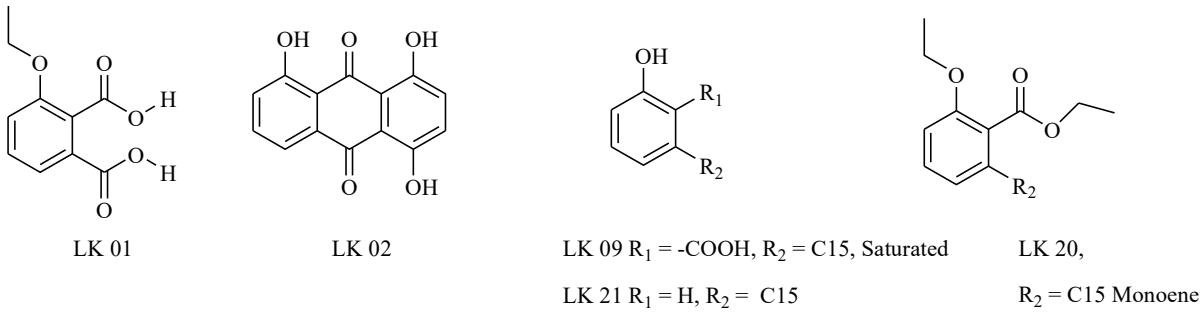

Figure 5. 1: Cashew nut shell liquid derived compounds

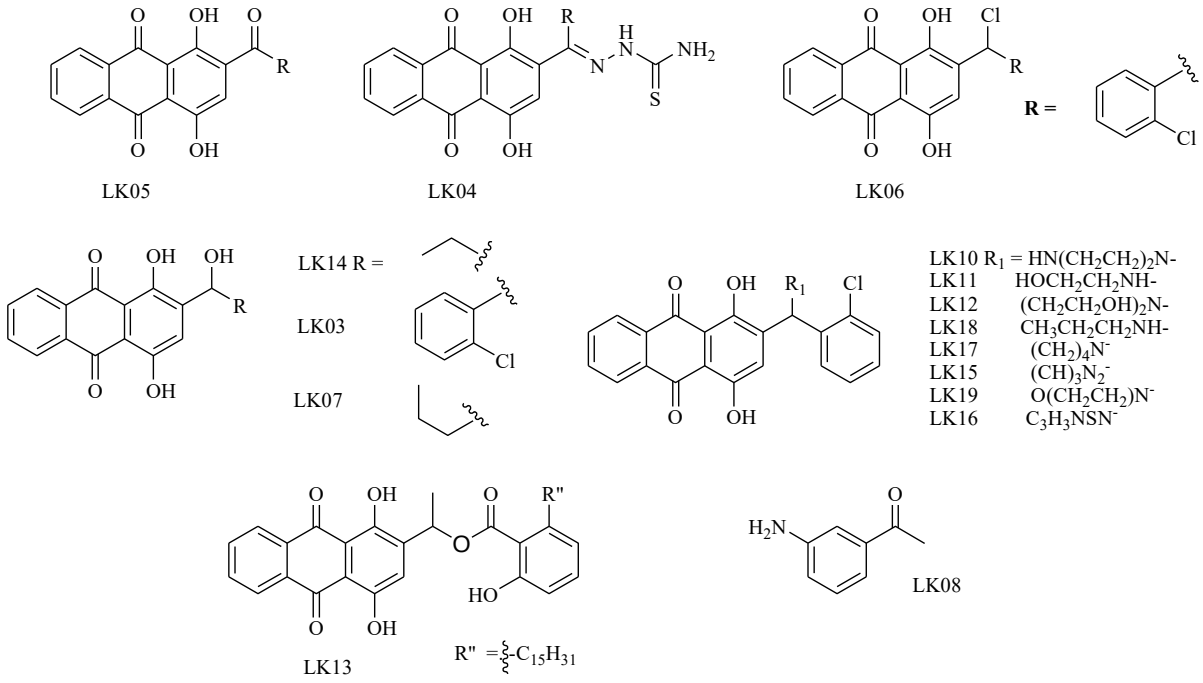

Figure 5. 2: The 1,4-dihydroxyanthraquinone derivatives and 2-amino acetophenone

5.31 *Trypanosoma brucei* assay

Test compounds (LK01-LK21) were evaluated for their anti-trypanosomal activity; compounds LK01, LK 02, LK09, and LK20 were synthetically derived from anacardic acid

63 (**Figure 2.12**) while LK21 was a saturated cardanol **64a** (**Scheme 4.22**). These were all obtained from the agro-waste cashew nut shell liquid. The rest of the compounds that were evaluated against trypanosomiasis were the 1,4-dihydroxyanthraquinone derivatives (**Figure 5.2**). Previous studies have reported that anthraquinones derivatives to be the agents for antimicrobial activities [160]. However, there are very limited studies that have been conducted on the anti-trypanosomal activity of the 1,4-dihydroxyanthraquinone. All the twenty-one compounds were first screened in vitro for their activity against trypanosomal parasites at an initial concentration of 20 μM. The compounds that showed viability below 20% were considered active and were put forwards to determine their IC_{50}. **Table 5.1** shows a summary of the % viability and IC_{50} for individual compounds. A careful analysis of the data in (**Table 5.1)** shows that cashew nut shell liquid-derived compounds LK09, LK20, and LK21 exhibited moderate activity against *T. brucei* parasites with IC_{50} value (3.10-5.04 μM). Cerone *et.al* has recently published a report on the medicinal value of the components of CNSL as potent compounds in the drug discovery for NTD [42]. Compounds LK01 and LK02 did not show activity against *T. brucei*. The activity of the cashew nut shell-derived hybrid against trypanosomes has been reported to be due to the inhibition of glyceraldehyde-3-phosphate dehydrogenase an important enzyme in the catalysis of cellular activities of the pathogen [161].

The 1,4-dihydroxyanthraquinone showed activity ranging from good to moderate, test compound LK04, LK05, LK11, LK12, and LK16 exhibited good activity against *T. brucei* with IC_{50} values ranging from 0.72-1.2 μM. Elaboration of the alcohol functionality of the 1,4-dihydroxyanthraquinone to thiosemicarbazide LK04, carbonyl LK05, to primary amine was important for the increased activity of the 1,4-dihydroxyanthraquinone skeleton. Test compounds LK06, LK07, LK10, LK14, and LK18 were found to exhibit moderate activity against *T. brucei* parasites (IC_{50} values ranging from 2.39-4.73 μM). The table shows the

hydroxyalkyl substituent group as a key determinant of the activity against the parasite. Sample compounds with aliphatic hydroxyalkyl substituents (LK07 and LK14) were active to *T. brucei* parasites while the hydroxyaryl substituent group (LK03) was inactive against *T. brucei* parasites.

Table 5.1: The residual % parasite viability and IC_{50} ± SD obtained for the individual compounds

Code	*Trypanosoma brucei*		*Plasmodium falciparum* strain	
	% Viability	IC_{50} (μM)	% Viability	IC_{50}(μM)
LK01	89.31 ± 4.24	-	103.24 ± 2.41	-
LK02	69.68 ± 1.83	-	19.76 ± 4.82	14.56 ±1.23
LK03	67.58 ± 4.96	-	51.79 ± 1.93	-
LK04	0.04 ± 0.20	0.72 ± 0.02	7.84 ± 3.37	3.17±0.07
LK05	1.83 ± 0.41	0.98 ± 0.005	53.15 ± 5.78	-
LK06	1.29 ± 0.06	2.39 ± 0.12	12.27 ± 0.96	4.27±0.62
LK07	3.30 ± 0.02	3.61 ± 0.07	53.15 ± 3.85	-
LK08	91.79 ± 0.43	-	98.81 ± 2.89	-
LK09	0.54 ± 0.05	5.04 ± 0.12	84.50 ± 0.96	-
LK10	0.23 ± 0.05	3.25 ± 0.23	65.08 ± 1.45	-
LK11	1.70 ± 0.19	1.14 ± 0.08	55.54 ± 3.37	-
LK12	-0.85 ± 0.10	1.10 ± 0.07	18.06 ± 3.37	9.10 ± 0.94
LK13	68.83 ± 1.72	-	84.16 ± 1.45	-
LK14	0.22 ± 0.01	4.73 ± 0.36	60.99 ± 5.30	-
LK15	90.43 ± 3.78	-	50.77 ± 5.30	-
LK16	0.96 ± 0.17	1.20 ± 0.01	52.13 ± 4.34	-
LK17	70.18 ± 6.88	-	16.01 ± 4.34	14.36±1.15

LK18	2.71 ± 0.35	2.59 ± 0.10	80.75 ± 3.37	-
LK19	61.36 ± 2.25	-	64.05 ± 0.96	-
LK20	0.22 ± 0.25	3.10 ± 0.005	54.86 ± 0.48	-
LK21	0.92 ± 0.03	3.79 ± 0.050	54.17± 2.41	-
Pentamidine standard		0.013	Chloroquine	0.01

The bar graph below **(Figure 5.3)** summarizes the % viability of *Trypanosoma brucei* for the test compounds at 20 µM

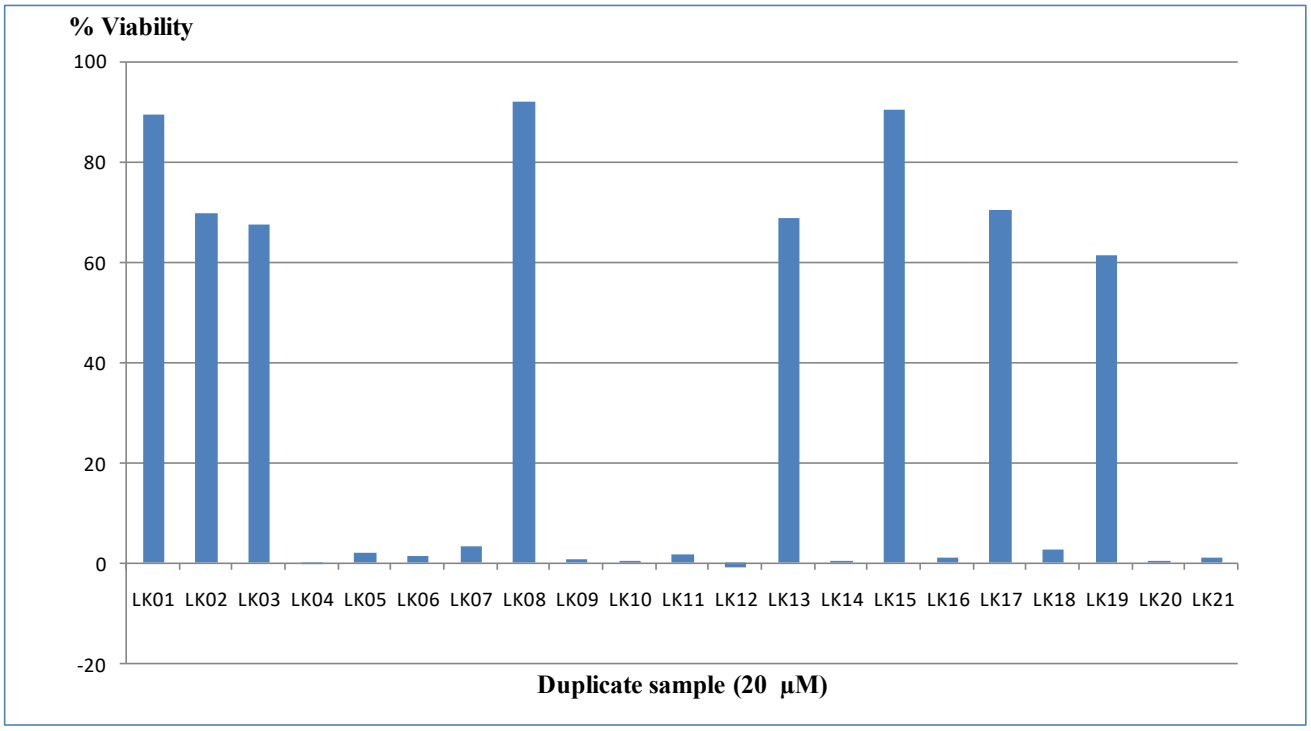

Figure 5. 3: Summary of the antitrypanosomal activity for teat compounds LK01-LK21

As shown from the figure sample compounds LK04, LK05, LK06, LK07, LK09, LK10, LK11, LK12, LK14, LK16, LK18, LK20, and LK21 displayed the viability below 10%. The IC_{50} of each of these compounds were determined.

To assess for anti-trypanosomal activity, compounds were tested in triplicate wells, and a standard deviation (SD) was derived. For each compound, percentage viability was then

plotted against Log (compound concentration) and the IC_{50} (50% inhibitory concentration) was obtained from the resulting dose-response curve by non-linear regression (**Appendix AA11 and AA12**).

5.32 pLDH (Malaria) assay – single concentration screen

The anti-plasmodial activity of the target compounds LK01- LK21 was evaluated against the chloroquine-sensitive 3D7 strain, *P. falciparum* parasite. Few of the test compounds displayed activity against malaria parasites. Test compounds LK04 and LK06 displayed good activity against malaria (IC_{50} = 3.17 and 4.27 µM). The 1,4-dihydroxyanthraquinone with diethanolamine (LK12) and pyrrole (LK17 substituent groups displayed moderate activity against trypanosomiasis (IC_{50} = 9.10 and 14.36 µM)

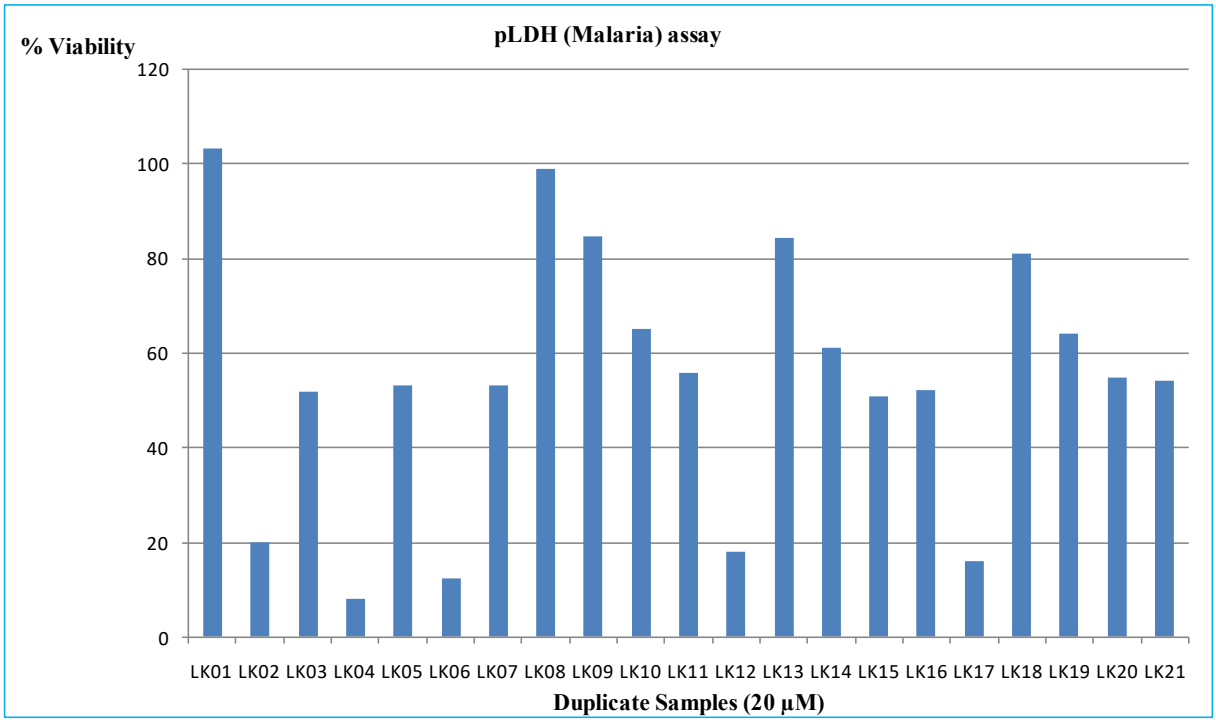

Figure 5.4: Summarized % viability *P. falciparum* parasites against test compounds LK01-LK21

Generally, none one of the CNSL derived compounds, except the 1,4,5-trihydroxyanthraquinone, LK02, showed activity against malaria parasites (**Table 5.1**), (IC_{50}

= 14.56 µM). It can be worthy to note that, the substitution of the hydroxyl group of the alkyl functionality of the 1,4-dihydroxyanthraquinone enhanced the activity of the test compounds.

The bar graph above (**Figure 5.4**) shows the % viability of the individual compounds at the initial concentration of 20 µM. Test compounds LK02, LK04, LK06, LK12, and LK17 were observed to display the % viability below 20% and they were active.

To assess for anti-malarial activity the compounds were tested in a range extending from 100 µM to 0.001693 µM (3 fold-dilution series). For each compound concentration, % parasite viability – the pLDH activity in compound-treated wells relative to untreated controls – is calculated. Compounds were tested in triplicate wells, and a standard deviation (SD) was derived.

For each compound, percentage viability was then plotted against log [C] (**Figure 5.5)** and the IC_{50} (50% inhibitory concentration) was obtained from the resulting dose-response curve by non-linear regression. For comparative purposes, chloroquine (an anti-malarial drug) was used as a drug standard (duplicate) and yields IC_{50} values in the range 0.01-0.05 µM.

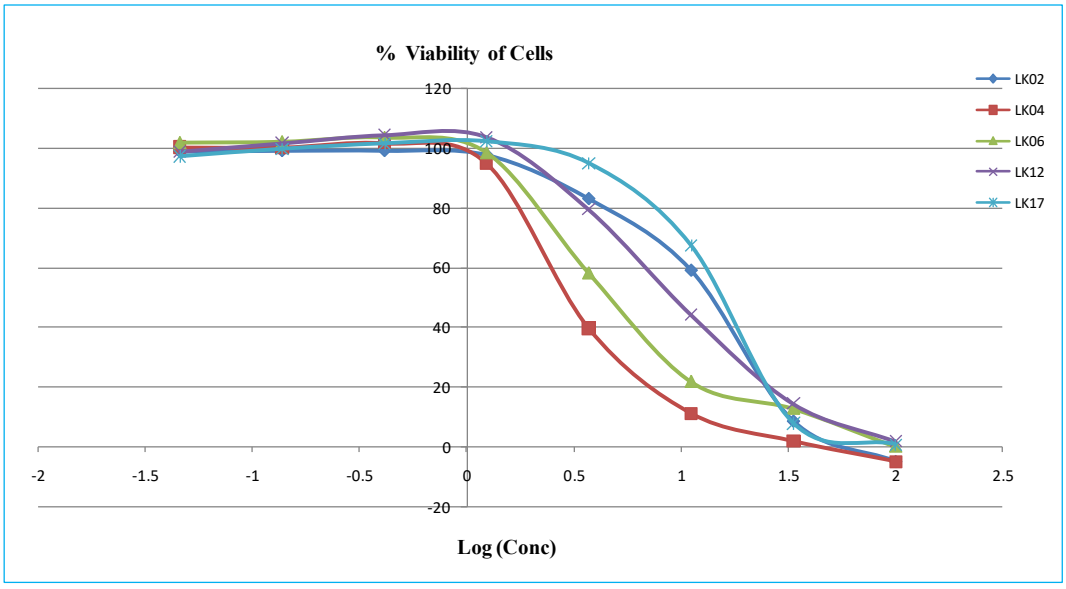

Figure 5. 5: Graph of Log [C] against percentage viability of *P. falciparum* parasites

5.33 Antibacterial assays

Twenty sample compounds were screened in vitro for their antibacterial activity against two bacterial strains, *Staphylococcus aureus,* and *Escherichia coli*. The results were expressed as percentage viability of cells of the treated cell against the untreated at the initial concentration of 50 µg/ml. Test compounds LK02, LK09, LK10, and LK12 showed % viability below 50% and were active against *Staphylococcus aureus* (**Figure 5.6**). Sample compounds LK09 and LK10 inhibited the viability of *Staphylococcus aureus* below 20% (**Figure 5.6**). None of the test compounds did show activity against *Escherichia coli*.

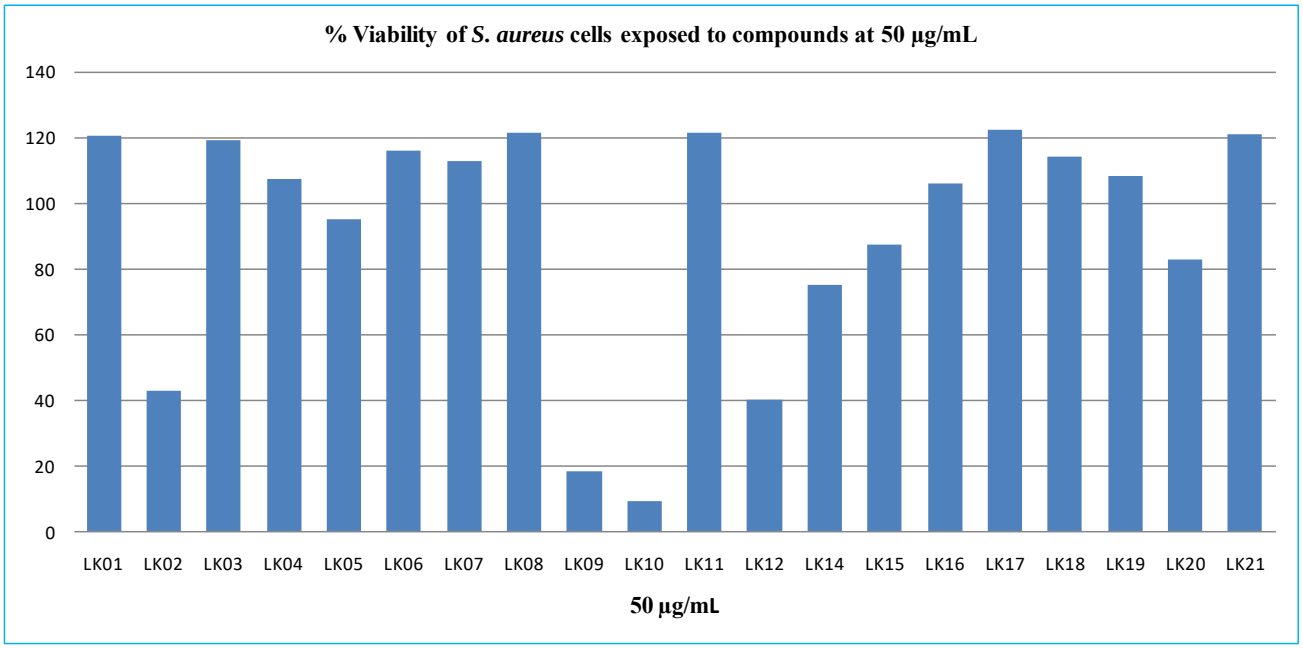

Figure 5.6: Summarized % viability of *S. aureus* at the concentration 50 µg/mL

5.34 Cytotoxicity assays

Twenty sample compounds were screened *in-vitro* for their cytotoxicity against HeLa cell lines. This assay was chosen as a suitable model for the assessment of the effect on a human cell of the test compounds. The results summarized on the bar graph (**Figure 5.7**) show that test compounds LK04, LK10, LK12, and LK14 reduced the viability of HeLa cells below

40%. These four compounds were found to be active against HeLa cells at the concentration of 50 µg/mL

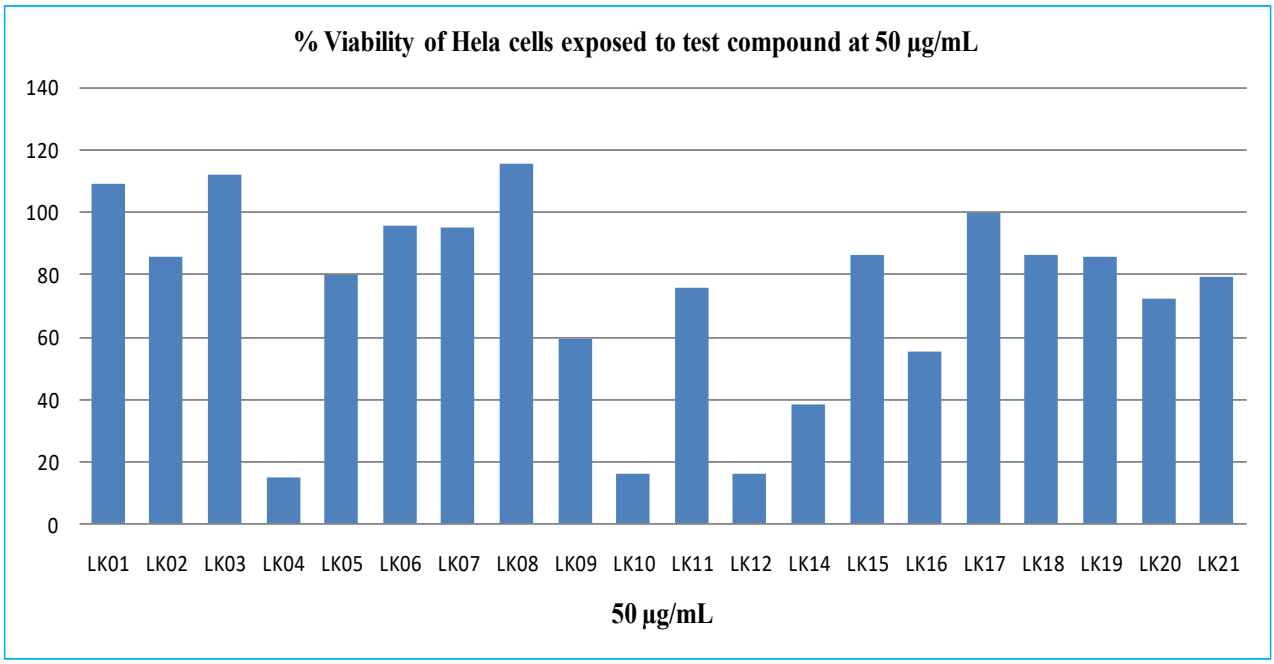

Figure 5.7: Summarized % viability of HeLa cells against test compounds at 50 µg/mL

5.4 *In silico* molecular docking analysis

Human African trypanosomiasis (HAT) is one of the most devastating neglected tropical diseases that occur in sub-Saharan Africa [162]. The causative agents for this disease are two species of protozoa: *Trypanosoma brucei gambiense* and *Trypanosoma brucei rhodesiense* [163]. Several drugs as reported earlier have been clinically approved for treating the disease [32]. Despite the available remedies, the mechanism of action of prescribed drugs for HAT is still unknown [164]. Nevertheless, the current drugs are reported to have severe side effects and to date, there is no vaccine developed against HAT [32]. This has necessitated the need for developing effective drugs to circumvent the existing side effects.

Several drug targets have been identified in *T. brucei* which are trypanothione reductase (TR), rhodesain, triosephosphate isomerase (TIM), farnesyl diphosphate synthase (FDS) [165] and L-threonine-3-dehydrogenase [164]. In this present work, twenty test compounds

from the natural and synthetic source were docked into T. *brucei* active sites using two docking procedures, Knime workflow, and the glide grid docking, the results were tabulated (**Table 5.6 and Table 5.7**) respectively.

The drug target was trypanothione reductase; PDB Id, 6BU7. The protein is a polypeptide with two chains, A and B. The active sites of the dipeptide (6BU7) (**Figure 5.8 A**) contain two ligands flavin-adenine dinucleotide (FAD) and the inhibitor RD_0 (1-[2-(piperidin-4-yl)ethyl]-5-{5-[1-(pyrrolidin-1-yl)cyclohexyl]-1,3-thiazol-2-yl}-1H-indole) both present in chain A and B [166]. Several other molecules present in the protein are sulphate ion (SO_4), 4-(2-hydroxyethyl)-1-piperazine ethanesulfonic acid (EPE), and Glycerol (GOL) [166]. Chain B was used in the glide grid docking (**Figure 5.8 B**)

Figure 5. 8: (A) Protein trypanothione reductase (6BU7), (B) Chain B, trimmed ligands labeled in red color, and EPE labeled in pink

Table 5. 2: Knime workflow docking results with enzyme 6BU7

Ligand code	Docking score	Energy
LK16	-6.530	27.221
LK02	-6.523	17.114
LK13	-6.479	43.373
LK14	-6.413	22.415
LK05	-6.229	37.913
LK15	-5.891	59.710
LK11	-5.828	39.826
LK07	-5.679	26.029
LK01	-5.437	9.460
LK19	-5.250	49.297
LK18	-5.225	45.142
LK10	-5.138	70.846
LK04	-5.007	19.173
LK06	-4.982	44.858
LK08	-4.965	17.240
LK09	-4.936	16.263
LK17	-4.894	55.833
LK21	-4.798	13.738
LK20	-4.581	19.554

The results shown from **table 5.2** above show anthraquinones LK16, LK02 and LK13 had higher docking scores with the target receptor protein 6BU7. The figure below shows both the 2D and the 3D interaction of the ligand with the protein

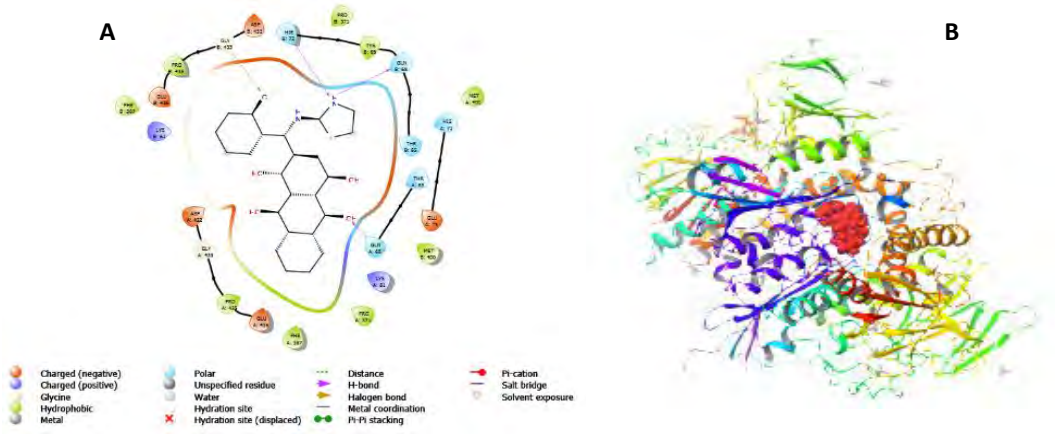

Figure 5.9: (A) 2D interaction of ligand LK 16 with target protein as visualized in maestro, three hydrogen bond interactions represented in purple lines, and one halogen bond represented in red colour. (B) 3D pose view interaction of ligand LK16 with the target protein docked using the ligand represented in red ball

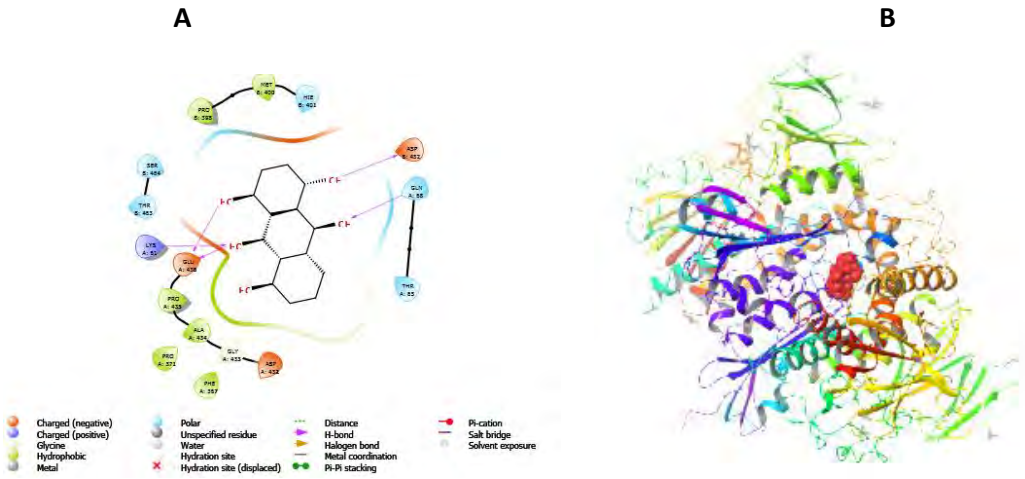

Figure 5. 10:(A) 2D interaction of ligand LK02 with target protein as visualized in maestro, the five-hydrogen bond interaction represented in purple lines (B) 3D pose view interaction of ligand LK02 with the target protein represented in red ball

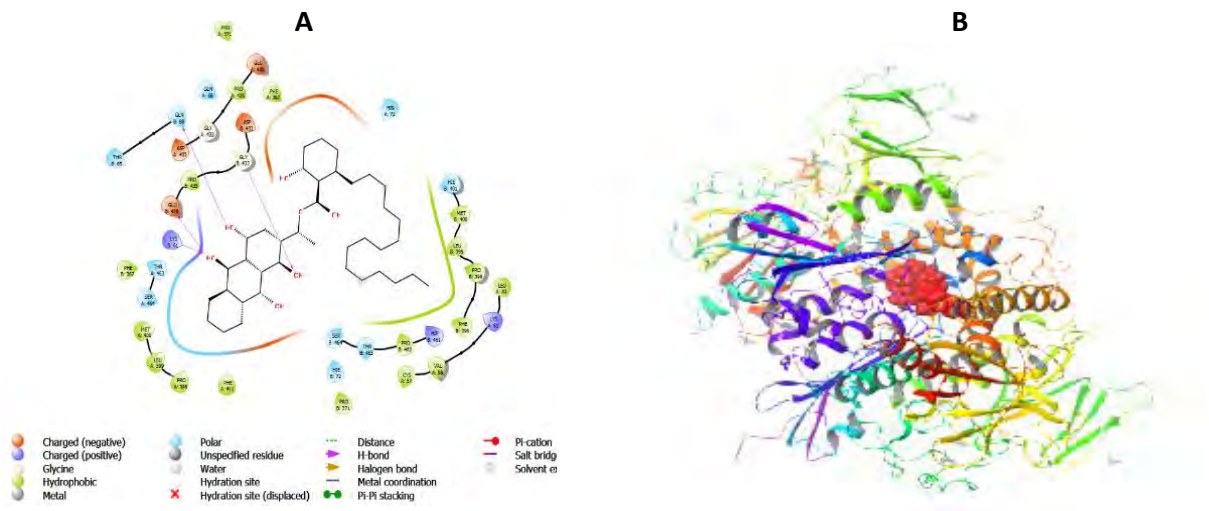

Figure 5.11(A) 2D interaction of ligand LK13 with target protein as visualized in maestro, four hydrogen bond interactions represented in purple lines. (B) 3D pose view interaction of ligand LK13 with the target protein with the ligand represented in red ball

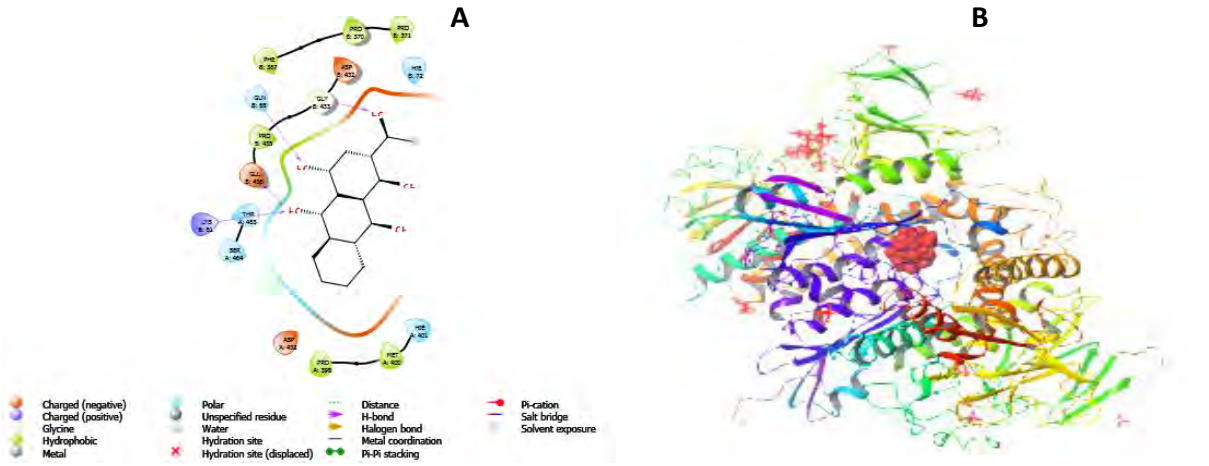

Figure 5.12:(A) 2D interaction of ligand LK 14 with target protein docked as visualized in maestro, the four-hydrogen bond interaction represented in purple lines (B) 3D pose view interaction of ligand LK14 with the target protein, the ligand represented in red ball

Table 5.3: Glide grid docking results with 6BU7

Ligand	Docking score	Glide score	Glide emodel
LK16	-7.351	-7.364	-53.057
LK02	-7.141	-7.141	-57.132
LK13	-8.775	-8.775	-74.202
LK14	-7.046	-7.047	-60.389
LK05	-5.426	-5.426	-38.654
LK15	-7.419	-7.886	-46.058
LK11	-6.653	-6.725	-53.024
LK07	-7.279	-7.280	-51.459
LK01	-7.596	-7.605	-65.694
LK19	-5.288	-6.979	-37.458
LK18	-6.713	-6.781	-54.144
LK10	-7.25	-7.312	-45.397
LK04	-5.683	-5.730	-54.738
LK06	-6.462	-6.464	-56.299
LK08	-6.797	-6.797	-44.224
LK09	-5.584	-5.584	-63.370
LK17	-6.426	-6.607	-32.999
LK21	-6.264	-6.265	-49.944
LK20	-5.731	-5.731	-75.003
LK12	-7.529	-7.691	-65.506
Pentamidine	-4.128	-4.128	-51.710
Eflornithine	-6.055	-6.335	-49.210
Camptothecin	-6.446	-6.446	-60.054

5.5 *In silico* molecular docking results and discussion

Anthraquinone test samples LK 04, LK 05, LK11, LK12, and LK 16 were active with minimum inhibitory concentration (IC_{50}) between this range 0.5-1.5μM against *T. brucei*. The in silico molecular docking studies indicated LK 16 and LK 12 have a good docking score -7.351 and -7.529 Kcal/mol. The diethanolamine anthraquinone compound LK 12 (**Figure 5.13**), was observed to show three H-bonding interactions with amino acid residues LYS 60, ALA 363 and ALA 365. while the 2-aminothiazole anthraquinone LK16 (**Figure 5.14)** showed two hydrogen-bonding interactions with amino acid residues LYS 60 and THR 335.

Table 5.4: Antitrypanosomal and molecular modelling evaluation of test compound

Code	*Trypanosoma brucei*	
	IC_{50} (μM)	Docking score
LK04	0.72 ± 0.02	-5.68
LK05	0.98 ± 0.005	-5.40
LK06	2.39 ± 0.12	-6.46
LK07	3.61 ± 0.07	-7.28
LK09	5.04 ± 0.12	-5.58
LK10	3.25 ± 0.23	-7.25
LK11	1.14 ± 0.08	-6.65
LK12	1.10 ± 0.07	-7.53
LK14	4.73 ± 0.36	-7.05
LK16	1.20 ± 0.01	-7.35
LK18	2.59 ± 0.10	-6.71
LK20	3.10 ± 0.005	-5.73
LK21	3.79 ± 0.050	-4.13

Pentamidine	0.013	-4.13

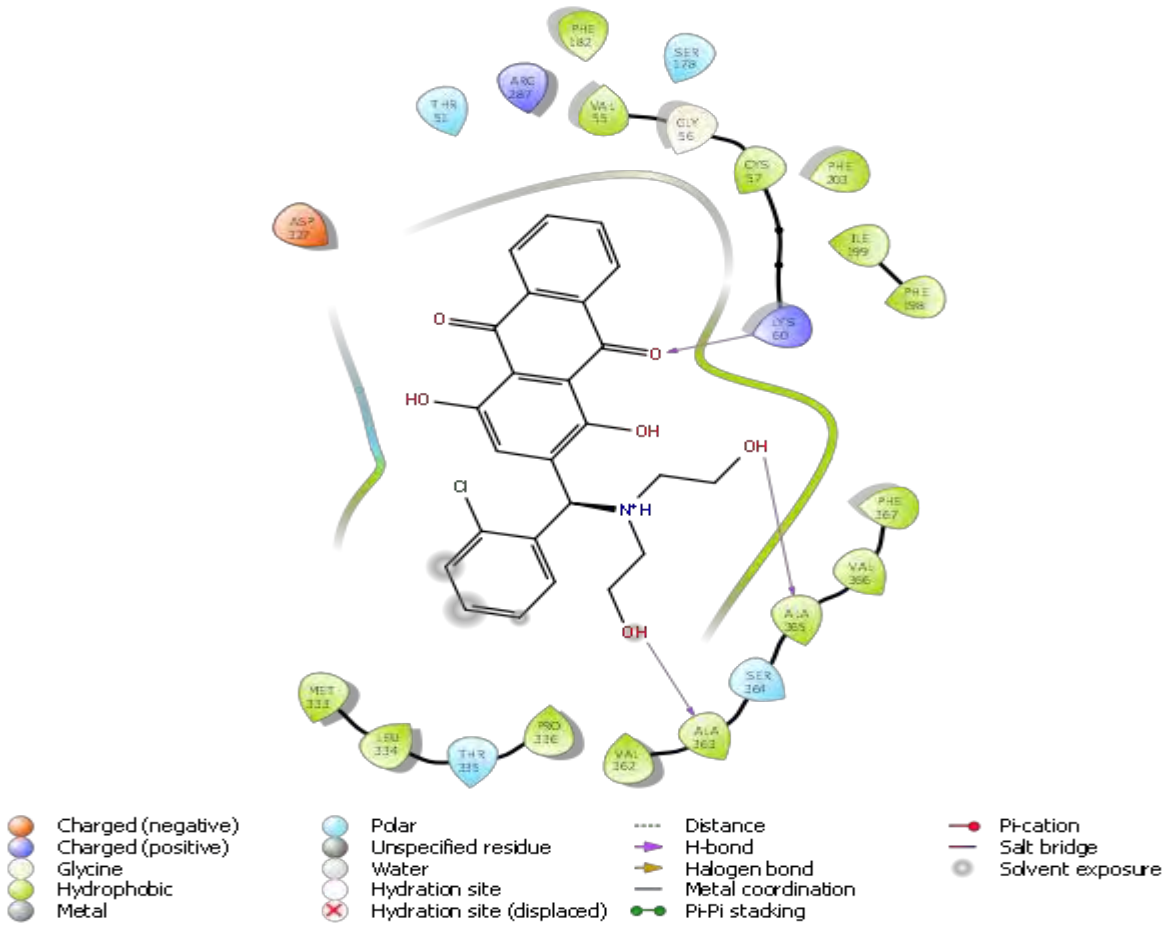

Figure 5. 13: The interactions of ligand LK 12 with the receptor protein molecule, the H-bonding interactions are indicated by the purple arrow

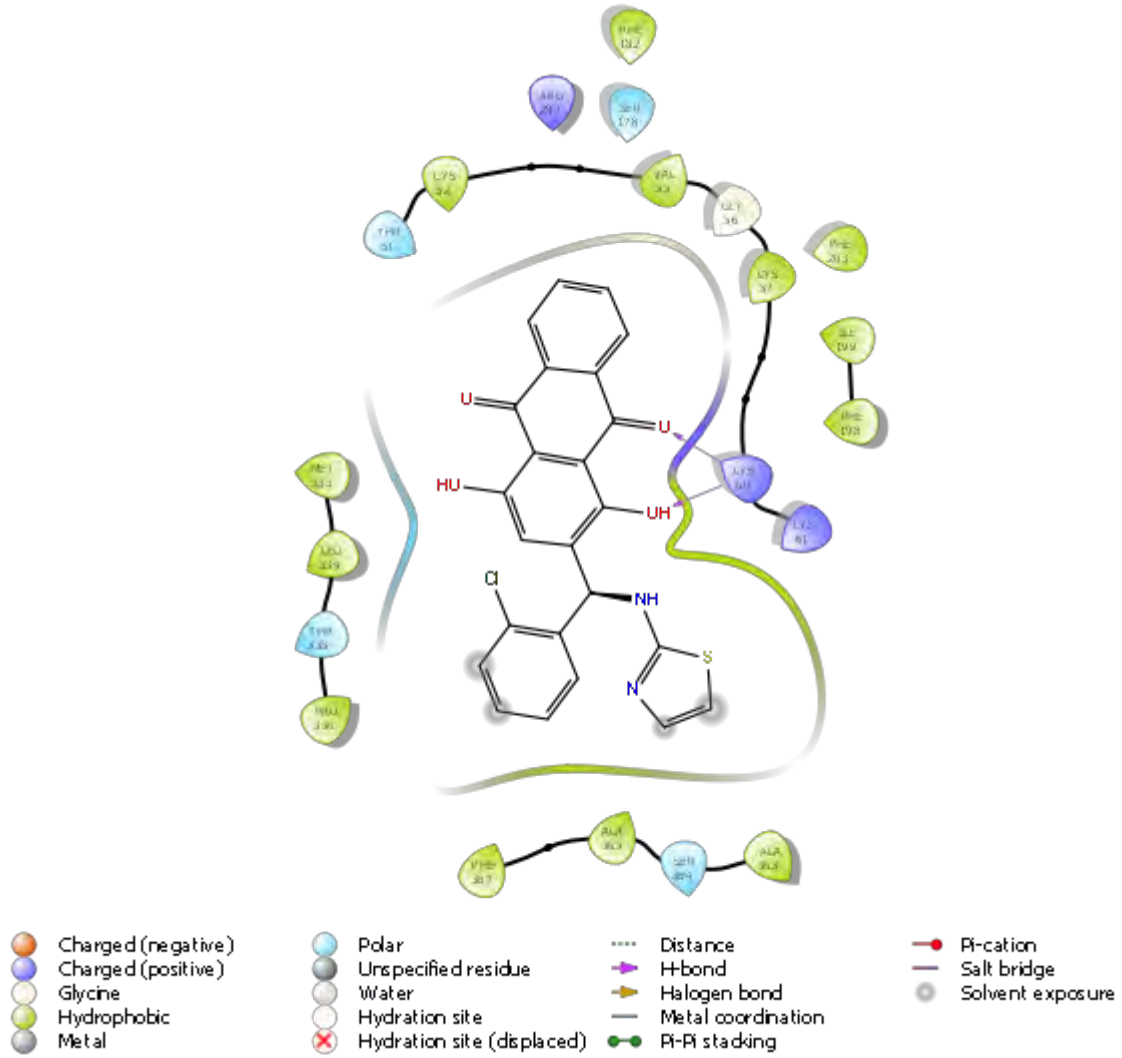

Figure 5.14: The interactions of ligand LK 16 with the receptor protein molecule, the H-bonding interactions are indicated by the purple arrow

Compounds LK04, LK05, and LK11 had moderate binding affinity -5.683, -5.40, and -6.653 kcal/mol, respectively. The bioassay studies show thiosemicarbazone anthraquinone LK 04 to be more active with IC_{50} 0.72 µM less than the rest of the compounds, that were tested against *T. brucei*. Despite the moderate binding energy results thiosemicarbazone LK04 (**Figure 5.13)** was found to show several binding interactions with the receptor protein molecule than LK 05 and LK11. Compound LK04 was found to appear in H-bonding interaction with amino acid residues SER 162, ARG 287, LEU 334 and THR 335, pi-pi stacking with PHE 198, pi-cation with ARG 287 and halogen bond interaction with CYS 57.

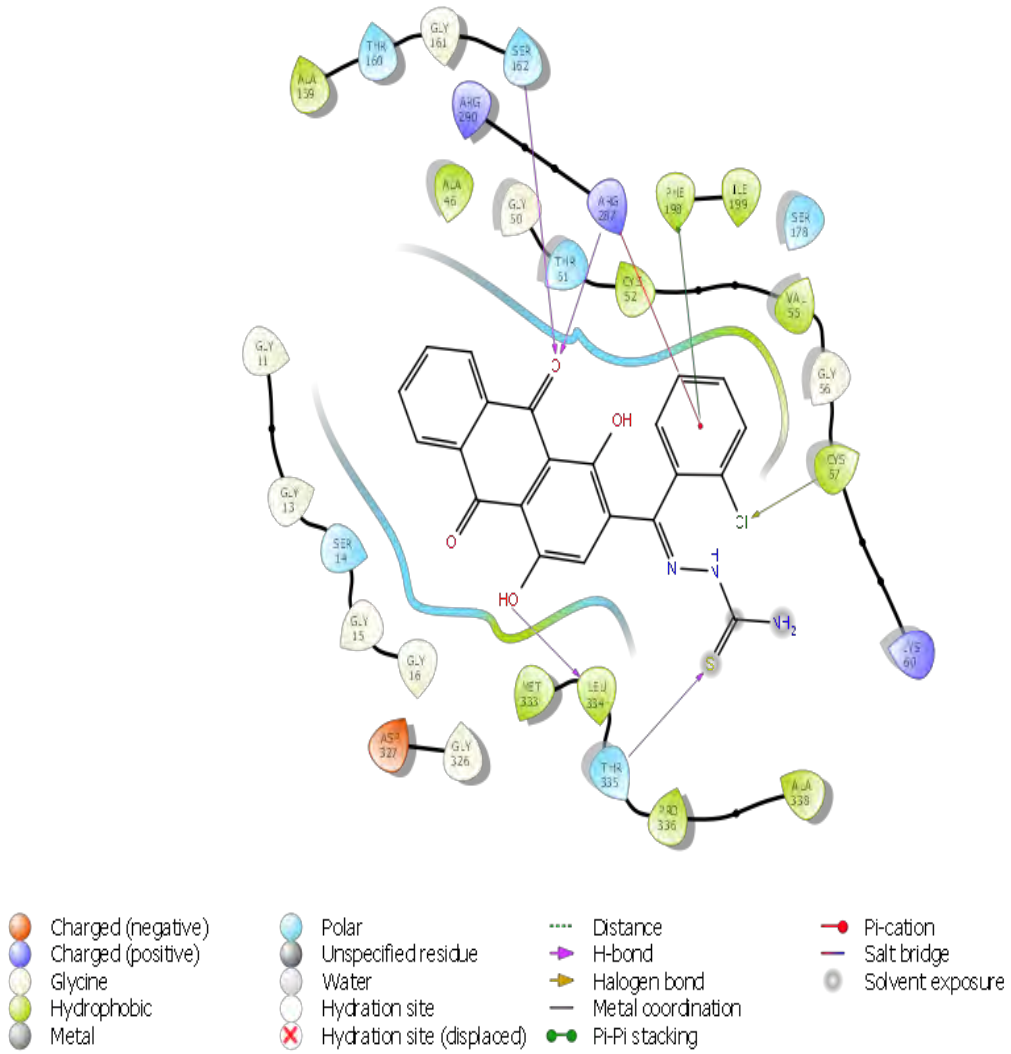

Figure 5. 15: The interactions of ligand LK 04 with the receptor protein molecule, showing H-bonding interactions, Pi-cation, halogen bond interaction, and pi-pi-stacking.

Compound LK 06, LK07, LK09, LK10, LK 14, LK 18, LK 20, and LK 21 showed moderate activity against *T. brucei* with IC_{50} ranging from 2.00-5.10 μM, The in silico molecular docking studies show that compound LK 07, LK10 and LK 14 have high binding affinity -7.279, -7.25 and -7.046 kcal/mol. These compounds formed an H-bonding interaction with at least two or three amino acid residues LYS 60, ASP 327, and ALA 363. Sample molecules LK09, LK18, LK20 and LK21 showed moderate binding energy of -5.584, -6.713, -5.731, and -6.264 kcal/mol, respectively. The interaction of these compounds with the receptor protein is included in the appendix (**AA4-AA7**)

Standard drugs pentamidine and eflornithine were found to bind to the receptor molecule with docking scores of -4.128 and -6.055 kcal/mol respectively; the receptor-ligand interactions are shown in appendices (**AA8** and **AA9**). Pentamidine forms H-bonding association with one key amino acid residue ALA 363 while eflornithine associates with amino acid residues ASP 327, THR 51 and SER 14. Camptothecin which is the human topoisomerases I (top I) was found to bind the active site of the protein 6BU7 with the slightly higher binding affinity of -6.446 kcal/mol (**AA10**). Camptothecin forms H-bonding interaction with amino acid residues such as LYS 60 and THR 335.

5.6 Swiss ADME results for ligands that were active against trypanosomiasis

The thirteen ligands that were found to be active against trypanosomiasis were passed through the SwissADME filter and were detected for their physicochemical properties, Lipophilicity, pharmacokinetics, solubility, and lead likeness (**Table 5.4**). The allowed molecular properties for the topological polar surface area (TPSA) ≤ 140; Consensus Log P ≤ 5; the number of rotatable bonds ≤ 10 [167]. As based on this preview compound LK04, LK09, LK20, and LK21 did not pass on the first filter. The results revealed that the CNSL

derived compounds LK09, LK20 and LK21 do not have drug-like properties and hence they were filtered out.

Table 5. 5: SwissADME results for the test ligands

Ligand	Physicochemical properties		Lipophilicity	Pharmacokinetics	Lead Likeness
	TPSA (Å²)	No of rot. bonds	Consensus Log P	GI Absorption	
LK04	157.10	4	3.44	Low	No
LK05	91.67	2	3.57	High	No
LK06	74.60	2	4.39	High	No
LK07	74.60	2	2.81	High	Yes
LK09	57.53	15	6.37	High	No
LK10	89.87	3	3.38	High	No
LK11	106.86	5	3.15	High	No
LK12	118.30	7	2.95	High	No
LK14	94.83	1	1.88	High	Yes
LK16	127.76	4	4.42	Low	No
LK18	86.63	5	4.30	High	No
LK20	35.53	17	7.04	Low	No
LK21	20.23	14	6.89	Low	No

5.7 Lipinski Rule of Five results

Eight ligands that had passed the SwissADME filter were subjected to be filtered further by the SCFBio Lipinski Rule of Five server. The Lipinski rule distinguished drug-like compounds and non-drug like compounds as based on five rules which are molar mass ≤ 500, partition coefficient (log P ≤ 5), hydrogen bond donor ≤ 5, hydrogen bond acceptors ≤ 10, and molar refractivity should be within 40 to 130 [164] [168]. Compounds meeting these five criteria are considered orally drug-like compounds. Test compound LK16 (**Table 5.5**) was filtered out as based on this rule it had a log P > 5. Generally, the results from the two table (**Table 5.4** and **Table 5.5**) has indicated that the 1,4-dihydroxyanthraquinone derivatives have great potential of orally being drug-like candidates.

Table 5.6: Lipinski Rule of Five Results

Ligand	Mass (g/mol)	H-acceptor	H-donor	Log P	Refractivity
LK05	378.76	5	2	3.75	97.96
LK06	399.22	4	2	4.85	102.22
LK07	298.00	5	3	2.31	78.32
LK10	448.90	6	3	3.52	120.81
LK11	423.85	6	4	3.19	111.46
LK12	467.50	7	4	2.66	121.18
LK14	284.26	5	3	1.92	73.71
LK16	462.90	6	3	5.18	122.11
LK18	421.87	5	3	4.61	114.66

CHAPTER 6

CONCLUSIONS

Generally in this study, we demonstrated our efforts on the synthesis of analogues of a natural anthraquinone utilizing starting materials from natural origin and synthetic sources. We successfully synthesized 1,4,5-trihydroxyanthraquinone which is a potential antiparasitic agent from the agro-waste cashew nut shells. The findings from this study, indicate that the components of CNSL and alkyl amino-substituted 1,4-dihydroxyanthraquinone derivatives can be used as agents for anti-trypanosomiasis. These compounds can serve as motifs to construct effective drugs active against trypanosomiasis. Since the components of CNSL showed no antiplasmodial activity, it is worthy to note that, they cannot be used for the construction of anti-malarial drugs.

The *in silico* molecular docking analysis results and the bioassay studies suggest that alky 1,4-dihydroxyanthraquinones can be good candidates in the preparation of drug-like compounds that can be used in the development of drugs effective against trypanosomiasis. In conclusion, the study has disclosed on the suitability of 1,4-dihydroxyanthraquinone derivatives as important scaffolds in the construction of pharmaceutical important drugs with varied bioactivities such as antiplasmodial, antibacterial, and anticancer.

RECOMMENDATIONS FOR FUTURE WORK

The current reported work has used the Friedel-Crafts acylation (FCA) method to synthesize the 1,4,5-trihydroxyanthraquinone from the agro-waste anacardic acid. The use of FCA to synthesize this derivative was limited due to low yields and lack of regioselectivity; these drawbacks need to be eliminated in the future. This study recommends thorough modifications of FCA method to synthesize 1,4,5-trihydroxyanthraquinone.

Since the components of CNSL and 1,4-dihydroxyanthraquinone derivatives displayed potency against trypanosomiasis, it is evident that these compounds need to be studied in detail to understand their mechanism of action and their structure-activity relationship. The modified Marschalk reaction was used as a motive to synthesize the 1,4-dihydroxyanthraquinone derivatives; these compounds need to be further studied with particular emphasis on stereoselective synthesis of enantiomerically pure anthraquinone amines, chlorides, and alcohols be tested for their biological activities.

REFERENCES

[1] T. Van Nguyen, M. D'Hooghe, S. Pattyn, and N. De Kimpe, "Synthesis of functionalized 1,4-dihydro-9,10-anthraquinones and anthraquinones by ring closing metathesis using Grubbs' catalyst," *Synlett*, no. 11, pp. 1913–1916, 2004, doi: 10.1055/s-2004-831299.

[2] V. Mohanlall and B. Odhav, "Antibacterial, anti-inflammatory and antioxidant activities of anthraquinones from Ceratotheca triloba (Bernh) Hook F," *J. Med. Plants Res.*, vol. 7, no. 14, pp. 877–886, 2013, doi: 10.5897/JMPR12.900.

[3] D. Hua *et al.*, "Syntheses, Molecular Targets and Antitumor Activities of Novel Triptycene Bisquinones and 1,4-Anthracenedione Analogs," in *Anti-Cancer Agents in Medicinal Chemistry*, vol. 6, no. 4, 2008, pp. 303–318.

[4] O. C. Mansour *et al.*, "New anthracenedione derivatives with improved biological activity by virtue of stable drug-DNA adduct formation," *J. Med. Chem.*, vol. 53, no. 19, pp. 6851–6866, 2010, doi: 10.1021/jm901894c.

[5] "Synthesis and activity of substituted anthraquinones against a human filarial parasite, Brugia malayi," *J. Med. Chem.*, vol. 48, no. 8, pp. 2822–2830, 2005, doi: 10.1021/jm0492655.

[6] U. Ramakrishna, A. Swathi, S. Banavath, and R. Suthakaran, "Design and Synthesis of Novel Hydroxy – Anthraquinone Derivatives As Anti-Leshmanial Agents," vol. 6, no. 16, pp. 759–764, 2017, doi: 10.20959/wjpr201716-10210.

[7] D. Lv, J. Cui, Y. Wang, G. Zhu, M. Zhang, and X. Li, "Synthesis and color properties of novel polymeric dyes based on grafting of anthraquinone derivatives onto O-carboxymethyl chitosan," *RSC Adv.*, vol. 7, no. 53, pp. 33494–33501, 2017, doi: 10.1039/c7ra04024e.

[8] L. F. Tietze, K. M. Gericke, and I. Schuberth, “Synthesis of highly functionalized anthraquinones and evaluation of their antitumor activity,” *European J. Org. Chem.*, no. 27, pp. 4563–4577, 2007, doi: 10.1002/ejoc.200700418.

[9] S. O. de Silva, M. Watanabe, and V. Snieckus, “General Route to Anthraquinone Natural Products via Directed Metalation of N,N-Diethylbenzamides,” *J. Org. Chem.*, vol. 44, no. 26, pp. 4802–4808, 1979, doi: 10.1021/jo00394a012.

[10] G. Tririya and M. Zanger, “Synthesis of anthracyclinone precursor: 5,12-dihydroxy-1,3,4- trihydronaphthacene-2,6,11-quinone,” *Synth. Commun.*, vol. 34, no. 17, pp. 3047–3059, 2004, doi: 10.1081/SCC-200028508.

[11] C.Avendano and J.C Menendez, *Medicinal Chemistry of Anticancer Drugs*. The Author(s). Published by Elsevier Ltd. This is an Open Access article under the CC BY-NC-ND 4.0 licence, 2008.

[12] L. M. Zhao, F. Y. Ma, H. S. Jin, J. Ma, H. Wang, and C. Z. Fu, “Facile installation of a hydroxyalkyl group into hydroxyanthraquinones and aminoanthraquinones through the modified Marschalk reaction,” *European J. Org. Chem.*, no. 31, pp. 7193–7199, 2013, doi: 10.1002/ejoc.201300891.

[13] N. Coufal and L. Farnaes, “Cancer Management in Man: Chemotherapy, Biological Therapy, Hyperthermia and Supporting Measures,” *Cancer Manag. Man Chemother. Biol. Ther. Hyperth. Support. Meas.*, no. January, 2011, doi: 10.1007/978-90-481-9704-0.

[14] J. V. McGowan, R. Chung, A. Maulik, I. Piotrowska, J. M. Walker, and D. M. Yellon, “Anthracycline Chemotherapy and Cardiotoxicity,” *Cardiovasc. Drugs Ther.*, vol. 31, no. 1, pp. 63–75, 2017, doi: 10.1007/s10557-016-6711-0.

[15] R. Article, “International Journal of Biotechnology and Bioengineering

Anthracyclines : Mechanism of Action , Classification , Pharmacokinetics and Future – A Mini Review," vol. 4, no. 4, pp. 81–85, 2018.

[16] Y. Liu, Y. Liang, J. Jiang, Q. Qin, L. Wang, and X. Liu, "Design, synthesis and biological evaluation of 1,4-dihydroxyanthraquinone derivatives as anticancer agents," *Bioorganic Med. Chem. Lett.*, vol. 29, no. 9, pp. 1120–1126, 2019, doi: 10.1016/j.bmcl.2019.02.026.

[17] L. M. Zhao, F. Y. Ma, H. S. Jin, S. Zheng, Q. Zhong, and G. Wang, "Design and synthesis of novel hydroxyanthraquinone nitrogen mustard derivatives as potential anticancer agents via a bioisostere approach," *Eur. J. Med. Chem.*, vol. 102, pp. 303–309, 2015, doi: 10.1016/j.ejmech.2015.08.006.

[18] J. J. E. Munissi, "New polycyclic ketides and other metabolitiesfrom cultures of some Tanzanian marine fungi," University of Dar es Salaam, 2011.

[19] H. Hussain, S. Aziz, B. Schulz, and K. Krohn, "Synthesis of a 4H-anthra[1,2-b]pyran derivative and its antimicrobial activity," *Nat. Prod. Commun.*, vol. 6, no. 6, pp. 841–843, 2011, doi: 10.1177/1934578x1100600621.

[20] G. Jin, G. Song, X. I. Zheng, Y. Kim, D. Sok, and B. Ahn, "Evaluation of Antitumor Activity," *Arch. Pharmacol. Res.*, vol. 21, no. 2, pp. 198–206, 1998.

[21] D. Sereno *et al.*, "Noninvasive biological samples to detect and diagnose infections due to trypanosomatidae parasites: A systematic review and meta-analysis," *Int. J. Mol. Sci.*, vol. 21, no. 5, pp. 0–49, 2020, doi: 10.3390/ijms21051684.

[22] A. A. M. Alkhaldi, H. P. de Koning, and S. N. A. Bukhari, "Antileishmanial and antitrypanosomal activity of symmetrical dibenzyl-substituted α,β-unsaturated carbonyl-based compounds," *Drug Des. Devel. Ther.*, vol. 13, pp. 1179–1185, 2019, doi: 10.2147/DDDT.S204733.

[23] I. Rohousova *et al.*, “Exposure to Leishmania spp. and sand flies in domestic animals in northwestern Ethiopia,” *Parasites and Vectors*, vol. 8, no. 1, pp. 1–10, 2015, doi: 10.1186/s13071-015-0976-1.

[24] P. O. Odeniran and I. O. Ademola, “A meta-analysis of the prevalence of African animal trypanosomiasis in Nigeria from 1960 to 2017,” *Parasites and Vectors*, vol. 11, no. 1, pp. 1–12, 2018, doi: 10.1186/s13071-018-2801-0.

[25] A. Geiger *et al.*, “Escaping deleterious immune response in their hosts: Lessons from trypanosomatids,” *Front. Immunol.*, vol. 7, no. MAY, pp. 1–21, 2016, doi: 10.3389/fimmu.2016.00212.

[26] M. Parsons, E. A. Worthey, P. N. Ward, and J. C. Mottram, “Comparative analysis of the kinomes of three pathogenic trypanosomatids: Leishmania major, Trypanosoma brucei and Trypanosoma cruzi,” *BMC Genomics*, vol. 6, pp. 1–19, 2005, doi: 10.1186/1471-2164-6-127.

[27] D. M. Walker, S. Oghumu, G. Gupta, B. S. Mcgwire, M. E. Drew, and A. R. Satoskar, “Mechanisms of cellular invasion by intracellular parasites Mechanisms of host cell invasion in Leishmania,” *Cell Mol Life Sci*, vol. 71, no. 7, pp. 1245–1263, 2014, doi: 10.1007/s00018-013-1491-1.Mechanisms.

[28] G. De Muylder, B. Vanhollebeke, G. Caljon, A. R. Wolfe, J. McKerrow, and J. C. Dujardin, “Naloxonazine, an Amastigote-Specific Compound, Affects Leishmania Parasites through Modulation of Host-Encoded Functions,” *PLoS Negl. Trop. Dis.*, vol. 10, no. 12, pp. 1–14, 2016, doi: 10.1371/journal.pntd.0005234.

[29] A. Ponte-Sucre, “An overview of trypanosoma brucei infections: An intense host-parasite interaction,” *Front. Microbiol.*, vol. 7, no. DEC, pp. 1–12, 2016, doi: 10.3389/fmicb.2016.02126.

[30] V. Kourbeli, E. Chontzopoulou, K. Moschovou, D. Pavlos, and T. Mavromoustakos, “An Overview on Target-Based Drug Design against Kinetoplastid Protozoan Infections : Human African Trypanosomiasis , Chagas Disease and Leishmaniases,” pp. 1–34, 2021.

[31] M. C. Field *et al.*, “Erratum: Anti-trypanosomatid drug discovery: an ongoing challenge and a continuing need (Nature reviews. Microbiology (2017) 15 4 (217-231)),” *Nat. Rev. Microbiol.*, vol. 15, no. 7, p. 447, 2017, doi: 10.1038/nrmicro.2017.69.

[32] A. Bhattacharya, A. Corbeil, R. L. Do Monte-Neto, and C. Fernandez-Prada, “Of drugs and trypanosomatids: New tools and knowledge to reduce bottlenecks in drug discovery,” *Genes (Basel).*, vol. 11, no. 7, pp. 1–24, 2020, doi: 10.3390/genes11070722.

[33] L. R. Tchokouaha Yamthe *et al.*, “ Antileishmanial effects of Sargassum vulgare products and prediction of trypanothione reductase inhibition by fucosterol ,” *Futur. Drug Discov.*, vol. 2, no. 3, p. FDD41, 2020, doi: 10.4155/fdd-2020-0002.

[34] G. A. Holloway *et al.*, “Trypanothione reductase high-throughput screening campaign identifies novel classes of inhibitors with antiparasitic activity,” *Antimicrob. Agents Chemother.*, vol. 53, no. 7, pp. 2824–2833, 2009, doi: 10.1128/AAC.01568-08.

[35] M. O. F. Khan, “Trypanothione Reductase: A Viable Chemotherapeutic Target for Antitrypanosomal and Antileishmanial Drug Design,” *Drug Target Insights*, vol. 2, no. 1999, p. 117739280700200, 2007, doi: 10.1177/117739280700200007.

[36] M. Beig, F. Oellien, L. Garoff, S. Noack, R. Luise Krauth-Siegel, and P. M. Selzer, “Trypanothione reductase: A target protein for a combined in vitro and in silico screening approach,” *PLoS Negl. Trop. Dis.*, vol. 9, no. 6, pp. 1–19, 2015, doi:

10.1371/journal.pntd.0003773.

[37] S. Kumar, M. R. Ali, and S. Bawa, “Mini review on tricyclic compounds as an inhibitor of trypanothione reductase,” *J. Pharm. Bioallied Sci.*, vol. 6, no. 4, pp. 222–228, 2014, doi: 10.4103/0975-7406.142943.

[38] A. Allouche, “Software News and Updates Gabedit — A Graphical User Interface for Computational Chemistry Softwares,” *J. Comput. Chem.*, vol. 32, no. 102, pp. 174–182, 2012, doi: 10.1002/jcc.

[39] M. A. Murcko, “What Makes a Great Medicinal Chemist? A Personal Perspective,” *J. Med. Chem.*, vol. 61, no. 17, pp. 7419–7424, 2018, doi: 10.1021/acs.jmedchem.7b01445.

[40] S. K. Koerner *et al.*, “Design and synthesis of emodin derivatives as novel inhibitors of ATP-citrate lyase,” *Eur. J. Med. Chem.*, vol. 126, pp. 920–928, 2017, doi: 10.1016/j.ejmech.2016.12.018.

[41] N. H. Mashour, G. I. Lin, and W. H. Frishman, “Herbal medicine for the treatment of cardiovascular disease: Clinical considerations,” *Arch. Intern. Med.*, vol. 158, no. 20, pp. 2225–2234, 1998, doi: 10.1001/archinte.158.20.2225.

[42] M. Cerone *et al.*, “Discovery of Sustainable Drugs for Neglected Tropical Diseases: Cashew Nut Shell Liquid (CNSL)-Based Hybrids Target Mitochondrial Function and ATP Production in Trypanosoma brucei,” *ChemMedChem*, vol. 14, no. 6, pp. 621–635, 2019, doi: 10.1002/cmdc.201800790.

[43] T. Matutino Bastos *et al.*, “Chemical Constituents of Anacardium occidentale as Inhibitors of Trypanosoma cruzi Sirtuins,” *Molecules*, vol. 24, no. 7, pp. 1–13, 2019, doi: 10.3390/molecules24071299.

[44] K. Tatyana *et al.*, “Inhibition of HIV-1 Ribonuclease H Activity by Novel Frangula-Emodine Derivatives,” *Med. Chem. (Los. Angeles).*, vol. 5, no. 5, pp. 398–410, 2009, doi: 10.2174/157340609789117840.

[45] H. Dave and L. Ledwani, “A review on anthraquinones isolated from Cassia species and their applications,” *Indian J. Nat. Prod. Resour.*, vol. 3, no. 3, pp. 291–319, 2012.

[46] Y. Caro, L. Anamale, M. Fouillaud, P. Laurent, T. Petit, and L. Dufosse, “Natural hydroxyanthraquinoid pigments as potent food grade colorants: an overview,” *Nat. Products Bioprospect.*, vol. 2, no. 5, pp. 174–193, 2012, doi: 10.1007/s13659-012-0086-0.

[47] E. M. M. and C. E. Muller, “Anthraquinones As Pharmacological Tools and Drugs,” *Med. Res. Rev.*, vol. 36, no. 4, pp. 705–748, 2016, doi: 10.1002/med.

[48] V. Mohanlall, P. Steenkamp, and B. Odhav, “Isolation and characterization of anthraquinone derivatives from Ceratotheca triloba (Bernh.) Hook.f.,” *J. Med. Plants Res.*, vol. 5, no. 14, pp. 3132–3141, 2011.

[49] J. S. Xu, Y. Cui, X. M. Liao, X. Bin Tan, and X. Cao, “Effect of emodin on the cariogenic properties of streptococcus mutans and the development of caries in rats,” *Exp. Ther. Med.*, vol. 8, no. 4, pp. 1308–1312, 2014, doi: 10.3892/etm.2014.1857.

[50] S. M. Abu-darwish, A. M. Ateyyat, and A. Salt, “The Pharmacological and Pesticidal Actions of Naturally Occurring 1,8-dihydroxyanthraquinones Derivatives,” *World J. Agric. Sci.*, vol. 4, no. 4, pp. 495–505, 2008, [Online]. Available: https://pdfs.semanticscholar.org/1d65/a3d7582c192a215d5919c1fc193f7c56775e.pdf.

[51] R. Sharma, A. B. Tiku, and A. Giri, “Pharmacological Properties of Emodin-Anthraquinone Derivatives,” *Share Your Innov. through JACS Dir. J. Nat. Prod. Resour. Visit J.*, vol. 3, no. 1, pp. 97–101, 2017, [Online]. Available:

http://www.jacsdirectory.com/jnpr.

[52] L. Zhang *et al.*, “Tyrosine kinase inhibitors, emodin and its derivative repress HER-2/neu-induced cellular transformation and metastasis-associated properties,” *Oncogene*, vol. 16, no. 22, pp. 2855–2863, 1998, doi: 10.1038/sj.onc.1201813.

[53] Y. Li and J. G. Jiang, “Health functions and structure-activity relationships of natural anthraquinones from plants,” *Food Funct.*, vol. 9, no. 12, pp. 6063–6080, 2018, doi: 10.1039/c8fo01569d.

[54] B. C. Lin *et al.*, “The anthraquinone emodin inhibits the non-exported FIKK kinase from Plasmodium falciparum,” *Bioorg. Chem.*, vol. 75, pp. 217–223, 2017, doi: 10.1016/j.bioorg.2017.09.011.

[55] A. Sakulpanich and W. Gritsanapan, “Determination of anthraquinone contents in Cassia fistula leaves for alternative source of laxative drugs,” *Planta Med.*, vol. 75, no. 09, pp. 28–31, 2009, doi: 10.1055/s-0029-1234665.

[56] L. Omur Demirezer, N. Karahan, E. Ucakturk, A. Kuruuzum-Uz, Z. Guvenalp, and C. Kazaz, “HPLC fingerprinting of sennosides in laxative drugs with isolation of standard substances from some senna leaves,” *Rec. Nat. Prod.*, vol. 5, no. 4, pp. 261–270, 2011.

[57] M. N. Preobrazhenskaya, A. E. Shchekotikhin, A. A. Shtil, and H. S. Huang, “Antitumor anthraquinone analogues for multidrug resistant tumor cells,” *J. Med. Sci.*, vol. 26, no. 1, pp. 1–4, 2006.

[58] S. M. M. Nor, M. A. H. M. Sukari, S. S. S. A. Azziz, W. C. Fah, H. Alimon, and S. F. Juhan, “Synthesis of new cytotoxic aminoanthraquinone derivatives via nucleophilic substitution reactions,” *Molecules*, vol. 18, no. 7, pp. 8046–8062, 2013, doi: 10.3390/molecules18078046.

[59] H. S. Huang, H. F. Chiu, W. C. Lu, and C. L. Yuan, “Synthesis and antitumor activity of 1,8-diaminoanthraquinone derivatives,” *Chem. Pharm. Bull.*, vol. 53, no. 9, pp. 1136–1139, 2005, doi: 10.1248/cpb.53.1136.

[60] K. Sweidan, H. Zalloum, D. A. Sabbah, G. Idris, K. Abudosh, and M. S. Mubarak, “Synthesis, characterization, and anticancer evaluation of some new N 1-(anthraquinon-2-yl) amidrazone derivatives,” *Can. J. Chem.*, vol. 96, no. 12, pp. 1123–1128, 2018, doi: 10.1139/cjc-2018-0145.

[61] X. Yang, G. Sun, C. Yang, and B. Wang, “Novel Rhein Analogues as Potential Anticancer Agents,” *ChemMedChem*, vol. 6, no. 12, pp. 2294–2301, 2011, doi: 10.1002/cmdc.201100384.

[62] J. L. Nitiss, “Targeting DNA topoisomerase II in cancer chemotherapy,” *Nat. Rev. Cancer*, vol. 9, no. 5, pp. 338–350, 2009, doi: 10.1038/nrc2607.

[63] K. Buzun, A. Bielawska, K. Bielawski, and A. Gornowicz, “DNA topoisomerases as molecular targets for anticancer drugs,” *J. Enzyme Inhib. Med. Chem.*, vol. 35, no. 1, pp. 1781–1799, 2020, doi: 10.1080/14756366.2020.1821676.

[64] S. Gattinoni, L. Merlini, and S. Dallavalle, “First total synthesis of topopyrone C,” *Tetrahedron Lett.*, vol. 48, no. 6, pp. 1049–1051, 2007, doi: 10.1016/j.tetlet.2006.11.164.

[65] Y. Baqi, “Anthraquinones as a privileged scaffold in drug discovery targeting nucleotide-binding proteins,” *Drug Discov. Today*, vol. 21, no. 10, pp. 1571–1577, 2016, doi: 10.1016/j.drudis.2016.06.027.

[66] Y. T. Han, “Synthesis of proposed structure of rennellianone B: A study on rearrangement of anthraquinonyl propargyl ether toward 2H-pyranoanthraquinone,” *Tetrahedron Lett.*, vol. 58, no. 6, pp. 556–558, 2017, doi: 10.1016/j.tetlet.2016.12.080.

[67] S. N. Fedorov, L. K. Shubina, A. S. Kuzmich, and S. G. Polonik, “Antileukemic properties and structure-activity relationships of O- and S-glycosylated derivatives of juglone and related 1,4-naphthoquinones,” *Open Glycosci.*, vol. 4, no. 1, pp. 1–5, 2011, doi: 10.2174/1875398101104010001.

[68] S. C. Chien, Y. C. Wu, Z. W. Chen, and W. C. Yang, “Naturally occurring anthraquinones: Chemistry and therapeutic potential in autoimmune diabetes,” *Evidence-based Complement. Altern. Med.*, vol. 2015, no. Figure 1, 2015, doi: 10.1155/2015/357357.

[69] M. Fouillaud, M. Venkatachalam, E. Girard-Valenciennes, Y. Caro, and L. Dufossé, “Anthraquinones and derivatives from marine-derived fungi: Structural diversity and selected biological activities,” *Mar. Drugs*, vol. 14, no. 4, 2016, doi: 10.3390/md14040064.

[70] S. Haider, “Heterocycles , Back Bone of Drug Design Phytochemistry & Biochemistry,” vol. 1, no. 1, p. 2017, 2017.

[71] K. H. Narasimhamurthy, A. M. Sajith, M. N. Joy, and K. S. Rangappa, “An Overview of Recent Developments in the Synthesis of Substituted Thiazoles,” *ChemistrySelect*, vol. 5, no. 19, pp. 5629–5656, 2020, doi: 10.1002/slct.202001133.

[72] N. Kerru, L. Gummidi, S. Maddila, K. K. Gangu, and S. B. Jonnalagadda, “A review on recent advances in nitrogen-containing molecules and their biological applications,” *Molecules*, vol. 25, no. 8, 2020, doi: 10.3390/molecules25081909.

[73] J. M. Liu *et al.*, “Novel 3-substituted fluorine imidazolium/triazolium salt derivatives: Synthesis and antitumor activity,” *RSC Adv.*, vol. 5, no. 78, pp. 63936–63944, 2015, doi: 10.1039/c5ra07947k.

[74] S. He *et al.*, “Discovery, Optimization, and Characterization of Novel Chlorcyclizine

Derivatives for the Treatment of Hepatitis C Virus Infection," 2016, doi: 10.1021/acs.jmedchem.5b00752.

[75] P. Goel, O. Alam, M. J. Naim, F. Nawaz, M. Iqbal, and M. I. Alam, "Recent advancement of piperidine moiety in treatment of cancer- A review," *Eur. J. Med. Chem.*, vol. 157, pp. 480–502, 2018, doi: 10.1016/j.ejmech.2018.08.017.

[76] A. Khazaei *et al.*, "Sulfonic acid functionalized imidazolium salts/ FeCl3 as novel and highly efficient catalytic systems for the synthesis of benzimidazoles at room temperature," *Sci. Iran.*, vol. 18, no. 6, pp. 1365–1371, 2011, doi: 10.1016/j.scient.2011.09.016.

[77] A. Castonguay, C. Doucet, M. Juhas, and D. Maysinger, "New ruthenium(II)-letrozole complexes as anticancer therapeutics," *J. Med. Chem.*, vol. 55, no. 20, pp. 8799–8806, 2012, doi: 10.1021/jm301103y.

[78] M. N. Aboul-Enein and and M. F. H. 1, Aida M. Abd El-Sattar El-Azzouny1, Fatma Abdel-Fattah Ragab2, "Design, Synthesis, and Cytotoxic Evaluation of Certain 7-Chloro-4- (piperazin-1-yl)quinoline Derivatives as VEGFR-II Inhibitors Mohamed," pp. 1–12, 2017, doi: 10.1002/ardp.201600377.

[79] A. Zhou *et al.*, "Synthesis and Evaluation of Paeonol Derivatives as Potential Multifunctional Agents for the Treatment of Alzheimer's Disease," pp. 1304–1318, 2015, doi: 10.3390/molecules20011304.

[80] B. Wang *et al.*, "Syntheses, biological activities and SAR studies of novel carboxamide compounds containing piperazine and arylsulfonyl moieties," 2016, doi: 10.1016/j.ejmech.2016.04.005.

[81] A. P. Kourounakis, "Morpholine as a privileged structure : A review on the medicinal chemistry and pharmacological activity of morpholine containing bioactive

molecules," no. May, pp. 1–44, 2019, doi: 10.1002/med.21634.

[82] P. Mahendran, J. R. A, S. Antony, S. Dhawa, and E. Kaliyappan, "Synthesis , molecular docking and in-vivo study of anti- hyperlipidemic activity in High fat Diet Animals for substituted morpholine derivatives," vol. 11, no. 6, pp. 2458–2474, 2019.

[83] 2 and Thoraya A. Farghaly 1 Ismail Althagafi 1,*, Nashwa El-Metwaly 1, "New Series of Thiazole Derivatives: Synthesis, Structural Elucidation, Antimicrobial Activity, Molecular Modeling and MOE Docking," vol. 24, 2019, [Online]. Available: 10.3390/molecules24091741.

[84] P. Yang, R. Wang, H. Wu, Z. Du, and Y. Fu, "Pd-Catalyzed C À H Arylation of Benzothiazoles with Diaryliodonium Salt : One-Pot Synthesis of 2-Arylbenzothiazoles," no. Iii, pp. 184–188, 2017, doi: 10.1002/ajoc.201600514.

[85] Y. Z. Hongrui Lei, Gang Hu, Yu Wang, Pei Han, Zijian Liu and and P. Gong, "Design, Synthesis, and Biological Evaluation of 4-Phenoxyquinoline Derivatives Containing Benzo[d]thiazole-2-yl Urea as c-Met Kinase Inhibitors," vol. 349, pp. 651–661, 2016, doi: 10.1002/ardp.201600003.

[86] W. Yu, L. Shi, G. Hui, and F. Cui, "Synthesis of biological active thiosemicarbazone and characterization of the interaction with human serum albumin," *J. Lumin.*, vol. 134, pp. 491–497, 2013, doi: 10.1016/j.jlumin.2012.07.040.

[87] P. Cai, Y. Xiong, Y. Yao, W. Chen, and X. Dong, "Synthesis, screening and biological activity of potent thiosemicarbazone compounds as a tyrosinase inhibitor," *New J. Chem.*, vol. 43, no. 35, pp. 14102–14111, 2019, doi: 10.1039/c9nj02360g.

[88] A. Saeed, A. Imran, P. A. Channar, M. Shahid, W. Mahmood, and J. Iqbal, "2-(Hetero(Aryl)Methylene)Hydrazine-1-Carbothioamides As Potent Urease Inhibitors," *Chem. Biol. Drug Des.*, vol. 85, no. 2, pp. 225–230, 2015, doi: 10.1111/cbdd.12379.

[89] K. S. A. Melha, “In-vitro antibacterial, antifungal activity of some transition metal complexes of thiosemicarbazone Schiff base (HL) derived from N4-(7′-chloroquinolin-4′-ylamino) thiosemicarbazide,” *J. Enzyme Inhib. Med. Chem.*, vol. 23, no. 4, pp. 493–503, 2008, doi: 10.1080/14756360701631850.

[90] H. J. Zhang, Y. Qian, D. Di Zhu, X. G. Yang, and H. L. Zhu, “Synthesis, molecular modeling and biological evaluation of chalcone thiosemicarbazide derivatives as novel anticancer agents,” *Eur. J. Med. Chem.*, vol. 46, no. 9, pp. 4702–4708, 2011, doi: 10.1016/j.ejmech.2011.07.016.

[91] M. S. Alam, L. Liu, Y. E. Lee, and D. U. Lee, “Synthesis, antibacterial activity and quantum-chemical studies of novel 2-arylidenehydrazinyl-4-arylthiazole analogues,” *Chem. Pharm. Bull.*, vol. 59, no. 5, pp. 568–573, 2011, doi: 10.1248/cpb.59.568.

[92] C. K. Oza, M. Jain, N. Jain, and D. Verma, “Synthesis, characterization, antimicrobial activities, and structural studies of Lanthanide (III) complexes with 1-(4-Chlorophenyl)-3-(4-fluoro/ hydroxyphenyl)prop-2-en-1-thiosemicarbazone,” *Phosphorus, Sulfur Silicon Relat. Elem.*, vol. 185, no. 2, pp. 377–386, 2010, doi: 10.1080/10426500902797483.

[93] R. H. Vekariya, K. D. Patel, D. P. Rajani, S. D. Rajani, and D. Patel, “Journal of the Association of Arab Universities for Basic A one pot , three component synthesis of coumarin hybrid thiosemicarbazone derivatives and their antimicrobial evolution A one pot , three component synthesis of coumarin hybrid thiosemicarbazone derivatives and their antimicrobial evolution,” *J. Assoc. Arab Univ. Basic Appl. Sci.*, vol. 23, pp. 10–19, 2018, doi: 10.1016/j.jaubas.2016.04.002.

[94] M. Sainsbury, “Aromatic Compounds with Three Fused Carbocyclic Ring Systems: Anthracene, Phenanthrene, and Related Compounds,” *Rodd’s Chem. Carbon Compd.*

A Mod. Compr. Treatise Second Ed., vol. 3, pp. 1–136, 1964, doi: 10.1016/B978-044453345-6.50675-1.

[95] E. H. Anouar, C. P. Osman, J. F. F. Weber, and N. H. Ismail, "UV/Visible spectra of a series of natural and synthesised anthraquinones: Experimental and quantum chemical approaches," *Springerplus*, vol. 3, no. 1, pp. 1–12, 2014, doi: 10.1186/2193-1801-3-233.

[96] K. K. and B. N, "Product Class 5: Anthra-9,10-quinones, Anthra-1,2-quinones, Anthra-1,4-quinones, Anthra-2,9-quinones, and Their Higher Fused Analogues," *ChemInform*, vol. 34, no. 46, 2006, doi: 10.1055/b-00000101.

[97] B. R. Madje, M. B. Ubale, J. V Bharad, and M. S. Shingare, "B(HSO 4) 3 : an efficient solid acid catalyst for the synthesis of anthraquinone derivatives," *Bull. Catal. Soc. India*, vol. 9, no. January 2011, pp. 19–25, 2011.

[98] R. Singh and Geetanjali, "Isolation and synthesis of anthraquinones and related compounds of Rubia cordifolia," *J. Serbian Chem. Soc.*, vol. 70, no. 7, pp. 937–942, 2005, doi: 10.2298/JSC0507937S.

[99] C. W. Smith, S. J. Ambler, and D. J. Steggles, "A VERSATILE SYNTHESIS OF HYDROXY-9,10-ANTHRAQUINONE-2-CARBOXYLIC ACIDS.," vol. 34, no. 46, pp. 7447–7450, 1993.

[100] D. Mal and P. Pahari, "Recent advances in the Hauser annulation," *Chem. Rev.*, vol. 107, no. 5, pp. 1892–1918, 2007, doi: 10.1021/cr068398q.

[101] J. Beck, O. Fuhr, M. Nieger, and S. Bräse, "A versatile Diels-Alder approach to functionalized hydroanthraquinones: Diels-Alder Approach to Anthraquinones," *R. Soc. Open Sci.*, vol. 7, no. 11, 2020, doi: 10.1098/rsos.200626rsos200626.

[102] K. B. Somai Magar, L. Xia, and Y. R. Lee, “Organocatalyzed benzannulation for the construction of diverse anthraquinones and tetracenediones,” *Chem. Commun.*, vol. 51, no. 41, pp. 8592–8595, 2015, doi: 10.1039/c5cc00623f.

[103] C. S. Kramer, M. Nieger, and S. Bräse, “Naphthoquinone diels-alder reactions: Approaches to the ABC ring system of beticolin,” *European J. Org. Chem.*, vol. 2014, no. 10, pp. 2150–2159, 2014, doi: 10.1002/ejoc.201301763.

[104] T. Komiyama, Y. Takaguchi, and S. Tsuboi, “Synthesis of anthraquinone derivatives: Tandem Diels-Alder-decarboxylation- oxidation reaction of 3-hydroxy-2-pyrone with 1,4-naphthoquinone,” *Synlett*, no. 1, pp. 124–126, 2006, doi: 10.1055/s-2005-922769.

[105] L. F. Tietze, K. M. Gericke, and C. Güntner, “First Total Synthesis of the Bioactive Anthraquinone Kwanzoquinone C and Related Natural Products by a Diels – Alder Approach,” pp. 4910–4915, 2006, doi: 10.1002/ejoc.200600634.

[106] “cl.1996.113.pdf.” .

[107] J. Roy, T. Mal, S. Jana, and D. Mal, “Regiodefined synthesis of brominated hydroxyanthraquinones related to proisocrinins,” *Beilstein J. Org. Chem.*, vol. 12, pp. 531–536, 2016, doi: 10.3762/bjoc.12.52.

[108] T.-S. W. and I. K. L. A. Mitscher, “A Useful Extension of the Marschalk Synthesis of 11-Deoxydoxorubicin Reaction Directed Toward Antitumor Antibiotics.,” *J. Chem. Inf. Model.*, vol. 24, no. 44, pp. 4809–4812, 1983, [Online]. Available: 10.1016/S0040-4039(00)94013-9.

[109] and A. J. HavliCkova L (Mrs.), “Anthraquinone Dyes. Part V.l A Contribution to the Study of the Marschalk reaction. Nuclear Methylation of 1 -Aminoanthraquinone Leuco-derivative,” 1970, [Online]. Available: 10.1039/J39700000567.

[110] KARSTEN KROHN and WAHYUDI PRIYONO, “SYNTHETIC ANTHRACYCLINONES-XXVII ANTHRACYCLINONES BY INTRAMOLECULAR MARSCHALK REACTION SYNTHESIS OF THE FEUDOMYCINONES AND RHODOMYCINONES,” vol. 40, no. 22, pp. 4609–4616, 1984.

[111] H. S. Jin and L. M. Zhao, “A contribution to the study of the modified Marschalk reaction: Hydroxymethylation of 6,8-O-dimethyl emodin,” *Chinese Chem. Lett.*, vol. 21, no. 5, pp. 568–571, 2010, doi: 10.1016/j.cclet.2010.01.013.

[112] F. B. Hamad and E. B. Mubofu, “Potential biological applications of bio-based anacardic acids and their derivatives,” *Int. J. Mol. Sci.*, vol. 16, no. 4, pp. 8569–8590, 2015, doi: 10.3390/ijms16048569.

[113] F. H. A. Rodrigues, J. P. A. Feitosa, N. M. P. S. Ricardo, F. C. F. De França, and J. O. B. Carioca, “Antioxidant activity of Cashew Nut Shell Liquid (CNSL) derivatives on the thermal oxidation of synthetic cis-1,4-polyisoprene,” *J. Braz. Chem. Soc.*, vol. 17, no. 2, pp. 265–271, 2006, doi: 10.1590/S0103-50532006000200008.

[114] M. R. Patel, B. Z. Dholakiya, T. Gandhi, M. Patel, and B. Kumar Dholakiya, “Studies on effect of various solvents on extraction of cashew nut shell liquid (CNSL) and isolation of major phenolic constituents from extracted CNSL,” *J. Nat. Prod. Plant Resour*, vol. 2012, no. 1, pp. 135–142, 2012, [Online]. Available: http://scholarsresearchlibrary.com/archive.html.

[115] M. Telascrêa, A. L. Leão, M. Z. Ferreira, H. F. F. Pupo, B. M. Cherian, and S. Narine, “Use of a Cashew Nut Shell Liquid resin as a potential replacement for phenolic resins in the preparation of panels - A review,” *Mol. Cryst. Liq. Cryst.*, vol. 604, no. 1, pp. 222–232, 2014, doi: 10.1080/15421406.2014.968509.

[116] M. Q. de Souza *et al.*, “Molecular evaluation of anti-inflammatory activity of phenolic lipid extracted from cashew nut shell liquid (CNSL),” *BMC Complement. Altern. Med.*, vol. 18, no. 1, pp. 1–11, 2018, doi: 10.1186/s12906-018-2247-0.

[117] M. C. Lubi and E. T. Thachil, “Cashew nut shell liquid (CNSL) - A versatile monomer for polymer synthesis,” *Des. Monomers Polym.*, vol. 3, no. 2, pp. 123–153, 2000, doi: 10.1163/156855500300142834.

[118] I. Kubo, N. Masuoka, T. J. Ha, and K. Tsujimoto, “Antioxidant activity of anacardic acids,” *Food Chem.*, vol. 99, no. 3, pp. 555–562, 2006, doi: 10.1016/j.foodchem.2005.08.023.

[119] M. Hemshekhar, M. Sebastin Santhosh, K. Kemparaju, and K. S. Girish, “Emerging roles of anacardic acid and its derivatives: A pharmacological overview,” *Basic Clin. Pharmacol. Toxicol.*, vol. 110, no. 2, pp. 122–132, 2012, doi: 10.1111/j.1742-7843.2011.00833.x.

[120] A. Omanakuttan *et al.*, “Anacardic acid inhibits the catalytic activity of matrix metalloproteinase-2 and matrix metalloproteinase-9,” *Mol. Pharmacol.*, vol. 82, no. 4, pp. 614–622, 2012, doi: 10.1124/mol.112.079020.

[121] A. L. N. Carvalho *et al.*, “Anacardic acids from cashew nuts ameliorate lung damage induced by exposure to diesel exhaust particles in mice,” *Evidence-based Complement. Altern. Med.*, vol. 2013, 2013, doi: 10.1155/2013/549879.

[122] S. M. Morais *et al.*, “Anacardic acid constituents from cashew nut shell liquid: NMR characterization and the effect of unsaturation on its biological activities,” *Pharmaceuticals*, vol. 10, no. 1, pp. 1–10, 2017, doi: 10.3390/ph10010031.

[123] E. Bloise *et al.*, “Sustainable preparation of cardanol-based nanocarriers with embedded natural phenolic compounds,” *ACS Sustain. Chem. Eng.*, vol. 2, no. 5, pp.

1299–1304, 2014, doi: 10.1021/sc500123r.

[124] “PDBsum Pictorial database of 3D structures in the Protein Data Bank. EMBL-EBI; 2013.” http://www.ebi.ac.uk/thornton-srv/%0Adatabases/cgi-bin/pdbsum/GetPage.pl?pdbcode=index.html.

[125] “Discovery Studio Visualizer. San Diego: Dassault Systèmes BIOVIA; 2017.” https://www.3dsbiovia.com/products/collaborative-science/%0Abiovia-discovery-studio/.

[126] R. Paramashivappa, P. Phani Kumar, P. J. Vithayathil, and A. Srinivasa Rao, “Novel method for isolation of major phenolic constituents from cashew (Anacardium occidentale L.) Nut shell liquid,” *J. Agric. Food Chem.*, vol. 49, no. 5, pp. 2548–2551, 2001, doi: 10.1021/jf001222j.

[127] N. S. Reddy, A. S. Rao, M. A. Chari, V. R. Kumar, V. Jyothy, and V. Himabindu, “Synthesis and antibacterial activity of sulfonamide derivatives at C-8 alkyl chain of anacardic acid mixture isolated from a natural product cashew nut shell liquid (CNSL),” *J. Chem. Sci.*, vol. 124, no. 3, pp. 723–730, 2012, doi: 10.1007/s12039-012-0253-1.

[128] J. H. Xu, Y. Q. Ma, J. P. Wei, F. M. Li, and X. H. Peng, “New insights into bromination process: Effective preparation of Ambroxol,” *Chem. Pap.*, vol. 69, no. 5, pp. 722–728, 2015, doi: 10.1515/chempap-2015-0077.

[129] S. W. Baldwin and T. H. O’Neill, “Benzylic Bromination With Bromotrichloromethane,” *Synth. Commun.*, vol. 6, no. 2, pp. 109–112, 1976, doi: 10.1080/00397917608072618.

[130] S. Lee and C. S. Ra, “Benzylic Brominations with N-Bromosuccinimide in 1,2-Dichlorobenzene: Effective Preparation of (2-Bromomethyl-phenyl)-

Methoxyiminoacetic Acid Methyl Ester," *Clean Technol.*, vol. 22, no. 4, pp. 269–273, 2016, doi: 10.7464/ksct.2016.22.4.269.

[131] L. P. L. Lograd*o et al.*, "Synthesis and cytotoxicity screening of substituted isobenzofuranones designed from anacardic acids," *Eur. J. Med. Chem.*, vol. 45, no. 8, pp. 3480–3489, 2010, doi: 10.1016/j.ejmech.2010.05.015.

[132] G. C. Flowers and J. E. Leffler, "Decomposition of Bis(p-methoxybenzoyl) Peroxide and the Carboxy Inversion Product on Silica," *J. Org. Chem.*, vol. 50, no. 22, pp. 4406–4408, 1985, doi: 10.1021/jo00222a048.

[133] P. Wolkoff, "Dehydrobromination of Secondary and Tertiary Alkyl and Cycloalkyl Bromides with 1,8-Diazabicyclo[5.4.0]undec-7-ene. Synthetic Applications," *J. Org. Chem.*, vol. 47, no. 10, pp. 1944–1948, 1982, doi: 10.1021/jo00349a023.

[134] E. A. Santalova and V. A. Denisenko, "Analysis of the configuration of an isolated double bond in some lipids by selective homonuclear decoupling," *Nat. Prod. Commun.*, vol. 12, no. 12, pp. 1913–1916, 2017, doi: 10.1177/1934578x1701201225.

[135] A. Sudalai, A. Khenkin, and R. Neumann, "Sodium periodate mediated oxidative transformations in organic synthesis," *Org. Biomol. Chem.*, vol. 13, no. 15, pp. 4374–4394, 2015, doi: 10.1039/c5ob00238a.

[136] F. Jia and Z. Li, "Iron-catalyzed/mediated oxidative transformation of C-H bonds," *Org. Chem. Front.*, vol. 1, no. 2, pp. 194–214, 2014, doi: 10.1039/c3qo00087g.

[137] A. Gonzalez-De-Castro and J. Xiao, "Green and Efficient: Iron-Catalyzed Selective Oxidation of Olefins to Carbonyls with O2," *J. Am. Chem. Soc.*, vol. 137, no. 25, pp. 8206–8218, 2015, doi: 10.1021/jacs.5b03956.

[138] T. M. Shaikh and F. E. Hong, "Iron-catalyzed oxidative cleavage of olefins and

alkynes to carboxylic acids with aqueous tert-butyl hydroperoxide," *Adv. Synth. Catal.*, vol. 353, no. 9, pp. 1491–1496, 2011, doi: 10.1002/adsc.201000899.

[139] Z. Zhang, X. Li, T. Song, Y. Zhao, and Y. Feng, "An anthraquinone scaffold for putative, two-face bim BH3 α-helix mimic," *J. Med. Chem.*, vol. 55, no. 23, pp. 10735–10741, 2012, doi: 10.1021/jm301504b.

[140] Q. D. Tu *et al.*, "Design and syntheses of novel N′-((4-oxo-4H-chromen-3-yl)methylene) benzohydrazide as inhibitors of cyanobacterial fructose-1,6-/sedoheptulose-1,7- bisphosphatase," *Bioorganic Med. Chem.*, vol. 21, no. 11, pp. 2826–2831, 2013, doi: 10.1016/j.bmc.2013.04.003.

[141] M. Korb and H. Lang, "The anionic Fries rearrangement: A convenient route to: Ortho-functionalized aromatics," *Chem. Soc. Rev.*, vol. 48, no. 10, pp. 2829–2882, 2019, doi: 10.1039/c8cs00830b.

[142] X. Chen, M. Tordeux, J. R. Desmurs, and C. Wakselman, "Thia-Fries rearrangement of aryl triflinates to trifluoromethanesulfinylphenols," *J. Fluor. Chem.*, vol. 123, no. 1, pp. 51–56, 2003, doi: 10.1016/S0022-1139(03)00106-4.

[143] J. L. Hicks, C. C. Huang, and H. D. H. Showalter, "Synthesis of double carbon-14 labeled CI-9371 and CI-942, potential new anticancer drugs," *J. Label. Compd. Radiopharm.*, vol. 24, no. 10, pp. 1209–1220, 1987, doi: 10.1002/jlcr.2580241008.

[144] A. B. Gamble, J. Garner, C. P. Gordon, S. M. J. O'Conner, and P. A. Keller, "Aryl nitro reduction with iron powder or stannous chloride under ultrasonic irradiation," *Synth. Commun.*, vol. 37, no. 16, pp. 2777–2786, 2007, doi: 10.1080/00397910701481195.

[145] S. Jiang, T. S. Yan, Y. C. Han, L. Q. Cui, X. S. Xue, and C. Zhang, "Hypervalent-Iodine-Mediated Formation of Epoxides from Carbon(sp2)-Carbon(sp3) Single

Bonds," *J. Org. Chem.*, vol. 82, no. 22, pp. 11691–11702, 2017, doi: 10.1021/acs.joc.7b00883.

[146] Q. Liu *et al.*, "A general electrochemical strategy for the Sandmeyer reaction," *Chem. Sci.*, vol. 9, no. 46, pp. 8731–8737, 2018, doi: 10.1039/c8sc03346c.

[147] S. Aziz *et al.*, "Efficient synthesis and biological evaluation of topopyrone C derivatives," *Chem. Nat. Compd.*, vol. 52, no. 1, pp. 58–61, 2016, doi: 10.1007/s10600-016-1546-2.

[148] K. Dziduch, P. Kolodziej, A. Paneth, A. Bogucka-Kocka, and M. Wujec, "Synthesis and anthelmintic activity of new thiosemicarbazide derivatives-A preliminary study," *Molecules*, vol. 25, no. 12, pp. 6–13, 2020, doi: 10.3390/molecules25122770.

[149] D. C. Reis *et al.*, "Structural studies and investigation on the activity of imidazole-derived thiosemicarbazones and hydrazones against crop-related fungi," *Molecules*, vol. 18, no. 10, pp. 12645–12662, 2013, doi: 10.3390/molecules181012645.

[150] P. Venkanna, M. S. Kumar, and K. C. Rajanna, "Trichloroisocynuric Acid / DMF as Efficient Reagent for Chlorodehydration of Alcohols Under Conventional and Ultrasonic Conditions Trichloroisocynuric Acid / DMF as Ef fi cient Reagent for Chlorodehydration of Alcohols Under Conventional and Ultrasonic Co," vol. 3174, 2015, doi: 10.1080/15533174.2013.819896.

[151] G. Gordon and M. J. Aziz, "No Title."

[152] H. L. Huang, M. Wang, J. Wang, H. C. Wang, and H. L. Liu, "Sensing of zinc-containing nanopollutants with an ionic liquid," *J. Nanomater.*, vol. 2010, pp. 10–13, 2010, doi: 10.1155/2010/309207.

[153] G. Jin, Y. You, Y. Kim, N. Nam, and B. Ahn, "Short Communication multifunctional

anticancer agents," vol. 36, pp. 361–366, 2001.

[154] J. Burgess, G. Trusiano, T. Burgess, R. Bongiovanni, and C. Joly-duhamel, "per fl uoropolyalkylethers (PFPAEs) based on hexa fl uoropropylene oxide units for," pp. 32664–32671, 2018, doi: 10.1039/c8ra06354k.

[155] J. H. P. Tyman and S. J. A. Iddenten, "The synthesis of oxime reagents from natural and semi-synthetic phenolic lipid and alkanoic acid resources for the solvent recovery of copper(II)," *J. Chem. Technol. Biotechnol.*, vol. 80, no. 11, pp. 1319–1328, 2005, doi: 10.1002/jctb.1312.

[156] J. Bonnet, C. Boudot, and B. Courtioux, "Overview of the Diagnostic Methods Used in the Field for Human African Trypanosomiasis: What Could Change in the Next Years?," *Biomed Res. Int.*, vol. 2015, 2015, doi: 10.1155/2015/583262.

[157] M. Llinás, Z. Bozdech, E. D. Wong, A. T. Adai, and J. L. DeRisi, "Comparative whole genome transcriptome analysis of three Plasmodium falciparum strains," *Nucleic Acids Res.*, vol. 34, no. 4, pp. 1166–1173, 2006, doi: 10.1093/nar/gkj517.

[158] F. Xavier, "The HeLa cell line originates from a cervical cancer tumor of a patient named Henrietta Lacks, who died of cancer in 1951." https://www.tebu-bio.com/blog/2017/11/28/hela-cells-the-first-cell-line/.

[159] N. Tani *et al.*, "Interlaboratory validation of the in vitro eye irritation tests for cosmetic ingredients. (8) Evaluation of cytotoxicity tests on SIRC cells," *Toxicol. Vitr.*, vol. 13, no. 1, pp. 175–187, 1999, doi: 10.1016/S0887-2333(98)00071-X.

[160] C. Balachandran, Y. Arun, V. Duraipandiyan, S. Ignacimuthu, K. Balakrishna, and N. A. Al-Dhabi, "Antimicrobial and cytotoxicity properties of 2,3-dihydroxy-9,10-anthraquinone isolated from Streptomyces galbus (ERINLG-127)," *Appl. Biochem. Biotechnol.*, vol. 172, no. 7, pp. 3513–3528, 2014, doi: 10.1007/s12010-014-0783-8.

[161] J. M. Pereira *et al.*, “Anacardic acid derivatives as inhibitors of glyceraldehyde-3-phosphate dehydrogenase from Trypanosoma cruzi,” *Bioorganic Med. Chem.*, vol. 16, no. 19, pp. 8889–8895, 2008, doi: 10.1016/j.bmc.2008.08.057.

[162] P. Büscher, G. Cecchi, V. Jamonneau, and G. Priotto, “Human African trypanosomiasis,” vol. 390, pp. 2397–2409, 2017, doi: 10.1016/S0140-6736(17)31510-6.

[163] D. Malvy and F. Chappuis, “Sleeping sickness,” *Clin. Microbiol. Infect.*, vol. 17, no. 7, pp. 986–995, 2011, doi: 10.1111/j.1469-0691.2011.03536.x.

[164] T. M. Dhorajiwala, S. T. Halder, and L. Samant, “Applied Biotechnology Reports Comparative In Silico Molecular Docking Analysis of L-Threonine-3-Dehydrogenase , a Protein Target Against African Trypanosomiasis Using Selected Phytochemicals,” vol. 6, no. 3, pp. 101–108, 2019, doi: 10.29252/JABR.06.03.04.

[165] I. V Ogungbe and W. N. Setzer, “Comparative Molecular Docking of Antitrypanosomal Natural Products into Multiple Trypanosoma brucei Drug Targets,” pp. 1513–1536, 2009, doi: 10.3390/molecules14041513.

[166] R. De Gasparo *et al.*, “Biological Evaluation and X-ray Co-crystal Structures of Cyclohexylpyrrolidine Ligands for Trypanothione Reductase, an Enzyme from the Redox Metabolism of Trypanosoma,” *ChemMedChem*, vol. 13, no. 9, pp. 957–967, 2018, doi: 10.1002/cmdc.201800067.

[167] M. A. de Brito, “Pharmacokinetic study with computational tools in the medicinal chemistry course,” *Brazilian J. Pharm. Sci.*, vol. 47, no. 4, pp. 797–805, 2011, doi: 10.1590/S1984-82502011000400017.

[168] C. A. Lipinski, “Lead- and drug-like compounds: The rule-of-five revolution,” *Drug Discov. Today Technol.*, vol. 1, no. 4, pp. 337–341, 2004, doi:

10.1016/j.ddtec.2004.11.007.

APPENDIX

AA 1: Mass spectrometry of carboxylic 71

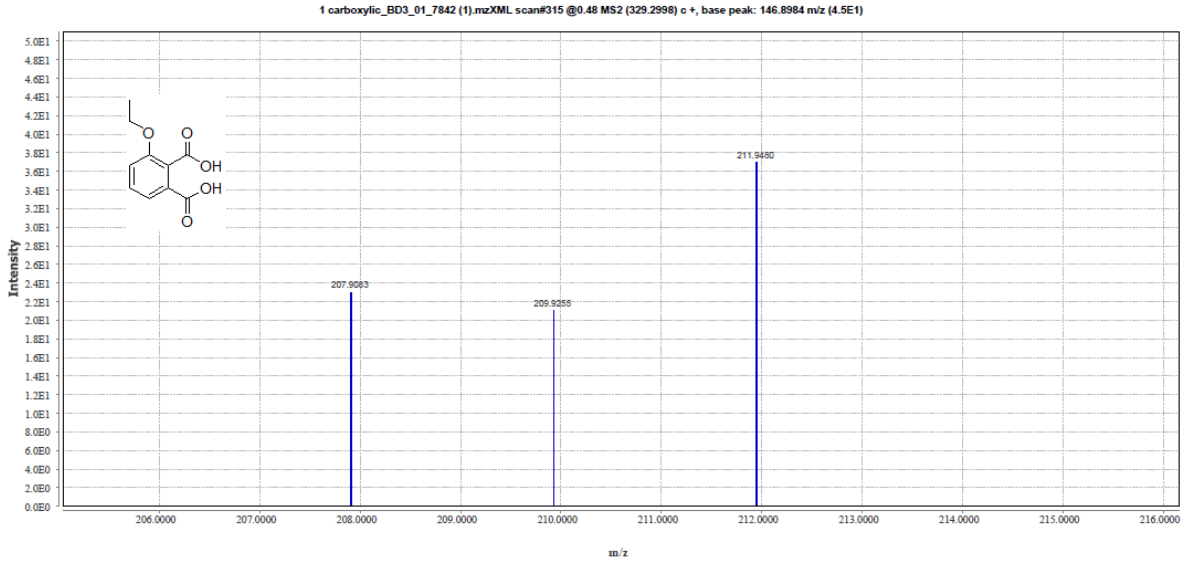

AA2: Mass spectrometry of imidazole anthraquinone 83

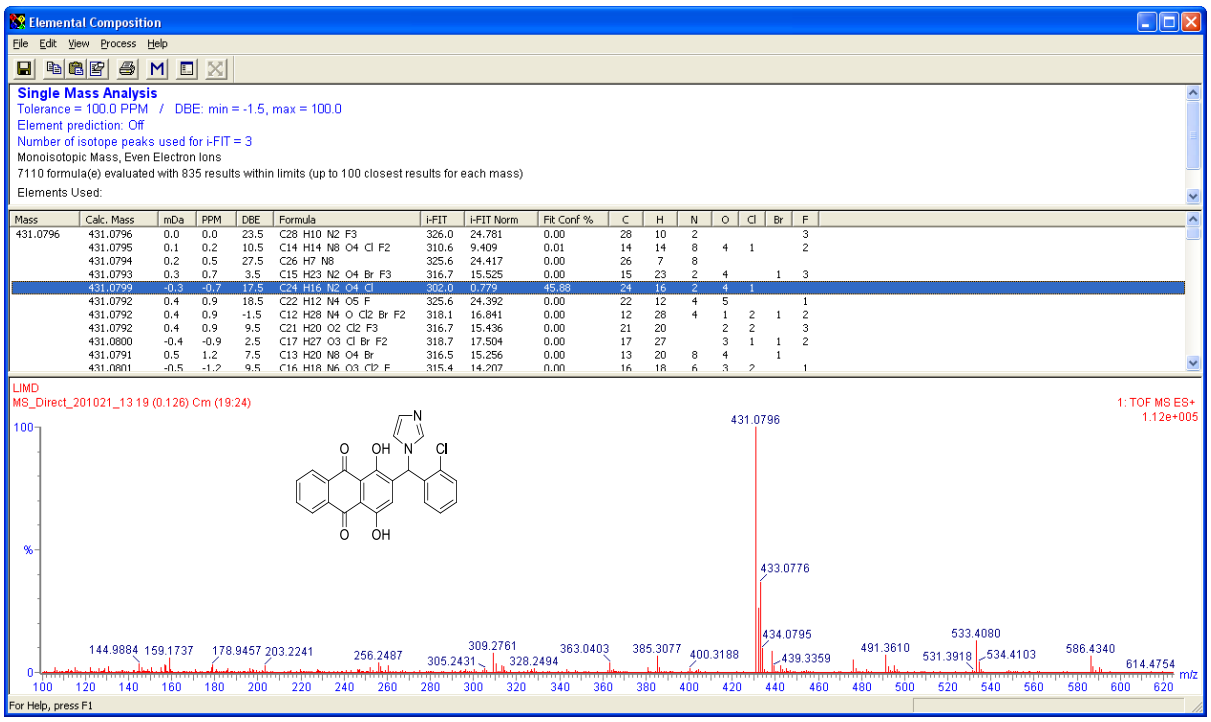

AA3: Mass spectrometry of thiazole anthraquinone 85

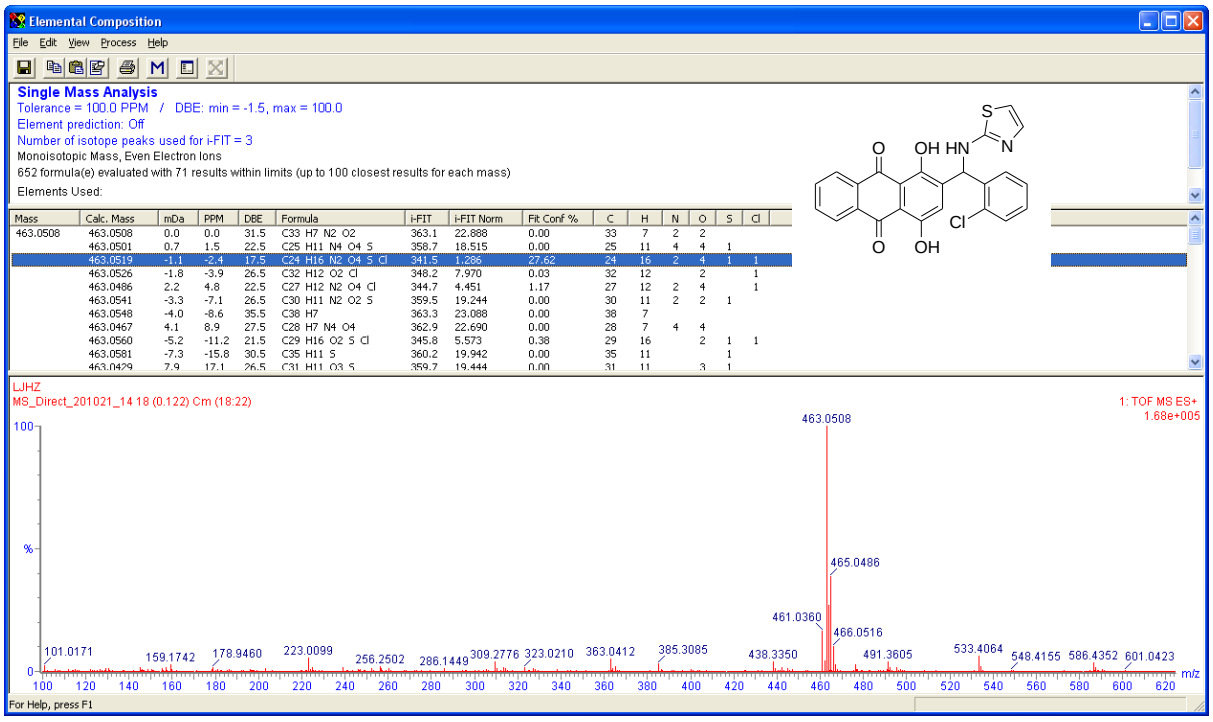

AA4: Protein ligand interaction-LK09

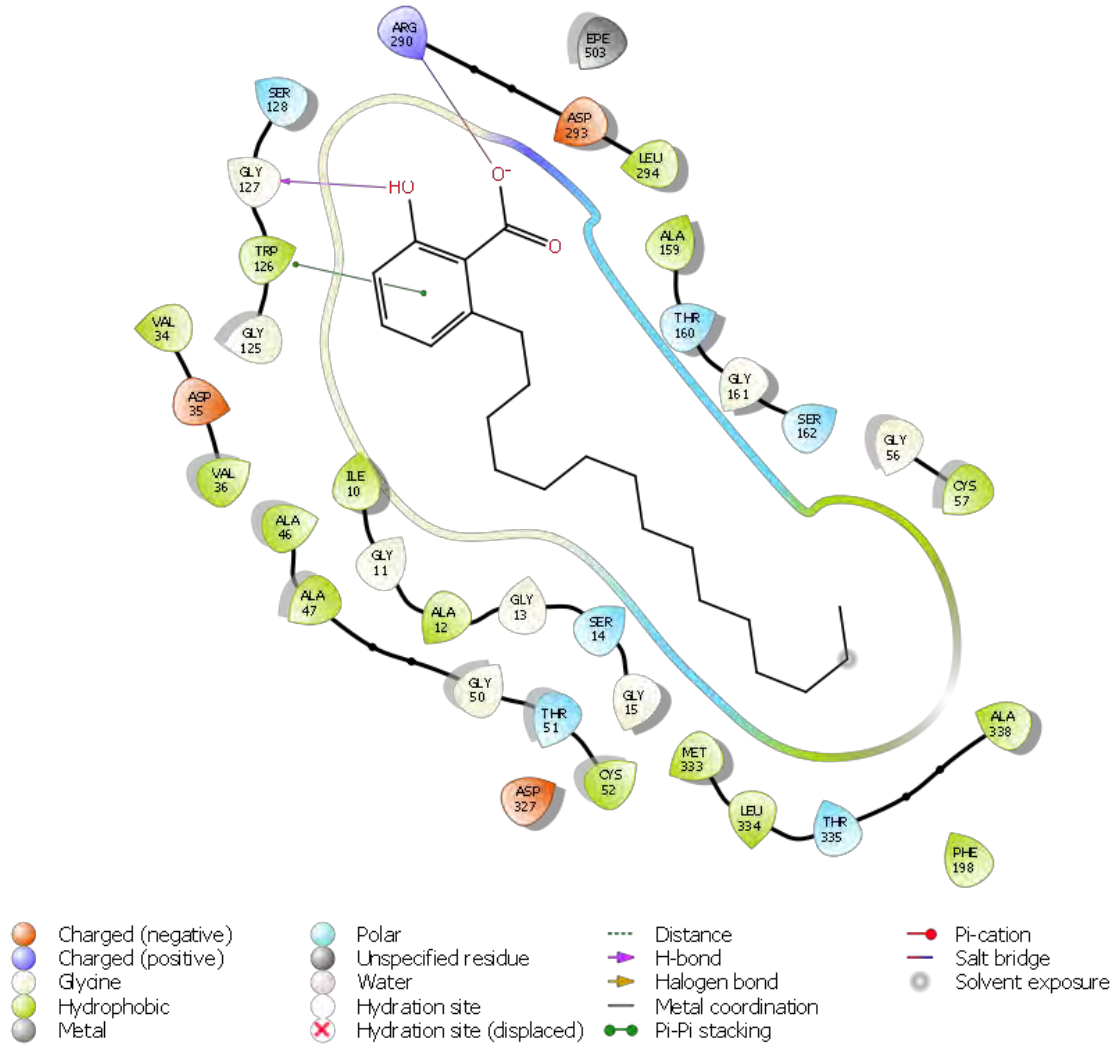

AA5: Protein ligand interaction-LK18

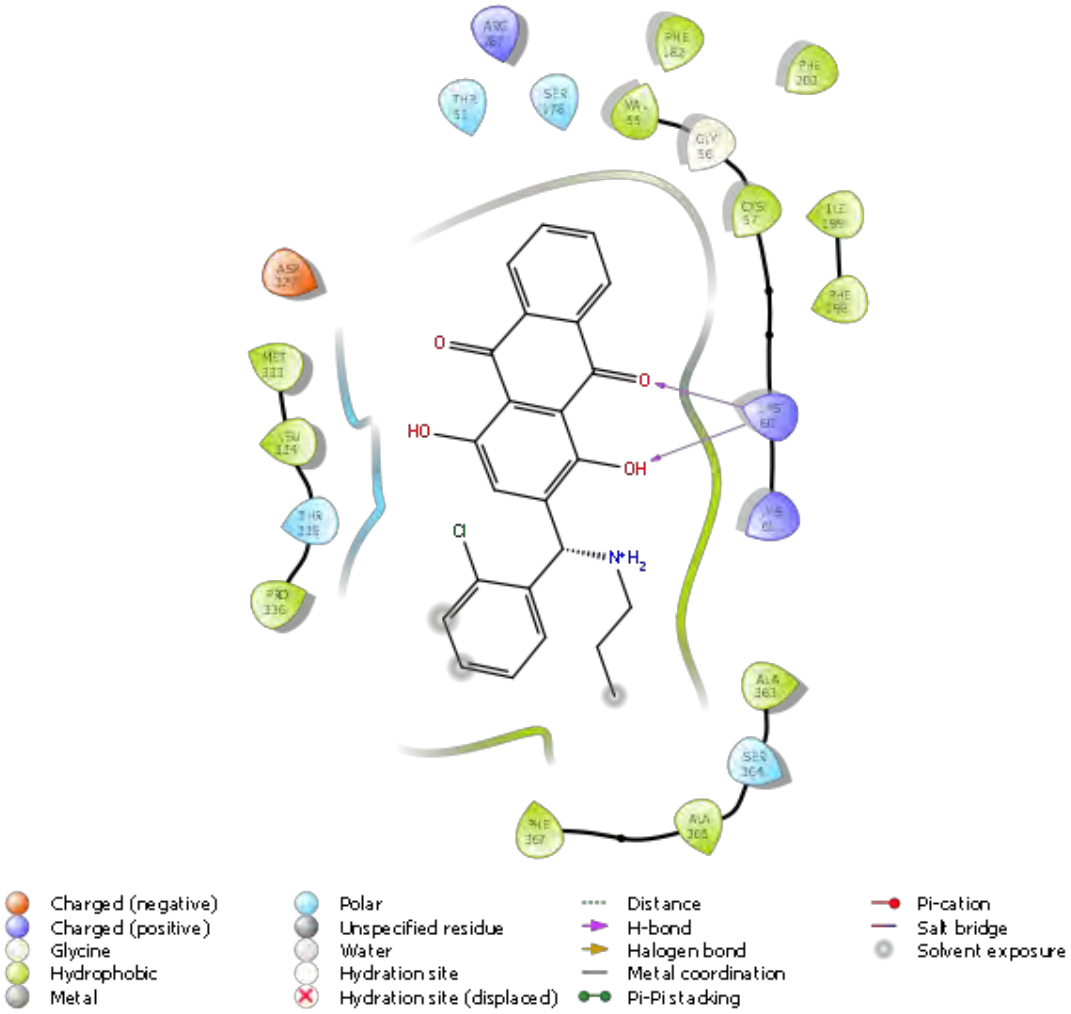

AA6: Protein ligand interaction-LK20

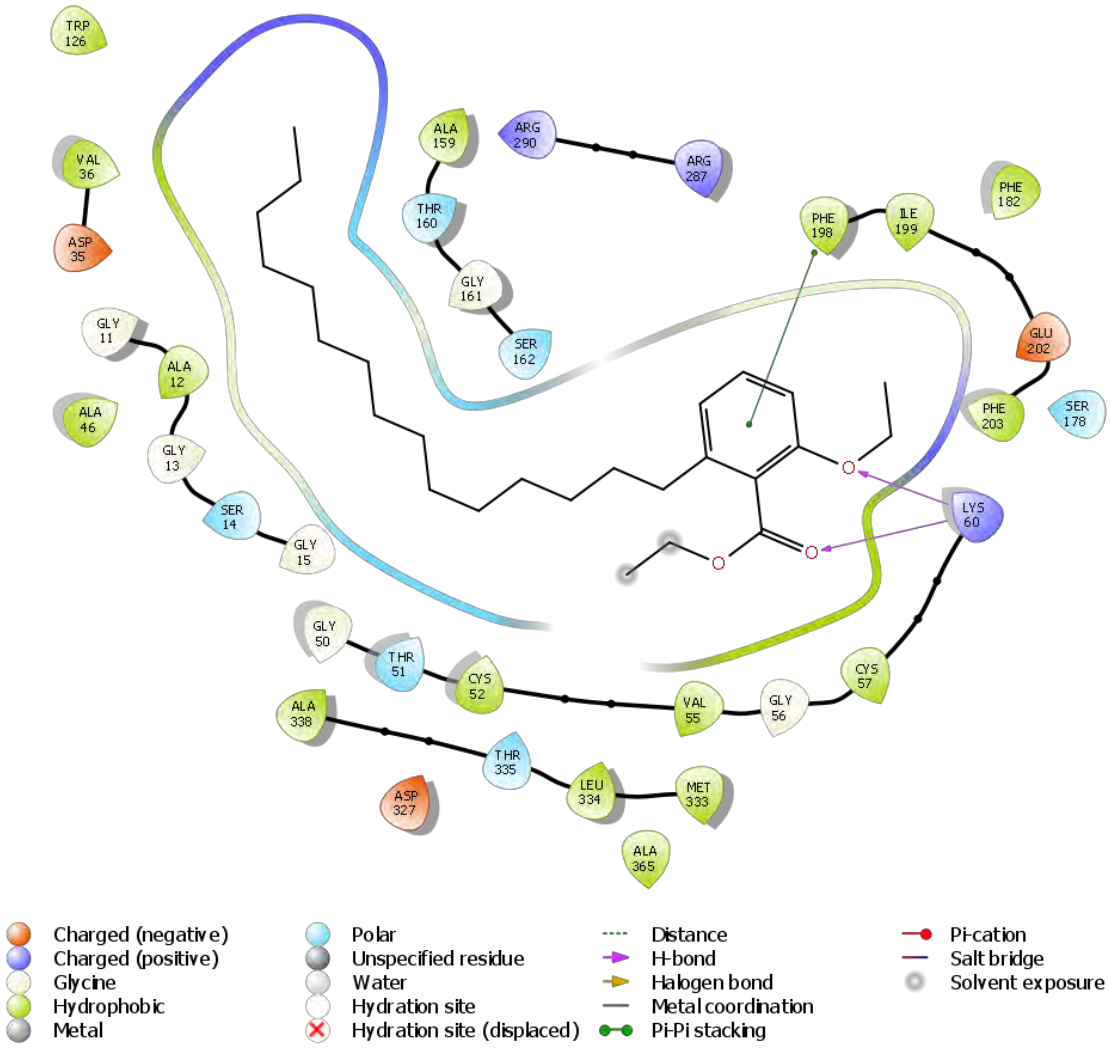

AA7: Protein ligand interaction-LK21

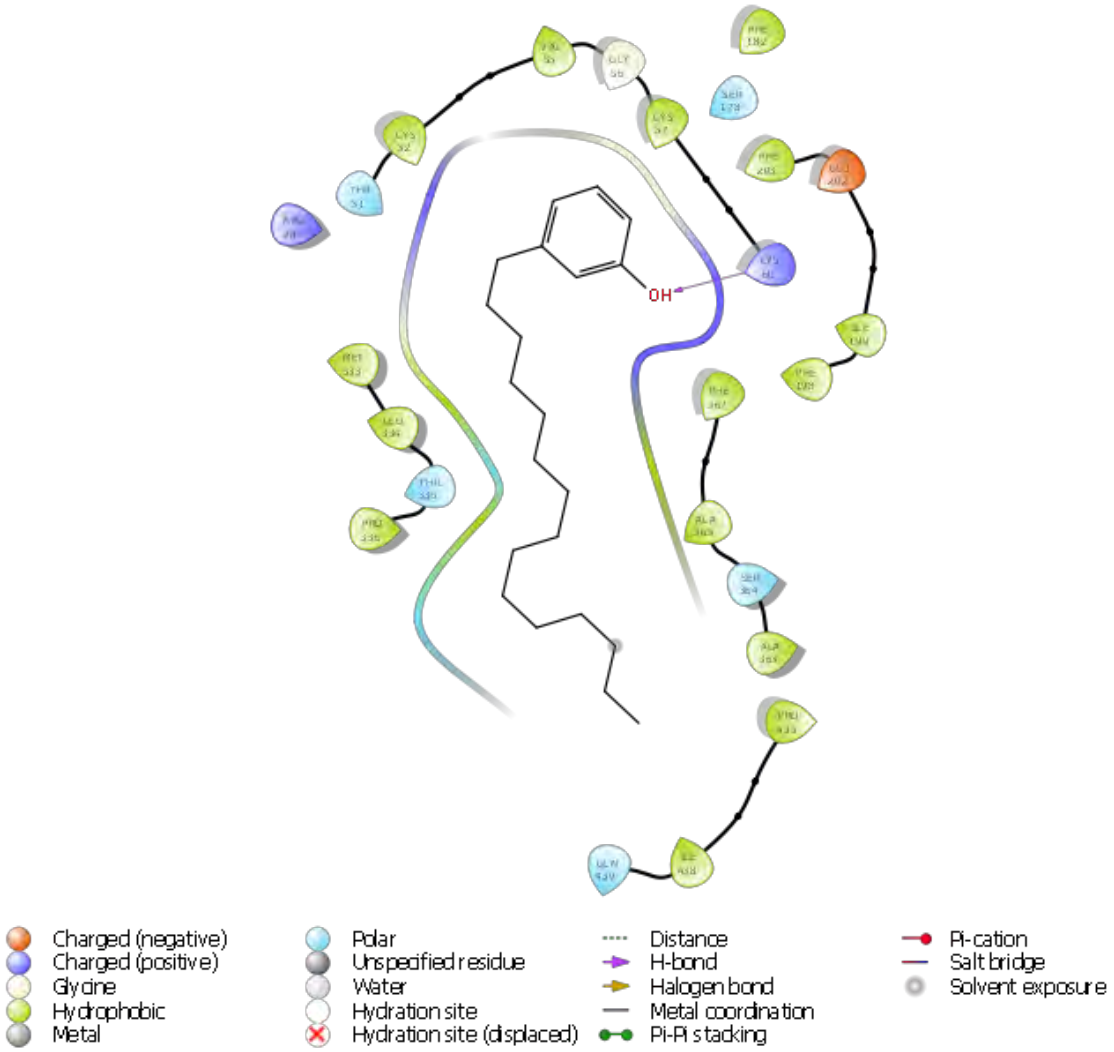

AA8: Protein ligand interaction- pentamidine

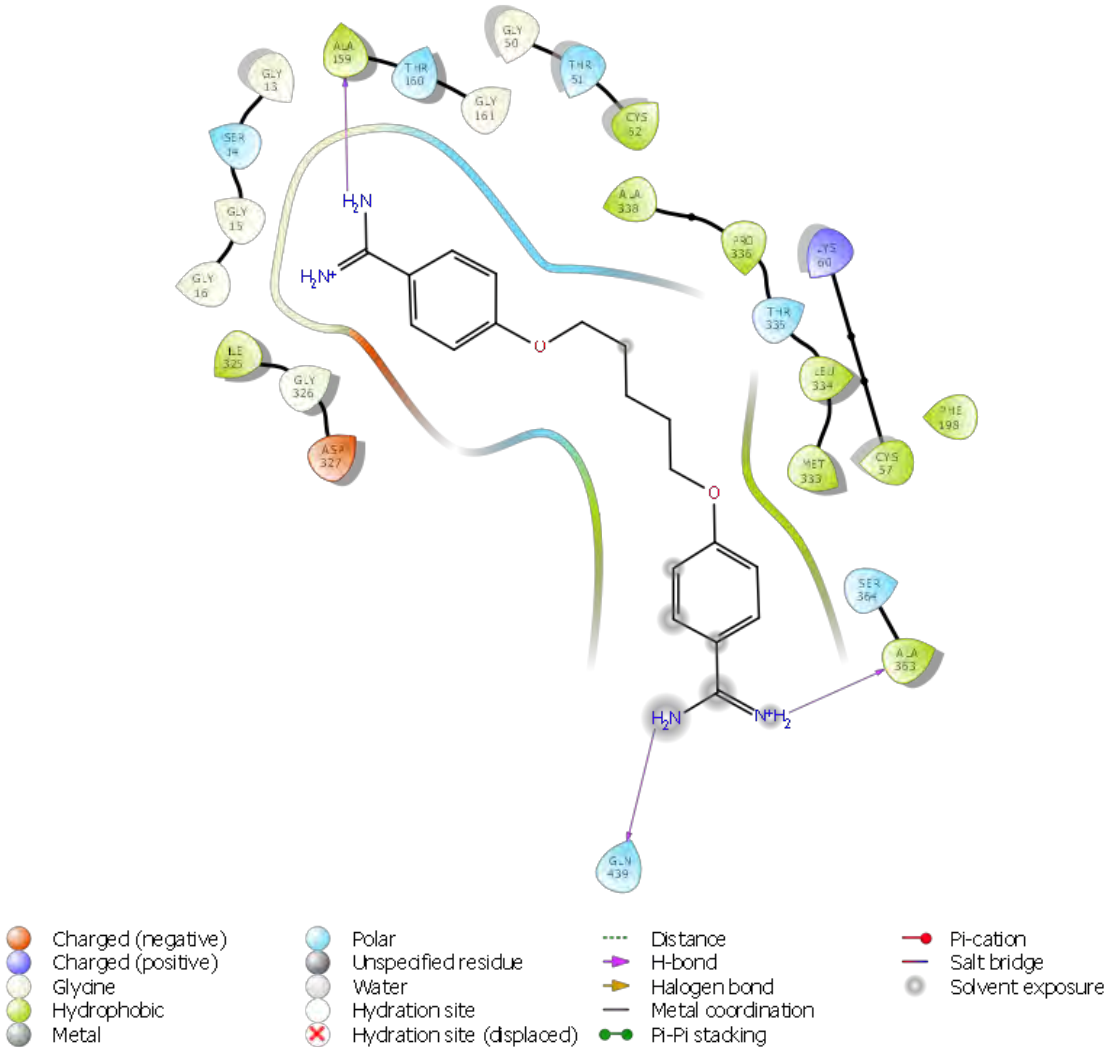

AA9: Protein ligand interaction- eflornithine

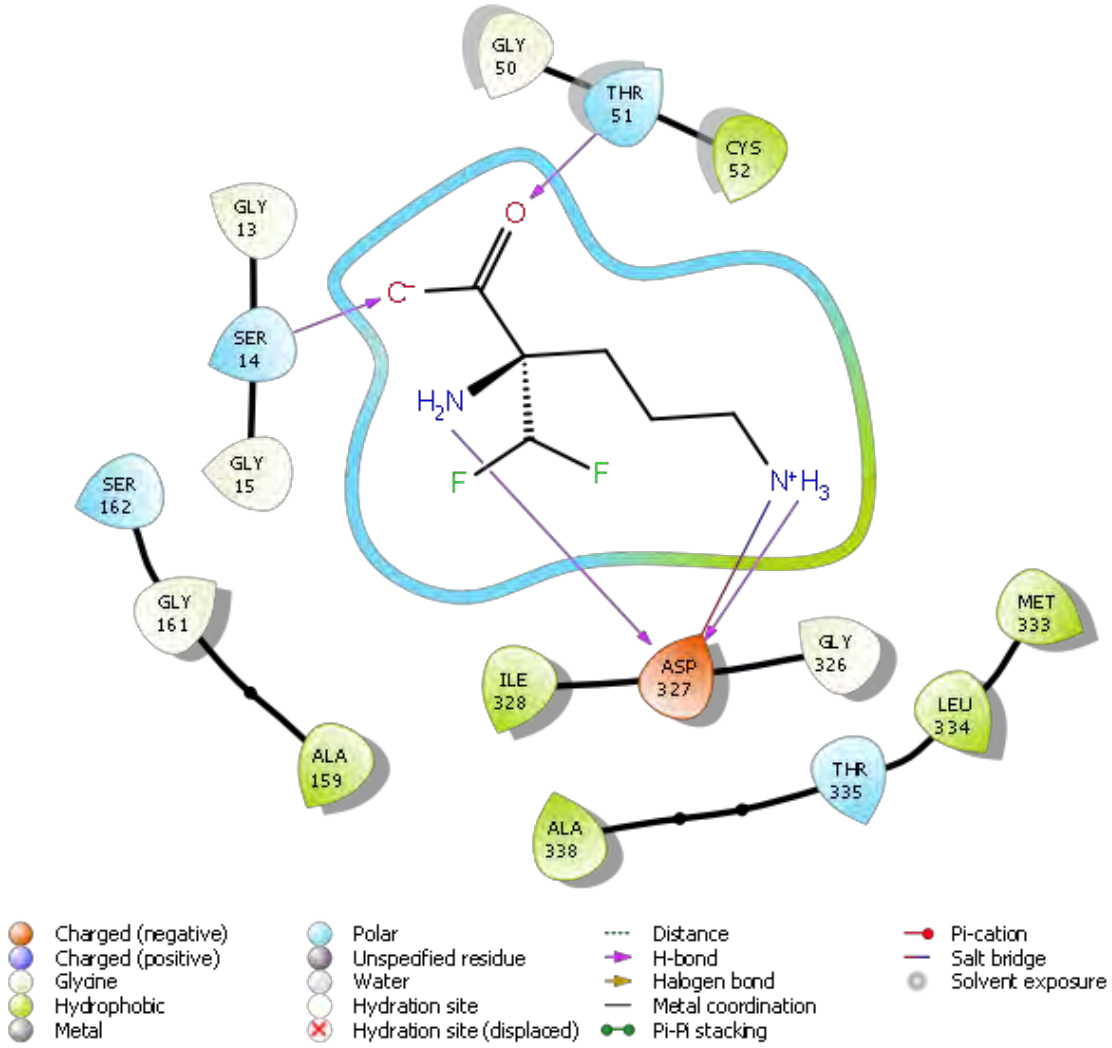

AA10: Protein ligand interaction- camptothecin

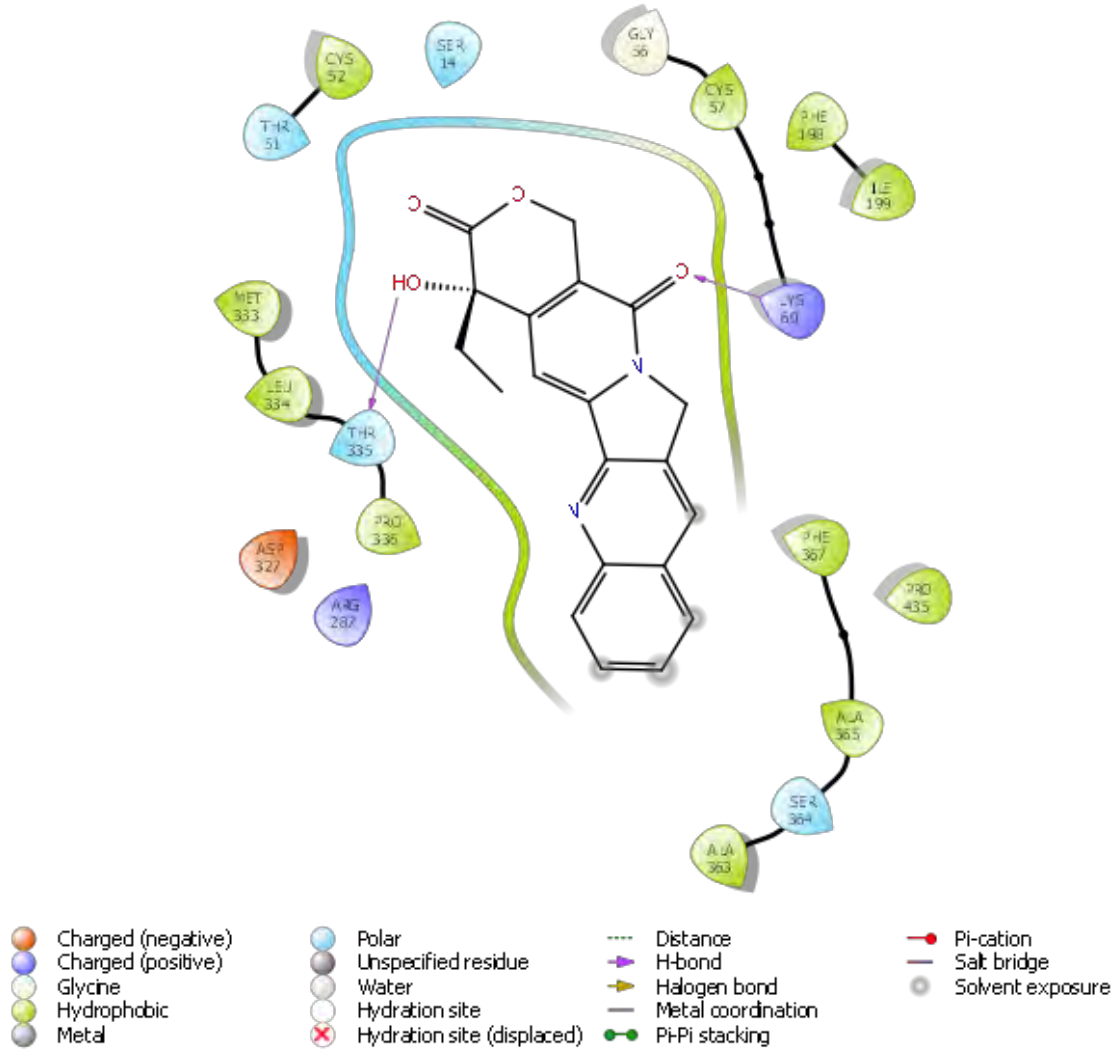

AA11: *Trypanosoma brucei brucei* % cell viability for compounds at the varied concentration

% Cell Viability								
Conc [C]	100	33.33	11.11	3.704	1.235	0.412	0.137	0.0457
Log [C]	2	1.523	1.046	0.568	0.091	-0.385	-0.863	-1.34
LK04	-0.54	1.20	1.51	1.60	21.32	80.74	100.97	99.23
LK05	1.06	2.89	6.58	10.99	31.73	101.19	102.20	102.55
LK06	1.63	1.17	5.02	21.61	90.61	99.63	102.02	100.66
LK07	-1.36	-0.70	2.90	46.57	98.84	98.00	97.54	97.70
LK09	-2.33	0.02	2.22	77.88	98.07	99.41	99.06	101.07
LK10	-3.17	-0.19	1.06	12.83	98.84	97.68	97.90	97.07
LK11	2.47	3.79	4.10	3.77	28.21	102.23	102.25	99.29
LK12	-1.47	-1.57	0.01	1.11	34.83	100.29	100.90	100.14
LK14	-2.97	-0.91	1.72	70.93	97.88	100.07	100.25	102.54
LK16	-2.69	-0.05	1.70	9.28	48.77	101.66	102.51	101.02
LK18	2.70	4.10	4.87	26.38	90.48	98.84	99.02	97.58
LK20	-0.30	0.58	1.49	29.37	98.66	100.76	100.33	98.83
LK21	-1.83	-0.72	0.74	52.70	100.93	101.15	99.17	98.37

AA12: Graph of % viability (*T. brucei* cells) against log [C] for sample LK01-LK21

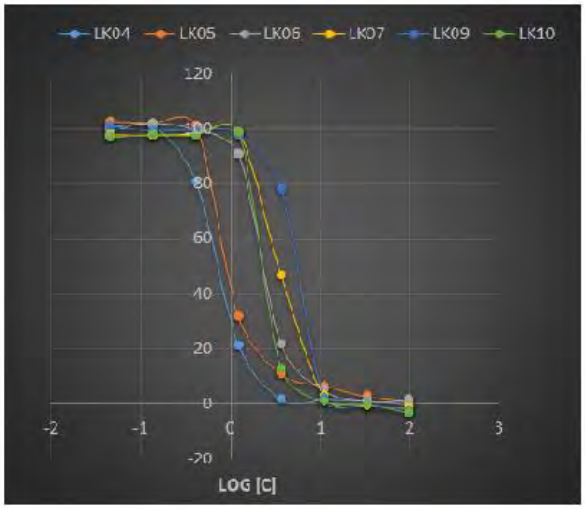

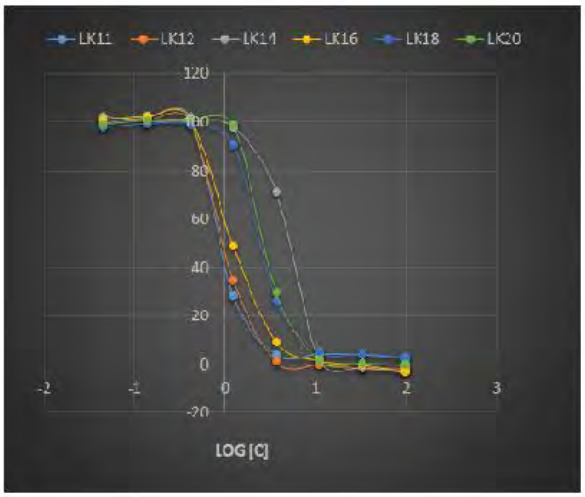

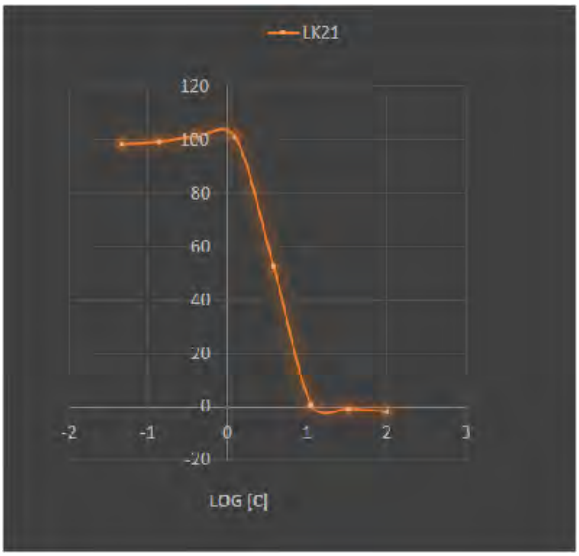

AA13: *P. falciparum* parasite % cell viability at the varied concentration (µM)

% Cell Viability								
Conc[C]	100	33.33	11.11	3.704	1.235	0.412	0.137	0.0457
Log C]	2	1.523	1.046	0.568	0.091	-0.385	-0.863	-1.34
LK02	-4.93	8.60	59.06	83.03	97.67	99.08	99.08	98.80
LK04	-4.93	1.83	11.13	39.61	94.86	101.62	102.21	102.21
LK06	0.14	12.83	21.85	58.21	98.52	102.59	102.18	101.90
LK12	1.88	14.44	44.12	79.28	103.48	104.17	101.43	98.69
LK17	0.74	7.82	67.41	95.03	102.34	101.66	99.83	97.32